Molecular Regulation

of Adrenal Androgen Biosynthesis

by

Jan Idkowiak

A thesis submitted to The University of Birmingham for

the degree of

DOCTOR OF PHILOSOPHY

School of Clinical and Experimental Medicine

College of Medical and Dental Sciences

University of Birmingham

August 2014

“More valuable than treasures in a storehouse are the treasures of the body, and the treasures of the heart are the most valuable of all. From the time you read this letter on, strive to accumulate the treasures of the heart!”

Nichiren Daishonin (1222-1282)

Abstract

The biosynthesis of adrenal androgens is catalysed by steroid-modifying enzymes. Over the past decade, co-factors were explored to regulate these enzymes: P450 oxidoreductase (POR) delivers electrons to the key androgen-producing cytochrome P450 enzyme CYP17A1. In addition, sulfation of the principal androgen precursor dehydroepiandrosterone (DHEA) catalysed by the enzyme SULT2A1, supported by its co-factor 3'-phosphoadenosine-5'-phosphosulfate (PAPS) synthase 2 (PAPSS2), has been found more recently as a gatekeeper of androgen activation.

Here, we have further characterised children with defects of enzymes of the androgen pathway, namely CYP17A1 and POR. We report the first human missense mutation of cytochrome b5, which supports electron transfer from POR to CYP17A1. In addition, we have explored the molecular regulation of DHEA sulfation by *in vitro* and *in vivo* studies.

The results from our studies provide important information on the clinical course, the diagnostic steroid fingerprint and underlying molecular mechanisms of conditions affecting androgen generation. The *in vitro* studies on DHEA sulfation confirm that the PAPSS2 isoform crucially regulates SULT2A1. Our *in vivo* study in children with deficiencies of the steroid sulfatase (STS) enzyme, the counterpart of SULT2A1, suggests that STS does not play a major role in DHEA metabolism but is more active before puberty.

Acknowledgements

I would like to express my gratitude to my supervisor, Prof Wiebke Arlt, for all her support, personal encouragement and foremost for her never ceasing confidence in this work. I am also grateful to my co-supervisor Prof Tim Barrett for his support.

I feel very fortunate to be part of the entire Arlt group and of the Centre of Endocrinology, Diabetes and Metabolism (CEDAM), where I met many wonderful people, great scientists and friends. I wish to thank them all, but I would like to specifically thank for their great support, friendship and laughter: Dr Vivek Dhir, Dr Nils Krone, Dr Silvia Parajes, Dr Nicole Reisch, Dr Jon Mueller, Mr Ian Rose, Dr Iwona Bujalska, Dr Mark Sherlock, Dr Laura Gathercole and Dr Fabian Hammer. A special thanks to Hannah Ivison for proofreading this thesis and (hopefully) correcting my Germanisms.

Thanks to mum and dad, who are supporting me throughout and are tolerant enough for me going away from Germany to seek my life and work mission in the UK, where I met my wonderful wife Vicki and her children Jamila and Jake. I am grateful to you all!!

I wish to dedicate this thesis to my mentor in life, Dr Daisaku Ikeda.

Table of contents

List of Figures

List of Tables

Abbreviations*

11β-HSD1	11β-hydroxysteroid dehydrogenase type 1
11β-HSD1	11β-hydroxysteroid dehydrogenase type 2
17OHP	17-hydroxyprogesterone
18S	18S ribosomal subunit
ACC	acetyl coenzyme A carboxylase
ACE	angiotensin converting enzyme
ACRD	apparent cortisone reductase deficiency
ACTH	adrenocorticotropic hormone
Adx	adrenodoxin
AdR	adrenodoxin reductase
AF	activation function domain
AIS	androgen insensitivity syndrome
AKR	aldo-keto reductase
AME	apparent mineralocorticoid excess
ANP	atrial natriuretic peptide
APS	adenosine-5'-phosphosulfate
ATP	adenosine triphosphate
AR	androgen receptor
BMI	body mass index
Bp	base pair
CAH	congenital adrenal hyperplasia
CAIS	complete androgen insensitivity syndrome
cAMP	cyclic adenosine-5'-monophosphate
cDNA	complementary deoxyribonucleic acid
CDS	coding sequence
CRD	cortisone reductase deficiency
CRH	corticotrophin releasing hormone
Ct	Cycle threshold
CYB5A	cytochrome b5 (isoform A)
CYP	cytochrome P450
DBD	DNA binding domain
dCt	delta cycle threshold
ddH_2O	double-filtered water
DHEA	dehydroepiandrosterone
DHEAS	dehydroepiandrosterone sulfate
DHT	dihydrotestosterone
DMEM	Dulbecco's modified eagles medium
DNA	deoxyribonucleic acid
DSD	disorders of sex development
dNTP	deoxynucleotide triphosphate
E	cortisone
E1	oestrione
E2	oestradiol
E3	oestriol
EDTA	ethylendiaminetetraacetic acid
ENaC	epithelial sodium channel
ER	oestrogen receptor; endoplasmic reticulum
F	cortisol
FAD	flavin-adenine dinucleotide
FCS	foetal calf serum

* Only those abbreviations are listed if they are used twice or more. Abbreviations of urinary steroid hormone metabolites are listed in **Table 9**

FGE	formylglycine generating enzyme
FGly	formylglycine
FMN	flavin mononucleotide
FSH	follicle stimulating hormone
FZ	foetal zone
GC	glucocorticoid
GC/MS	gas chromatography/ mass spectrometry
GnRH	gonadatrophin releasing hormone
GPCR	G-protein coupled receptor
GR	glucocorticoid receptor
GRE	glucocorticoid response element
H_2O	water
H6PDH	hexose-6-phosphate dehydrogenase
HCL	hydrochloride acid
HCG	human chorionic gonadotrophin
HPA	hypothalamic-pituitary-adrenal
HPG	hypothalamic-pituitary-gonadal
HRE	hormone responsive element
Hrs	hours
HSD	hydroxysteroid dehydrogenase
HSP	heat-shock protein
IGF	insulin-like factor
IMM	inner mitochondrial membrane
IPA	idiopathic premature adrenarche
HSD	hydroxysteroid dehydrogenase
LB	Luria Bertani broth
LBD	ligand-binding domain
LC/MSMS	liquid chromatography/ tandem mass spectrometry
LH	luteinizing hormone
LiAc	lithium acetate
LPL	lipoprotein lipase
MAPK	mitogen-activated protein kinase
MC	mineralocorticoid
MCS	multiple cloning site
Min	minute
MLPA	multiplex ligand probe amplification
MOPS	3-(N-morpholino-)propanesulfonic acid
MR	mineralocorticoid receptor
mRNA	messenger ribonucleic acid
MTBE	methyl tert-butyl ether
NaAc	sodium acetate
NaCl	sodium chloride
NaOH	sodium hydroxide
NAD	nicotinamide adenine dinucleotide
NBD	nucleotide-binding domain
NADH	dihydronicotinamide adenine dinucleotide
NADPH	nicotinamide adenine dinucleotide phosphate
NCAH	non-classical congenital adrenal hyperplasia
NTD	N-terminal domain
OD	optical density
OGTT	oral glucose tolerance test
OMIM	online mendelian inheritance in man
OMM	outer mitochondrial membrane
ORF	open reading frame
P	p-value
PA	premature adrenarche
PAIS	partial androgen insensitivity syndrome
PAPS	3’-phosphoadenosine 5’-phosphosulphate
PAPSS	3’-phosphoadenosine 5’-phosphosulphate synthase
PBS	phosphate buffered saline

Pc	post conceptionem
PCOS	polycystic ovary syndrome
PCR	polymerase chain reaction
PEG	polyethylene glycol
PKA/C	protein kinase A/C
POR	P450 oxidoreductase
PORD	P450 oxidoreductase deficiency
PP	premature pubarche
RAAS	renin angiotensin aldosterone system
RNA	ribonucleic acid
ROMC	renal outer medullary potassium channel
Rpm	revolutions per minute
RAAS	renin-angiotensin-aldosterone system
RT	room temperature *or* reverse transcriptase
RT-PCR	reverse-transcriptase PCR
SD	standard deviation of the mean
SDS	sodium dodecyl sulphate
SDM	site-directed mutagenesis
SDR	short chain dehydrogenase/reductase
SE	standard error of the mean
SEMD	spondylometaphyseal dysplasia
SF-1	steroidogenic factor 1
SGA	small for gestational age
Sec	second
SHBG	sex hormone binding globulin
SNP	single nucleotide polymorphism
SRY	sex-determining region of the Y-chromosome
StAR	steroidogenic acute regulatory protein
STS	steroid sulfatase
STSD	steroid sulfatase deficiency
SULT	sulfotransferase
SUMF	sulfatase modifying factor
T	testosterone
Taq	*thermus aquaticus*
THE	tetrahydrocortisone
THF	tetrahydrocortisol
TLC	thin-layer chromatography
UV	ultra violet
WT	wild type
WT1	Wilms' tumour suppressor gene 1
ZF	zona fasciculata
ZG	zona glomerulosa
ZR	zona reticularis

1. CHAPTER 1: GENERAL INTRODUCTION

Parts of this chapter have been published as:

Premature adrenarche: novel lessons from early onset androgen excess.

Idkowiak J, Lavery GG, Dhir V, Barrett TG, Stewart PM, Krone N, Arlt W.

Eur J Endocrinol. 2011 Aug;165(2):189-207. doi: 10.1530/EJE-11-0223.

1.1. THE ADRENAL CORTEX AND STEROID BIOSYNTHESIS

1.1.1. Anatomy, function and regulation of the adrenal gland

The adrenal gland is a paired, quadrilateral-shaped organ situated in the retroperineum on the upper pole of each kidney. The right adrenal is more triangular-shaped while the left adrenal has a semilunar shape. The weight of one adult adrenal is about 4g from autopsy specimens in cases of sudden death; hospital specimens are up to 50% heavier due to stress-induced proliferation (Pohorecky and Wurtman, 1971). Macroscopically, the adrenal gland can be divided into two separate parts: the medulla and the cortex, with the latter comprising 90% of its total weight. Medulla and cortex are of different embryological origins, the medulla is derived from neural crest cells, the cortex develops from mesenchyme (Moore, 1988).

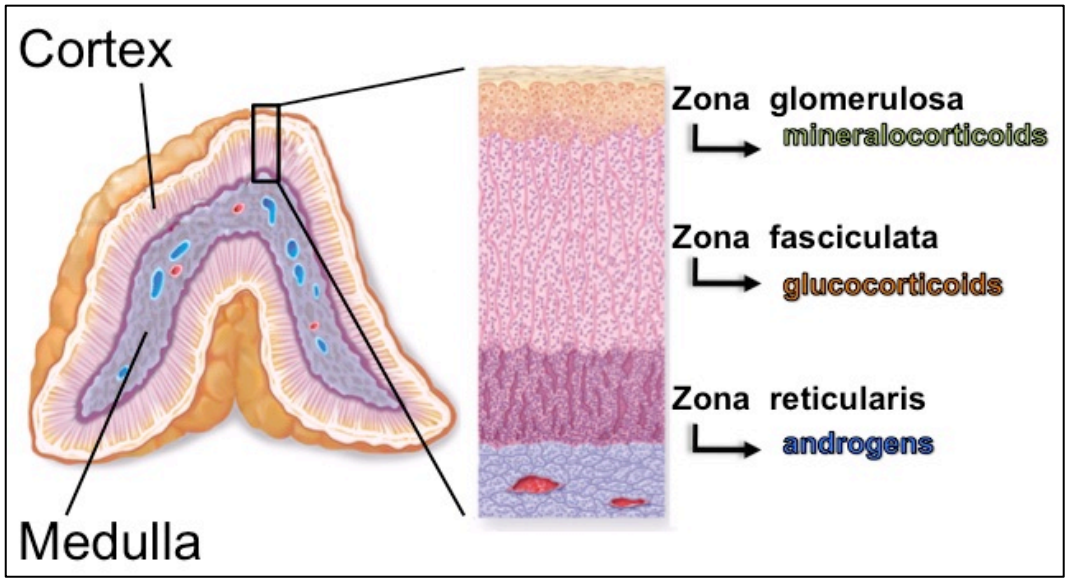

Figure 1: Schematic depiction of the structure (left) of the adrenal gland and the zonation of the adrenal cortex (right).

The adrenal medulla is the body's main source of secreted catecholamines, namely epinephrine (adrenaline) and nor-epinephrine (noradrenaline). It consists of so-called chromaffin cells, a name derived from the characteristic brown staining

when exposed to chromic acid salts. Catecholamines are derived from the amino acid tyrosine, which is subsequently converted to epinephrines via different enzymes with tyrosine hydroxylase representing the rate-limiting step converting tyrosine to dihydroxyphenylalanine (DOPA) (Pacak et al., 2008). The acute release of these hormones activates immediate physical reactions in preparation for a muscular action (also called “flight-or-fight response”), first described by Walter Bradford Cannon (Cannon, 1915). The medulla is exposed to high concentrations of glucocorticoids produced in the adrenal cortex, and it has been shown that cortisol induces the enzyme phenylethanolamine-N-methyltransferase, which converts norepinephrine to epinephrine (Wurtman and Pohorecky, 1971). This observation revealed the existence of an intriguing cross-talk between these two morphologically and embryologically distinct compartments of the adrenal gland.

The adrenal cortex is devoted to the production of steroid hormones. Within the adrenal cortex, three concentric cellular layers (or zones) can be histo-morphologically distinguished: the outer zona glomerulosa (ZG), the zona fasciculata (ZF) and, adjacent to the adrenal medulla, the zona reticularis (ZR) (**Figure 1**). The morphological differences of these three zones reflect their molecular endowment as their cells express a specialized set of steroidogenic enzymes generating the three major subclasses of steroid hormones. These are mineralocorticoids produced in the ZG, glucocorticoids synthesized in the ZF and sex steroids generated in the ZR (**Figure 1**).

The actions of the three subtypes of steroid hormones are complex. In brief, mineralocorticoids regulate salt and water balance; glucocorticoids are essential for glucose metabolism and stress response, but also have various immune-modulatory functions. Sex steroids, which are also produced in the gonads of the foetus and after

birth from puberty onwards, promote gender-specific sexual characteristics, including prenatal sexual differentiation, postnatal sexual maturation and fertility.

Classically, they act via intracellular receptors that initiate the translational machinery in the nucleus, thereby affecting the transcription of various target genes (see section 1.1.5).

1.1.2. Principles of steroid hormone biosynthesis and action

All steroid hormones are derived from cholesterol and have a closely related structure in the form of the cyclopentanophenanthrene 4-ring. It comprises three cyclohexane rings (A, B and C) and a cyclopentane ring (D) (**Figure 2**).

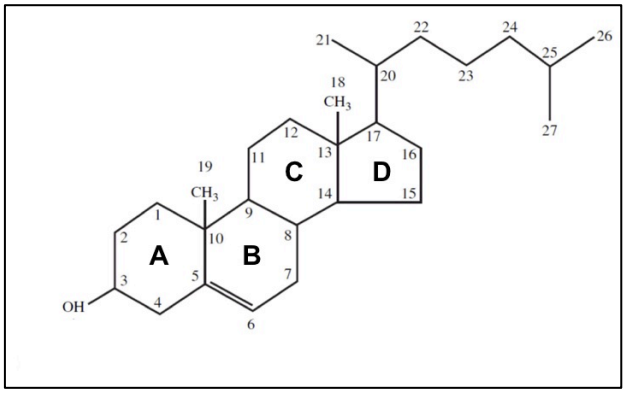

Figure 2: Conventional nomenclature of steroids shown by the example of cholesterol, the precursor for all steroid hormones. The basic structure is a cyclopentanophenanthrene 4-ring. *Letters (A-D)* refer to the rings; the carbon atoms are indicated by *numbers*.

The differences in the various subclasses of steroid hormones and its precursors are determined 1) by the total number of carbon atoms and 2) the functional groups attached to the four-ring core and 3) the oxidation state of the rings. A lot of effort has been made in the past to correlate steroid structure with their physiological activities; however, when the steroid hormone receptors were cloned and characterized, it became clear that not the chemical structure of a steroid defines its activity, but rather its affinity to a certain receptor (Miller and Auchus, 2011).

Two major groups of enzymes are involved in steroid biosynthesis: cytochrome P450s (CYPs) and hydroxysteroid dehydrogenases (HSDs). The direction of the conversion is almost always unidirectional for the CYPs; hence, in biochemical terms, an accumulation of a product does not reverse the flux towards the precursors. However, HSD reactions are mechanistically reversible and under certain conditions can run in either direction *in vitro*; however, *in vivo*, each HSD drives the reaction predominantly either towards the direction of reduction or oxidation (Agarwal and Auchus, 2005).

The human genome codes for 57 cytochrome P450s, six of them are involved in human steroidogenesis (**Table 1**); the majority of non-steroidogenic type 2 CYPs are hepatic enzymes involved in drug metabolism and detoxification of xenobiotics. The most widely accepted nomenclature is to designate the gene name (and the enzyme itself) with the abbreviation CYP; this is followed by a number indicating the gene family, then a capital letter for the subfamily and another number indicating the individual gene (Nelson et al., 1996). Italicizing the name of the CYP (i.e. *CYP17A1*) refers to the gene; otherwise it refers to the enzyme. The current nomenclature of the CYPs is under constant revision and updates are available on the P450 cytochrome homepage (http://drnelson.uthsc.edu/CytochromeP450.html).

Table 1: Molecular characteristics and functions of cytochrome P450 (CYP) involved in human steroidogenesis.

CYP enzyme	Type	mRNA size (Kb)	Protein size (aa)	Substrate	Function
CYP11A1	1	2.0	521	Cholesterol	Synthesis of pregnenolone
CYP11B1	1	4.2	574	11-deoxycortisol, 11-deoxycorticosterone	Cortisol synthesis
CYP11B2	1	4.2	503	11-deoxycorticosterone	Aldosterone synthesis
CYP17A1	2	1.9	508	(17OH-)progesterone, (17OH-)pregnenolone	Biosynthesis of GC and sex steroid precursors
CYP21A2	2	2.0	494	(17OH-)progesterone	Biosynthesis of GC and MC precursors
CYP19A1	2	1.5-4.5	503	Androstenedione, Testosterone	Generation of oestrogens

The common features of all CYPs are a single haeme group and a size of about 500 amino acids, ranging from 45 to 60 kDa. The name cytochrome “P450” derives from the chemical properties that absorb light at 450nm when in the reduced state. CYPs use their haeme centre to activate molecular bound oxygen and to transfer electrons derived from reduced nicotinamide adenine dinucleotide phosphate (NADPH). A common catalytic cycle of CYPs has been elucidated in detail on the molecular level (Meunier et al., 2004), but the exact catalytic reactions carried out by the CYP enzyme can vary and largely depends on the substrate and on the enzyme itself.

The diversity of catalytic reactions and also the structural properties are much more diverse for the hydroxysteroid dehydrogenases (HSDs). In contrast to CYPs, they do not contain haeme groups, but they do employ NADPH or NADP+ to oxidize or reduce a steroid via hybrid transfer mechanisms (Agarwal and Auchus, 2005; Miller and Auchus, 2011). Their molecular masses range from 35 to 45 kDa (Miller and Auchus, 2011). Based on their structure, HSDs can be divided in two sub-

groups: the short-chain dehydrogenases/reductases (SDRs) and the aldo-keto reductases (AKRs). **Table 2** provides an overview of the HSDs that are involved in human steroidogenesis.

Table 2: Overview and central functional properties of key hydroxysteroid dehydrogenase (HSD) enzymes involved in steroid metabolism. For steroid abbreviations please refer to the abbreviation table at the beginning of the thesis. Adapted from (Miller and Auchus, 2011).

HSD enzyme	Co-factor	Preferred direction	Tissue expression (key tissues)	Function
HSD3B1	NADPH	Reductase	Placenta, liver, skin; various tissues	Both: Preg → Prog, 17Preg → 17OHP, DHEA → d4dione
HSD3B2	NADPH	Reductase	Adrenal cortex, gonads, placenta	
HSD11B1	NADPH	Reductase	Liver, adipose, muscle	E → F
HSD11B2	NAD+	Oxidase	Kidney, colon, salivary glands	F → E
HSD17B1	NADPH	Reductase	Placenta, ovary	E1 → E2
HSD17B2	NAD+	Oxidase	Placenta, endometrium	E2 → E1; T → d4dione; DHEA → 5-diol
HSD17B3	NADPH	Reductase	Testis	d4dione → T; 5α-Androstane-3α,17βdiol → DHT
HSD17B6 (RODH)	NAD+	Oxidase	Testes, liver, adrenal cortex	androstanediol → DHT
HSD17B7/12	NADPH	Reductase	multiple	E1 → E2
AKR1C3 (HSD17B5)	NADPH	Reductase	Ovary; multiple tissues (foetal) adrenals	d4dione → T
AKR1C4				
SRD5A1	NADPH	Reductase	Various tissues: liver, intestine, bone, muscle, brain	GC inactivation, Testosterone → DHT
SRD5A2	NADPH	Reductase	Prostate, testicles, skin	Testosterone → DHT

Most HSDs catalyse the formation of a ketone from a secondary alcohol (or *vice versa*); the human 5α-reductases (SRD5A), which are grouped within the HSD family for convenience, reduce an olefinic carbon-carbon double bond to the saturated state (Miller and Auchus, 2011). The two human 3β-hydroxysteroid dehydrogenases (HSD3Bs) exhibit two catalytic reactions as the dehydrogenation is accompanied by

the isomerization of a carbon-carbon double bond from carbons 4 and 5 (‘delta 5’) to carbon 5 and 6 (‘delta 4’). In contrast to the CYP enzymes, each of the reactions catalyzed by HSDs can be carried out by different isozymes, which are sometimes structurally very different.

1.1.3. Co-factor regulation of steroidogenesis

For all CYPs, electrons are derived from NADPH and their transfer, crucial for the enzyme’s catalytic activity, is facilitated by cofactors.

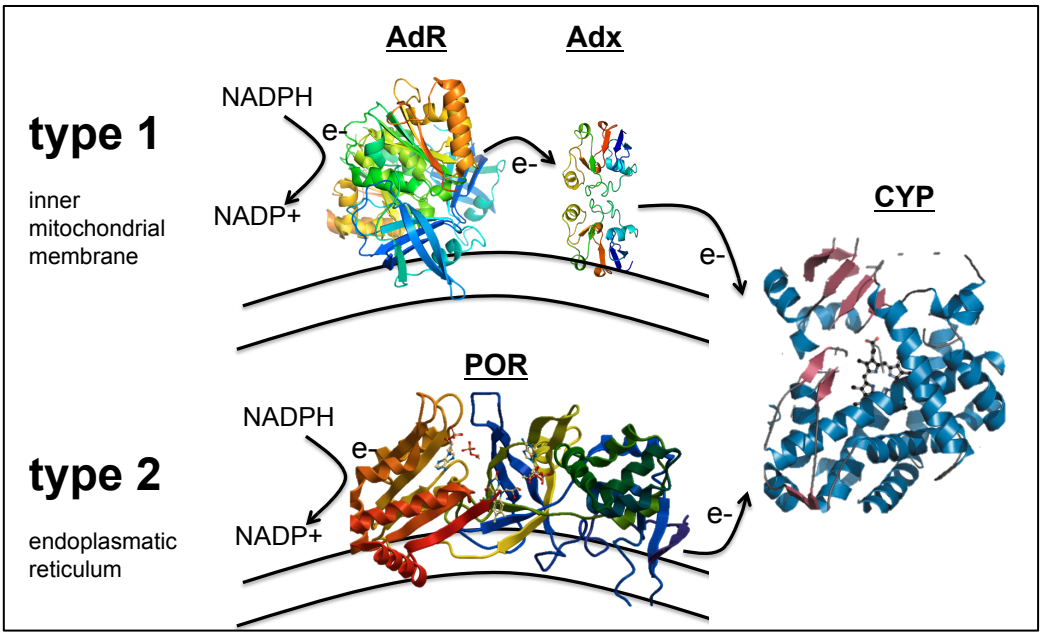

Figure 3: Schematic illustration of the two different routes of electron transfer for mitochondrial type 1 and microsomal type 2 CYPs. For type 1 enzymes, electrons are transferred via adrenodoxin reductase (AdR) and adrenodoxin (Adx). Type 2 enzymes receive electrons via the flavoprotein P450 oxidoreductase (POR). The crystal structures of the indicated proteins are shown in this figure: for the CYP enzyme, the crystal structure of CYP2D6 was chosen as a representative example. Data were retrieved from the pdb online protein databank; PDB IDs: FDR: 1CJC; FDX1: 3P1M; POR: 3QFS; CYP2D6: 2F9Q.

Depending on the redox-cofactor system, which also determines their sub-cellular localization, CYPs are further sub-classified into two main groups: seven human CYPs are expressed in the mitochondria and are termed “type 1” enzymes. They receive electrons via the flavoprotein adrenodoxin (Adx; also ferredoxin), which is in turn reduced by its co-enzyme adrenodoxin reductase (AdR; also ferredoxin

reductase); the other 50 “type 2” CYPs are found in the endoplasmic reticulum (ER) and electron transfer from NADPH is facilitated by the single flavoprotein P450 oxidoreductase (POR) (**Figure 3**).

1.1.3.1. Adrenodoxin (Adx) and Adrenodoxin reductase (AdR)

Adrenodoxin (Adx) and adrenodoxin reductase (AdR) are expressed in the mitochondrial matrix and inner mitochondrial membrane (IMM) of various tissues, in particular steroidogenic cells, where they support electron flux to type 1 CYPs.

Adx is a soluble iron-sulfur protein that is only loosely attached to the IMM and mainly resides freely within the mitochondrial matrix. AdR is a flavoprotein attached to the IMM containing a flavin adenine dinucleotide (FAD) in its core domain and binds NADPH at its N-terminal domain, which interacts with the FAD domain when ’activated’ by NADPH to allow electron transfer to the FAD. The FAD domain forms a positively charged ‘cleft’ docking to the negatively charged surface of the interaction domain of Adx, which is in proximity to the Fe_2/S_2 core of the core domain (Ziegler et al., 1999). There is evidence that the same surface area that docks to the AdR protein also interacts with the positively charged co-factor binding site of the CYPs (Vickery, 1997).

1.1.3.2. P450 oxidoreductase (POR)

POR is a membrane-bound flavoprotein that supports electron transfer from NADPH to all microsomal (type 2) CYPs. Only three CYPs are involved in steroidogenesis, namely CYP17A1, CYP21A2 and CYP19A1 (see **Table 1**).

The wide tissue distribution of the POR protein indicates that it supports many biological processes, including electron transfer to all major drug-metabolising CYP enzymes, and it has been shown that POR not only supports electron transfer to

CYPs, but also to other redox systems involved in crucial metabolic processes like squalene monooxygenase (Ono and Bloch, 1975), haeme oxygenase (Wilks et al., 1995), fatty acid elongase (Ilan et al., 1981) and post-translational modification of proteins involved in the hedgehog signalling pathway (Aguilar et al., 2009).

The structural and biochemical properties of POR have been studied extensively based on the rat crystal structure, which shares 94% amino acid identity with the human protein (Wang et al., 1997), but also the human POR protein has recently been crystallised (Xia et al., 2011). POR contains two derivatives of the nucleic acid riboflavin: a flavin adenine dinucleotide (FAD) and a flavin mononucleotide (FMN), which are located in major domains forming the two main lobes of the POR protein responsible for electron transfer. The N-terminal FMN domain is flexibly connected with the FAD domain by several α-helices forming the connecting domain, which brings the two riboflavin domains together once electrons are received by the C-terminal NADPH binding domain and transferred to the FAD moiety. A further 25 amino acid hinge region loosely connects the FMN with the connecting domain, suggesting a high flexibility in between these domains. NMR and x-ray crystallographic studies revealed drastic conformational changes during intra-molecular electron transfer: once electrons are received by the FAD domain, the two lobes (FAD and FMN domains) come close together, like wings of a butterfly, and the electrons are passed on from the FAD to the FMN domain (Ellis et al., 2009; Miller and Auchus, 2011). Subsequently, negative surface charges at the FAD domain ‘dock’ POR to positively charged basic residues of the co-factor binding site of the CYP protein to bring the FMN domain in close proximity to the CYP haeme centre, thereby passing on the electrons (Miller and Auchus, 2011).

The POR gene is located on chromosome 7q11.2 and consists of 16 exons, of which the first one is not transcribed. The coding region is 2043 base pairs long and encodes for the 681 amino acid protein. The human POR gene is highly polymorphic and sequencing analysis in over 800 subjects from different ethnicities indicate a variety of sequence variants, some of which have some impact on CYP-mediated activities and cytochrome c reduction and NADPH oxidation (Huang et al., 2008). There does not seem to be a hotspot for polymorphisms or mutations within the gene structure of *POR* (Huang et al., 2008; Krone et al., 2007a; 2012).

1.1.3.3. Cytochrome b5 (CYB5A)

Cytochrome b5 (CYB5A) is a small (~ 16kDa) membrane-bound protein that contains a haeme molecule as its prosthetic group. A soluble isoform lacking the C-terminal membrane anchor is expressed in erythrocytes, the full protein containing the transmembrane domain and the haeme-domain is expressed in various tissues, but with high levels in liver, adrenals and gonads (Dharia et al., 2004; Suzuki et al., 2000).

CYB5A interacts with POR and CYP17A1 to further support electron flux from NADPH, in particular the higher demand for electrons required for its 17,20 lyase activity (see also section 1.1.8.1). However, the redox-potential between POR and CYB5A is unfavourable and hence makes it unlikely that CYB5A receives electrons in the context of CYP reduction, although its prosthetic group would be able to carry electrons. In addition, *in vitro* studies show that truncated CYB5A protein lacking the prosthetic group (apo-b5) stimulates the 17,20 lyase activity of CYP17A1 equally to holo-b5, suggesting that this co-factor supports allosteric interaction between POR and CYP17A1, rather than conducting the flux of electrons directly (Auchus et al., 1998).

In a broader context, CYB5A has been shown to support other physiological processes like fatty acid desaturases (Guillou et al., 2004) and other P450 monooxigenases (Schenkman and Jansson, 2003), including hepatic CYPs involved in steroid metabolism and drug detoxification (Yamazaki et al., 1996a; 1996b). Recent *in vitro* studies also suggest additional roles of CYB5A in steroidogenesis, in particular by enhancing HSD3B activity leading to an increase of androstenedione production (Goosen et al., 2013; 2011; Storbeck et al., 2013).

1.1.4. The first step in human steroidogenesis

Cholesterol is the substrate for steroid hormones. Prior to the various catalytic reactions generating active steroid sub-class molecules, hydrophobic cholesterol needs to meet its first steroidogenic enzyme CYP11A1 (also termed 'cytochrome P450 side chain cleavage', P450scc) at the inner mitochondrial membrane (IMM).

The adrenal cortex is able to produce cholesterol *de novo* from acetate, but the majority of the cholesterol that feeds into steroid biosynthesis comes from low density lipoproteins (LDL) derived from dietary cholesterol (Gwynne and Strauss, 1982). The regulation of the intracellular cholesterol-bioavailability is complex, but largely orchestrated by sterol response-element binding proteins (SREBPs), a family of transcription factors regulating transcription of target genes involved in cholesterol biosynthesis (Horton et al., 2002). The steroidogenic acute regulatory protein (StAR) itself is responsible for carrying cholesterol from the outer (OMM) to the inner mitochondrial membrane (IMM). The exact molecular mechanism of how StAR promotes steroidogenesis and cholesterol transport are not fully elucidated; further interactions with other proteins are required for StAR function at the OMM (Liu et al., 2006; Rone et al., 2009). StAR gene transcription and its activation through phosphorylation is rapidly induced by pituitary ACTH (Stocco et al., 2005), allowing a

fast flux of cholesterol molecules from the cytosol to the IMM, where it serves as the substrate for the first and rate-limiting P450 enzyme, CYP11A1 (Stocco and Sodeman, 1991).

The biosynthesis of pregnenolone from cholesterol at the IMM is achieved by three subsequent and distinct catalytic reactions, all carried out by the one enzyme CYP11A1: (1) hydroxylation at position 22, (2) 20-hydroxylation of 22(R)-hydrocholesterol and (3) the side chain cleavage reaction via oxidative scission of the C20-22 bond of 20(R),-22(R)-dihydroxycholesterol yielding pregnenolone. Each catalytic reaction requires two electrons, provided by NADPH via the electron donors Adx and AdR (**Figure 3**). As CYP11A1 is the key-initiating and rate-limiting step in human steroidogenesis, its expression marks cells or tissues as steroidogenic (Miller and Auchus, 2011). CYP11A1 expression is regulated by ACTH/cAMP in the adrenal ZF/ZR, but also in the testis and the ovary (John et al., 1986). Intracellar calcium and protein kinase C (PKC) regulate CYP11A1 expression in the ZG (Barrett et al., 1989). In addition, adrenal and gonadal steroidogenic tissues require the presence of the transcription factor SF1 (steroidogenic factor 1) for CYP11A1 expression (Parker and Schimmer, 1997).

Once synthesized, hydrophobic pregnenolone leaves the mitochondrion without any active transport mechanism or carrier proteins serving as a substrate for further conversion in steroidogenic pathways. The fate of the pregnenolone molecule solely depends on the endowment of the respective adrenocortical cell type with steroidogenic enzymes, yielding mineralocorticoids, glucocorticoids or sex steroids (**Figure 4**).

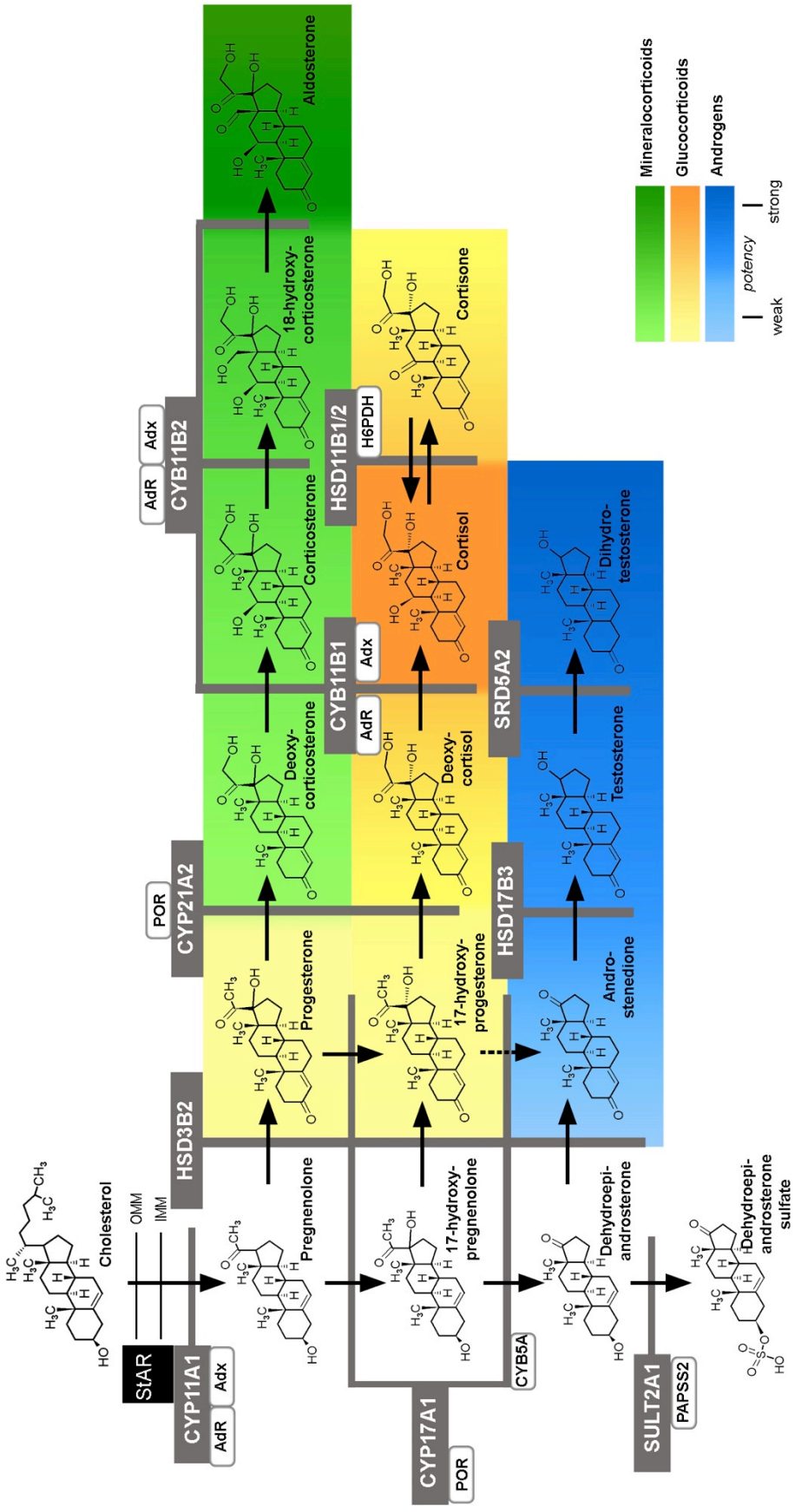
Mineralocorticoids
Glucocorticoids
Androgens
potency
weak
strong
Cholesterol
OMM
IMM
StAR
CYP11A1
AdR
Adx
Pregnenolone
HSD3B2
Progesterone
17-hydroxy-pregnenolone
17-hydroxy-progesterone
CYP17A1
POR
CYB5A
Dehydroepi-androsterone
SULT2A1
PAPSS2
Dehydroepi-androsterone sulfate
CYP21A2
Deoxy-corticosterone
Deoxy-cortisol
Androstenedione
HSD17B3
SRD5A2
Testosterone
Dihydro-testosterone
CYB11B1
Corticosterone
Cortisol
HSD11B1/2
H6PDH
Cortisone
CYB11B2
18-hydroxy-corticosterone
Aldosterone

Figure 4 (previous page): Overview of human adrenal steroidogenesis with key intermediate metabolites and steroidogenic enzymes involved. The three subclasses of steroids are colour-coded with green for MCs, yellow/orange for GCs and blue for androgens; the intensity of the colour indicates the affinity of the steroid to its receptor. The steroidogenic enzymes are shown in grey with co-factors in white. Arrows indicate the direction of the enzymatic reactions; dashed arrows indicate that the efficiency of the reaction is weak. POR: P450 oxidoreductase; Adx: adrenodoxin; AdR: Adrenodoxin reductase; H6PDH: Hexo-6-phosphate dehydrogenase; PAPSS2: 3'-phosphoadenosine-5'-phosphosulfate (PAPS) synthase 2.

1.1.5. Principles of steroid hormone action

Steroid hormones exert their effects mainly via targeting and activating intracellular receptors that act as ligand-dependent transcription factors initiating gene transcription. The glucocorticoid receptor (GR), the mineralocorticoid receptor (MR), the androgen receptor (AR) and the oestrogen receptor (ER) belong to the subfamily 3 of the large family of nuclear receptors (Lu et al., 2006).

The molecular composition and the mechanism of action of nuclear receptors are similar and based on the arrangement of five distinct domains with different functions (**Figure 5**): the sequence of the N-terminal domain is the most variable one amongst the different nuclear receptors and contains the activation-function 1 (AF1) site initiating gene transcription independent of ligand binding. The sequence of the DNA-binding domain (DBD) is highly conserved amongst various subfamilies of nuclear receptors and contains, as a typical molecular feature, two zinc-ions each coordinated by four cysteine residues. The DBD recognizes hormone-responsive elements (HREs) within the genome, binds to DNA as homodimers and initiates gene transcription. A hinge region connects the DBD with the ligand-binding domain (LBD). A unique arrangement of eleven α-helices and four small β-strands form a highly selective ligand-binding pocket at its core that recognizes the steroid ligand. This selectivity is assured by (1) unique surface charges due to a 'hydrogen network' within the binding pocket, (2) the shape of the topology inside the binding pocket and (3) the relative position of the binding pocket within the LBD (Lu et al., 2006). The C-

terminal domain is highly variable in sequence amongst the various nuclear receptors.

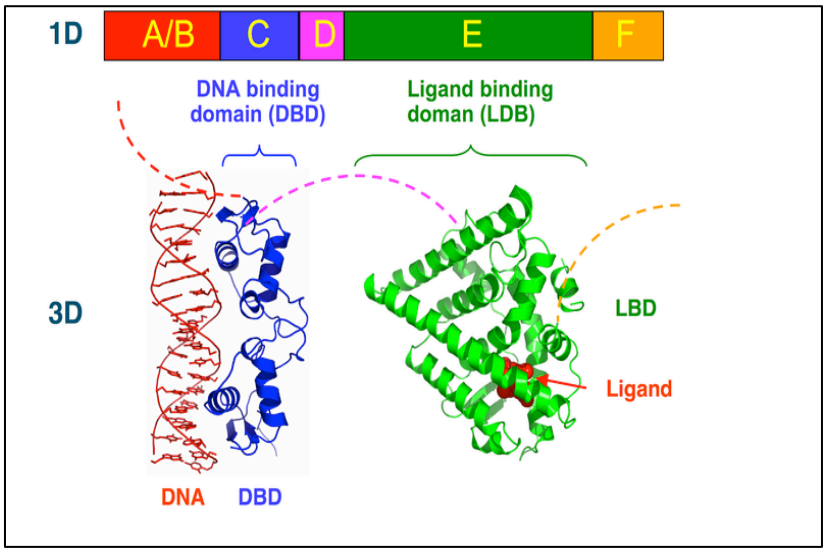

Figure 5: Schematic representation of the structure of nuclear receptors, including steroid hormone receptors from the one-dimensional (1D, top) and three-dimensional (3D, bottom) perspectives. The crystal structures of the DNA binding domain (DBD) and ligand binding domain (LBD) are derived from the oestrogen receptor protein. To simplify illustration of the functional domains, the structures of the N-terminal domain (A/B), the hinge region (D) and the C-terminal domain (F) are not shown, but they are represented as red, purple and yellow dashed lines, respectively. Source: Wikipedia

Steroid hormone receptors also have a similar mechanism of activation. If not activated by the steroid ligand, they are found in the cytosol bound in complexes with heat shock proteins (HSPs); these are chaperones preventing the receptor from endosomal degradation and holding them in a high affinity conformation. Upon ligand binding, the receptor dissociates from the HSPs, homo-dimerizes and translocates into the nucleus of the cell where it binds via its DBD to HREs of the genomic DNA initiating gene transcription. The transport of the receptor from the cytosol to the nucleus is facilitated by active transport mechanisms and mediated by nuclear targeting sequences usually found in the hinge region of the receptor (**Figure 5**) (Lu et al., 2006).

A number of proteins have been identified that modulate gene transcription of steroid hormone receptors and function as either co-activators or co-suppressors.

Classically, co-regulators interact with the translational machinery; but in addition they also exert many other activities beyond the interaction with the translational machinery such as mRNA translation and transport and post-translational modification of the synthesized protein (Lonard and O'Malley, 2006).

Beside the genomic effects of steroid hormones initiating gene transcription, which usually takes minutes to hours, they can also exert more rapid effects occurring within seconds independently of gene transcription. These non-genomic effects of steroid hormones are mediated via several signalling pathways ranging from the activation of G-protein coupled receptors (GPCRs) to the activation of distinct kinases like mitogen activated protein kinase (MAPK), protein kinase A (PKA) and protein kinase C (PKC) (Hammes and Levin, 2007). These non-genomic effects of steroid hormones are well documented for the rapid effects of oestrogens on breast cancer proliferation and in the cardiovascular system (Simoncini et al., 2000; Márquez and Pietras, 2001), of androgen on cell proliferation in the prostate (Kampa et al., 2006), and for glucocorticoids on the suppression of ACTH release (Iwasaki et al., 1997).

1.1.6. Mineralocorticoids (MC)

1.1.6.1. MC biosynthesis

The site of mineralocorticoid biosynthesis is the ZG of the adrenal cortex, uniquely expressing the enzyme systems required to generate the most potent mineralocorticoid, aldosterone, from pregnenolone (**Figure 1** and **Figure 4**).

Pregnenolone can either be hydroxylated to 17α-hydroxy-pregnenolone (17Preg) by the 17α-hydroxylase activity of CYP17A1 or converted to progesterone by HSD3B2. Although the substrate binding affinity of CYP17A1 for pregnenolone is

much higher for CYP17A1 than for HSD3B2, CYP17A1 is virtually not expressed in the ZG; in contrast HSD3B2 is strongly expressed in ZG cells throughout all age groups (Suzuki et al., 2000). HSD3B2 has two catalytic reactions, supported by the two-fold oxidation of a single NADPH molecule: (1) with its dehydrogenase activity it oxidizes the hydroxyl group at carbon 3 to a keto group and (2) subsequently with its Δ4→Δ5 isomerase activity, HSD3B2 isomerases the carbon-carbon double bond from the position between C5/6 (‘Δ5’) to C4/5 (‘Δ4’). HSD3B2 has similar affinities to all Δ4 steroids, i.e. pregnenolone, 17-Preg and DHEA (Miller and Auchus, 2011).

Progesterone generated by HSD3B2 is subsequently hydroxylated by CYP21A2 to form 11-deoxycorticosterone (DOC), a mineralocorticoid intermediate able to bind and activate the mineralocorticoid receptor. Finally, the enzyme aldosterone synthase, CYP11B2, produces aldosterone from DOC in the mitochondrion in three consecutive catalytic reactions: (1) 11β-hydroxylation of DOC yielding corticosterone, (2) 18-hydroxylation of corticosterone to form 18-hydroxy corticosterone and finally (3) the 18-methyl oxidation of corticosterone generating aldosterone (Miller and Auchus, 2011). CYP11B2 is predominantly expressed in the adrenal ZG and is closely related to its isozyme CYP11B1, which is highly expressed in the ZF generating cortisol from 11-deoxycortisol. CYP11B1, which is not expressed in the ZG, is also able to perform the first two catalytic reactions of CYP11B2, however, the 18-methyl oxidation generating aldosterone is unique to the type 2 isozyme.

In essence, the absence of CYP17A1 17α-hydroxylase activity and the presence of CYP11B2 and HSD3B2 are the key molecular characteristics of the adrenal ZG and essential to produce mineralocorticoids.

1.1.6.2. MC regulation

MCs are the key regulators of the body's salt and water balance and blood pressure. As the plasma levels of most endocrine hormones are regulated via negative feedback mechanisms, so to the production and excretion of MCs from the adrenal ZG are inhibited by low intravascular potassium, high sodium concentrations and high blood pressure. A cascade of proteases forming the renin-angiotensin-aldosterone system (RAAS) mediates this feedback cross-talk between the kidneys and the ZG of the adrenal cortex. Specialized cells within the glomeruli of the kidneys, as part of the juxtaglomerular apparatus, secrete the protease renin in response to a decrease of the glomerular filtration rate. Renin converts angiotensin to the inactive peptide-hormone angiotensin I. Secondly, the angiotensin converting enzyme (ACE), mainly expressed in the vascular endothelium of the lungs and kidneys, converts the deca-peptide angiotensin I to the active octa-peptide angiotensin II, which acts as a strong inducer of *CYP11B2* expression in the ZG of the adrenal cortex. Beside its effects on the adrenal cortex, angiotensin II acts a potent vasoconstrictor targeting the smooth muscles of arteries thereby increasing arterial blood pressure. MC synthesis and secretion is also directly stimulated by high potassium levels and inhibited via direct and indirect effects by the atrial natriuretic peptide (ANP) (Ganguly, 1992). To a lesser extend, the ZG also responds to pituitary ACTH, the key stimulus for glucocorticoid synthesis in the ZF (Honda, 1976).

1.1.6.3. MC action

Aldosterone is the principal mineralocorticoid as it has the highest affinity to the mineralocorticoid receptor (MR), a classical intracellular steroid hormone receptor and part of the subfamily 3 of nuclear receptors (see section 1.1.5 and **Figure 5**). A MC-responsive cell is characterized by the expression of the MR. However, as the

MR is highly promiscuous with cortisol, the concomitant expression of the HSD11B2 enzyme is crucial to 'protect' the MR from cortisol as HSD11B2 converts active cortisol to inactive cortisone (Kornel, 1994).

Cells that express the MR and HSD11B2 are found in the epithelium of distal tubules and collecting ducts of the kidneys, where MCs play a main role in the regulation of salt and water homeostasis; the MR is also expressed in other epithelial cells like sweat and salivary glands (ductal cells) and in enterocytes of the distal colon. In addition, non-epithelial cells of the heart muscle, central nervous system (hippocampus) (Meijer, 2002), adipose tissue (Caprio et al., 2007) and blood vessels (Lombès et al., 1992) express the MR. Aldosterone enters freely into the cells and binds to the LBD of the receptor. Once activated through ligand binding, the MR translocates as a homodimer into the nucleus and initiates gene transcription by recognizing HREs, thus executing its classic genomic effects (see section 1.1.5). Similar to other steroid hormone receptors, a wide range of co-regulators have been identified to modulate gene transcription or MR-induced protein synthesis on the post-transcriptional level (Yang and Fuller, 2012). Their main physiological sites of action are the kidneys where they initiate transcription of genes involved in sodium reabsorption and potassium secretion.

1.1.7. Glucocorticoids (GCs)

1.1.7.1. GC biosynthesis

The adrenal zona fasciculata (ZF) is the site of glucocorticoid (GC) synthesis. Cortisol is the principal product of this pathway having the highest affinity for the glucocorticoid receptor (GR). 17α-progesterone (17OHP) is the immediate precursor metabolite for GC synthesis and substrate of the enzyme CYP21A2. CYP17A1 17α-

hydroxylase activity generates 17OHP directly from progesterone; it also catalyses the 17α-hydroxylation of pregnenolone yielding 17α-hydroxypregnenolone (17Preg), which serves as a substrate for the HSD3B2 enzyme to generate 17OHP. Hence, the presence of CYP17A1 17α-hydroxylase activity in the ZF is the rate-limiting step in the generation of GC precursors and biochemically distinguishes the ZF from the MC-producing ZG, which lacks CYP17A1. Two further catalytic reactions are required to produce cortisol from 17OHP: CYP21A2 catalyses hydroxylation of carbon 21, yielding 11-deoxycortisol, which is then hydroxylated at carbon 11 by CYP11B1 to generate cortisol.

1.1.7.2. GC regulation and metabolism

Adrenal GC secretion is regulated by the hypothalamic-pituitary-adrenal (HPA) axis (**Figure 6**). The hypothalamus is generally considered as a connector between the central nervous and the endocrine systems, as it regulates the secretion of various stimulating hormones in the pituitary gland. The paraventricular nucleus of the hypothalamus secretes upon central nervous influences and regulatory feedback mechanisms the corticotropin-releasing hormone (CRH) into the portal-vein system connecting the hypothalamus with the anterior lobe of the pituitary. Here, it stimulates corticotrophic cells and the transcription of the *POMC* gene coding for pre-pro-opiomelanocortin (pre-POMC), a 285-amino acid peptide. POMC has multiple cleavage sites and undergoes various post-translational processes to generate a variety of biologically active substances, including melanocyte stimulating hormone (α/β-MSH), β-endorphin and the adrenocorticotrophic hormone ACTH (Pritchard et al., 2002). ACTH binds to its melanocortin-2 receptor (MC2R), a G-protein-coupled receptor predominantly expressed in the adrenal ZF and ZR. Its activation induces cAMP-mediated expression of genes that facilitate cholesterol import into the

mitochondrion, where it serves as substrate for CYP11A1 generating pregnenolone, the first step in human steroidogenesis (see 1.1.3.1). Beside the rapid increase of cholesterol influx, ACTH also induces gene expression of various steroidogenic enzymes, including *CYP11A1*, *CYP21A2* and *CYP11B1*. Both actions ultimately lead to the initiation of adrenal glucocorticoid synthesis (Sewer and Waterman, 2003).

The release of hypothalamic CRH and pituitary ACTH/POMC is regulated by cortisol itself via negative feedback (see **Figure 6**). However, a variety of other stimuli alter HPA drive and cortisol secretion, which follows a diurnal rhythm with higher levels during late night/early morning and a nadir around midnight. Beside the circadian variation of cortisol levels, a variety of other stimuli alter adrenal GC secretion, such as stress (both physical and emotional), mood, appetite/food intake, infection/pro-inflammatory cytokines. Depending on these factors, the daily GC secretion rates can vary drastically and increase more than five-fold above the normal daily production rates of 8-12 mg for cortisol (Esteban and Yergey, 1990; Kerrigan et al., 1993; Salem et al., 1994).

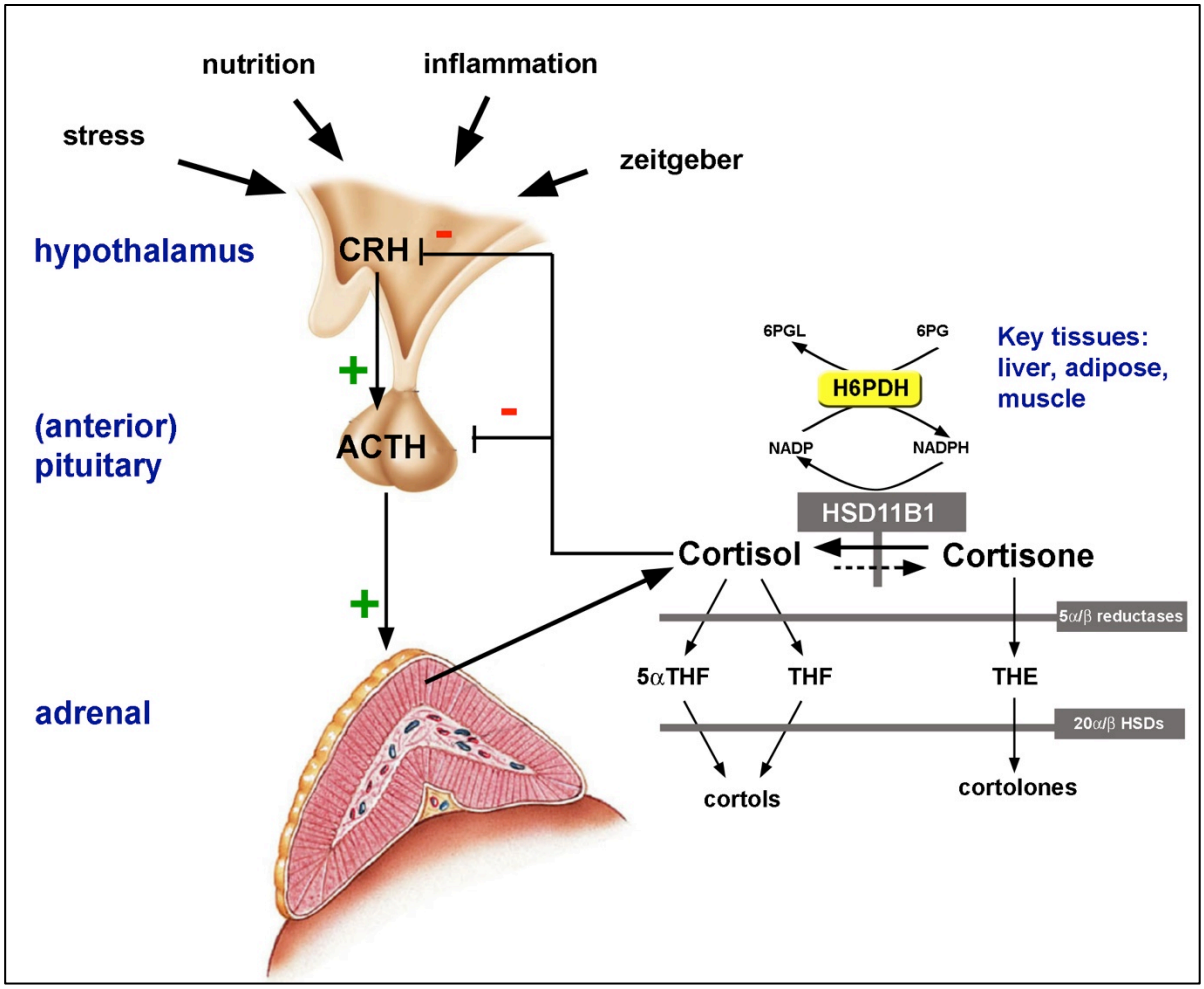

Figure 6: The hypothalamic-pituitary-adrenal (HPA) axis and peripheral cortisol (re)generation by HSD11B1.

While the HPA axis regulates the secretion of cortisol from the ZF, the availability of cortisol in peripheral tissues is modulated by the enzyme 11-β hydroxysteroid dehydrogenase type 1 (HSD11B1) regenerating active cortisol from inactive cortisone (Agarwal et al., 1989; Tomlinson et al., 2004). In fact, this enzyme, in contrast to its type 2 isoform, acts in two directions, either as a reductase to regenerate cortisol, or as an oxidase to 'inactivate' cortisol to cortisone. However, the predominant direction is the reduction of cortisone, and *in vitro* and *in vivo* studies revealed that this activity depends on the availability of NADPH, which is provided by its co-enzyme hexose-6-phosphate dehydrogenase (H6PDH) (Draper et al., 2003). H6PDH, expressed in the lumen of the endoplasmic reticulum, generates NADPH

from $NADP^+$ utilizing glucose-6-phosphate (G6P) as a substrate, which is reduced to 6-phosphogluconate (6PGL).

Due to the fluctuating levels of cortisol and cortisone, it is not possible to assess changes of activity in the HSD11B1 enzyme with simple blood sample measurements. However, urinary steroid profiling of cortisol and cortisone metabolites provide an important diagnostic tool to assess the current bio-availability of cortisol and cortisone ultimately reflecting the *in vivo* activity of HSD11B1 (**Figure 6**): Both cortisol and cortisone are further metabolised by 5α- and 5β-reductases to their respective 5α- and 5β-reduced metabolites tetra-hydrocortisol (THF) and tetra-hydrocortisone (THE). Subsequently, hydroxylation at carbon 6 and 20 by 20α/β HSDs converts these tetrahydro-metabolites to cortols and cortolones, respectively (**Figure 6**).

In summary, the global activity of HSD11B1 determines the ratio of cortisol to cortisone. Hence, a change in the activity of this enzyme will affect this ratio with an immediate impact on the activity of the HPA axis (**Figure 6**).

1.1.7.3. GC action

The glucocorticoid receptor (GR) is expressed in virtually all cells in the body, underpinning the huge variety of effects GCs exert in normal human physiology and pathophysiology (Buckingham, 2006). From a mechanistic point of view, the GR functions in the same way as other nuclear receptors in the steroid receptor sub-family. Once activated by ligand binding, it classically homo-dimerises, translocates to the nucleus and initiates gene transcription targeted by the recognition of HREs by the DBD of the receptor. The HREs are typically inverted repeats of 'TGTTCT' motifs with three base pairs in between as a spacer ('AGAACA-XXX-TGTTCT'). Co-activators facilitate and regulate gene expression as described in section 1.1.5.

Uniquely, the GR can also act as a monomer and interact with other transcription factors to modulate gene expression, a process called transrepression. This mode of GR action leads to inhibition of target gene transcription and is responsible for the anti-inflammatory effects of GCs. Examples of pro-inflammatory proteins, that are transrepressed as a consequence of the monomeric activity of the GR, are the transcription factors AP-1 and NF-κB (Ray and Prefontaine, 1994).

The immediate actions of GCs can be roughly classified as metabolic and immunologic. The name 'glucocorticoid' was given based on early observations that they are able to increase blood sugar levels and are hence involved in glucose metabolism. GCs stimulate gluconeogenesis in liver and muscle by utilizing alternative, 'non-sugar' substrates like amino acids and glycerol. Simplified, the metabolic effects of GCs can be described as catabolic to increase the availability of energy substrates (carbohydrates) as required in stress or during severe illness/infection (Buckingham, 2006).

Other metabolic effects of GCs include thinning of the skin due to a reduction of collagen synthesis, resulting in increased vulnerability and prolonged wound healing. In bone, GCs suppress osteoblast activity resulting in reduction of bone mineralization due to the prevailing catabolic activity of osteoclasts.

GCs exert a range of immune-modulatory effects and have profound anti-inflammatory and immunosuppressive activities. They are able to reduce the amount of circulating neutrophils and effectively block the synthesis of the two main inflammatory cytokines, prostaglandins and leukotrienes. A schematic overview of the various effects of GCs in the human body is shown in **Figure 7**.

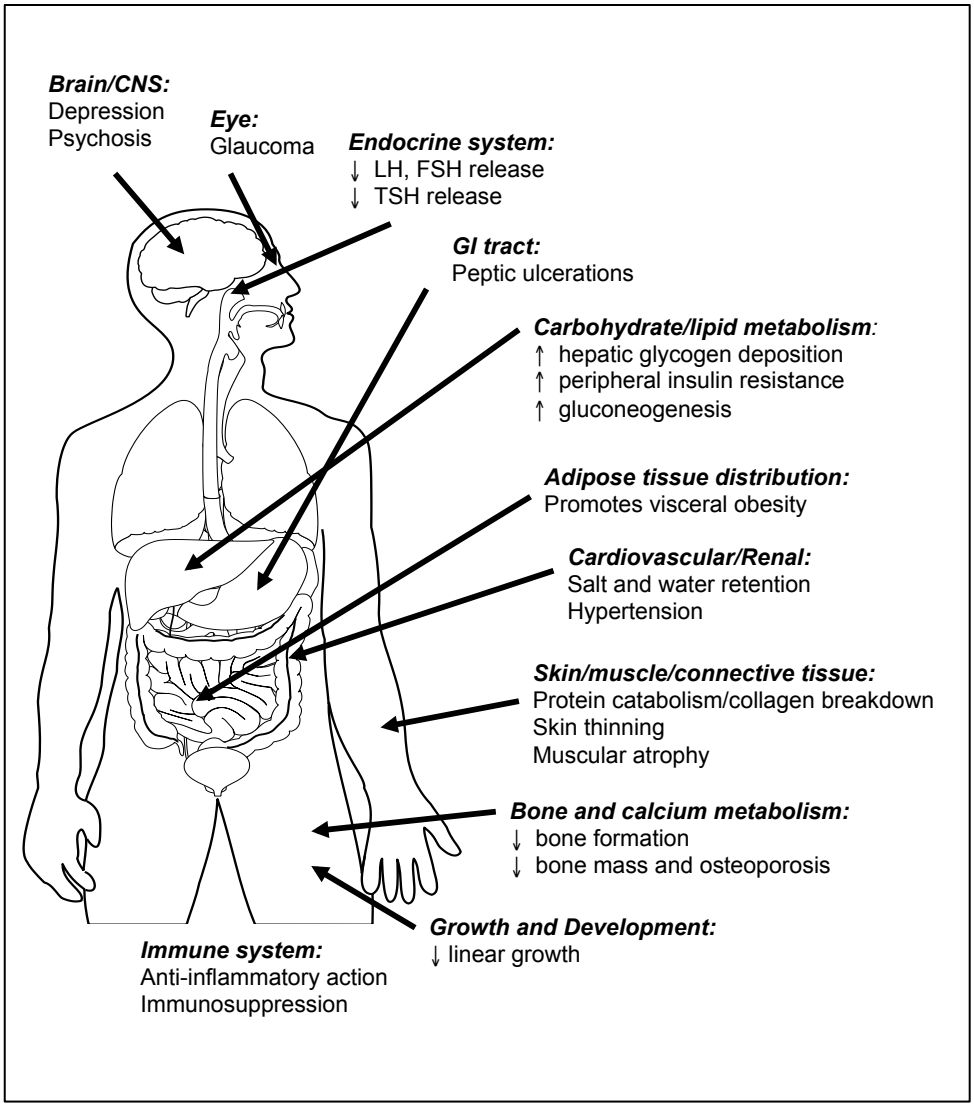

Figure 7: Overview of the key actions and clinical consequences of GCs in the human body. With kind permission from Paul Stewart.

1.1.8. Androgen precursors

1.1.8.1. Biosynthesis of DHEA

The principal precursor for all androgens in humans is dehydroepiandrosterone (DHEA). It is synthesized from cholesterol in the adrenal ZR and the gonads by the action of the two enzymes CYP11A1 and CYP17A1 (**Figure 4**). CYP11A1 is located in the mitochondrion and cleaves the cholesterol side chain, yielding pregnenolone (see 1.1.3.1; **Figure 4**).

The microsomal enzyme CYP17A1 is the qualitative regulator of steroid synthesis and exerts two distinct catalytic activities: (1) its 17α-hydroxylase activity catalyses the production of the glucocorticoid precursors 17OHP and 17Preg (see 1.1.7.1). (2) The 17,20 lyase activity of CYP17A1 catalyses their subsequent conversion to the adrenal androgen precursors androstenedione and dehydroepiandrosterone (DHEA), respectively. Of note, the 17,20 lyase activity of CYP17A1 has approximately a 100-fold higher substrate preference for 17Preg over 17OHP (Auchus et al., 1998). Hence, in the physiological situation, almost all androgen synthesis proceeds through DHEA.

The regulation of CYP17A1 17,20 lyase activity has been of interest for many years as alterations in this activity can be causative for androgen deficiency as well as androgen excess. The availability of electrons determines whether CYP17A1 performs only 17α-hydroxylation or whether it also performs 17,20 bond scission. Hence, co-factors involved in electron transfer have been considered and identified to regulate this activity. For both catalytic activities of microsomal CYP17A1, electrons are provided by the flavoprotein POR from NADPH (see **Figure 3**, see section 1.1.3). High molar ratios of POR to CYP17A1 have been shown *in vitro* to increase 17,20 lyase activity over its 17α-hydroxylase activity (Yanagibashi and Hall, 1986). Secondly, cytochrome b5 (CYB5A) has been thought to facilitate allosteric interaction between POR and CYP17A1, thereby increasing the electron flux from POR and specifically enhancing 17,20 lyase activity (Auchus et al., 1998) (see section 1.1.3.3). In addition, *in vitro* data suggest that phosphorylation of serine and threonine residues of CYP17A1 facilitate 17,20 lyase activity by a cAMP-dependent protein kinase (Zhang et al., 1995), which has recently been identified as p38α (Tee and Miller, 2013).

While CYP11A1 and CYP17A1 are essential and theoretically sufficient to create the biochemical environment of the ZR, other steroidogenic enzymes also affect androgen synthesis. HSD3B2 converts the Δ5 steroids Preg and 17Preg to the Δ4 steroids Prog and 17OHP, thus crucially facilitating MC and GC synthesis (**Figure 4**).

As it competes with CYP17A1 for substrate, decreased HSD3B2 activity will results in increased DHEA synthesis. Indeed, the ZR cell expresses low levels of HSD3B2 with CYP11A1 and CYP17A1 in abundance (Suzuki et al., 2000; Nakamura et al., 2009).

1.1.8.2. Regulation of adrenal androgen secretion

Cells of the ZR express the ACTH receptor responding with DHEA synthesis upon stimulation by pituitary ACTH; however, a negative feedback mechanism similar to the inhibitory effects of cortisol on ACTH release does not exist for DHEA or downstream androgens. The physiological role of androgen secretion in the context of central/pituitary activation is unclear, but it could be due to the immune-modulatory effects of DHEA and DHEAS during stress and illness, in particular infections (Hazeldine et al., 2010; Radford et al., 2010).

The mechanisms by which ACTH stimulates adrenal androgen synthesis are essentially via the same cascades that increase GC generation in the ZF, i.e. increased cholesterol uptake and transport to the IMM (StAR-mediated) with upregulation of CYP11A1 expression (see sections 1.1.5 and 1.1.7.2). In addition, *in vitro* studies show that ACTH/cAMP-stimulation of adrenal human cell lines or bovine primary cultures increase the expression of CYP17A1 (Miller and Auchus, 2011; Rodriguez et al., 1997; Sewer and Waterman, 2002; Bischof et al., 1998; Lund et al., 1990).

The adrenal ZR is not present from infancy until mid-childhood. The processes leading to its emergence, an event called adrenarche, is not understood and remains one of the big riddles in steroid endocrinology (see 1.2.3).

1.1.8.3. Adrenal androgens and androgen receptor activation

Androgens promote their actions via the androgen receptor (AR), a member of the subfamily 3 of nuclear receptors. The AR gene is located on the X-chromosome (Xq11-12). Its structure is similar to the MR and GR (see sections 1.1.5, 1.1.6.3 and 1.1.7.3) and consists of four domains: 1) a large NTD with an activation function 1 (AF1), 2) the NBD followed by the 3) hinge region (HR) that contains a nuclear localization signal (NLS). 4) The LBD contains the activation function 2 (AF2) domain (**Figure 8**).

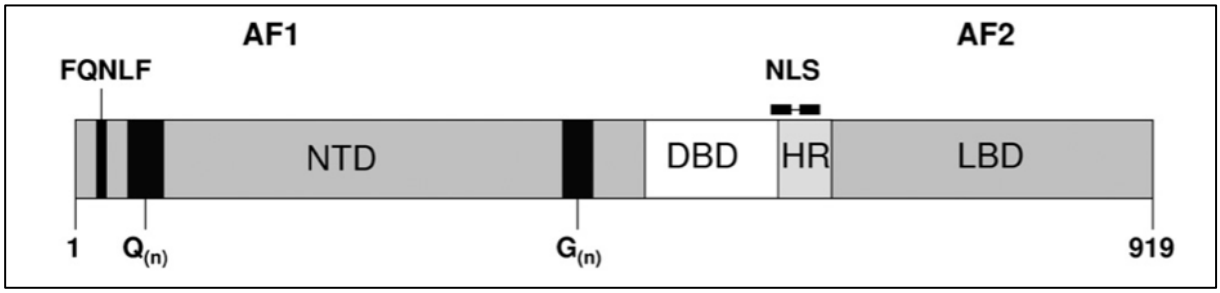

Figure 8: Schematic illustrating the protein structure of the AR (919 aa). NTD: N-terminal domain; DBD: DNA-binding domain; HR: hinge-region; LBD: ligand-binding domain; AF1/2: activation function 1 and 2; NLS: nuclear localization signal; a FQNLF-motif at the N-terminus is crucial for the interaction with AF2 upon ligand binding, resulting in conformational changes of the molecule. With kind permission from (Werner et al., 2010).

The protein structure of the AR in relation to its function has been studied extensively (Moras and Gronemeyer, 1998). More than 200 co-regulators of the AR have been identified, that either directly interact with the AR molecules and modulate gene transcription, or post-translationally modify gene products of the AR by phosphorylation, ubiquitination, sumoylation, methylation, or others (van de Wijngaart et al., 2012). The co-factor binding pocket of the AR seems to be unique compared to

other steroid hormone receptors, as it recognizes preferentially LxxLL or FxxLF motifs of the protein sequence of co-regulators (van de Wijngaart et al., 2012).

The detailed effects and actions of androgens across lifespan are described in detail in section 1.2 of this chapter.

1.1.8.4. Conversion of DHEA to active androgens

DHEA has virtually no affinity for sex steroid receptors. It is released into the blood stream to serve as a substrate for extra-adrenal steroidogenic enzymes activating DHEA to potent sex steroids, with dihydrotestosterone (DHT) and oestradiol (E2) having the highest affinity to the androgen and oestrogen receptors, respectively. This 'activation' of DHEA takes place in peripheral target tissues, which express the steroidogenic enzyme systems required for the formation of active hormones (**Figure 9**). This field of endocrinology describing intra-cellular activation and action of hormones derived from circulating precursors is called 'intracrinology', and peripheral adrenal androgen activation is one of the best described examples of this field (Labrie et al., 1988; Labrie, 2003).

The conversion of DHEA to androstenedione is the first step of sex steroid activation, and this reaction is catalysed by the two isoforms of the HSD3B enzyme. The adrenal ZG and ZF expresse the type 2 isoform HSD3B2, which is also crucial for the generation of MC and GC precursors (see sections 1.1.6.1, 1.1.7.1; **Figure 4**). However, the ZR expresses HSD3B2 to a lesser extent than the two outer zones (Suzuki et al., 2000). Still, 50% of plasma androstenedione levels are still derived from the adrenal glands in pre-menopausal women (Judd et al., 1974). HSD3B2 is exclusively expressed in the adrenals, gonads and the placenta, while the HSD3B1 isoform is expressed in many 'non-steroidogenic' tissues, including liver, skin, adipose, kidney and brain. Inactivating mutations in the *HSD3B2* gene result in a

severe form of congenital adrenal hyperplasia (CAH) characterized by salt-wasting crisis due to MC and GC deficiencies with increased DHEA generation due to HPA axis activation; however, the fact that these patients develop androgen excess, reflects the increased peripheral activation of DHEA by the (intact) HSD3B1 enzyme.

17β-hydroxysteroid dehydrogenases (HSD17Bs) are a large group of enzymes with at least 14 human isoforms known (Kong et al., 1992; Miller and Auchus, 2011). Like many other HSDs, they can act in two directions, either as an oxidase or a reductase. However, most HSD17Bs catalyse a reaction in one preferential direction. Six HSD17Bs are involved in steroid metabolism, in particular in the inter-conversion of sex steroid precursors. Their roles in sex steroid metabolism and tissue expression are summarized in **Table 2** and illustrated in **Figure 9**.

5α-reduction of testosterone yields 5α-dihydrotestosterone (DHT), the most potent androgen. This reaction is irreversible. Two isoforms of the enzyme 5α-reductase (SRD5A) have been cloned and characterized (Andersson and Russell, 1990; Andersson et al., 1991; Jenkins et al., 1992) and differ mainly regarding their tissue-specific distribution: the type 2 isoform (SRD5A2) is expressed in the tissues of the male reproductive tract, but also in foetal genital skin; SRD5A1 is widely expressed in peripheral tissues, but mainly in liver and skin (Luu-The et al., 1994).

All oestrogens are derived from androgens by the activity of the enzyme P450 aromatase (CYP19A1). CYP19A1 uses three electrons, derived from NADPH via POR, to oxidize and demethylate androgenic C19 steroids, yielding a C18 steroid with an aromatic A-ring (Miller and Auchus, 2011). Its main substrates are androstenedione and testosterone yielding oestrone (E1) and oestradiol (E2), respectively. During pregnancy, 16-hydroxy-DHEA, which is 16α-hydroxylated in the foetal liver, is aromatized to oestriol (E3), which reaches high levels in the maternal

circulation. E2 is the oestrogen with highest affinity for the oestrogen receptor (ER) and mediates the development of secondary female characteristics during puberty and the gain of fertility. CYP19A1 is mainly expressed in granulosa cells of the ovarian follicle and placenta, but also in adipose, the growth plate of long bones and the brain (Simpson et al., 1994).

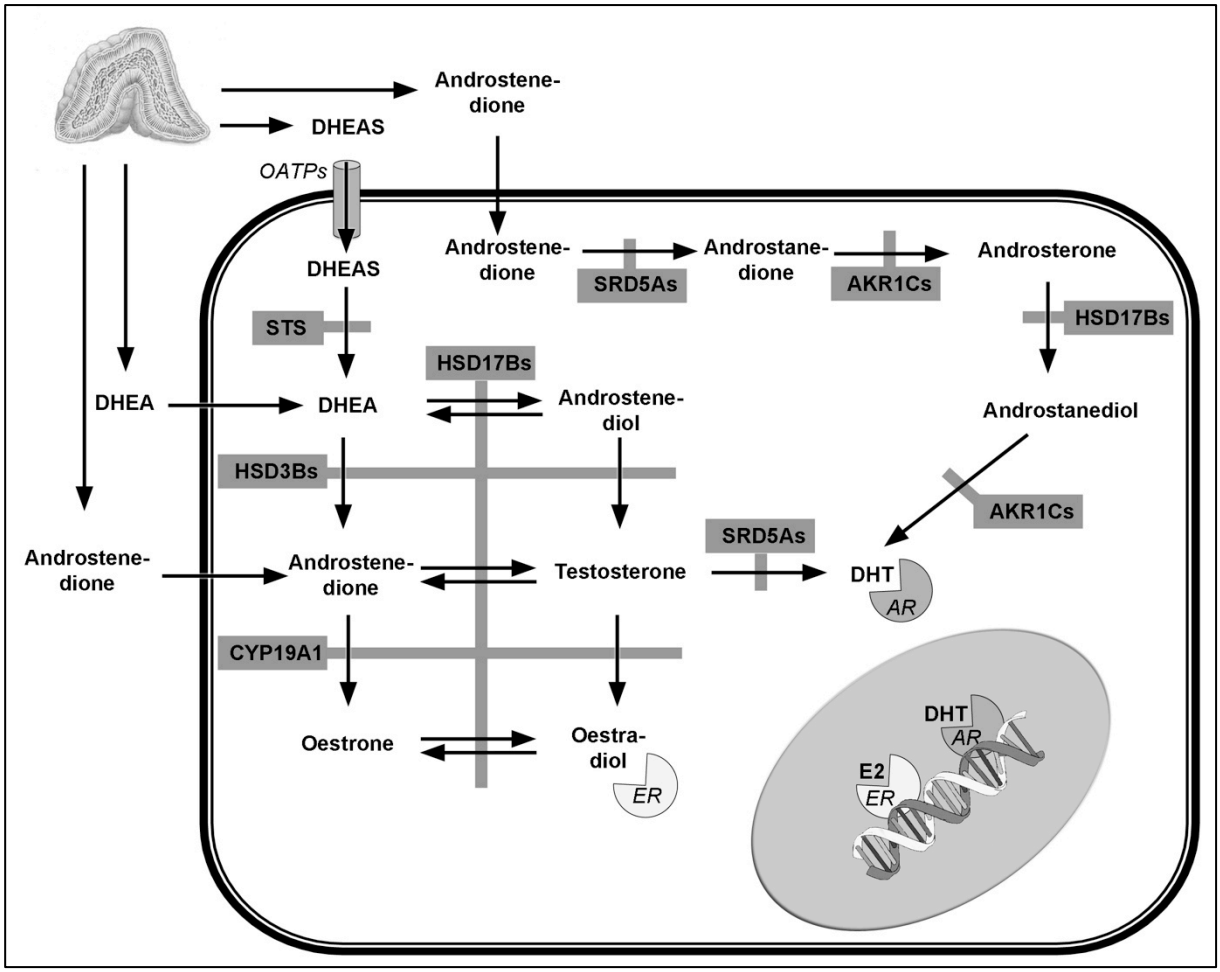

Figure 9: Schematic illustration of the activation of adrenal androgen precursors in peripheral target cells by the action of various steroidogenic enzymes. Dihydrotestosterone (DHT) is the most potent androgen with the highest transactivation capacity of the androgen receptor (AR); its biosynthesis is realised by 5α-reduction of testosterone by SRD5As. Testosterone is produced from DHEA and androstenedione by the action of the two HSD3B isoforms and various HSD17Bs isoforms. The sulfate moiety of DHEAS is hydrolysed by the enzyme steroid sulfatase (STS), yielding DHEA. Due to the hydrophilic properties of DHEAS, it needs active transport into the cell by OATPs. An alternative pathway from androstenedione to DHT without the use of testosterone is illustrated to the top and right part of this figure. Oestrogens are derived from androstenedione and testosterone by the action of CYP19A1. ER: Oestrogen receptor.

1.1.9. DHEA sulfation pathways and interconversion of DHEA and DHEAS

The main product of the adrenal ZR and also the most abundant steroid hormone in the circulation is DHEAS, the sulfoconjugated form of DHEA. The daily DHEAS production in adult women of reproductive age is up to 20 mg, compared to 3-6 mg for DHEA, 1-6 mg for androstenedione and 0.1-0.4 mg for testosterone (Burger, 2002).

DHEAS is in the context of AR activation an inactive metabolite and cannot directly be converted to active androgens. DHEAS has strikingly different biochemical properties than DHEA: as a hydrophilic molecule, it is not able to cross lipid membranes freely as most other steroids and has to rely on active transport mechanisms. DHEAS is bound to plasma proteins (mainly albumin) and thus has a much longer plasma half-life of about 20 hours compared to 3-6 hours for DHEA. The sulfation of DHEA is catalysed by the enzyme DHEA sulfotransferase (SULT2A1) and predominantly occurs within the ZR (Falany et al., 1989; Strott, 2002). The enzyme steroid sulfatase (STS), which is mainly expressed in peripheral tissues, cleaves the sulfate moiety off the DHEAS molecule to regenerate DHEA, which can be converted further downstream to active sex steroids. Hence, through the counter-actions of SULT2A1 and STS, circulating, albumin-bound DHEAS has been thought to represent a storage pool for amplification of sex steroid signalling in peripheral target tissues. However, little is known about the exact impact of the DHEA sulfation system and its role during childhood development.

1.1.9.1. DHEA sulfotransferase (SULT2A1) and 3’-phosphoadenosine-5’-phosphosulfate (PAPS) synthases (PAPSS)

The sulfoconjugation of substances is a major metabolic pathway in humans and involved in many key cellular and metabolic processes, crucial for growth and

development (Strott, 2002; Dawson, 2011). Sulfation is a catalytic reaction where a sulfate group (SO_4^{2-}) is transferred to an acceptor molecule. The introduction of a sulfate group into a molecule results in striking alterations of the molecule's biochemical properties, mainly an increase in water solubility as well as conformational changes.

Sulfation reactions are catalysed by sulfotransferases (SULTs), and more than 50 SULTs have been cloned and characterized in humans (Strott, 2002).

Depending on their cellular localization and chemical properties, two super-families can be distinguished: 1) soluble, cytosolic SULTs and 2) membrane-bound SULTs that are usually located within the Golgi apparatus (Strott, 2002). Members of the cytosolic group of SULTs are involved in steroid and drug metabolism, the membrane-associated SULTs sulfo-conjugate carbohydrates, peptides and proteins.

SULT2A1, a member of the subfamily 2 of cytosolic SULTs, has been traditionally named DHEA sulfotransferase, as it utilizes DHEA as its major substrate (Kong et al., 1992). However, it has a broad substrate specificity and also sulfates other Δ4 steroids, like pregnenolone or 17-hydroxypregnenolone, but also testosterone, oestradiol and bile acids (Radominska et al., 1990; Falany, 1997). Usually, the 3α/β- or the 17β-hydroxyl-groups of these molecules undergo sulfation by SULT2A1. Other SULTs involved in steroid metabolism have been identified; in particular SULT1B1 with its two isoforms SULT1B1a and SULT1B1b is able to sulfate hydroxysteroids (Whitnall et al., 1993; Strott, 2002).

SULT2A1 is robustly expressed in the cytosol of many steroidogenic tissues, in particular tissues involved in androgen production and metabolism, which are adrenal cortex, testicles, ovaries, prostate and liver but also the digestive tract (Javitt et al., 2001).

The sulfate group for sulfation reactions mediated by SULTs needs to be 'activated' and is delivered by an organic compound named 3'-phosphoadenosine-5'-phosphosulfate (PAPS). In fact, PAPS serves as the universal sulfate donor for all sulfation reactions, and all tissues in mammals are able to produce PAPS from ATP and inorganic sulfate (Mulder, 2003). The generation of PAPS requires two distinct catalytic reactions carried out by the bi-functional enzyme PAPS synthase (PAPSS): First, ATP is sulfurylated yielding adenosine-5'-phosphosulfate (APS) as an intermediate, which is secondly further phosphorylated to form PAPS. While both enzymatic reactions, ATP sulfurylase and APS kinase, are located in plants, yeast and bacteria on different polypeptide chains, they are fused to one enzyme in metazoans forming the PAPSS enzyme (Strott, 2002; Mueller and Shafqat, 2013). Two PAPSS isoforms exist in humans, and their genes are located on two separate chromosomes: PAPSS1 (chromosome 4q25-26) is highly conserved amongst different species, including rodents, guinea pig and drosophila (Venkatachalam, 2003; Yanagisawa et al., 1998). It has about 80% amino acid identity with the human PAPSS2 isoform (chromosome 10q23-56) (Strott, 2002), which was discovered in a search for the genetic cause of a bone malformation disorder in a large consanguineous pedigree with affected members suffering from distinct bone malformations called spondylepimatephyseal dysplasia (SEMD) (Haque et al., 1998).

Both isoforms have a very similar structure, genomic arrangement (12 exons with similar intro/exon boundaries), length (614 and 624 amino acids, respectively) and distribution of catalytic domains with the ATP sulfurylase domain being located at the N-terminus and the APS kinase domain at the carboxy-terminus (Xu et al., 2000). Two splice variants exist for the human PAPSS2 isoform, PAPSS2a and PAPSS2b: PAPSS2b has an additional exon comprising 5 amino acids ('GMALP') within the

ATP sulfurylase domain (van den Boom et al., 2012; Fuda et al., 2002). However, there are differences between the two PAPSS isoforms in regards to their tissue expression: PAPSS1 is virtually ubiquitously expressed, while PAPSS2 is mainly in cartilage, adrenal, gonads, placenta, colon and liver (Fuda et al., 2002; Stelzer et al., 2007). Furthermore, a different subcellular distribution of PAPSS isoforms has been reported. Sulfation reactions are essentially taking place within the cytoplasm for most substrates, including steroids; however, sulfation of oestrogens has been reported to occur in the nucleus for rodents and guinea pig (Mancini et al., 1992; Whitnall et al., 1993). Strikingly, Besset et al. reported that the human PAPSS1 isoform is located in the nucleus whereas PAPSS2 is expressed in the cytoplasm of mammalian cells (Besset et al., 2000). Recently, Schröder et al. showed that the distribution pattern of both PAPSS isoforms is much more variable and both enyzmes are expressed dynamically in the cytosol and the nucleus of mammalian cells (Schröder et al., 2012). Interestingly, work from the same group has shown that PAPSS2 is less stable with a half-life of several minutes for the unfolding protein, whereas PAPSS1 remains structurally intact at physiological temperatures (van den Boom et al., 2012). In addition, Grum et al. has shown that PAPSS isoforms associate as hetero-dimers, suggesting the possibility of co-synergistic regulation of intracellular sulfation pathways (Grum et al., 2010).

However, the functional consequences of the differences regarding their dynamic sub-cellular localization patterns, *in vitro* protein stability and dimerisation, in particular in the context of androgen pre-receptor metabolism, are still unknown and remain to be established.

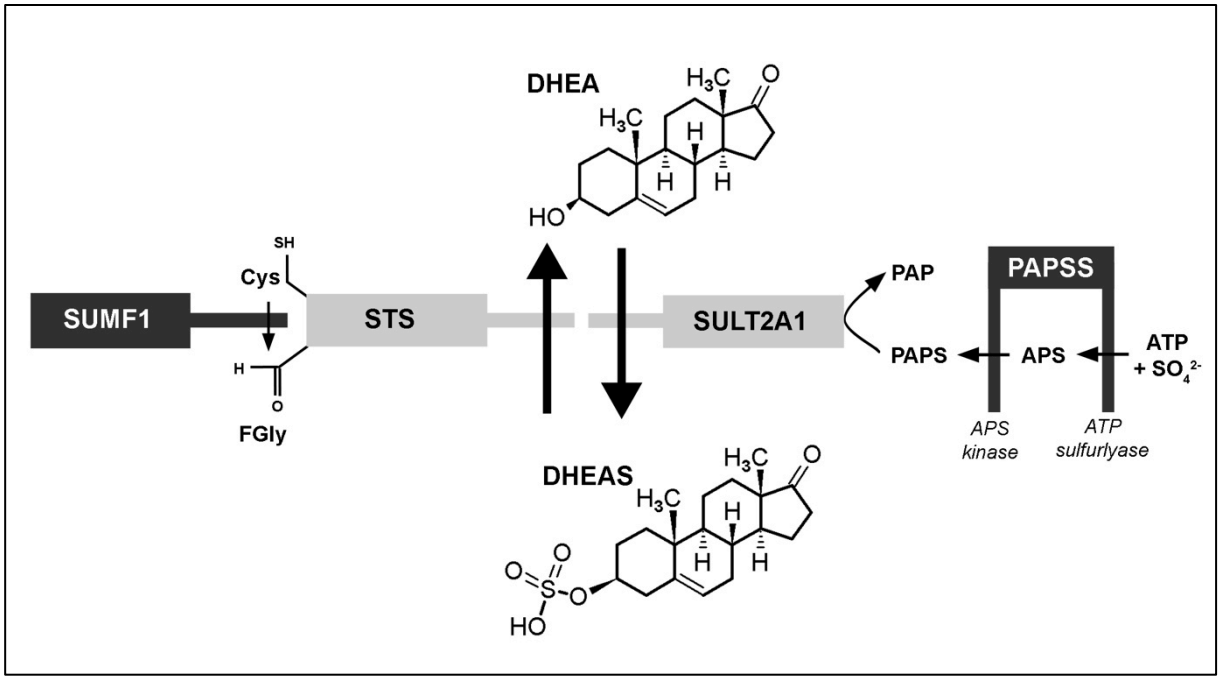

Figure 10: Interconversion of DHEA and DHEAS. The sulfation of DHEA is catalysed by the enzyme DHEA sulfotransferase (SULT2A1); the opposite direction, the hydrolysis of the sulfate moiety from DHEAS, is performed by steroid sulfatase (STS). Both enzymes depend on co-factors: SULT2A1 requires the activated sulfate compound PAPS, generated by the enzyme PAPS synthase (PAPSS) via two catalytic activities: (1) ATP is sulfurylated to APS by the ATP sulfurylase activity, (2) APS is further phosphorylated to form PAPS. A cysteine residue of the STS enzyme needs to be post-translationally activated to a formylglycine (FGly) by the mono-oxigenase formylglycine-generating enzyme (FGE), encoded by the SUMF gene. FGly is further hydroxylated, crucial for the hydrolysis of the sulfate moiety catalysed by STS.

1.1.9.2. Steroid sulfatase (STS) and sulfatase-modifing factors (SUMFs)

Steroid sulfatase (STS, *aka* as arylsulfatase C) is a membrane-bound microsomal enzyme and member of a highly conserved family of arylsulfatases (ARS) (Reed et al., 2005). Sulfatase enzymes act in the opposite direction of sulfotransferases and catalyse the cleavage of the sulfate moiety from a variety of substrates, including conjugated steroids and other hormones, proteoglycans, post-translationally modified proteins and aromatic compounds.

The action of STS is implicated in the regeneration of steroids and its precursors from their inactive sulfo-conjugated esters, thereby enhancing their availability in peripheral target cells on the pre-receptor level. It hydrolyses the sulfate

group of 3β-hydroxysteroid sulfates, including DHEAS, pregnenolone sulfate, 17-Preg sulfate, sulfated oestrogens, but also of cholesterol sulfate (Reed et al., 2005).

The *STS* gene is localized on the short arm of the X-chromosome (Xp22.3), which is part of the pseudo-autosomal region escaping X-inactivation (Ballabio et al., 1987a). It encodes a protein of 583 amino acids and has a mass of about 65kDA (Stein et al., 1989).

Genetic abnormalities of the *STS gene* causes steroid sulfatase deficiency (STSD) resulting in the skin condition X-linked ichthyosis, a common inborn error of metabolism with a prevalence of 1:6,000 (Fernandes et al., 2010). It is characterized by thickening of the epidermis and large, brown scales of the skin; the pathomechanism is thought to be due to accumulation of cholesterol sulfate in the stratum corneum of the epidermis. Abnormal steroid metabolism has been reported in small cohorts of patients with STSD as well as elevated levels of sulfated steroids, like DHEAS and oestrogen sulfates (Lykkesfeldt et al., 1985a; Milone et al., 1991; Delfino et al., 1998).

The molecular mechanisms underlying STS catalytic activity have been studied in detail and are highly conserved amongst different human sulfatase enzymes (Reed et al., 2005; Ghosh, 2007): a highly conserved cysteine residue resides in the catalytic centre of the sulfatase, which is post-translationally modified to form a formylglycine (FGly) residue. FGly is catalytically active and ‘attacks’ the sulfate moiety of substrates and is essential to hydrolyse the sulfate ester bond (Recksiek et al., 1998; Dierks et al., 1998; Ghosh, 2007) (**Figure 10**). The modification of the cysteine to form the FGly is mediated by the co-enzyme formylglycine generating enzyme (FGE), which is encoded by the gene *sulfatase-modifying factor 1* (*SUMF1*). Mutations in *SUMF1* cause multiple sulfatase

deficiency, a rare and fatal autosomal recessive disorder characterized by absent activity of all sulfatase enzymes (Cosma et al., 2003; Dierks et al., 2003).

STS is believed to be expressed in virtually all human adult and foetal tissues in very small amounts (Strott, 2002). Immunohistochemistry studies have demonstrated that STS is localized in the endoplasmic reticulum and Golgi apparatus (Willemsen et al., 1988). A systemic expression analysis employing semi-quantitative RT-PCR, immunohistochemistry and biochemical detection by activity assays detected either absent or very low STS expression and activity in a variety of human foetal and adult tissues, with low-moderate STS detection in lung, aorta, adrenal gland, thyroid, mammary gland, testis, prostate and endometrium (Miki et al., 2002). However, the richest source for STS is the syncytiotrophoblast of the human placenta.

1.2. ADRENAL ANDROGENS DURING HUMAN PRE- AND POSTNATAL DEVELOPMENT

1.2.1. The adrenal gland during foetal development

About one month *post conceptionem* (*pc*), the human adrenal gland can be morphologically distinguished from the surrounding tissue and starts to express steroidogenic enzymes at 50-52 *days pc* (*dpc*) (Val et al., 2006; Goto et al., 2006; Val and Swain, 2010). At 8 *weeks pc* (*wpc*) cortisol is produced in human foetal primary cultures, which are also responsive to ACTH and forskolin stimulation (Goto et al., 2006). The micro-architecture of the foetal adrenal cortex, however, is different from the postnatal situation, as only two layers are present before birth: an outer ‘definite zone’ (DZ) and an inner larger ‘foetal zone’ (FZ), which comprises about 75% of the entire foetal cortex of the organ (Mesiano and Jaffe, 1997). Steroidogenic enzymes able to synthesize cortisol *de novo* from cholesterol are expressed in the

FZ from 50-52 *dpc* onwards. The expression of HSD3B2 within the FZ is weak and decreases during further development; this is accompanied by an increased activity of CYP17A1 17,20 lyase, which makes the large FZ capable of producing large amounts of androgens (Goto et al., 2006). As SULT2A1 is strongly active in the FZ, DHEAS is the main product of the foetal adrenal gland (Miller and Auchus, 2011). Foetal DHEAS requires cleavage of the sulfate moiety to be further processed into sex steroids; the abundant expression of STS in the placenta therefore regenerates DHEA from circulatory DHEAS. Through the actions of placental STS, HSD17B1, HSD3B1 and CYP19A1, the placenta produces large amounts of oestrogens. As the placenta does not express CYP17A1, it itself is not able to produce androgens and relies on the foetal adrenal to generate oestrogens. Therefore, as both organs are linked to a common task – creating the oestrogenic environment of pregnancy – they are functionally connected to build the so-called 'foetal-placental unit'.

The exact role of oestrogens during pregnancy is unclear. Foetuses with inborn errors in androgen or oestrogen biosynthesis develop normally until term and abnormal parturition has not been reported.

1.2.2. Sex determination and differentiation

During foetal development, androgens play a central role in the development of male external genitalia. This second phase of male sexual development is called sex differentiation and is mechanistically distinct from the initial phase of sexual determination, which is mainly regulated by transcription factors and signalling molecules other than steroids.

Genetically male (46,XY) and female (46,XX) foetuses do not differ morphologically until about 6 weeks *post conceptionem (wpc)*, when sexual dimorphism occurs due to the differentiation of the bipotential gonadal anlage into

either testes or ovaries. In 1990, a gene on the Y-chromosome was identified as being responsible for the initiation of male sex determination, and called 'sex-determining region of the Y-chromosome' (SRY) (Berta et al., 1990; Sinclair et al., 1990). Since the discovery of SRY, numerous rodent and human studies have unravelled complex developmental pathways that mediate the determination of the gonadal phenotype in mammals, with the majority of these genes being discovered because of genetic abnormalities found in patients with disordered sexual development (DSD); see (Eggers and Sinclair, 2012) for an extensive review. In brief, the presence of SRY, which is expressed in the bipotential gonad, initiates the expression of the transcription factor SOX9, which stimulates in turn FGF9; both SOX9 and FGF9 suppress WNT4 and establish a testis-specific pathway. In ovarian development, WNT4 initiates canonical Wnt-signalling in the gonadal anlage, crucial for the establishment of the ovarian-specific pathway.

Both mammalian steroidogenic tissues, the gonads and adrenals, are derived from a common embryological origin, the adreno-gonadal primordium (AGP). This has been suggested by histological studies as well as the detection of distinct steroidogenic enzymes (CYP11A1, HSD3B2, CYP19A1, CYP17A1) in both the gonadal and adrenal anlage during early mammalian development (Val et al., 2006; Val and Swain, 2010). Studies in mice implicate certain genes in the development of the AGP, and knock-out mice lacking these factors do not develop either gonads or adrenals. Steroidogenic factor-1 (SF1), a nuclear receptor from the subfamily 5 (NR5A1), acts as a key regulator in steroidogenic cell-differentiation and function, with important implications for male sex differentiation (El-Khairi and Achermann, 2012). *SF1* knock-out mice are not able to maintain adrenal primordia and show a male-to-female sex reversal (Luo et al., 1994). Upstream of SF1, the Wilms' tumour

gene 1 (WT1) has been implicated in murine *SF1* transcription, modulating adrenal cortex differentiation (Val et al., 2007).

In the course of male sex determination, the bipotential gonad develops into a testis consisting of functional Sertoli and Leydig cells. The Sertoli cells secrete the Muellerian inhibitory substance (MIS) at 8 *wpc*, inhibiting the development of the para-mesonephric ducts ('Muellerian' ducts) into uterus and vagina. At 9 *wpc*, testicular Leydig cells start to secrete testosterone (Siiteri and Wilson, 1974). Androgen actions are mediated by the androgen receptor (AR), which is expressed in the urogenital tract from 8 *wpc*. There are no differences in AR expression between male and female foetuses at this stage (Sajjad et al., 2004b; 2004a). AR activation by androgen action results in growth and differentiation of the male external genitalia and the prostate gland, respectively. From a stage of phenotypic ambiguity, androgens support the fusion of the two bilateral genital swellings, which forms the scrotum; in addition, the genital tubercle enlarges and forms the penis shaft (Werner et al., 2010). The critical developmental time window for the external male genitalia to masculinise opens between 8 and 10 *wpc* only (Goto et al., 2006) (see **Figure 11**).

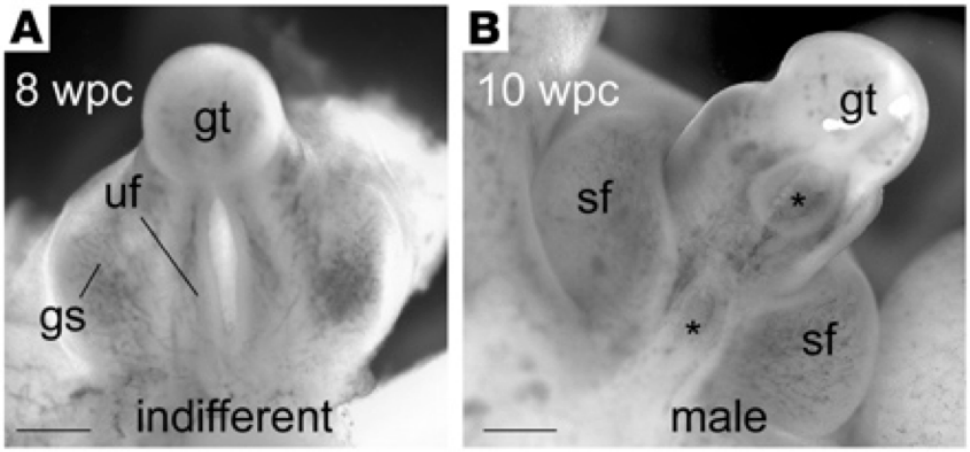

Figure 11: External male genitalia at 8 *wpc*, showing an indifferent/ambiguous stage (**panel A**), which masculinizes under the influence of testicular androgens at 10 *wpc* (panel B). gs: genital swelling; uf: urethral fold; gt: genital tubercle. Asterisks indicate patency of the scrotal fusion. Bar: 500 µm. With kind permission from Goto et al., 2006.

1.2.3. Adrenarche

Adrenarche refers to the developmental maturation of the adrenal gland, observed only in the human, chimpanzee, and gorilla (Dhom, 1973; Cutler et al., 1978; Conley et al., 2012; Arlt et al., 2002). At adrenarche, the innermost layer of the human adrenal cortex, the ZR, starts to produce increasing amounts of DHEA and DHEAS (Rege and Rainey, 2012; Auchus and Rainey, 2004; de Peretti and Forest, 1978; 1976). The term “adrenarche” was coined by Fuller Albright and Nathan Talbot in the 1940s when they linked the developmental rise in adrenal androgens to the appearance of pubertal and axillary hair, which they called “sexual hair” (Marshall and Tanner, 1969; Albright, 1947; Marshall and Tanner, 1970; Talbot et al., 1943).

Adrenarche is a physiological mystery because it is not well understood how the development of the ZR is initiated or controlled [see (Arlt et al., 1999; Auchus and Rainey, 2004) for review] nor why adrenal androgens are significant for human pre-pubertal development. Adrenal androgens contribute to changes in body composition and transient growth acceleration but without having a major impact on final height or subsequent developmental milestones like puberty. From the evolutionary perspective it has been suggested that adrenarche is a key component of ‘juvenility’, a period that emerges during evolution in the late *Hominides* and prolongs the transition from childhood to adolescence and adult life; juvenility may serve the adaptation of body composition and metabolic status to environmental conditions (Binder et al., 2009; Hochberg, 2010). Another interesting hypothesis refers to the neuro-modulatory effects of DHEAS that may help to protect more metabolically active regions of the cerebral cortex to support brain maturation in the developing pre-pubertal child (Remer et al., 2004; Campbell, 2011; Voutilainen et al., 1983; Sopher et al., 2011).

The postnatal reappearance and increase in circulating DHEAS has been traditionally perceived as a relatively sudden surge, physiologically occurring between six to eight years of age (Counts et al., 1987; de Peretti and Forest, 1976; Sklar et al., 1980; de Peretti and Forest, 1978). However, previous studies employing immunoassays for determination of serum DHEAS only identified increasing levels once they went above the lower limit of detection. In a recent study that applied highly sensitive steroid mass-spectrometry indicates that “biochemical” adrenarche starts with a detectable increase in DHEA and related androgenic steroids at about three years of age (Martin, 2004; Remer et al., 2005). In addition, histological studies in the 1970s from human adrenal samples taken throughout childhood, revealed that focal ZR cell islets are present from the age of three years onwards (Arlt, 2006; Dhom, 1973) (**Figure 12**).

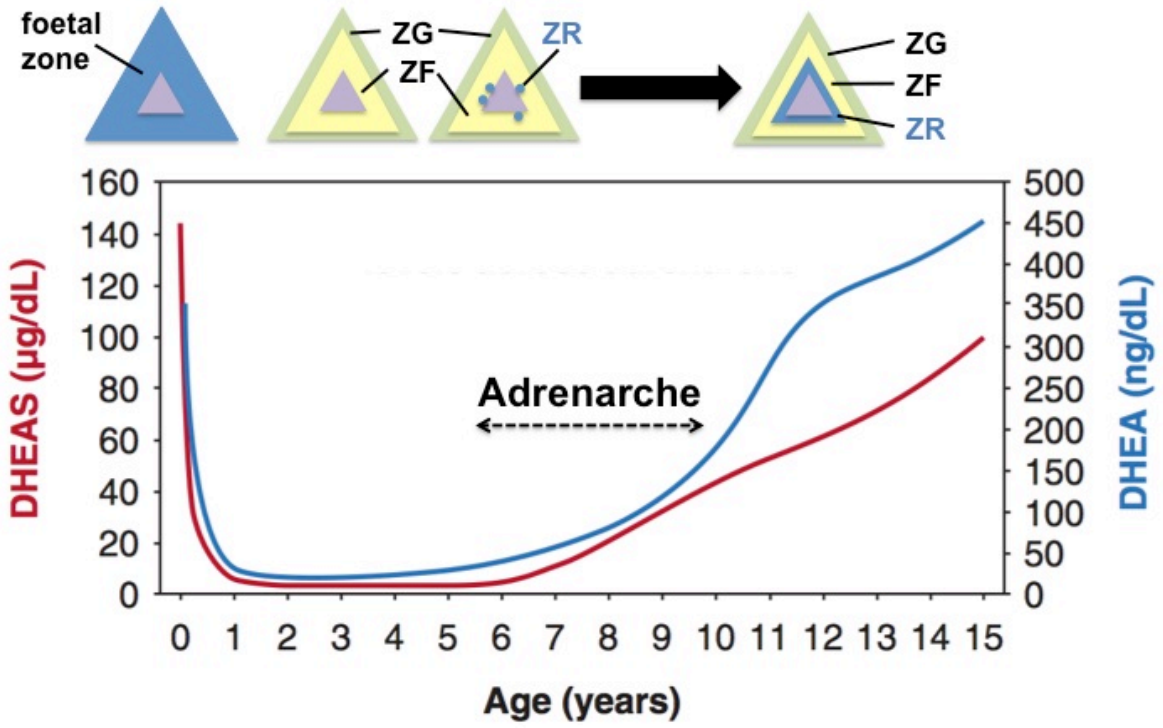

Figure 12: Schematic representing the morphological changes of the adrenal cortex with the rise of adrenal plasma androgens. DHEA and DHEAS slowly increase during mid-childhood, which correlates with the development of adrenal ZR cells present as focal islets in mid-childhood and then forming a continuous layer over a time span of several years until adolescence. Adapted from (de Peretti and Forest, 1976; 1978; Rege and Rainey, 2012).

These islets progressively form a continuous layer of ZR cells until early adolescence. These findings suggests that adrenarche, both as a biochemical and morphological phenomenon, is a long lasting developmental process rather than a sudden event.

There are no sex-differences in androgen excretion in pre- and early-pubertal age groups (Remer et al., 2005) and consequently, these results may challenge the well-accepted cut-off for the definition of premature adrenarche including sex differences (age 8 in girls and 9 in boys), derived from Marshall and Tanner's clinical observations that the appearance of pubic hair occurs about one year earlier in girls than in boys (Marshall and Tanner, 1969; 1970) (see section 1.3.2). The reason for earlier pubarche in girls might be that girls are more susceptible to peripheral androgen action and develop clinical signs earlier than boys.

In normal development, the first appearance of pubic hair, i.e. pubarche, from the age of 8 years onwards is the direct result of the physiological rise in adrenal androgen production during adrenarche (**Figure 12**). DHEA is converted to active androgens in the gonads and peripheral target tissues of androgen action, including the skin, resulting in the development of pubic and also axillary hair. Women with acquired adrenal insufficiency without physiologic DHEA production suffer from a lack of axillary and pubic hair, which reappears after initiation of DHEA replacement therapy (Arlt et al., 1999). Physiologically, increasing androgen production during adrenarche manifests with distinct changes in body odour, oily skin and hair, followed by the first appearance of pubic and axillary hair. In addition, the rise in adrenal androgens can result in transient growth acceleration and contributes to bone maturation (Voutilainen et al., 1983; Remer et al., 2004).

Generally, adrenarche appears to represent a developmental process independent of the maturation of the gonads (Sklar et al., 1980; Counts et al., 1987) Gonadarche, i.e. the onset of sex steroid production by the gonads, manifests with testicular enlargement and penile growth in boys and breast development and menarche in girls. Children with precocious puberty have no corresponding advance in the timing of adrenarche; their basal and ACTH-stimulated adrenal androgens are lower than in children matched for pubertal stage and only slightly higher than in age-matched children (Wierman et al., 1986). Conversely, children with isolated hypogonadotropic hypogonadism and subsequent lack of spontaneous puberty were found to have no corresponding delay in adrenarche (Counts et al., 1987; Sklar et al., 1980).

1.3. ANDROGENS AND HUMAN DISEASE

1.3.1. Monogenic causes of impaired androgen synthesis and metabolism

Defects in steroidogenic enzymes and their co-factors can affect androgen production. These comprise a variety of disorders inherited in an autosomal-recessive mode.

When androgen-generating enzymes or their co-factors are affected directly, androgen production is decreased. In contrast, disruptions in distinct pathways of steroidogenesis or metabolism may increase androgen generation due to compensatory regulatory mechanisms.

Table 3 and **Table 4** provide an overview of all known enzymatic defects of human steroidogenesis and co-factor mutations affecting steroid biosynthesis and metabolism, respectively.

Table 3: Overview and key clinical features of known steroidogenic disorders, where enzymes are affected directly. The (direct and indirect) effects on androgen metabolism are highlighted in **bold**.

Gene (Defect)	**Key clinical features**	**Affected reaction**
CYP11A1 (CYP11A1 deficiency)	**Sex steroid deficiency** at birth (46,XY DSD) and GC deficiency. *Only partially inactivating mutations (ie 'non-classical' forms)*	Cholesterol → Preg
CYP11B1 (11β-hydroxylase deficiency)	Classical form: Isolated GC deficiency; ACTH-mediated **androgen excess** and accumulation of MC precursors. Non-classical forms: partial GC deficiency, may presenting as androgen excess only.	11-deoxycortisol → F
CYP11B2 (aldosterone synthase deficiencies)	Isolated MC deficiency; may present at different ages with broad variety of symptoms.	DOC → B → 18OH-B → Aldo
CYP17A1 (17α-hydroxylase deficiency)	Classical form: GC and **sex steroid deficiency** and ACTH-mediated MC excess. Spectrum of non-classical forms with predominant sex steroid deficiency and without/partial GC deficiency/MC excess reported. Rare: 'isolated 17,20 lyase' (= sex steroid) deficiency.	17α-hydroxylase: Preg → 17-Preg; Prog → 17OHP 17,20 lyase: 17Preg → DHEA (17OHP → androstenedione)
CYP21A2 (21-hydroxylase deficiency)	Classical form: Severe MC and GC deficiency ('salt-wasting crisis') with ACTH-mediated **androgen excess** (i.e. 46,XX DSD). 'Simple-virilising' forms: 46,XX DSD at birth without adrenal crisis. Non-classical forms: androgen excess and compensated GC deficiency.	Prog → DOC 17OHP → 11-deoxycortisol
CYP19A1 (aromatase deficiency)	**Prenatal androgen excess** due to decreased placental aromatisation ('inactivation') of foetal androgens: 46,XX DSD	1) T → E2 2) A'dione→ E1 3) DHEA → E3
HSD3B2 (3β-HSD type 2 deficiency)	Classical form: GC and MC deficiencies (salt-wasting crisis). **Androgen excess** as accumulating DHEA can be converted down-stream to active androgens by the HSD3B type 1 isozyme. Non-classical form: androgen excess with compensated GC/MC deficiencies.	Preg→ Prog 17Preg→ 17OHP DHEA→ A'dione
SRD5A2 (5α-reductase deficiency)	**Androgen deficiency** at birth (46,XY DSD)	T → DHT
HSD17B3 (17β-HSD type 3 deficiency)	**Androgen deficiency** at birth (46,XY DSD)	A'dione → T
HSD11B1 (cortisone reductase deficiency)	Various degrees of postnatal **androgen excess**, i.e. PCOS or premature adrenarche/pubarche.	E → F

Table 4: Overview and key clinical features of known co-factor deficiencies affecting human steroidogenesis and steroid metabolism. The (direct and indirect) effects on androgen metabolism are highlighted in **bold**.

Gene (Defect)	Key clinical features	Affected reaction
POR (P450 oxidoreductase deficiency)	Broad spectrum of GC deficiency. Postnatal **sex steroid deficiency and prenatal androgen excess** (DSD in both sexes).	Supports all microsomal type 2 CYPs (CYP17A1, 21A2, 19A1)
PAPSS2 (apparent DHEA sulfotransferase deficiency)	**Androgen excess** (premature adrenarche, PCOS-like phenotype) and bone malformations.	Supports SULT2A1 (DHEA → DHEAS)
H6PD (apparent cortisone reductase deficiency)	Various degrees of **androgen excess**, i.e. PCOS or premature adrenarche/pubarche.	Supports HSD11B1 (E → F)

1.3.1.1. CYP17A1 17α-hydroxylase deficiency and isolated 17,20 lyase deficiency

Inactivating mutations in the *CYP17A1* gene cause 17α-hydroxylase deficiency (17OHD), an autosomal recessive disorder and a rare variant of CAH accounting for about 1% of all CAH cases (Krone and Arlt, 2009). More than 50 mutations have been identified so far and the vast majority of them cause impairment of both 17α-hydroxylase and 17,20 lyase activities of CYP17A1 resulting in combined sex steroid and glucocorticoid deficiency (Geller et al., 1997; 1999; Miller and Auchus, 2011). The low glucocorticoid levels stimulate pituitary ACTH secretion resulting in adrenal hyperplasia with an excess of mineralocorticoid production and hypokalaemic, hyporeninaemic hypertension.

A few mutations in *CYP17A1* have been reported in patients who present without MC excess and with apparently normal GC production, indicating that the 17α-hydroxylase activity is not impaired but only the 17,20 lyase activity is affected.

Hence, a selective decrease of sex steroid biosynthesis but normal GC and MC production is the clinical manifestation of this rare syndrome termed “isolated 17,20 lyase deficiency” (Gupta et al., 2001). So far, there are about 25 cases of isolated 17,20 lyase deficiency described in the literature (Yanase, 1995; Miller and Auchus, 2011); however, in only four of them could inactivating mutations in the *CYP17A1* gene be identified as the cause of this condition (Miller and Auchus, 2011; Geller et al., 1997; Sherbet et al., 2003; Van Den Akker et al., 2002). Further functional characterizations of these mutations including *in silico* analysis on the protein model of CYP17A1 revealed novel insights into CYP17A1 function, in particular the regulation of 17,20 lyase activity (Geller et al., 1999): two of these mutations (p.R347H and p.R358Q) are located in the redox partner binding site of CYP17A1, that is crucial for the interaction with POR and CYB5A, and change electrostatic charge distribution disturbing sufficient electron flux to support 17,20 lyase activity. So far, only one missense mutation in the *POR* gene (p.G539R) has been reported to selectively disrupt CYP17A1 17,20 lyase activity in one family with several members affected (Hershkovitz et al., 2008). A *CYB5A* nonsense mutation resulting in early truncation of protein has been described in a patient with 46,XY DSD diagnosed with isolated 17,20 lyase deficiency (Kok et al., 2010). Hence, interaction of the three proteins CYP17A1, POR and CYB5A are essential for 17,20 lyase activity generating androgen precursors. It appears that the abundance of electrons sustained by co-factor interaction is crucial to support CYP17A1 17,20 lyase over 17α-hydroxylase activity while inactivating mutations that disrupt the electron flux completely or interact with substrate binding, affect the efficacy of both catalytic activities (Auchus and Miller, 1999).

1.3.1.2. P450 oxidoreductase deficiency (apparent combined 21-hydroxylase and 17-hydroxylase deficiencies)

P450 oxidoreductase (POR) is the electron donor to all microsomal (type 2) CYPs, which play central roles in adrenal steroidogenesis, but are also involved in other metabolic processes, mainly hepatic drug metabolism (see section 1.1.3.2). Consequently, inactivating mutations in the *POR* gene, resulting in POR deficiency (PORD), is a multi-system disorder with manifold implications on human metabolism.

The biochemical evidence for a syndrome with concomitant impairment of 21-hydroxylase and 17-hydroxylase/17,20 lyase activities was initially reported in the 1980s in patients with adrenal insufficiency and ambiguous genitalia (Peterson et al., 1985; Augarten et al., 1992; Małunowicz et al., 1987); in addition, distinct bone malformations as part of the Antley-Bixler syndrome have been reported in some patients with a similar biochemical fingerprint (Shackleton et al., 2004).

In 2004, homozygous and compound heterozygous mutations in the *POR* gene were reported as the genetic basis of this syndrome (Flück et al., 2004; Arlt et al., 2004). To date, more than 50 mutations of the *POR* gene have been reported in patients with PORD presenting with a variety of clinical and biochemical phenotypes (Huang et al., 2005; Fukami et al., 2006; 2009; Krone et al., 2012).

The impact of mutant POR on human steroidogenesis, in particular apparent inhibition of 21-hydroxylation of GC and MC precursors by the enzyme CYP21A2, makes PORD a new and unique form of CAH. In contrast to 21-hydroxylase deficiency due to inactivating mutations in the CYP21A2 gene, the commonest form of CAH, the accumulating steroid precursors cannot drain downstream into the androgen pathway, as the catalytic activities of CYP17A1 are also impaired by

mutant POR. Thus, the combined apparent inhibition of these two enzymes affects MC and GC synthesis as well as androgen/sex steroid production.

However, clinically apparent MC deficiency with abnormal electrolytes or hypotension has not yet been reported in PORD; in fact, evidence from urinary steroid profiling suggests that MC metabolites are indeed slightly elevated, most likely as a consequence of the accumulation of MC precursors due to impaired 17α-hydroxylase activity (Krone et al., 2012). Circulating cortisol levels in PORD are often normal, but frequently fail to increase appropriately after ACTH stimulation, indicating partial adrenal insufficiency. In contrast, sex steroids are postnatally always low (Fukami et al., 2009; Homma et al., 2006; Krone et al., 2012), indicating that the 17,20 lyase activity of CYP17A1 greatly depends on POR, which has also been consistently described by *in vitro* functional activity assays (Huang et al., 2005; 2008; Fluck et al., 2008; Dhir et al., 2007). 17OHP levels are increased and can be clinically used as a screening tool in suspected cases; importantly, they are not as high as in (classical) 21-hydroxylase deficiency (Krone et al., 2012).

Disordered sex development (DSD) is a frequent finding in affected 46,XY males and can readily be explained as a consequence of prenatal androgen deficiency. However, 46,XX females can also present with ambiguous genitalia indicating prenatal androgen excess, similar to how 46,XX babies present in CYP21A2 deficiency. This puzzling and intriguing finding has been proposed to be caused by the presence of an alternative pathway towards androgen synthesis, that only exists prenatally and does not require testosterone as an intermediate step (Arlt et al., 2004). This pathway has been previously described in the tammar wallaby pouch young (Wilson, 2003) but its existence in the human foetus still needs to be conclusively proven. According to this hypothesis, 17OHP enters the alternative

pathway and is 5α-reduced to the intermediate 5α-pregnane-17α-ol-20-dione by the SRD5A1 isozyme. Further reduction at carbon 3 forms 5α-pregnane-17α-20-dione (also '5p-dione'), catalysed by HSD3As. Subsequently, 5p-dione serves as a substrate for the CYP17A1 17,20 lyase reaction (**Figure 13**) for the generation of androsterone. 17,20 lyase is also the key reaction to generate DHEA in the front door pathway (see section 1.1.8.1), and for both pathways, POR is required to deliver electrons from NADPH to CYP17A1 (see section 1.1.3.2); however, when 5p-diol (and not 17Preg) is the substrate for human CYP17A1, the catalytic efficiency is drastically increased and further increases 3-fold when CYB5A is added *in vitro* (Nebert and Russell, 2002; Gupta et al., 2003; Auchus, 2004). Androsterone is then further oxidized to androstanediol by HSD17B3 and finally its reduction at the A-ring via AKRCs yields DHT.

The existence of an alternative, prenatally active androgen pathway in humans seems to be conclusive and explains the masculinization observed in female PORD foetuses. It also explains the frequent observation that pregnant mothers carrying affected children experience virilization during pregnancy as 5α-reduced androgens produced in excess via the alternative pathway cannot be inactivated by placental aromatase prior to entering the maternal blood stream.

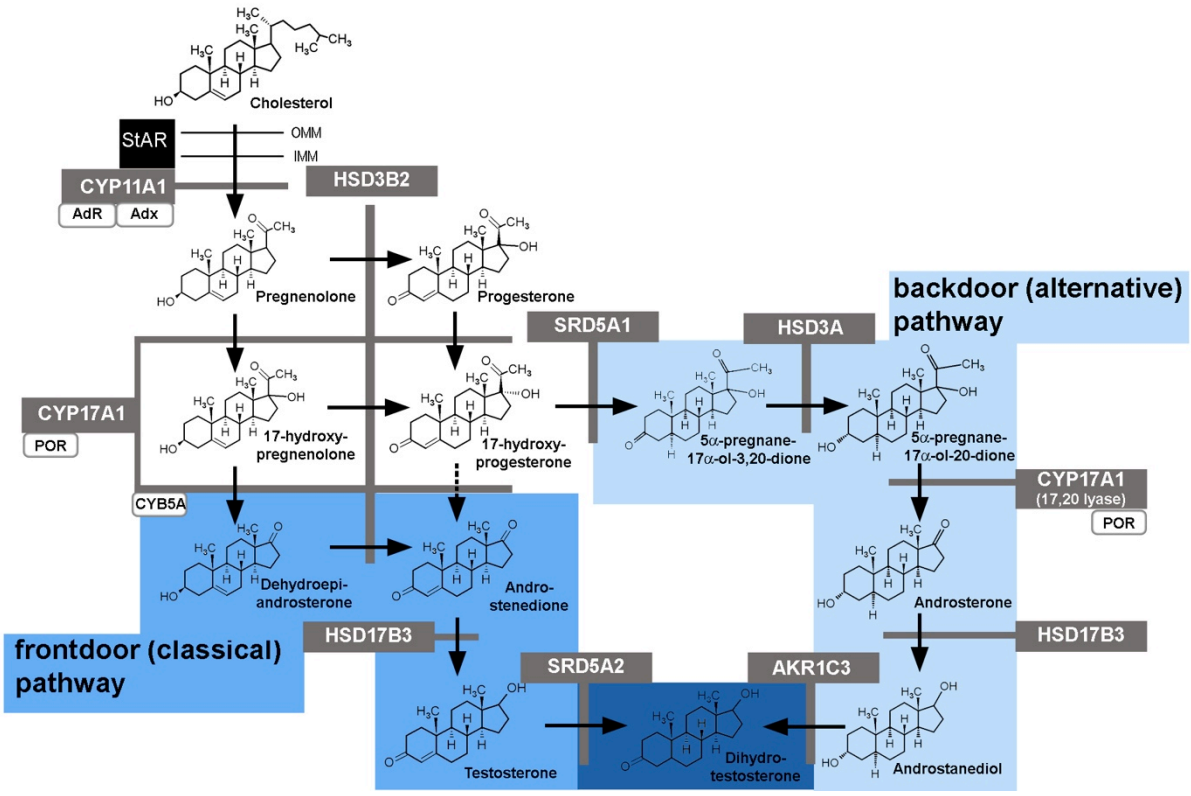

Figure 13: Schematic illustration of the classical (front door) and suggested alternative (backdoor) pathway to dihydrotestosterone.

Apart from abnormal steroid metabolism, the second striking and almost consisting finding in PORD is skeletal malformations. They are described as the Antley-Bixler syndrome (ABS) malformation phenotype, which can also be caused by mutations in the *FGFR2* gene (OMIM 207410). Malformations in PORD patients comprise a wide spectrum including craniosynostosis, midface hypoplasia/proptosis with choanal stenosis, as well as limb deformities (femoral/radio/humeral bowing) and arachno- and camptodactyly. The underlying mechanisms of how POR is involved in skeletal development still remain to be fully elucidated; however, it has been thought that mutant POR disrupts the activity of enzymes involved in sterol metabolism (14α-sterol demethylase, CYP51A1; squalene epioxygenase) (Kelley et al., 2002). In addition CYP26 iso-enzymes, which are involved in retinoic acid

metabolism, also require POR-dependent electron transport (Schmidt et al., 2009). Lastly, impairment of heptic drug metabolism has been reported in patients with PORD, which is due to the effects of impaired liver CYPs involved in the detoxification of xenobiotics (Tomalik-Scharte et al., 2010). This includes a significant involvement in key drug-metabolising enzymes CYP1A2, CYP2C9, CYP2C19, CYP2D6, and CYP3A4, which metabolise more than 80% of known drugs and xenobiotics; some of them are also involved in the inactivation of steroid hormones (Nebert and Russell, 2002).

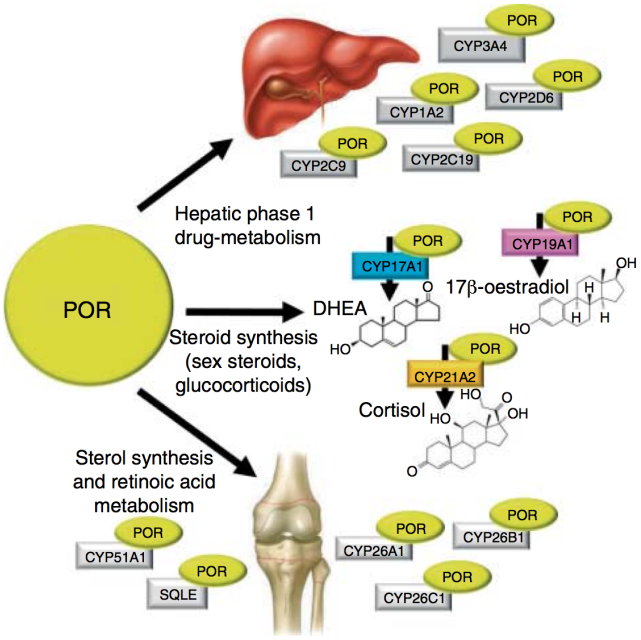

Figure 14: Overview of the key metabolic pathways that are supported by POR in human physiology. With kind permission from (Tomalik-Scharte et al., 2010).

The clinical presentation in PORD varies extensively with regards to GC deficiency, masculinization of 46,XX foetuses, maternal virilization and skeletal malformations (Fukami et al., 2009; Flück et al., 2004; Krone et al., 2012; Arlt et al., 2004; Adachi et al., 2004). Genotype-phenotype analysis and *in vitro* functional studies revealed that distinct POR mutations act differently on certain CYP enzymes. For example, the most common mutation in the Caucasian population, p.A287P,

predominantly inhibits CYP17A1 but catalytic activities for CYP21A2 and CYP19A1 are nearly fully retained (Dhir et al., 2007). In contrast, the global founder mutation most frequently found in the Asian population, p.R457H (Adachi et al., 2006), severely impairs CYP19A1 (Pandey et al., 2007) and CYP17A1 catalytic activities (Huang et al., 2005). Similarly, homozygous p.A287P has been consistently found in masculinized 46,XX females and is a predictor for moderate malformation severity; however, the overall genotype-phenotype prediction from larger cohorts is poor (Krone et al., 2012).

1.3.1.3. CRD and ACRD (HSD11B1 and H6PDH deficiencies)

The enzyme 11β-hydroxysteroid dehydrogenase type 1 (11β-HSD1) is important for amplifying glucocorticoid signals in target tissues such as liver, adipose and muscle by interconverting cortisol and its metabolically inactive metabolite cortisone (see section 1.1.7.2). Within the endoplasmic reticulum, 11β-HSD1 oxo-reductase activity, facilitating the regeneration of cortisol from cortisone, is dependent upon the maintenance of a high NADPH/$NADP^+$ ratio and NADPH is supplied by the enzyme H6PDH (1.1.7.2). However, as the 11β-HSD1 enzyme is not directly affected the altered ER redox environment subsequent to loss of H6PDH function permits an increase in 11β-HSD1 dehydrogenase activity, resulting in increased inactivation of cortisol to cortisone. In H6PDH KO mice this leads to insensitivity to feedback suppression of the HPA axis and resultant ACTH-mediated adrenal hyperplasia and elevated circulating glucocorticoid levels.

In humans, ‘apparent‘ cortisone reductase deficiency (ACRD) is characterized by decreased urinary excretion of cortisol metabolites and ACTH-driven adrenal androgen excess manifesting as premature adrenarche and PCOS (Draper et al., 2003; Lavery et al., 2008; 2012). To date, approximately twelve cases have been

reported in the literature that have a biochemical and clinical presentation consistent with ACRD. In six of these cases, a complete clinical, biochemical and genetic work-up has been published (Lavery et al., 2008; 2012). In all cases hyperandrogenaemia was confirmed with markedly elevated serum levels of DHEAS, androstenedione, and testosterone.

Genetic analyses determined a normal sequence of the *HSD11B1* gene in all affected individuals, but revealed inactivating mutations in the *H6PD* gene encoding H6PDH, including homozygous and compound heterozygous nonsense, missense and splicing mutations, which were all shown to disrupt enzymatic activity (Lavery et al., 2008; 2012). Thus, in ACRD, loss of H6PDH activity yields reduced 11β-HSD1 oxo-reductase activity and a concurrent gain in 11β-HSD1 dehydrogenase activity, resulting in enhanced peripheral clearance of cortisol thereby reducing the negative feedback suppression of the hypothalamic-pituitary-adrenal (HPA) axis, which in turn increases the ACTH drive and an ACTH-mediated increase in adrenal androgen secretion (see 1.1.7.2; **Figure 6**).

In most cases serum cortisol levels were within the normal range, as might be expected due to the compensatory increase in HPA axis activity. However, the urinary levels of cortisone metabolites were grossly elevated in all affected individuals, resulting in characteristically decreased ratios of cortisol over cortisone metabolites (5αTHF+THF/THE and cortols/cortolones, see **Figure 6**).

Only recently, heterozygous mutations of the HSD11B1 gene have been identified in two children presenting with milder forms of androgen excess (Lawson et al., 2011); these patients with ‘true’ cortisone reductase deficiency (CRD) showed a very similar biochemical fingerprint as the previous ACRD cases.

1.3.1.4. PAPSS2 and apparent DHEA sulfotransferase deficiency

Noordam and co-workers have reported a case in point, a girl who presented with premature adrenarche manifesting with pubic hair development at the age of 6 years (Noordam et al., 2009). She subsequently developed acne and hirsutism at 11 years of age and secondary amenorrhoea at 13 years of age, i.e. a phenotype progressing from premature adrenarche to a presentation resembling PCOS. Lab investigations revealed increased serum androstenedione and mildly elevated testosterone, with her body weight progressing from overweight to the obese range. However, her serum DHEAS levels were undetectable throughout whereas serum DHEA was at the upper limit of normal, suggestive of impaired DHEA sulfation as the driver of androgen excess. Surprisingly, genetic analysis did not reveal any mutations in the *SULT2A1* gene, which led to further exploration of mechanisms potentially impacting on DHEA sulfation. For catalytic activity SULT2A1 crucially depends on sulfate provision by the universal sulfate donor PAPS, which is generated by the two human isozymes PAPS synthase type 1 (PAPSS1) and type 2 (PAPSS2) (see section 1.1.9.1). Sequencing of the *PAPSS2* gene in the index patient revealed compound heterozygous mutations: a nonsense mutation, R329X, resulting in early truncation of the PAPSS2 ATP sulfurylase subdomain, and a missense mutation, T48R, located in an area of the PAPSS2 APS kinase domain that is crucial for protein function. *In vitro* assays demonstrated complete disruption of DHEA sulfation by the R329X nonsense mutation while T48R maintained 5% residual activity (Noordam et al., 2009). Interestingly, the mother of the patient, who carried R329X on one allele, developed symptoms of PCOS including obesity, oligomenorrheoa and hirsutism at the age of 30 years, suggestive of a possible impact of milder genetic variation in *PAPSS2* on presentation with androgen excess.

Of note, the patient also had short stature and showed mild signs of bone dysplasia that were not clinically apparent but revealed by x-ray. A severe bone phenotype [spondylometaphyseal dysplasia (SEMD)] has been previously reported to be linked with homozygous *PAPSS2* mutations void of any catalytic function in a large consanguineous Pakistani kindred (Haque et al., 1998). An androgen phenotype was not reported but the researchers were only allowed to examine male family members and learned that affected female individuals suffered from infertility.

These findings indicate that PAPSS2 deficiency has to be considered a multi-system disorder, which in principle is not surprising, as sulfation is a major metabolic reaction occurring in multiple tissue types and organs such as liver, bone and cartilage and is also involved in other endocrine pathways such as neuropeptide, thyroid and catecholamine signalling (Strott, 2002). Importantly, PAPSS2 deficiency reveals DHEA sulfation as a major regulator of human androgen synthesis, with impaired sulfation of DHEA to DHEAS resulting in increased conversion of DHEA to active androgens and subsequent androgen excess, which manifests with premature adrenarche and PCOS.

1.3.2. Premature adrenarche

Premature adrenarche describes the precocious onset of adrenal androgen secretion, traditionally defined as occurring as early as 8 years in girls and 9 years in boys. It is important to note that premature adrenarche is *not* equivalent to premature pubarche, i.e. the early appearance of pubic hair only. Indeed, there is some inconsistency in the literature where premature pubarche is often used synonymously for premature adrenarche.

A recently proposed definition of premature adrenarche is the concurrent presence of adrenal androgen levels increased above the age- and sex-specific

reference range and clinical signs of an increase in androgen action, such as adult-type body odour, oily hair and skin and/or premature pubarche, occurring before the age of 8 years in girls and 9 years in boys (Utriainen et al., 2007) (**Table 5**). The definition of the exact age limits should take influences of ethnicity into account. Two studies in Caucasian populations found pubic hair Tanner stage 2 or above before the age of 8 years in girls in 0.6% and 0.8% of American and Lithuanian girls, respectively (Zukauskaite et al., 2005; Rosenfield et al., 2009). By contrast, a five-fold higher incidence of premature pubarche was reported in girls of Afro-American descent (Herman-Giddens et al., 1997). All these studies focused on the premature appearance of pubic hair only and did not report on the incidence of other signs of increased androgen action such as adult-type body odour or oily skin. Thus the overall incidence of premature adrenarche may well be higher. Generally, the reported prevalence of premature adrenarche is about 10-fold higher in girls than in boys (Rosenfield, 1994).

Constitutional or idiopathic premature adrenarche (IPA) is most often observed, which is a diagnosis of exclusion. Distinct conditions manifesting with premature adrenarche include non-classic variants of CAH that have been diagnosed in 0-40% of children with premature pubarche (Utriainen et al., 2009; Armengaud et al., 2009; Dacou-Voutetakis and Dracopoulou, 1999; Temeck et al., 1987; del Balzo et al., 1992; Balducci et al., 1994), depending on the pre-selection bias applied to the studied cohorts. Other causes potentially underlying a presentation with premature adrenarche are summarized in **Table 5**.

Table 5: Definition and differential diagnosis of disorders presenting with childhood androgen excess.

Definition	Causes
Premature adrenarche = **Increased adrenal *androgen secretion*** above the age- and sex-specific normal reference range before the age of 8 years in girls and 9 years in boys (= premature biochemical adrenarche) AND **Clinical signs of *androgen action*** before the age of 8 years in girls and 9 years in boys including adult-type body odour oily hair and skin, acne pubic hair (= **premature pubarche)**, axillary hair AND **No signs of pubertal development** (i.e. no development of secondary sexual characteristics including breast development in girls or testicular/penile growth in boys)	**Most frequent:** Idiopathic (constitutional) premature adrenarche **Rare:** *Defects in steroid synthesis, metabolism or action:* Congenital adrenal hyperplasia - 21-hydroxylase deficiency - 11β-hydroxylase deficiency - 3β-hydroxysteroid dehydrogenase deficiency - Cushing's disease - Glucocorticoid resistance - (Apparent) Cortisone reductase deficiency - Apparent DHEA sulfotransferase (PAPSS2) deficiency *Other:* - Virilizing tumours originating from adrenals or gonad - Exogenous testosterone treatment
Precocious pseudo-puberty = Development of secondary sexual characteristics (penile growth, breast development, menarche) before the age of 8 years in girls or 9 years in boys AND Low gonadotrophins before and after GnRH stimulation GnRH-independent; usually non-harmonic chronology of sexual characteristics, e.g. lack of bilateral testicular enlargement in boys (exceptions: gonadal tumours, familial testotoxicosis) also termed *peripheral precocious puberty*	**Rare:** *Defects in steroid synthesis, metabolism or action:* Congenital adrenal hyperplasia - 21-hydroxylase deficiency - 11β-hydroxylase deficiency *Other:* - Virilizing tumours originating from adrenals or gonads - Exogenous sex steroid treatment - *LH- or HCG-driven stimulation of adrenal androgen production due to* - β-HCG-secreting tumours - Familial testotoxicosis (due to activating LH receptor (*LH/CGR*) mutations) - McCune-Albright-syndrome (due to activating Gsα protein (*GNAS1*) mutations)
Precocious puberty = Development of secondary sexual characteristics (testicular/penile growth, breast development, menarche) before the age of 8 years in girls or 9 years in boys AND Increase in gonadotrophins after GnRH stimulation GnRH-dependent; usually harmonic chronology of sexual characteristics, e.g. bilaterally enlarged testicular volume in boys	**Most frequent**: Idiopathic (constitutional) precocious puberty **Rare:** - Central nervous system lesions, e.g. glioma, astrocytoma, hypothalamic hamartoma, arachnoid cysts - post-infectious (e.g. meningitis, encephalitis) - post-traumatic - Hypothyroidism - activating mutations in the genes encoding kisspeptin1 (*KISS1*) and its receptor KISS1R (*GPR54*)

If in addition to the clinical signs and symptoms associated with premature adrenarche, progressive signs of pubertal development are present, such as breast development or menarche in girls and penile or testicular growth in boys, a diagnosis of precocious puberty or precocious pseudo-puberty has to be considered (**Table 5**). The clinical picture of these two distinct conditions is relatively similar. However, they can be distinguished by analysing the gonadotrophin response to GnRH stimulation. Accordingly, in precocious pseudo-puberty the gonadotrophins are low and remain low after GnRH stimulation. The condition is rare and most of the identified cases in boys are due to simple virilizing and non-classic CAH variants. In CAH, transition from precocious pseudo-puberty to secondary central precocious puberty has been observed and is thought to be due to the induction of the GnRH pulse generator by persistently increased sex steroids (Pescovitz et al., 1984).

1.3.2.1. Metabolic risk in premature adrenarche

Traditionally, idiopathic premature adrenarche (IPA) has been considered to be an extreme variation of normal (Silverman et al., 1952; Voutilainen et al., 1983; Ibanez et al., 1992). However, a series of studies in children with early onset androgen excess provide increasing evidence for the notion that IPA in girls may precede the development of the polycystic ovary syndrome (PCOS). PCOS manifesting during adolescence or early adulthood carries a significantly increased risk of developing the metabolic syndrome (Rosenfield, 2007; Ibáñez et al., 2000; 2009; Ehrmann, 2005) and represents the leading cause of female infertility (Ibanez et al., 1993; Ibáñez et al., 1999; Asuncion et al., 2000). IPA and adolescent PCOS are linked by two similarities, early onset androgen excess and an increased prevalence of insulin resistance.

The first evidence for a link between premature androgen excess and metabolic syndrome emerged in 1995 from a study in American-Hispanic girls who presented with premature pubarche and evidence of insulin resistance (Oppenheimer et al., 1995). Later on, Ibanez and co-workers published a series of case-control studies in lean Spanish (Catalonian) girls with a history of premature pubarche (PP) that showed evidence of insulin resistance based both on fasting insulin levels and the insulin response to a standard oral glucose tolerance test (oGTT) (Ibanez et al., 1996; Ibáñez et al., 1997; 1998; 2002; Potau et al., 2003). In PP girls from North America, an inverse correlation between insulin sensitivity and ACTH-stimulated Δ5-androgen precursors (17-hydroxypregnenolone, DHEA) has been found, however, the study population was not BMI matched (Vuguin et al., 1999). Overall, impaired insulin sensitivity is a consistent finding in the majority of studies. However, an association of PA/PP with dyslipidaemia, PCOS and neonatal growth restriction is a matter controversy with reported as an inconsistent finding in various study cohorts [see (Idkowiak et al., 2011) for an extensive review].

In conclusion, more research and in particular well-controlled longitudinal studies are required to confidently correlate early-onset androgen excess with metabolic risk in later life.

1.4. AIMS AND HYPOTHESES

The aim of this thesis is to investigate the role and the regulation of androgen producing enzymes of the adrenal gland in human disease states characterized by androgen deficiency or androgen excess. Of particular interest in this work are co-factors or co-enzymes supporting steroid modifying enzymes, like P450

oxidoreductase, cytochrome b5 and PAPS synthases (see chapters 1.1.3 and 1.1.9.1).

This will be examined in the first part of this thesis (chapter 3-6) by clinical, biochemical, genetic and *in vitro* experimental studies of individual children presenting with a distinct clinical phenotype. In all studies, we will explore *ex vivo* steroid mass-spectrometry techniques to elucidate underlying conditions and hypothesize that they provide powerful diagnostic tools to diagnose, and differentiate between, distinct steroidogenic defects and co-factor deficiencies.

Secondly, in chapter 7 we will investigate in *in vitro* studies the regulation of DHEA sulfation by the two known PAPS synthase isoforms, PAPSS1 and PAPSS2. As only deficient PAPSS2 has been previously shown to cause androgen excess (Noordam et al., 2009), we addressed the question why ubiquitously expressed PAPSS1 can not compensate for defect PAPSS2. We hypothesize that a different pattern of subcellular localization of the two isoforms explains the observed superiority of PAPSS2 in the context of DHEA sulfation.

In chapter 8 of this thesis, we will further investigate the concept of DHEA sulfation in pre-receptor androgen metabolism. We have conducted a clinical study in boys and young men with a genetic defect in the steroid sulfatase (STS) enzyme. STS counteracts DHEA sulfation and thus works in the opposite direction of DHEA sulfotransferase and PAPS synthases. The aim of this study is to explore androgen metabolism in these individuals and we hypothesize, in line with previous observations (Hammer, 2005), that STS does not play a major role in the regulation of active androgen levels. Ultimately, we anticipate gaining a deeper understanding of the physiological role of STS during childhood adrenarche.

2. CHAPTER 2: GENERAL METHODS

2.1. CELL CULTURE TECHNIQUES

2.1.1. Human embryonic kidney (HEK) 293 cells

HEK293 cells are derived from human embryonic kidneys extracted from an aborted foetus in the 1970s and generated by transformation with adenovirus 5 DNA (Graham et al., 1977). The cells were purchased from the American Type Culture Collection (ATCC). HEK293 cells were propagated in Minimal Essential Medium (Sigma, Pool, UK) supplemented with 10% foetal calf serum (FCS) (PAA, Etobicoke, Canada). To avoid bacterial contamination 1% penicillin/streptomycin was added to the medium (PAA, Etobicoke, Canada). The medium was replaced every two to three days and cells were passaged when reached they 90 and 100% confluence. The cells were discarded after reaching passage numbers more than P20.

2.1.2. COS7 cells

COS cells are derived from renal tissue of an African Green Monkey (*Cercopithecus aethiops)* and are fibroblast-like cells in nature. They were immortalized following transformation with an SV40 virus expressing the WT virus T-antigen. Cells were available in the lab from internal collaborators and propagated in Dulbecco's Modified Eagle's Medium (DMEM) supplemented with 10% foetal calf serum and 1% penicillin/streptomycin (all: PAA, Etobicoke, Canada). The medium was replaced every two to three days and cells were passaged when they reached 90 and 100% confluence. The cells were discarded after reaching passage numbers more than P30.

2.1.3. NCI-H295R cells

The NCI-H295 cell lines were derived in 1980 from a 48-year old female patient with an adrenal cortical carcinoma (Gazdar et al., 1990; Rainey et al., 2004). After changing growth conditions with alternative serum supplements, a substrain was developed (NCI-H295R) growing in adherent monolayer with a population doubling time reduced from five to two days; different substrains were generated and biochemically as well as enzymatically characterized (Rainey et al., 2004). For this work, the NCI-H295R1 substrain was used for siRNA knock-down and immunofluorescence studies, as it grows conveniently in monolayers and optimised transfection protocols were available. The R3 substrain, which has zona reticularis-like characteristics and grows in cell lumps, was used for fractionation studies only. The cells were obtained from Prof W. Rainey (Ann Arbor, Michigan, USA). The cells were propagated in Dulbecco's Modified Eagle's Medium/ Ham's F12 medium (1:1) supplemented with 2% Nu-Serum, 1% ITS plus (both Collaborative Biomedical Products, Bedford, MA, USA), 1% penicillin/streptomycin and 0.01% gentamicin (both Invitrogen, Carlsbad, USA). The medium was replaced every two to three days and cells were passaged after growing more than 90% confluent. Only cells with a low passage number (P6-12) were used for experiments.

2.1.4. Transient transfections of plasmid DNA into mammalian cells

Transfections for enzymatic activity assays and immunofluorescence studies were carried out in 6-well plates (Greiner Bio-One, Stonehouse, UK). 24 hours before transfection cells were seeded at the appropriate concentration (cells/well as determined in pilot experiments; see **Table 6**) to reach 70-90% confluency for assays (10-20% for IF studies allowing the observation of single cells) prior to transfection. Cells were transiently transfected with 2 µg of plasmid DNA and XtremeGene HP®

transfection reagent (for each cell-type, an optimal amount of transfection reagent [µl] has been determined in preliminary experiments to reach a transfection efficiency of 60-90%; see **Table 6**). The manufacturer's protocol was followed meticulously.

Table 6: Optimised conditions for transient transfections according to the different cell-types used for this work. IF: immunofluorescence.

Cell line	No. of cells to seed in a 6-well plate 24h prior to transfection	Ratio transfection reagent (µl): plasmid DNA (µg)
HEK 293	Assays: 75×10^4 IF: 30×10^4	2:2
COS7	Assays: 30×10^4 IF: 10×10^4	2:2
NCI-H293R	Assays: 100×10^4 IF: 20×10^4	5:2

Prior to the experiment, the transfection reagent (kept at -20C) was transferred to room temperature, allowing equilibration to +15 C° - +25 C°. Per transfection, 2 µg of plasmid DNA (dissolved in ddH_2O) was diluted into a total volume of 100 µl with serum-free cell culture medium in a 1.5 ml reaction tube. Then, the vial containing the transfection reagent was vortexed for 2-3 seconds at low force and the optimised amount (**Table 6**) was pipetted into the DNA containing tube, without touching the wall of the tube. The reaction was gently mixed and incubated for 15 minutes at RT. Medium from the cells was replaced with 2 ml of fresh, pre-warmed (37°C) full growth medium. Then, the transfection complex was added dropwise to the cells and subsequently the well was gently swirled for about 5 seconds for mixing. The expression optimum was usually between 36 and 50 hours post transfection. Cells were then processed as described in sections 7.2.5 and 2.5.3.4.

2.2. RNA AND DNA METHODS

2.2.1. RNA extraction using TriReagent®

For isolation of total RNA from cultured cells or tissues, TriReagent® (Sigma, Pool, UK) was used. The method is based on a protocol published by Chomczynski using the acid guanidinium thiocyanate following a phenol-chloroform extraction (Chomczynski and Sacchi, 1987).

Usually, 1 ml of TriReagent® was added to one to three wells of confluent monolayer cells growing in six-well cell-culture plates (Greiner Bio-One, Stonehouse, UK). The cells were incubated for one to five minutes, which resulted in homogenization and lysis of the cells. Then, the homogenate was transferred into 1.5 ml microcentrifuge tubes. Per 1 ml of TriReagent®, 0.2 ml of chloroform was added, mixed and incubated for 15 minutes at RT. During centrifugation (4°C; 12,000 g for 10 minutes), the solution separated into 3 phases: an upper aqueous phase containing the RNA, a middle white-dense layer containing (genomic) DNA, and the bottom pink organic phase containing protein. The upper aqueous phase was carefully removed into a new tube and 0.5 ml of isopropanol was added to precipitate the RNA. After gentle mixing and 15 minutes incubation at RT, the solution was centrifuged (4°C, 15,000 g for 20 minutes) to form a solid, white pellet. The pellet was washed once in 70% ethanol and centrifuged again for 10 minutes (4°C for 10 minutes). The supernatant was removed and the pellet was dried in air for not more than 15 minutes at RT. Finally, the pellet was resuspended in nuclease-free water, immediately processed (all steps on ice) or stored at -80°C.

Prior to processing the RNA to cDNA synthesis, the integrity of the sample was checked by agarose gel electrophoresis containing 1:10,000 GelRed® staining for nucleic acids. Intact totalRNA samples should show clear bands for 18S and 28S

ribosomal bands after visualization under ultraviolet light, with the 28S ribosomal band being twice as intense as the 18S band.

2.2.2. Quantification of RNA/DNA

The concentration of the RNA and DNA was measured by spectrophotometry using a Nanodrop ND-1000 device (Thermo Scientific, Cheshire, UK). Nucleic acids absorb maximum light at 260 nm, which is the principle of this method to determine the optical density (OD) of a nucleic-acid containing solution. One OD_{260} unit is equivalent to 40 µg single stranded RNA (or 50 µg for double-stranded DNA). Simultaneous measurement at 280 nm indicates protein contamination of the sample. A 'clean' sample should have a 260/280 nm OD ratio between 1.8-2.0.

2.2.3. Reverse transcriptase (RT) cDNA synthesis from RNA

Reverse transcriptase (RT) is an enzyme derived from a recombinant Moloney murine leukaemia virus (rMoMuLV) that uses single stranded RNA as template in the presence of a primer to generate single stranded, complementary DNA (cDNA). As primers, hexamers were used that bind randomly to the RNA template.

The kit MultiScribe™ Reverse Transcriptase (Life Technologies, Carlsbad, USA) was used for all RT reactions. 700 ng of total RNA (extracted as described under 2.2.1) was used as a template. In the presence of 5.5 mM $MgCl_2$, 500 µM dNTPs (each), 2.5 µM random hexamers, 0.5 U/µl RNAse inhibitor and 3.125 U/µl RT, the RNA was incubated in the supplied reaction buffer in a final volume of 20 µl for 10 minutes at 25°C, with further incubation steps at 37°C (60 minutes) and 48°C for 30 minutes. Subsequently, the reaction was stopped and the enzyme denatured at 95°C for five minutes. Reactions were carried out in a thermal cycler (TProfessional Basic, Biometra, Goettingen, Germany). For further PCR analysis and processing, the reaction was 1:20 diluted with ddH_2O.

2.2.4. Agarose gel electrophoresis

PCR products, total RNA, but also plasmids and inserts following restriction digest for molecular cloning were analysed by agarose gel electrophoresis. 1% (w/v) SeaKam® agarose (Lonza, Amboise, France) was dissolved in Tris borate buffer (TBE; 89 mM Tris base, 89 mM boric acid, 2 mM EDTA). To dissolve the agarose, the solution needs to be heated until boiling in a microwave and gently stirred by shaking in a conical glass flask. Upon cooling down to 40-50°C, GelRed® Nucleic Acid Stain (Biotium, Hayward, CA, USA) solution was added in a 1:10,000 dilution and gently stirred until the dye dissolved in the liquid agarose. Then, the solution was poured into a gel cast and cooled down until solid. Nucleic acid solutions were loaded into the gel pockets in an appropriate amount (minimum estimated DNA amount: 100 ng) and electrophoresis was carried out at 100-120V in TBE buffer for 60 minutes. As a loading control, HyperLadder I (Bioline, London, UK) was used. The bands were analysed under UV light and documented employing a gel doc system with digital camera (SynGene G:Box, Geneflow, UK).

2.2.5. Ethanol precipitation of DNA

DNA was precipitated in the presence of positive ions and abundance of ethanol. Generally, 1/10 volume of sodium acetate (NaAc; 3M, pH 5.2) was added to the DNA sample in a 1.5 ml reaction tube and gently mixed by pipetting up and down. Then, 3 x volume of at least 95% ethanol was added to the sample, thoroughly mixed and incubated for 15 minutes at RT. The DNA was pelleted by centrifugation for at least 30 minutes at > 14,000 g in a table-top centrifuge at 4°C (model 5451R; Eppendorf, Cambridge, UK). The supernatant was carefully removed with a pipette and then 70% ethanol was added and the tube briefly vortexed to wash the pellet. Following centrifugation at > 14,000 g for 10 minues, the ethanol was removed and

the pellet dried for 15-20 minutes at RT. Finally, the DNA was dissolved in nuclease-free water.

2.2.6. Extraction of DNA from agarose gels

For DNA extraction from agarose gel, a kit ('QIAquick gel extraction kit') was used and the instructions from the protocol provided by the manufacturer were followed (Qiagen, Manchester, UK). After separation of the DNA by agarose gel electrophoresis (2.2.4), the bands were visualized under UV light and carefully isolated by using a fresh scalpel. The DNA/agarose fragments were transferred into reaction tubes and weighed. The agarose was dissolved in QG buffer at 50°C and subsequently loaded on a column provided with the kit. After centrifugation with a tabletop centrifuge (model 5451R; Eppendorf, Cambridge, UK) for one minute at 13,000 g, the flow-through was discarded and the membrane washed by centrifugation with additional QG buffer to reduce agarose contamination. Then, the membrane was washed with PE buffer containing ethanol and completely dried by a final centrifugation step at full speed for one minute. Finally, to wash the DNA off the membrane, ddH_2O or TE buffer (30-50 µl) was loaded on the membrane of the column, which was placed in a fresh reaction tube; after incubation for one minute, the column was centrifuged again at full speed for one minute and the DNA-containing flow-through was used for subsequent experiments.

2.2.7. Transformation of plasmids into bacteria

A competent *E.coli*-based cell strain (K12 background) was used for chemical transformation of plasmid DNA (α-select; Bioline, London, UK). For routine sub-cloning of plasmid DNA, bronze-efficient cells were used; for plasmid construction and cloning of limited amounts of plasmid DNA, gold-efficient cells were used. The plasmid DNA was pipetted into a pre-chilled (on ice) 1.5 ml reaction tube and the

bacteria, stored at -80°C, were gently thawed on ice for 10-15 minutes. Then, 20-50 µl of bacteria where added to the DNA, gently mixed by pipetting 2-3 times up and down and subsequently incubated for 30 minutes on ice. Then, the bacteria were heat-shocked for 30 seconds at 42°C and then immediately transferred back to the ice. After 2 minutes incubation, the bacteria were suspended in 500 µl of LB-medium and incubated for 30 minutes at 37°C. Bacteria were then pelleted by gentle centrifugation (1,000 g for 1 minute), the supernatant was discarded and the bacteria dissolved in 50 µl of LB medium. With the use of a spreader, the bacteria were plated on pre-warmed (37°C) LB-agar plates containing the appropriate antibiotics. After 18-24 hours incubation at 37°C, single colonies grew on the plates, which were picked for plasmid preparation and analysis (see next section).

2.2.8. DNA plasmid purification from bacteria

A kit was used for plasmid preparation from cultures of transformed DH5α E.coli strains (Qiagen, Manchester, UK). Depending on the amount of bacterial culture, the 'mini' (up to 10 ml) or 'midi' (up to 150 ml) kit was used, and the instructions as stated in the manufacturer's protocol were followed. The principle is based on a method for alkaline lysis of bacteria (Birnboim and Doly, 1979). Under alkaline conditions, the cytosolic plasmid is released (lysis) and following neutralization under high salt conditions, the DNA is selectively bound to a silica membrane, then washed and purified.

All steps were carried out at RT using a tabletop centrifuge (model 5451R; Eppendorf, Cambridge, UK). Overnight cultures (5-10 ml) were pelleted at 5,000 g for 10 minutes; the supernatant was discarded and the pellet re-dissolved in 250 µl buffer P1. Then, 250 µl NaOH-containing buffer P2 was added to initiate the cell lysis, and the tube was gently inverted 8-10 times to ensure homogenization of the

sample. Finally, 350 µl of neutralising buffer P3 was added, resulting in protein precipitation. The whole lysate was centrifuged at full speed (13,000 g for 10 minutes) and the supernatant was carefully poured onto the columns containing the silica membrane. After centrifugation (full speed, 1 minute), the flow-through was discarded and the membrane was washed with 750 µl ethanol-containing PE buffer by centrifugation (1 minute, full-speed). Following removal of the flow-though, the column was centrifuged for another minute at full speed to remove residual buffer. Finally, 50 µl of ddH_2O was added onto the membrane and incubated for one minute to elute the DNA. After centrifugation in a fresh reaction tube, the DNA content of the flow-through was quantified with spectrophotometry.

2.2.9. Polymerase chain reaction (PCR)

The PCR is a technique that amplifies DNA by using the enzyme DNA polymerase. Two pre-designed oligonucleotides (primers) anneal to distinct, complementary parts of the DNA, one at the 5'-position, the other one at the 3'-position of the desired fragment to be amplified. Then, the polymerase, traditionally derived from *thermus aquaticus*, hence called Taq polymerase, extends the DNA downstream (5'→3') from the primer, generating a new DNA strand. This strand serves as a template for the generation of further DNA strands in subsequent cycles of the reaction, yielding an exponential amplification of DNA fragments.

The standard Taq polymerase was purchased from Bioline (London, UK); for PCR-based cloning, a mixture of two polymerases, Taq- and Tgo-polymerase, were used, as the latter one, derived from *thermococcus gorgonarius*, possesses a pronounced 3'→5' exonuclease activity. This 'proofreading' ability of the enzyme reduces the error rate from 1.3×10^5 (Taq) to 4.9×10^7 (Tgo) resulting in a high fidelity of DNA synthesis (Keohavong and Thilly, 1989). The enzymes were

purchased from Roche as part of the Expand High Fidelity PCR System™ (Roche, Basel, Switzerland).

All reactions were carried out in a 25 µl total reaction volume. The following components were added (final concentration): reaction buffer (1x), $MgCl_2$ (1.5-4 mM), forward and reverse primer (0.4 µM), dNTPs (200 µM each) (Bioline, London, UK), DNA polymerase (0.05 U/µl), 10-15 ng of DNA template.

Reactions were carried out in 200 µl reaction tubes (Sigma, Pool, UK) in a thermal cycler (TProfessional Basic gradient, Biometra, Goettingen, Germany). After one initial denaturation step (95°C, 5 minutes), 32-35 cycles followed with 1) 95°C for 1 minute (denaturation), 2) 60°C for 30 seconds (primer annealing) and 3) 72°C between 30 seconds and 2 minutes (elongation). After the last cycle, a final elongation step of 5 minutes at 72°C was performed. The duration of cycle step 3) depends on the length of the DNA fragment to be amplified; it was calculated based on the capacity of the polymerase, which is about 1000 bp per minute. Fragments were analysed by agarose gel electrophoresis (2.2.4).

2.2.10. Real-time quantitative (RTQ) PCR

RTQ-PCR is an enhancement of the PCR and measures the amplification of DNA strands at each cycle, i.e. in real time. Essentially, it has the same components of a standard PCR; its principle relies on the 5'→3'-exonuclease activity of the polymerase and the presence of a 20-60 bp oligonucleotide probe that binds to the DNA template in-between the primer pairs. This probe has a fluorophore at its 5' end and a quencher at its 3' end, that silences the emission of fluorescence when both quencher and probe are in close proximity, as in intact oligonucleotides. During amplification, the probe binds to the synthesized DNA strands and gets degraded by the 5'→3'-exonuclease activity of the enzyme, which removes the quencher from the

fluorophore. Then, the probe is able to emit fluorescent light when excited and the amount of fluorescence detected in the sample directly correlates with the amplified DNA in the sample, but it also correlates to the amount of DNA template that was initially added into the PCR reaction.

During the initial RTQ-PCR cycles, the DNA is amplified exponentially, until the amplification is saturated, mainly as a consequence of the consumption of the dNTPs or exhaustion of the enzyme. To compare the amount of DNA in a sample, a threshold needs to be determined when the DNA is amplified exponentially; the threshold allows the calculation of threshold cycles (Ct) for each target, which essentially correspond to the amount of template added to the sample or the mRNA-expression in a sample, whose RNA was extracted and transcribed into cDNA by RT reaction. Importantly, the lower the Ct values are, the higher the gene of interest is expressed. To determine the relative expression of a gene, the Ct values of a constantly expressed housekeeping gene (i.e. 18S) can be subtracted from the gene-specific Ct values; these resulting delta Ct (dCt) values correct for equal sample loading and were used for calculations.

All assays (a pre-mix of gene-specific primers and probes) and the Taq polymerase mastermix were purchased from Applied Biosystems (Quarrington, UK). The RTQ-PCR reactions were carried out in a 7500 ABI qPCR machine (Applied Biosystems, Quarrington, UK) and the data were analysed with the product-specific software. The total reaction volume was 10 µl, consisting of 5 µl mastermix, 0.5 µl TaqMan gene expression assays and 4.5 µl of cDNA sample (see 2.2.3; 7.8 ng mRNA-equivalent cDNA). Reactions were carried out in duplicate and 18S was used as a housekeeping gene. All TaqMan assay probes were labelled with 6-carboxyfluorescein (FAM), the 18S probe with the VIC® fluorophore.

2.2.11. Sequencing analysis

DNA sequencing analysis was performed after obtaining informed consent and assent from patients and their parents with approval of the local institutional review board committees.

After genomic DNA extraction from peripheral leukocytes utilizing a blood and cell culture DNA kit (Qiagen, Hilden, Germany), the mutation analysis was performed by PCR of the respective gene with primer pairs covering the whole coding region, including the intron-exon boundaries (**Table 7**). The PCR conditions are described in section 2.2.9. The PCR fragments were checked for integrity and correct size (**Table 7**) by agarose gel electrophoresis (section 2.2.4) and subsequently purified with the QIAquick PCR purification kit, following the manufacturer's protocol (Qiagen, Hilden, Germany). 5-10 ng of purified DNA template with 3.2 pmol of primer (the same as used for PCR amplification; see **Table 7**) was processed for electrophoresis on an automated ABI PRISM 310 Sequencer and analysed with the ABI SeqScape 1.1 software (Applied Biosystems Inc., Weiterstadt, Germany). Sequencing analysis was performed using Lasergene® software (DNASTAR Inc., Madison, USA) and mutation numbering was carried out referring to the NCBI reference sequences: POR: NG_008930.1 (genomic) and NP_000932 (protein); CYP17A1: NG_007955.1 (genomic) and NP_000093 (protein); *CYB5A*: NG_023211.1 (genomic), NP_683725.1 (protein). For DNA numbering, the nucleotide designated +1 was the A of the ATG start codon.

Table 7: Primer sequences, annealing temperatures (T_m) and expected fragment sizes following PCR amplification of the exons of *CYP17A1, POR and CYB5A* from genomic DNA.

Name	Sequence (5'-3')	Tm (C)	Fragment size (bp)
CYP17A1			
CY17A1 - 1F	TCTAGGCTCAGAGAGAGGTG	65.1	650
CY17A1 - 1R	GGGCTCCAGGAGAATCTTTC	63.9	
CY17A1 - 2F	GGTGTGAGATTCCTACGCC	61.1	676
CY17A1 - 3R	TCTACAGAACCTGAAGGCAG	57.8	
CY17A1 - 4F	GGTGGAGTAGGAACTTCCAS	60.1	316
CY17A1 - 4R	TGTGCCAGGTTCTCTGCTT	66.6	
CY17A1 - 5F	CCTGCCCAGACTTGCTCTAC	63.9	935
CY17A1 - 6R	CTGACTTTAGGTTGGCCAGCA	66.3	
CY17A1 - 7F	AGCTGTTCAGACAGAAGCGC	64.6	1259
CY17A1 - 8R	GGCATTGCCACAAGCTGAAA	68.3	
POR			
POR - 1F	AGT GAC CAT TTC CTG CAG	58.7	368
POR - 1R	ACT GCT TGG AGT GGT GAC AG	63.0	
POR - 2F	ATG ACA CCT GCC TCC CAC	63.8	159
POR - 2R	GAC TTG ATT ACA TGC CCA TCG	64.1	
POR - 3F	GTG GCT GAG GTC TGT GGC	64.9	241
POR - 3R	TAC AGA CCT GCT CCC TGT CC	64.3	
POR - 4F	TTG AAC AGG CTC AGT CAT GG	63.9	236
POR - 4R	TGG AGT CCC CAG GGA GG	66.5	
POR - 5F	CCA CTG GTC AGG TCG AGG	64.6	232
POR - 5R	CAC GGC CCC TGC CTA AG	66.8	
POR - 6F	ACA GTC CTG AGC TTT GGG G	64.2	303
POR - 6R	CTT CTA ACC TTG CTG CGA CC	63.7	
POR - 7F	TGT AGT CCA ACC CCT CCC TC	65.2	218
POR - 7R	AGT GGC CAT AGA GCC GTC TG	66.6	
POR - 8F	GTG CTT TGT GCA ACC AGA AG	63.5	515
POR - 9R	GCC TAA GCA GAA GCT CAA CC	63.0	
POR - 10F	GAG CAT AGG CCT TGT TTC CA	64.0	544
POR - 11R	CTT GCA CTC TGC CTG CTG T	64.6	
POR - 12F	CTG CAG AAC GGG ACT TGG	64.6	649
POR - 13R	AAG GGT GGT GCT GTG AGG	63.9	
POR - 14F	AGC AGT CCC ACA AGG TGA GA	64.9	583
POR - 15R	GGC TGA GGA GGA TGC AC	62.1	
CYB5A			
CYB5A - 1F	GCTCTGCTCCACCCCGAC	65.0	246
CYB5A - 1R	CAGTGAACCCCCAAACCC	65.3	
CYB5A - 2F	TGGTTAAATAAATTTCTGGCCG	62.4	276
CYB5A - 2R	GACTAGGGTAAGGTCATCTGATAGC	62.0	
CYB5A - 3F	AAGTCAGCATTTTGGAAGTGG	62.9	175
CYB5A - 3R	CCCTCTGCCTTCAGTTTGAC	63.7	
CYB5A - 4F	AAGTTCAGATTCCCTTGAAC	62.0	144
CYB5A - 4R	CAAACCTGGACCCATGACC	64.3	
CYB5A - 5F	AGTCCACCACAGTGCACATC	63.9	199
CYB5A - 5R	GCAATGGCTTCTTTTCTCCC	64.3	

2.3. PROTEIN METHODS

2.3.1. Protein preparations

Protein for Western blot analysis was either derived from whole cell lysates of mammalian adherent cell lines or from purified yeast microsomes (see sections 3.2.4 and 6.2.6).

Adherent cells were usually grown until confluency in 6-well plates; cells from one or two wells (combined) were used for protein extraction. All steps were performed on ice with PBS containing proteinase inhibitor (Complete™ Protease Inhibitor Cocktail, Roche, Basel, Switzerland). After washing (2x in PBS) the cells to reduce contamination with cell culture medium and serum, the adherent monolayer was gently detached with a scraper in 0.5 ml PBS/well and loose cells transferred into 1.5 ml reaction tubes. To release the protein and disrupt the cell membrane, the homogenate was sonicated (three times for 15 seconds, medium power) with a Bioruptor® Professional sonicator (Diagenode, Liege, Belgium). The cell lysate was subsequently centrifuged with a tabletop centrifuge (4°C) at 10,000 g for 10 minutes and the supernatant containing the protein transferred into a fresh reaction tube.

2.3.2. Protein quantification

Protein extracts were quantified with a colourimetric assay (Bio-Rad Protein Assay, Bio-Rad, Hemel Hempstead, UK), which is based on the Lowry method (Lowry et al., 1951). The reaction of the protein with 1) an alkaline copper tartrate solution and 2) folin reagent, which reduces the protein-copper complexes, results in a characteristic blue-coloured staining with maximum absorbance at 750 nm. The measurements were carried out on a 96-well microtiter plate. The protein concentration was derived from a standard curve, which was generated by a calibration series of known protein concentrations.

According to the manufacturer's protocol, 5 µl of protein standard (0, 0.5, 1, 2, 5, 8 and 10 mg/ml bovine serum albumin) or sample was added to each well (all reactions in duplicate). Then, 25 µl of solution A (containing Cu^{2+}-tartrate) followed by 200 µl Solution B (Folin reagent) were added to the protein sample. After 10-15 minutes incubation, the absorbance was measured at OD_{690nm} on a Victor3 1420 multilabel counter (Perkin Elmer, Bucks, UK).

2.3.3. Western blot

Western blotting is a technique to semi-quantify protein, i.e. to measure the relative content of a distinct protein in a heterogeneous protein extract. After the separation of proteins according to their size by denaturing SDS polyacrylamide gel electrophoresis (PAGE), the proteins are transferred onto a membrane, which consisted of nitrocellulose in this thesis. To detect and visualize the protein, indirect immunostaining with a primary antibody, targeted against the protein of interest, and a secondary antibody, which is labelled with a dye or enzyme (horseradish peroxidase [HPE], in this thesis) is performed. Incubation of the membrane with chemiluminescent agents result in light generation by HPE, which can be recorded by photographic film. To compare the protein content between different samples, the membrane can be co-stained with an antibody against a housekeeping protein to demonstrate that the amount of protein loaded has been kept constant.

Solutions for Western blot:

- **Loading buffer (4x):** 50 mM Tris-HCl pH 6.8, 2% SDS, 10% glycerol, 1% 14.7 M β-mercaptoethanol, 12.5 mM EDTA, 0.02% bromophenol blue.
- **Running buffer (20x):** NuPAGE MOPS SDS (Invitrogen).
- **Transfer buffer (10x stock):** 30.3 g Tris base, 144 g glycine in 1 litre of distilled water, adjusted using 5M HCL to pH 8.3.

- **Transfer buffer (working solution):** for 1 litre, 100 ml 10x stock solution + 200 ml 100% methanol + 700 ml H_2O
- **Washing solution:** 0.1% Tween 20 (Sigma, Pool, UK) in PBS.
- **Blocking solution:** 5% non-fat resuspended dried milk in washing solution.

All Western blot equipment was purchased from Invitrogen (Carlsbad, USA), unless stated otherwise.

Between 10 – 20 µg of protein were loaded per lane on a pre-cast NuPAGE® 10% SDS Bis-Tris gel and samples were run for 60 min at 200V in the XCell SureLock® Mini Cell Running Chamber in NuPAGE® MOPS running buffer. Subsequently, the protein-containing PAGE was transferred to a Hybond ECL nitrocellulose membrane (GE Healthcare), either immersed in transfer buffer at 30V for one hour in a transfer module, or by employing the iBLOT® DryBlotting system. To confirm the successful transfer of the protein, the nitrocellulose membrane was incubated with 1 ml of Ponceau S solution (Sigma, Pool, UK) for one minute at RT. Then, to block unspecific antigen binding, membranes were incubated with 10% (m/v) skimmed milk powder in phosphate-buffered saline containing 0.05% Tween 20 (PBST) (Sigma, Pool, UK) for one hour at room temperature on an orbital shaker. Subsequently, membranes were incubated with a primary antibody (concentrations varied between 1:200 and 1:1000 in 10% milk/PBST) overnight at 4°C. After washing with PBST (3 times for 10 mins), membranes were incubated with an IgG antibody conjugated with horseradish peroxidase (1:1000 in 10% milk/PBST) targeted against the species of the primary antibody for about one hour at room temperature. After washing with PBST, the protein bands were briefly incubated in enhanced chemiluminescence reagent (ECL, GE Healthcare, Bucks, UK) and exposed to a photographic film (Perkin Elmer, Surrey, UK) in a dark room for 30 seconds to 1 hour.

Films were developed in a Compact X4 automatic film processor (Xograph Imaging Systems, Gloucestershire, UK).

2.4. MOLECULAR CLONING AND SITE-DIRECTED MUTAGENESIS

To assess steroidogenic enzyme activities, different *in vitro* systems have been used to express either wild type or mutant enzymes. The functionality of these proteins was investigated by steroid conversion assays (see section 2.5).

In this work, human steroidogenic enzymes were either generated and subsequently isolated in baker's yeast (*saccharomyces cerevisiae*) or expressed in mammalian non-steroidogenic cell lines.

2.4.1. Expression vectors

2.4.1.1. pDE2 and V10 yeast expression vectors

For co-expression of POR with the respective CYP proteins (i.e. CYP21A1, CYP17A1 and CYP19A1) in *saccharomyces cerevisiae*, yeast expression vectors V10 and pDE2 (Hadfield et al., 1987; Pompon et al., 1996) containing the enzymes' cDNA were employed [kindly donated by Prof Walter Miller (University of California, San Francisco, USA)].

2.4.1.2. pcDNA™6/V5-6xHis mammalian expression vector

The pcDNA™6/V5-6xHis expression vector was employed for cloning human CYP17A1 cDNA before subcloning the WT and mutant variants (generated by site-directed mutagenesis) into the pIRES vector. The vector contains a V5-tag downstream of the multiple cloning sites, which is attached to the CYP17A1 cDNA during subcloning into pIRES in order to perform accurate Western blot analysis.

2.4.1.3. pIRES™ mammalian expression vector

The mammalian expression vector pIRES (Clontech, Mountain View, USA) was used for *in vitro* functional assays in HEK293 cells. It contains two cloning sites (A + B) downstream of a single CMV promotor, which are separated by an internal ribosome entry site (IRES) sequence derived from the encephalomycarditis virus. The IRES cassette allows ribosomal binding and initiation of translation from an additional internal site of the mRNA, which is usually only permitted at its 5'-cap. Hence, it allows the translation of two open reading frames (ORFs) from one mRNA and consequently equal expression of two proteins of interest.

The pIRES vector was employed to express a steroidogenic enzyme with a co-factor, i.e. CYP17A1 and CYB5A (see chapters 5 and 6) and SULT2A1 with PAPS synthase isoforms (see section 7.2).

2.4.2. Molecular cloning

Molecular cloning in this context means the targeted insertion of the CDS of a distinct protein into an expression vector. This is facilitated by the use of restriction endonucleases. For most expression vectors, a designated 'multiple cloning site' (MCS) downstream of the promotor contains a variety of restriction sites for enzymes to cut. The CDS can be enzymatically ligated into the linearized vector at this site, if it contains the same nucleotide overhang(s) at its ends. If both vector and insert were digested with the same two enzymes, there is only one possible orientation of the insert/CDS ('directional cloning').

2.4.2.1. Restriction digest

Restriction endonucleases are usually enzymes derived from bacteria that recognize nucleotide motifs (restriction sites) within double-stranded DNA molecules and cut the DNA. They evolved as defence mechanisms to protect the cell from viral

DNA. Most enzymes cut the DNA at restriction sites (type I enzymes); others cut the DNA a short distance away from the respective nucleotide motif. Each enzyme has a specific restriction site and a specific way of cutting the DNA, creating either blunt or sticky ends (**Figure 15**).

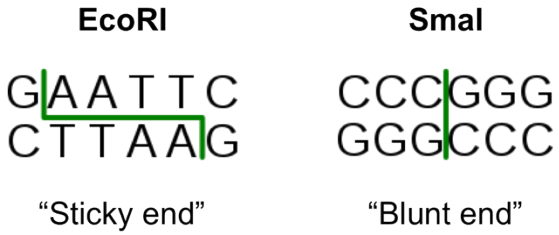

Figure 15: Two examples of restriction endonucleases. EcoRI (left) performs a sticky end digest and SmaI (right) a blunt end digest. The enzyme-specific recognized motifs are shown with the exact course of the cut indicated by the green line.

The protocols for restriction digests are similar for different enzymes: a specific buffer assuring optimum activity for the enzyme is crucial. The amount of the enzyme added and the length of the incubation varied, depending on the particular circumstances like the type of enzyme, amount of DNA, single/multiple cutting. The enzymes are delivered in unit per volume. By definition, one unit is the amount of enzyme necessary to digest 1 µg of λ DNA at 25°C in one hour in a total reaction volume of 50 µl. Some enzymes exhibit unspecific digestion outside the restriction sites (“star activity”), which makes it necessary to restrict the incubation time to a minimum. Double digests of DNA simultaneously with two different enzymes are possible, if the enzymes work well in the same reaction buffer.

For this work, all restriction enzymes were purchased from New England BioLabs (Ipswich, MA, USA).

For the digest of 1 µg of plasmid DNA with the restriction enzyme EcoRI (single cut), the following exemplary protocol has been used:

Reaction Buffer (10x)	5 µl
Template DNA (1 µg)	x µl
ddH_2O	x µl to a final volume of 50 µl
then add EcoRI (20,000 units/ml)	1-2 µl

Incubation for 60 minutes at 37°C, followed by heat inactivation of the enzyme for 5 minutes at 65°C. Subsequently, the digested DNA was analysed to check the completion of the digest by agarose gel electrophoresis (section 2.2.4) and then further processed for cloning after purification by ethanol precipitation (section 2.2.5).

2.4.2.2. Cloning with T4 DNA ligase

T4 DNA ligase is a bacteriophage-derived enzyme that catalyses the formation of phosphodiester linkages of adjacent nucleotides of double-stranded DNA molecules in an ATP-dependent fashion. The enzyme was purchased from Promega (Madison, USA).

The DNA insert was PCR-amplified with special hybrid primers that contain the gene-specific sequence at their 3'-ends and the restriction sites required for ligation into the vector at their 5'-end. By using these primers during a standard PCR with High-Fidelity®Taq/Pfo polymerases (section 2.2.9) the generated DNA contained the restriction sites at both ends. Following separation by agarose gel electrophoresis (section 2.2.4) and extraction from the gel (section 2.2.6), the purified DNA was digested with the appropriate restriction enzymes (section 2.4.2.1). The purified and digested insert and vector DNA were quantified to calculate the amount of vector and insert for the ligation reaction.

Usually, a 3:1 molar ratio of insert:vector was used for all ligation reactions and the amounts of DNA calculated by using the following formula:

$$\frac{ng\ vector\ x\ kB\ size\ of\ the\ insert}{kB\ size\ of\ the\ vector}\ x\ \frac{3}{1} = ng\ of\ insert$$

The standard protocol used to ligate a 1.5 kB insert into a 5 kB vector (50 ng) with a 3:1 molar ratio of vector to insert is as follows:

Ligase Buffer (10 x)	1 µl
Vector DNA (50 ng)	x µl
Insert DNA (75 ng)	x µl
T4 DNA Ligase (10 U)	1 µl
ddH_2O	x µl to a final volume of 10 µl

The mixture was incubated either in the fridge (4°C) overnight or at RT (20°C) for 4-6 hours. The ligation reaction as a whole, without purification necessary, was transformed into DH5α bacteria as described in section 2.2.7. Single colonies were picked and grown in small scale to prepare plasmid DNA, which was analysed by either direct sequencing or restriction digest.

2.4.2.3. Cloning with the In-Fusion™ kit

In-Fusion™ (Clontech, Mountain View, USA) is a PCR-based cloning method that works without the use of the ligase enzyme and is useful to clone either multiple DNA-fragments into one single vector or to facilitate cloning that is difficult with the traditional ligase-based technique.

First, PCR fragments are generated with gene-specific primers that have 15 bp extensions homologous to the ends of the linearized vector. The purified fragments are then fused into the vector by the In-Fusion™ enzyme that creates single-stranded regions at the end of insert and vector. Finally, the generated constructs are transformed into bacteria for selected amplification.

The primer sequences were designed based on the manufacturer's specification with the help of an online tool provided by Clontech (http://bioinfo.clontech.com/infusion/) and purchased from Sigma (Pool, UK). The PCR was performed under standard conditions with the High-Fidelity Taq/Pfo polymerase (see section 2.2.9). Plasmids were linearized by restriction digest (section 2.4.2.1), and both linearized plasmids and PCR products were run on an agarose gel (section 2.2.4), purified by extraction from the gel (section 2.2.6) and quantified (section 2.2.2).

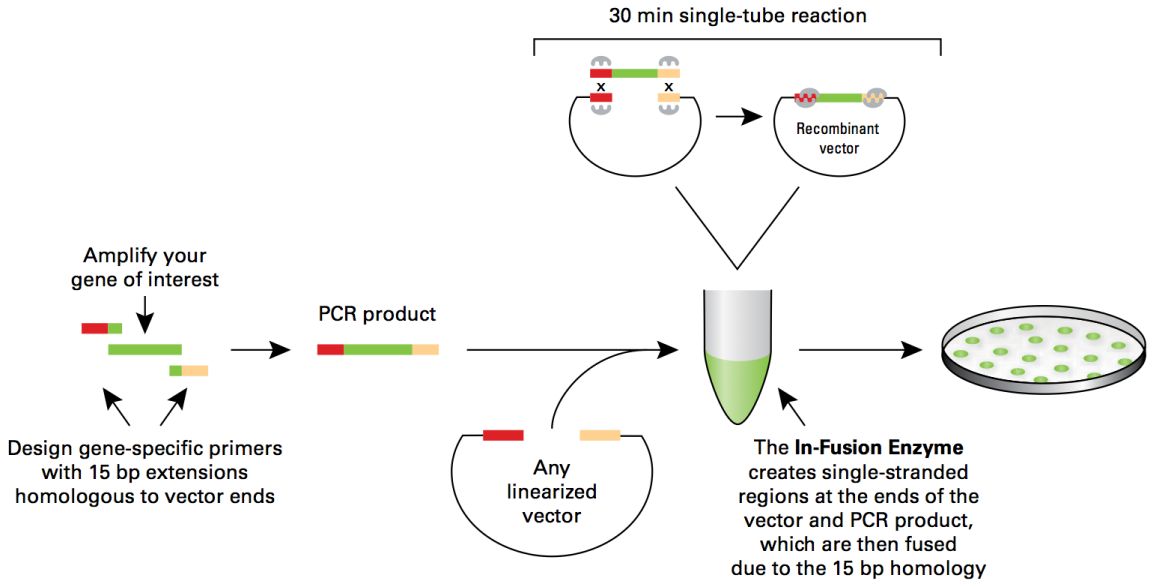

Figure 16: Overview of the In-Fusion™ cloning method (from the manufacturer's protocol).

For a standard cloning procedure with linearized vector and column-purified insert, the following reagents were combined in a 200 µl PCR-reaction tube:

Reaction Buffer (5x)	2 µl
Linearized Vector DNA (100 ng)	x µl
Insert DNA (50 ng)	x µl
In-Fusion™ Enzyme	1 µl
ddH_2O	x µl to a final volume of 10 µl

Then, the mixture was incubated for 15 minutes at 37°C, followed by another incubation step for 15 minutes at 50°C. Then, the mixture was kept on ice and brought to a volume of 50 µl with TE-buffer (pH 8). 2.5 µl of this mixture were added to 50 µl of gold-efficient DH5α cells for transformation as described in section 2.2.7. Single colonies grown on LB-agar plates with an appropriate antibiotic drug were selected for restriction digest and subsequently Sanger sequenced to check the integrity of the insert and to exclude mutations caused by faulty amplification of the polymerase.

2.4.3. Site-directed mutagenesis

Site-directed mutagenesis (SDM) modifies expression vectors to change the structure of a protein and further investigate the relationship between structure/mutation and functional abilities of the protein.

It is a PCR-based technique, where the entire vector DNA is amplified with primers introducing the desired mutation into the coding sequence of the protein. For all SDMs, the Quick-Change® II XL Site-Directed Mutagenesis kit was used (Agilent Technologies, Santa Clara, USA). The procedure is divided into three parts: 1) PCR amplification of the plasmid, 2) digestion of the plasmid template and 3) transformation of the modified plasmid into bacteria.

The primers were designed based on guidelines provided in the manufacturer's protocol: the desired length for the mutagenic oligos is 25-45 base pairs with a melting temperature (T_m) > 75°C. The following formula has been used to calculate the Tm of the primers:

$$T_m = 81.5 + 0.41(\%GC) - 675/(\text{number of nucleotides}) - \%\ \text{mismatch}$$

The desired mutation should be in the middle of the oligos, with equal amounts of nucleotides (10-15) on both sides; the GC content should be between 40% and 60%.

The digest of the parental template plasmid was performed with the endonuclease *Dpn* I (target sequence: 5'-Gm^{6}ATC-3'), which selectively digests methylated and hemi-methylated DNA, thereby selectively targeting the bacterial-derived template but not the PCR-amplified plasmid DNA.

The following components have been added into a 200 µl PCR-tube:

Reaction Buffer (10 x)	5 µl
Template DNA (10 ng)	x µl
Oligo Primer 1 (125 ng)	x µl
Oligo Primer 2 (125 ng)	x µl
dNTP Mix	1 µl
QuickSolution	3 µl
ddH_2O	x µl to a final volume of 50 µl
Then: *Pfu*Ultra HF DNA polymerase	1 µl

The following settings were used for all SDMs in a GeneAmp 9700 thermal cycler (Applied Biosystems, Foster City, USA):

Step	**Temperature**	**Length**	**Cycles**
1)	95°C	1 minute	1 cycle
2)	95°C	50 seconds	
	60°C	30 seconds	18 cycles
	68°C	10 minutes	
3)	68°C	7 minutes	1 cycle

After amplification, 1 µl (10 U/µl) of the *Dpn* I enzyme was added, gently mixed by pipetting up and down and then incubated for 60 minutes at 37°C to digest the non-mutated, supercoiled DNA. After digestion, the DNA was precipitated with 500 µl 100% ethanol in a 1.5 ml reaction tube for 2 hours at -20°C. After centrifugation (60 minutes, 13,200 g at 4°C in a 5415R Eppendorf centrifuge), the supernatant was

carefully removed and the pellet washed once in 70% ethanol. After a further 15 minutes of centrifugation (same settings as above), the supernatant was removed and the pellet was dried at RT for 15 minutes. Finally, the dry pellet was re-suspended in 10 µl of ddH_2O.

For the transformation, XL10-Gold ultracompetent cells were thawed on ice and an aliquot of 45 µl was transferred into a 1.5 ml reaction tube. 2 µl β-mercaptoethanol (provided with the cells) were added to the bacteria, gently swirled and incubated for 10 minutes on ice (with intermittent swirling every 2 minutes). Then, the bacteria were added to the DNA, gently homogenized by swirling the tube and incubated on ice for 30 minutes. The plasmid DNA was transformed by heat-shocking the cells at 42°C for 30 seconds, followed by 2 minutes incubation on ice. Then, 200 µl of LB medium was added and the bacteria were incubated for 30 minutes at 37°C. Finally, the bacteria were plated on LB-agar plates containing the appropriate antibiotic for selection and incubated overnight at 37°C until single colonies grew. 2-3 single colonies were picked, grown in 5 ml of LB medium (+ antibiotic) at 37°C, with shaking, overnight to prepare the plasmid DNA (see section 2.2.8). Finally, the whole coding sequence was analysed by direct sequencing (see 2.2.11).

2.5. ENZYMATIC ACTIVITY ASSAYS

2.5.1. Principle

The catalytic enzyme activity of intact cells expressing steroidogenic enzymes (and co-factors, if necessary) or purified proteins can be assessed by incubating the cells/protein with steroid precursors and measuring the product generated after incubation. By correlating the amount of substrate to the amount of product, the activity of the enzyme can be determined. Steroids are extracted from the incubation medium by using an organic solvent.

In this thesis, two different methods were used to quantify substrate conversion rates: 1) indirect quantification of substrate conversion rates after co-incubation of radiolabelled substrates, followed by steroid separation by thin-layer chromatography (TLC) and quantification on a bioscanner; 2) direct quantification of steroids with liquid-chromatography/tandem mass-spectrometry (LC/MSMS).

For TLC, the assay was performed in the presence of a known concentration of steroid substrate and a small molar quantity of tritiated (^{3}H) steroid substrate. The radiolabelled steroid is converted to the respective product (in the same fashion as the nonlabelled steroid), and co-migrates in the optimised mobile phase during TLC.

For the LC/MSMS method, the direct quantification of the substrates and precursors after extraction is employed to calculate subtrate conversion rates. The addition of non-radioactively labelled (deuterated) steroids prior to extraction, which usually run about two mass transitions behind the original compound, rectifies for loss of steroids during the extraction procedure.

2.5.2. Calculation of steroid conversion and enzyme kinetics

To calculate enzyme conversion rates following incubation and steroid extraction, the amount of steroid product and substrate can either be quantified as total *counts* with a radio-detector (TLC) or as total *mass* (LC/MSMS). Then, conversion rates can be deduced based on substrate concentration (µmol), protein content (µg/mg) and incubation time (h) as molar conversion per mg protein per hour.

However, the optimised incubation time at a given substrate concentration and amount of protein has to be determined in pilot experiments in order to assess the enzyme's linear phase. The linear phase is the initial period of an enzymatic reaction when it produces the product at a certain rate. When the reaction continues and substrate is consumed, this rate slows down. Therefore, to assess the activity of an

enzyme, assays were carried out during the initial step of the reaction, which is – by definition – up to 40% of substrate conversion.

As steroidogenic P450 cytochrome enzymes perform single-substrate reactions, they follow the Michaelis-Menten kinetic model of enzymatic reactions. This model describes how the activities of distinct enzymes vary and is illustrated in **Figure 17**: with increasing amounts of substrate (x-axis) the reaction rate or velocity (v) of the enzyme increases (y-axis). This is a linear relationship at low substrate concentrations. However, at higher amounts of substrate the curve becomes asymptotic as the enzyme's capacity to convert the substrate is saturated until its maximum velocity (V_{max}) is reached.

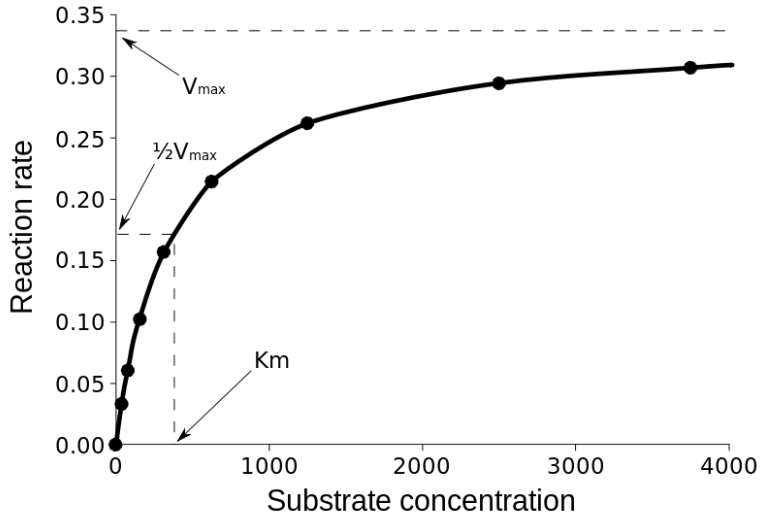

Figure 17: Michaelis-Menten curve of a single-substrate reaction.

The Michaelis-Menten constant Km is an experimentally derived number and defines the substrate concentration at which the enzyme operates at ½ Vmax. Michaelis-Menten curves, as shown in **Figure 17**, are calculated from experiments where the enzyme is incubated with different concentrations of substrate. The catalytic efficiency of the enzyme is defined as Vmax/Km and frequently used to compare the activity of a mutant protein to WT.

The linear (or double reciprocal) Lineweaver-Burk plot is commonly used to illustrate kinetic data (**Figure 18**). This plot is generated by taking the reciprocal of both axes from the Michaelis-Menten plot. Important information can be obtained directly from this graph, in particular when comparing enzyme activities (WT/mutant) in one plot: the gradient of the straight line reflects Km/Vmax and is steeper when the catalytic efficiency is reduced. The intercepts of the axes and the line reflect the reciprocals of Vmax (y-axis) and Km (x-axis).

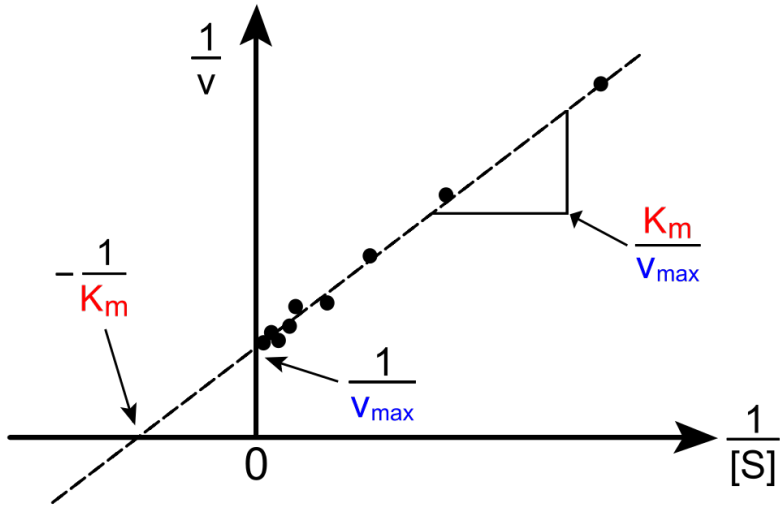

Figure 18: An example of a Lineweaver-Burk plot, the common way to illustrate kinetic data.

For all kinetic experiments, the software 'EnzFitter' (BioSoft; version 2.0.9.1) was used to obtain fitted curves and kinetic parameters.

2.5.3. Yeast activity assays

Yeast cells (from baker's yeast; *saccharomyces cerevisae*) are a robust eukaryotic system to yield large amounts of purified protein. They grow fast and are relatively simple to transform with expression vectors encoding human steroidogenic enzymes. Double-transformations are possible if the impact of mutant co-factor proteins on CYP enzymatic activities is assessed.

For this work, the W303B wild type strain (JC 104, Matα/ leu+/his+ / trp 1-1/ ura 3-1/ ade 2-1) was used to generate protein for assessing the catalytic activities of

three steroidogenic CYPs, i.e. CYP17A1, CYP21A2 and CYP19A1 in the presence of a mutant POR protein. The functional assays were performed with purified yeast microsomes employing TLC.

2.5.3.1. General procedures for yeast

Solutions:

YPD medium *(whole nutrient medium)*

For 500 ml:

- 5 g yeast extract (Fisher Biotech)
- 10 g peptone (Sigma, Pool, UK)
- (10 g agar; 2% [Fisher Biotech]; for plates only)
- 475 ml dH_2O

The solution was autoclaved and 25 ml glucose (Sigma, Pool, UK) 40% in ddH_2O (sterile filtered) were added.

SD medium *(selective media for vector-transformed yeast)*

For 500 ml:

- 0.85 g Yeast Nitrogen Base (YNB; Difco)
- 2.5 g NH_4SO_4 (Sigma, Pool UK)
- 470 ml dH_2O
- (for plates: 10 g agar; 2%)

The solution was autoclaved and 25 ml glucose (Sigma, Pool, UK) 40% in ddH_2O (sterile filtered) were added. Amino acids (final concentration: 20 mg/l) were added after cooling down to hand-warmth.

Amino acids (all purchased from Sigma, Pool, UK)

Stock solution: 2 g/l (200 mg/100 ml) in dH_2O.

All amino acid solutions have been sterile filtered; adenine to be kept at RT, tryptophan to be stored at 4°C (fridge) and light protected (wrapped with aluminium foil), Uracil to be kept at 4°C (fridge).

2.5.3.2. Transformation of yeast cells

The W303B yeast strain was transformed by a lithium-acetate method (Delfino et al., 1998; Auchus et al., 1998). The selection process after transformation of the plasmid DNA is based on the ability of the successfully transformed yeast clones to produce essential amino acids. The W303B strain cannot produce the amino acids adenine, uracil and tryptophan (ade-/trp-/ura-). The yeast expression vectors containing the protein of interest also carry coding sequences generating essential amino acids and thus can serve as a selection tool when transformed cells are incubated in minimum selective medium.

Solutions: (All reagents were purchased from Sigma [Pool, UK])

10 x Tris-EDTA (TE) stock *(100 mM Tris, 10 mM EDTA)*	12.1 g Tris-base were dissolved in 400 ml of dH_2O. Then, 1.68 g EDTA-disodium was added and adjusted to pH 7.5 by adding 1M HCL. Finally, dH2O was added to top up the final volume to 500 ml.
1 x TE *(100 mM Tris, 10 mM EDTA)*	For 10 ml, add 1ml of 10xTE and 9 ml of dH_2O.
Tris-EDTA (TE) /LiAc	For 1 ml, add 100 µl of 1M LiAc, 100 µl 10xTE and 800 µl of dH_2O.
PEG/LiAc	For 1 ml, add 800 µl 50% PEG 3350, 100 µl 10xTE and 100 µl 1M LiAc.
Sorbitol/TE	For 10 ml, add 2.5 ml of 4M sorbitol, 1 ml 10xTE and 6.5 ml dH_2O.

10-15 ml YPD medium was inoculated with a pipette tip of W303B yeast and left on the bench to grow at RT in a 50 ml tube with a loosened lid to assure oxygenation of the culture. After 2-3 days, a white-brown pellet of yeast cells formed at the bottom of the tube. The evening before transformation, a dilution series (1:1000; 1:1500;

1:2000) in YPD medium was prepared and left on the bench top overnight; the next morning, cultures were incubated at 30°C in an orbital incubator (220 rpm) for 3-5 hours. To obtain yeast in the linear range of growth, ideal for transformation, the OD at 600 nm needed to be between 0.3 and 0.5. OD measurements were carried out with a Unicam Helios gamma photometer (Life Technologies, Carlsbad, USA). 1 ml of the optimum density yeast cultures were transferred into a 1.5 ml reaction tube and centrifuged at 12,000xg (RT) on a bench top centrifuge. Then, the supernatant was removed and the pellet carefully resuspended in 100 µl TE/LiAc. Then, 700 µl of freshly prepared PEG/LiAc was added to each transformation. Subsequently, 5 µl of herring sperm DNA (after denaturation at 95°C for 5 min) was added and the tube was inverted gently several times for homogenization. Finally, 1-2 µg of plasmid DNA (in less than 10 µl of total volume) was added and, again, the tube was gently inverted to assure distribution of the DNA within the mixture. After 30 minutes incubation at 30°C, the yeast was heat-shocked at 42°C for 15 minutes (waterbath). Then the transformed yeast cells were centrifuged for 5 mins (12,000xg), the supernatant removed and the pellet was resuspended in 200 µl Sorbitol/TE buffer by pipetting and vortexing (medium velocity). After another 5 mins centrifugation (12,000xg), the supernatant was removed and the pellet resuspended in 100 µl TE buffer by pipetting. Then, the yeast cells were immediately plated on appropriate selection plates and incubated at 30°C for 3-4 days until single colonies formed.

For double transformation to yield microsomes containing the CYP proteins and the WT/mutant POR protein, W303B yeast cells were first transformed with the V10 (ura+) plasmid containing the CDS of human CYP21A2, CYP17A1 and CYP19A1, respectively. Transformed yeast cells were plated on SD-Agar plates containing 20 mg/l adenine and tryptophan. Selected yeast clones were subsequently grown in liquid SD (ade+/trp+) medium and the second transformation was performed with the

pYdE2 plasmid (trp+) containing the WT and mutant POR sequence, respectively. The selection was then carried out on SD (ade+) medium agar plates. Single colonies were then selected to grow in large scale cultures for microsome preparations.

2.5.3.3. Microsome preparation

Solutions: (All ingredients were purchased from Sigma [Pool, UK], unless stated otherwise.)

Te-K *(50 mM Tris pH 8.0, 1 mM EDTA, 0.1 mM KCl)*	For 100 ml, add 0.2 ml 0.5M EDTA (pH 8.0) to 5 ml TrisHCl, 3.3 ml 3M KCl and 91.5 ml dH_2O
TES-B *(50 mM Tris pH8.0, 1 mM EDTA, 0.6 M sorbitol)*	For 100 ml, add 0.2 ml 0.5M EDTA (pH 8.0) to 5 ml TrisHCl, 15 ml 4M sorbitol and 80 ml dH_2O
TE-G *(50 mM Tris pH 8.0, 1 mM EDTA, 20 % glycerol [v/v])*	For 100 ml, add 0.2 ml 0.5M EDTA (pH 8.0) to 5 ml TrisHCl, 25 ml 80% glycerol and 70 ml dH_2O

Stock solutions:

4M Sorbitol	54 g sorbitol in 75 ml dH_2O, sterile filtered
0.5M EDTA, pH 8.0	97.5 g EDTA-Na2 in 500 ml dH_2O; adjust to pH 8.0 with 1M NaOH
1M Tris-base, pH 8.0	121 g Tris-base dissolved in 1l dH_2O; adjust pH to 8.0 with 1M HCl
3M KCl	22.5 g KCl in 100 ml dH_2O, autoclaved

Pre-cultures of transformed yeast clones were grown in 15 ml selective medium for 2-3 days. This assures viability of the cells, and allows the synchronization of the various clones (i.e. wild type/mutant protein).

5 ml of the saturated pre-cultures were diluted in 300 ml selective SD medium and cultures were incubated in a large orbital incubator at 30°C for 15-20 hours to grow to a density of 1 or higher at OD_{600}. Then, the saturated cultures were centrifuged 5 minutes at 6,000 rpm (Avanti J-20XP with a JLA 16.2500 rotor). The supernatant was subsequently discarded and the pellet resuspended in 5 ml TE-K buffer by carefully pipetting up and down. The solution was transferred to 50 ml reaction tubes with screwed lid, left at RT for 5 minutes and then spun down (5 mins at 4,000 g; BOSRAG64 rotor; Harrier 18/80 MSE centrifuge, Jepson Bolton, Watford, UK). The pellet was re-dissolved in 2 ml TES-B (containing proteinase inhibitor cocktail; one tablet in 15 ml [Roche, Basel, Switzerland]) and acid-washed glass-beads (Sigma, Pool, UK) were added up to the top of the fluid level in a 50 ml reaction tube. All subsequent steps were performed on ice. For breaking-down the yeast cell membranes, the tubes were briskly shaken and vortexed at high speed. Seven cycles of one minute shaking (30 seconds shaking and 30 seconds vortexing) and 30 seconds incubation on ice were performed. Subsequently, the supernatant was transferred into 50 ml polycarbonate screw-top centrifuge tubes. The remaining glass beads were washed twice with 2 ml TES-B, which was also transferred and added to the centrifuge tubes. To separate the cell debris, the tubes were then centrifuged for 10 minutes at 9,000 RCF (4°C) in a Beckman J26XP centrifuge with a JA25.5 rotor (Beckman Coulter, High Wycombe, UK). Subsequently, the supernatants were transferred into polycarbonate ultracentrifuge tubes, placed into a perfectly balanced pre-chilled Ti-70 rotor of an LE-80K ultracentrifuge and spun down at 32,000 rpm (100,000 g) for 90 minutes at 4°C. After centrifugation the supernatant

was discarded and the pellet resuspended in 250/500 µl of TE-G. The pellet was first homogenized with 19G needles and then with 25G needles, using a 2 ml syringe. The protein content of the solution was measured with the BioRad method (section 2.3.2); 10-20µl aliquots were made and immediately transferred to -80°C for storage.

2.5.3.4. Activity assays

Yeast microsomes stored at -80°C were gently thawed on ice and transferred into a 50 mM potassium phosphate reaction buffer (pH 7.4) [1M potassium phosphate stock solution = 80.2 ml 1M K_2HPO_4 + 19.8 ml 1M KH_2PO_4] in 13 x 100 mm borosilicate glass tubes (Thermofisher, Loughborough, UK). The reaction volume was 196 µl, including steroid substrate at the appropriate concentration, tritiated steroid substrates (normally 3 µl of a 1:10 dilution from the stock) and CYB5A protein for CYP17A1 17,20 lyase reaction only. The reaction was initiated by adding 4 µl of 100 mM NADPH. The enzymatic reaction was carried out at 37°C and was terminated by adding 5 ml of dichloromethane. Then, steroids were extracted as described in section 2.5.5.

2.5.4. Activity assays in mammalian cells

2.5.5. Steroid extraction

A liquid-liquid extraction with the inorganic solvent dichloromethane (DCM) or methyl tert-butyl ether (MTBE) was used to release steroids from the reaction buffer and protein following steroid conversion assays. 5 ml of DCM (2 ml of MTBE) was added to the reaction buffer or cell culture supernatant in a 10 ml borosilicate glass tube (Appleton Woods, Birmingham, UK). The tubes were sealed with plastic caps and the tube was vortexed vigorously for 30 seconds at highest velocity. Then, the tubes were centrifuged at 500 g for 10 minutes. Buffer and protein form a thin layer on the top of the DCM solvent; this layer was carefully removed with glass pipettes

and the samples were evaporated for 30-40 minutes under constant airflow at 60°C. When MTBE extraction was performed, the buffer/protein layer was at the bottom of the tube, overlaid by the solvent. Here, the samples were frozen at -20°C for 60 minutes. Then the MTBE supernatant was carefully transferred by pouring into a fresh glass tube and evaporated as above.

2.5.6. Thin layer chromatography (TLC)

Thin layer chromatography (TLC) for separation of extracted steroids was performed on PE SIL G/UV silica gel plates (Whatman, Maidstone, UK). The steroids extracted as decribed in section 2.5.5 were eluted in 70 µl of DCM by vigorous vortexing for 15-30 seconds. The solvent was then transferred dropwise with a glass pipette onto points marked on the silica gel plate. For the separation of the steroids, the plate was vertically transferred with the steroids at its bottom, into a tank containing a mixture of anorganic solvents. The separation of the respective steroids depends on the assay and requires different conditions concerning the exact mixture of solvents and the running time. They are summarized in **Table 8**.

Table 8: Overview of solvent systems for the separation of steroids by TLC.

Steroid precursor	Steroid product	Enzyme activity	Solvent	Running time
Prog	17OHP	CYP17A1 (17α-hydroxylase)	3:1 chloroform/ethyl acetate	45 min
17 Preg	DHEA	CYP17A1 (17,20 lyase)		
Prog	DOC	CYP21A2 (21-hydroxylase)		
A'dione	E1	CYP19A1 (aromatase)	12:1 dichloromethane/acetone	45 min
DHEA	DHEAS	SULT2A1 (DHEA sulfotransferase)	8:2:4:2:1 chloroform/methanol/acetone/ acetic acid/water	120 min

Following separation, the plates were dried for 1-2 hours at room temperature and radio-counts were quantified with a Bioscan 2000 image analyzer (Lablogic, Sheffield, UK).

2.6. STEROID HORMONE MEASUREMENT BY RADIOIMMUNOASSAYS

Most serum steroid hormone measurements of individual case reports in this thesis were performed by collaborators across the world (chapters 3, 4, 5 and 6). The steroid assays applied for the diagnostic work-up are radio-immunoassays (RIAs) and were performed in the routine hospital clinical chemistry department. These are all certified laboratories with approved age-specific reference ranges for each individual assays, which are stated in the respective chapters of this thesis.

2.7. STEROID HORMONE MEASUREMENT BY STEROID MASS SPECTROMETRY

2.7.1. Principles

Mass spectrometry (MS) identifies and quantifies steroids in a sample according their mass-to-charge ratio (m/z). This requires a series of subsequent physical-chemical steps: (1) ionization of the steroids molecules in a gaseous phase, (2) separation of the ionized molecules according to their m/z ratio and (3) detecting the ions and quantifying the relative abundance of each m/z ratio. These reactions are carried out within the three major components of a mass-spectrometer (see **Figure 19**): The ionization source, the mass analyser and the detector.

Prior to steroid detection and quantification by MS, steroids need to be extracted from the respective sample. As steroids are polar molecules, they move easily from an aqueous to an organic phase and liquid-liquid extractions with organic solvents is commonly applied for this purpose. Then, to allow the determination of several steroids in a single experiment, chromatography is usually coupled to MS analysis. In this thesis, either liquid chromatography (LC) or gas chromatography (GC) has been applied. Both methods have their own strengths and disadvantages

(see (Krone et al., 2010) for a recent and detailed review). LC/MS is suited for the rapid and highly sensitive analysis of individual steroids from a small sample volume. It therefore is considered as the gold standard for steroid measurements from serum, replacing conventional radioimmunoassays (RIAs), which are often unspecific due to cross-reactivity of the employed antibodies.

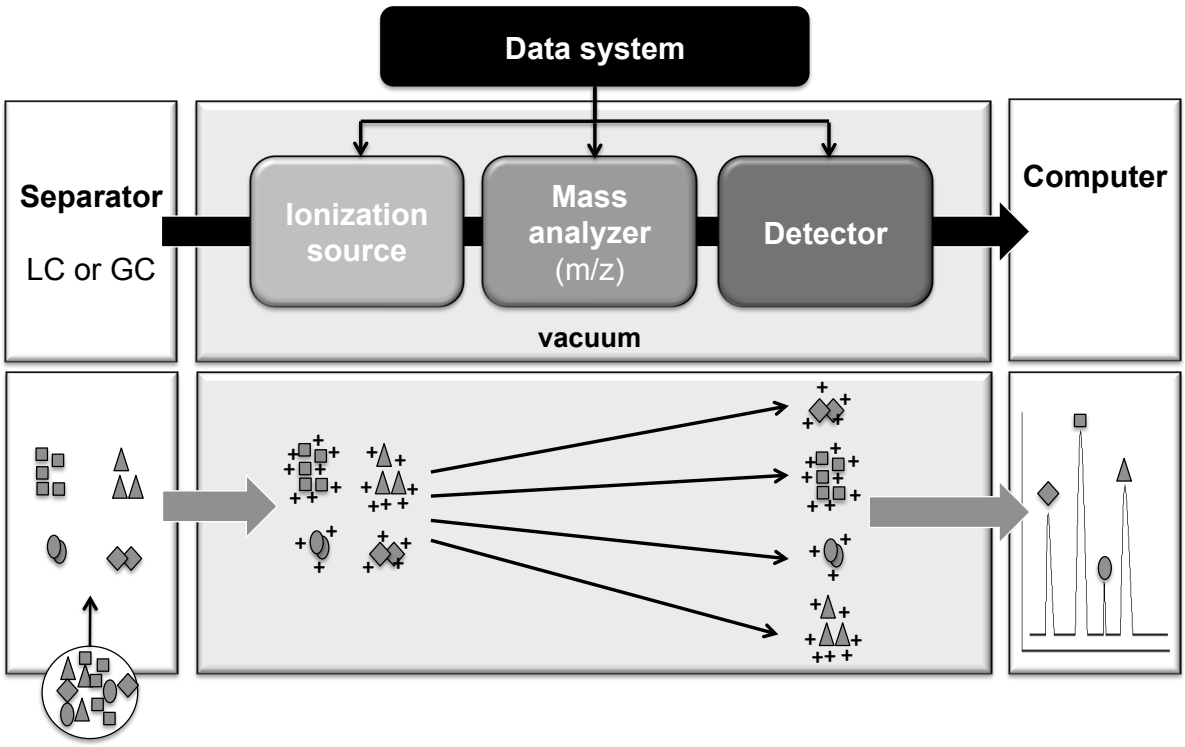

Figure 19: Schematic illustration of the key procedures involved in steroid mass spectrometry analysis. The upper panel shows the technical components and the bottom panel illustrates the biochemical and physical processes occurring to a mixture of analytes carried out by these components: the different analytes (illustrated by grey symbols) are separated by chromatography (liquid: LC or gas: GC) before they enter the mass spectrometer (grey-shaded box). The ionization source produces gaseous ions of the molecules. Then, the analyser resolves the ions according to their mass-to-charge ratio (m/z). Finally, the detector counts the relative abundance of each ionic species. A computer 'translates' the detector signals into peaks and numbers. The three main steps of mass spectrometry analysis is under close control by computerised systems and are carried out under vacuum to avoid collisions of the ions with other molecules.

LC/MS is always 'targeted', i.e. restricted to the detection of either single or a small panel of steroids. In contrast, GC/MS allows the detection of all steroid compounds within a sample and is often used to measure steroid hormone metabolites as well as their respective precursors. This technique is already available since the 1970s and is a powerful tool to explore new steroid 'metabolomes' as a

comprehensive run detects all steroids present in the sample. As a 'scanned' run including sample preparation takes a couple of days, the method is time-consuming (and expensive) compared to the fast, much cheaper high-throughput LC/MS approach. Therefore, GC/MS analysis has its role in research to explore novel steroid profiles while LC/MS is about to facilitate and maybe revolutionize steroid hormone analysis in the clinical setting (Krone et al., 2010).

2.7.2. Urinary steroid profiling with gas-chromatography/mass-spectrometry (GC/MS)

Analysis of urinary steroid metabolite excretion was performed by a quantitative GC/MS selected ion-monitoring method, that allows for selective identification and quantification of all major metabolites of androgens, glucocorticoids, mineralocorticoids and their respective precursors (**Table 9**, **Figure 20**). Steroids were enzymatically released from conjugation and, after extraction, chemically derivatized before GC/MS analysis (Shackleton, 2008): First, steroids were extracted from urine with a SepPak column (Waters, Milford, Ma, USA): 5 ml of urine sample were loaded after washing the columns with 4 ml methanol and 4 ml of ddH_2O. Then, the loaded column was washed with 4 ml ddH_2O and the steroids were eluded in 4 ml methanol into a clean borosilicate tube. After evaporation (heat block at 55°C under N_2), sulfate and glucoronide groups were enzymatically removed from conjugated steroids by incubating for 3 hours at 55°C in the hydrolysis buffer (3 ml 0.1M acetate buffer [pH 4.8-5.0] + 10 mg ascorbate + 10 mg sulfatase/glucoronidase; all ingredients purchased from Sigma, Pool, UK). The cooled sample was then loaded again on a SepPak column and eluded into a clean glass tubes with 4 ml methanol. Derivatization: After evaporation, three drops of 2% methoxyamine-pyridine was added; the tube was vortexed vigorously and incubated at 55°C for one

hour. After evaporation under N_2, 75µl of N-trimethylsilylimidazole (Sigma, Pool, UK) were added, vortexed and incubated at 120^{o}C overnight. Then, the samples were extracted by adding (1) 2 ml cyclohexane and (2) 2 ml dH_2O (vortexing after each step). After centrifugation (1,000g for 5 minutes), the bottom later layer was removed into waste. Then, another 2 ml dH_2O were added, vortexed, centrifuged and removed. Finally, the top layer containing the extracted steroids in cyclohexane was transferred into injection vials. The samples were then injected into an Agilent 5973 GC mass-spectrometer.

Table 9: Overview of (urinary) steroid hormone metabolites with full names and abbreviations and the steroid hormone(s) they are derived from.

Abbreviation	Full name	Metabolite of
An	Androsterone	Androstenedione, testosterone, 5α-dihydrotestosterone, DHEA
Et	Etiocholoanolone	Testosterone, DHEA
DHEA (and DHEAS)	Dehydroepiandrosterone	Dehydroepiandrosterone and -sulfate
11β-OH-An	11β-Hydroxy-androsterone	11β-OH-androstenedione, cortisol
11β-OH-Et	11β-Hydroxy-etiocholanolone	Cortisol
11-OXO-Et	11-Oxo-etiocholanolone	Cortisol
16α-DHEA	16α-Hydroxy-	Dehydroepiandrosterone and -sulfate
PD	Pregnadienol	Progesterone, 11-deoxy-corticosterone
5PD	Pregnadienol	Pregnenolone
Pregnadienol	Pregnadienol	Pregnenolone
17HP	17-Hydroxy-pregnanolone	17-Hydroxy-progesterone
3α-5α-17HP	3α5α-17-OH-pregnanolone	17-Hydroxy-progesterone and other fetal origin
PT	Pregnatrienol	17-Hydroxy-progesterone
5PT	5-Pregnatrienol	17-Hydroxy-pregnenolone
PTONE	Pregnanetriolone	21-Deoxycortisol
THDOC	Tetrahydrodeoxycorticosterone	11-Deoxycorticosterone
5αTHDOC	5α-Tetrahydro-deoxycorticosterone	11-Deoxycorticosterone
THS	Tetrahydro-11-deoxycortisol	11-Deoxycortisol
THA	Tetrahydro-11-dehydrocorticosterone	Corticosterone
5αTHA	5α-Tetra-11-dehydrocorticosterone	Corticosterone
THB	Tetrahydrocorticosterone	Corticosterone
5αTHB	5α-Tetrahydrocorticosterone	Corticosterone
THALDO	Tetrahydroaldosterone	Aldosterone
THE	Tetrahydrocortisone	Cortisol, cortisone
THF	Tetrahydrocortisol	Cortisol
5αTHF	5α-Tetrahydrocortisol	Cortisol
α-cortolone	α-cortolone	Cortisol, cortisone
β-cortolone	β-cortolone	Cortisol, cortisone
α-cortol	α-cortol	Cortisol
β-cortol	β-cortol	Cortisol
6β-OHF	6β-Hydroxy-cortisol	Cortisol

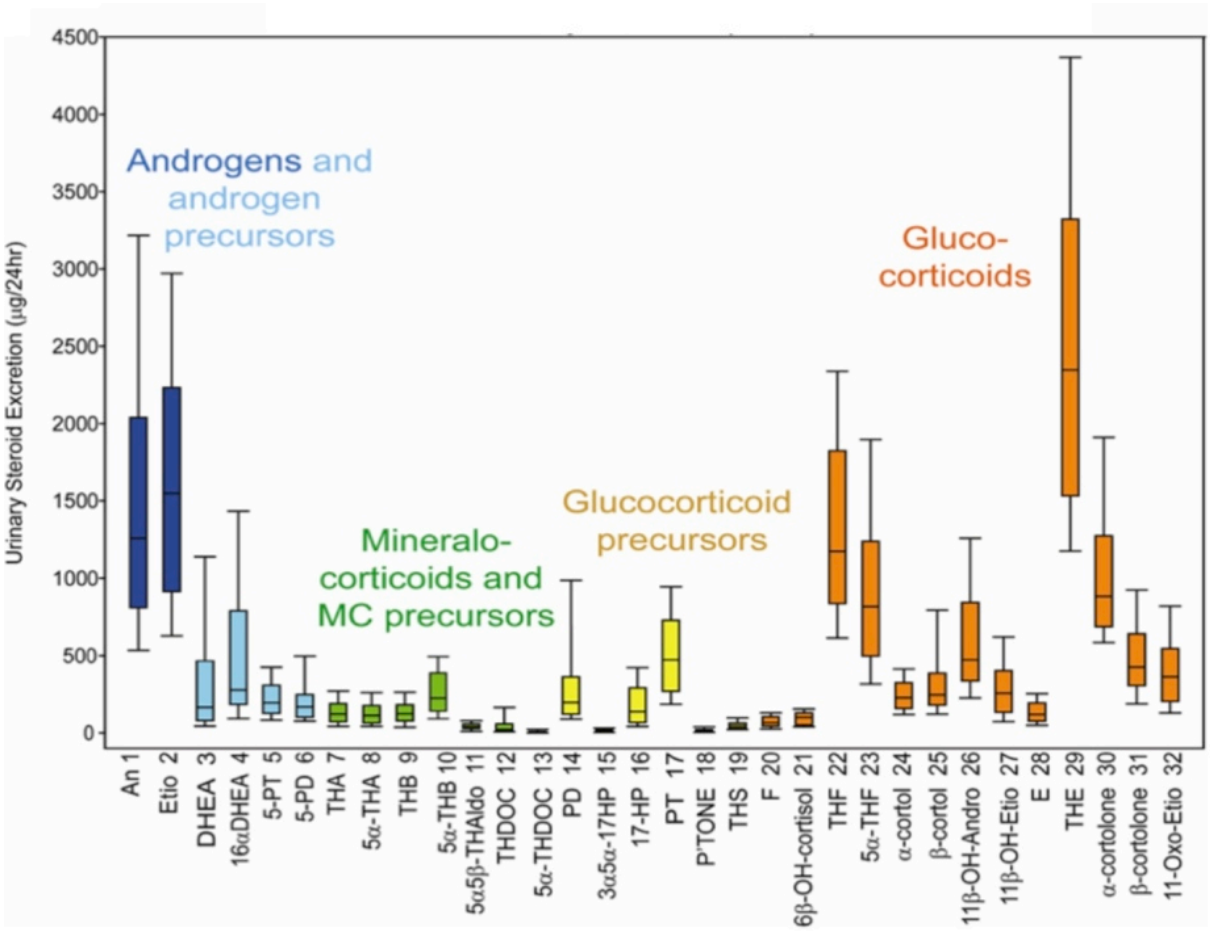

Figure 20: The 24-h urinary steroid metabolite excretion in healthy controls (n = 88). Box plots represent median and interquartile ranges; the whiskers represent 5th and 95th percentile, respectively. Colour coding of steroid metabolites mirrors that used for depicting the major adrenal corticosteroid classes. With kind permission from (Krone et al., 2010).

2.7.3. Steroid measurements with liquid chromatography/tandem mass spectrometry (LC/MSMS)

Steroids were measured by liquid chromatography/ tandem mass spectrometry (LC/MSMS) employing a Waters Xevo mass spectrometer with Acquity uPLC system, fitted with a HSS T3, 1.8 mm, 1.2 x 50 mm column. LCMS/MS conditions were an electrospray ionization source with capillary voltage 4.0 kV, a source temperature of 150°C, and a desolvation temperature of 500°C. Steroid oxime analysis, which facilitates enhanced detection, i.e. increased sensitivity, by formation of oxime derivatives of the steroid oxo-groups (Kushnir et al., 2010), was employed

for the measurement of DHEA and androstenedione and carried out in positive mode, whereas DHEAS measurement was performed in negative mode. Steroids were extracted from cell-culture supernatant or serum using 2 ml tert-butyl-methyl-ether. Steroids were derivatized into oximes employing 100 ml derivatization mixture (0.16 g hydroxylamine in 8 ml pyridine). For protein precipitation and extraction of DHEAS and Cholesterol-sulfate, 20ml $ZnSO_4$ 0.1 mM and 100 ml acetonitrile were added to 20 ml serum before evaporation under constant flow of nitrogen. All steroids were separated using an optimised gradient system consisting of methanol with 0.1% formic acid and quantified referring to a linear calibration series with appropriate internal standards, ranging from 0.1 to 250ng/ml for steroid oxime analysis and 250 to 100 000 ng/ml for DHEAS/ Cholesterol-sulfate analysis. Each steroid was identified by matching retention times and two mass transitions in comparison to a deuterated reference compound.

3. CHAPTER 3: CONCOMITANT MUTATIONS IN THE P450 OXIDOREDUCTASE AND ANDROGEN RECEPTOR GENES PRESENTING WITH 46,XY DSD AND ANDROGENISATION AT ADRENARCHE

This chapter has been published as:

Concomitant mutations in the P450 oxidoreductase and androgen receptor genes presenting with 46,XY disordered sex development and androgenization at adrenarche.

Idkowiak J, Malunowicz EM, Dhir V, Reisch N, Szarras-Czapnik M, Holmes DM, Shackleton CH, Davies JD, Hughes IA, Krone N, Arlt W.

J Clin Endocrinol Metab. 2010 Jul;95(7):3418-27. doi: 10.1210/jc.2010-0058.

3.1. INTRODUCTION

Disordered sexual development (DSD) in genetic males (46,XY DSD) can be due to a number of distinct mutations compromising different stages of sex determination and differentiation (Mendonca et al., 2009; Ahmed and Rodie, 2010). The most common cause of 46,XY DSD is androgen insensitivity syndrome (AIS) due to inactivating mutations of the *androgen receptor* (*AR*) gene, which has an incidence of 1:20,000 life births (Hughes and Deeb, 2006). More than 300 mutations are listed in the AR database (http://androgendb.mcgill.ca) leading to different degrees of androgen resistance from azoospermia to complete androgen insensitivity syndrome (CAIS). Missense and nonsense mutations in specific regions of the *AR* gene have distinct effects on AR function and can affect ligand binding, transactivation or N-terminal-/C-terminal-interaction of the androgen receptor molecule (Bevan et al., 1996; Ghali et al., 2003; Jääskeläinen et al., 2006). However, the *in vitro* assessment of AR function may not always match the observed clinical phenotype in patients with AIS, with variable degrees of undervirilization in different individuals carrying the same distinct *AR* (Hughes and Deeb, 2006; Hughes and Evans, 1987).

Upstream of AR action, androgen synthesis may be affected and result in 46,XY DSD (Mendonca et al., 2009; Krone et al., 2007b). Five enzymes and six catalytic reactions are required for the conversion of cholesterol to the most potent androgen, 5α-dihydrotestosterone (DHT) (see section 1.1.8). Mutations in the genes required for these conversions (*CYP11A1*, *CYP17A1*, *HSD17B3*, *HSD3B2* and *SRD5A2*) represent distinct causes of 46,XY DSD, manifesting with a broad phenotypic spectrum. The identification of inactivating mutations in the P450 oxidoreductase gene (*POR*) (Flück et al., 2004; Arlt et al., 2004) has demonstrated

that sex steroid synthesis may also be disrupted by mutations in co-factor enzymes (see section 1.3.1).

Here, we have investigated a patient with 46,XY DSD and concomitant, disease-causing mutations in the *AR* and *POR* genes, both fully established causes of undervirilization in their own right.

3.2. METHODS

3.2.1. Case report

The patient was born at term after an uneventful pregnancy as the first child of non-consanguineous parents of Polish origin (birth weight was 2850g (-1.3 SDS), length 52 cm (0.89 SDS), Apgar score 5/8). The postnatal adaptation went well and no neonatal complication occurred. However, at birth, the attending pediatrician noticed ambiguous genitalia. The external genitalia looked predominantly female, but the clitoris was enlarged and a common urogenital sinus and blind ending vaginal pouch were present. The gonads were palpable within the inguinal canal. No other abnormalities or malformations were noted. The karyotype was 46,XY.

At the age of 14 days a slightly elevated serum 17-hydroxyprogesterone (17OHP) was measured (**Table 10**). Circulating androgens and androgen precursors were low and testosterone showed a poor response to hCG stimulation while the gonadotrophin response to LHRH stimulation was normal (**Table 10**). Urinary steroid profiling by gas chromatography/mass spectrometry (GC/MS) at the age of 14 days showed undetectable androsterone, normal levels of foetal adrenal zone steroids, normal cortisol and 17OHP metabolite excretion and no evidence of 5α-reductase deficiency.

Table 10: Hormonal assessment in the patient at 1-2 months and at 9 years. Bilateral gonadectomy had been carried out at the age of four years. * age-specific normal reference range; ** age-specific reference ranges for androgens are listed for both girls (f) and boys (m)

	1-2 months		9 years	
17OHP (nmol/L)	9.38 (1.8-7.5)*		37.9 (< 6)	
60 min after ACTH 250µg/m2 i.v.	-		47.2	
Cortisol (nmol/L)	-		391	
60 min after ACTH 250 µg/m^2 i.v.	-		494	
DHEAS (µmol/L)	0.23	(f: 0.04 -1.32)** (m: 0.04-1.96)	2.49	(f: 0.23 - 2.37) (m: 0.42 -2.13)
Androstenedione (nmol/L)	0.41	(f: 0.7 - 1.9) (m: 1.3 – 4.25)	0.73	(f: 0.3 – 1.2) (m: 0.2 – 2.8)
4 days after hCG 2000 IU/m^2 i.m.	0.35		-	
Testosterone (nmol/L)	< 0.20	(f: 0.17 -0.40) (m: 1.4 – 8.2)	< 0.17	(f: 0.17 - 0.30) (m: 0.15 – 0.65)
4 days after hCG 2000 IU/m^2 i.m.	2.15		-	
ACTH (pg/ml)	-		50.9 (10-60)	
LH (U/L)	0.4		-	
60 min after LHRH 75 µg/m^2 i.v.	3.7		-	
FSH (U/L)	2.0		-	
60 min after LHRH 75 µg/m^2 i.v.	6.7		-	

The initial presentation with 46,XY DSD had prompted genetic analysis of the androgen receptor (AR) gene, which revealed the hemizygous mutation p.Q798E. Despite the finding of low circulating androgens the diagnosis of partial AIS (PAIS) was made. The patient was assigned female gender and underwent bilateral removal of the inguinal gonads at the age of four years; histopathologic examination identified the removed tissue as immature testis.

Follow-up was inconsistent due to poor clinic attendance. However, at the age of 9 years the patient presented with progressive clitoral enlargement over the preceding 18 months. At examination, no other external signs of puberty were noticed (Tanner stages PH 1, B1, A1); clitoral length was 3 cm. Except for the bilateral gonadectomy, no genital reconstruction surgery had been performed yet, largely due to parental doubts about the gender identification of her daughter (male hobbies and roles, aggressive behaviour). Psychological assessment including

thorough evaluation of her gender preference was offered but declined by the parents. Her growth chart showed normal linear growth along the 50th percentile, the bone age was significantly delayed (-3 yrs).

Hormonal assessment again revealed mildly elevated serum 17OHP. However, DHEAS levels were raised slightly above the age-specific reference ranges of both girls and boys (**Table 10**). Serum testosterone was below sensitivity of the employed radioimmunoassay (**Table 10**). Urinary steroid profiling with gas-chromatography/mass spectrometry (GC/MS) was performed and showed a profile suggestive of combined inhibition of 21-hydroxylase and 17α-hydroxylase activities and thus indicative for PORD (for detailed analysis see section 3.3.1). A short synacthen test revealed a normal baseline cortisol but an impaired cortisol response to ACTH stimulation (**Table 10**). Subsequently, hydrocortisone replacement therapy for intercurrent stress, illness and surgery was recommended and patient and parents were educated accordingly.

3.2.2. Urinary steroid profiling

Analysis of urinary steroid metabolite excretion was performed as described previously by a quantitative gas chromatography/mass spectrometry (GC/MS) selected ion-monitoring method (section 2.7.1). Steroids quantified included corticosterone metabolites (THB, 5αTHB, THA), the progesterone metabolite PD, 17-hydroxyprogesterone metabolites (PT, 17HP), the 17-hydroxypregnenolone metabolite 5-PT, the 21-desoxycortisol metabolite P'TONE, cortisol metabolites (THF, 5αTHF and THE), and androgen metabolites (An, Et, DHEA) and 16-OH-DHEA (see **Table 9** for abbreviations of steroid metabolites).

Following quantification of steroid metabolites by GC/MS, the following substrate/product ratios were calculated to determine the approximate *in vivo* net

activity of specific steroidogenic enzymes: corticosterone over cortisol metabolites (17α-hydroxylase; (THA+THB+5αTHB)/(THF+5αTHF+THE)), 17-hydroxy-progesterone over androgen metabolites (17,20-lyase; (17HP+PT)/(An+Et)), 17-hydroxyprogesterone over cortisol metabolites (21-hydroxylase; (100xP'TONE/ (THF+5αTHF+THE)), and the ratio of progesterone over cortisol metabolites (combined 21-hydroxylase and 17-hydroxylase activities, i.e. specific for PORD; PD/(THF+5αTHF+THE)). These diagnostic ratios were compared to ratios obtained from urine analysis in a normal age matched female reference cohort (n=10).

3.2.3. Genetic analysis

DNA sequencing analysis was carried out with approval of the local research ethics committee, after obtaining informed consent from patients and their parents. Direct sequencing of the coding regions of *POR* gene including 15 exons and exon-intron junctions were performed as described in section 2.2.11. Exon 8 of the *androgen receptor* gene (Batch et al., 1992; Bevan et al., 1996) was performed by our collaborators (Prof Ieuan Hughes, Department of Paediatrics, Cambridge, UK). Sequencing results were analysed using Lasergene® software (DNASTAR Inc., Madison, USA) and mutation numbering was carried out referring to the appropriate NCBI reference sequences (see section 2.2.11). The coding sequence variant of the androgen receptor was numbered according to M20132.1 (where A of the ATG translation initiation codon is +363bp), the protein mutation was numbered relative to AAA51729.1.

3.2.4. *Site-directed mutagenesis and in vitro* enzymatic activity assays

The cDNA of the *POR* missense mutant p.Y607C POR, generated by site-directed-mutagenesis, was cloned into the yeast expression vector pDE2 and used

for microsomal co-expression assays in comparison to wild type POR (WT) described in section 2.5.2. For site-directed mutagenesis, the following primer pairs were used to introduce the p.Y607C mutation into the WT POR cDNA: forward sequence : 5'-GGGAGCAGTCCCACAAGGTCT**G**CGTCCAGCAC-CTGCTAAAGC-3'; reverse sequence: 5'-TGCTTTAGCAGGTGCTGGACG**C**AGACCTTGTGGGACT-GCTCCC-3'. The detailed conditions are described in section 2.4.3.

For *in vitro* activity assays, yeast microsomes co-expressing wild type or mutant Y607C POR and wild type human CYP17A1, CYP21A2 and CYP19A1, respectively (see section 2.5.3.2), were incubated with 0.5-5 μM progesterone or 17-hydroxypregnenolone for 17α-hydroxylase and 17,20-lyase activities of CYP17A1, 0.5-5 μM progesterone for 21-hydroxylase (CYP21A2) activity, and 50-500 nM androstenedione for aromatase (CYP19A1) assays. Steroids were added to the final reaction volume of 200 μl in 4 μl ethanol also containing 10,000 cpm [^{3}H] steroid substrate (all 55.4 Ci/mol). Purified recombinant cytochrome b5 (Invitrogen, Paisley, UK) was added in a final concentration of 10 pM to the 17,20-lyase assays. All reactions were initiated by the addition of 200 nM NADPH and subsequently incubated at 37°C. Steroids were extracted and TLC performed (see section 2.5 for detailed descriptions). The obtained data represent the results of three independent experiments carried out in triplicate and are expressed as mean ± standard error of the mean (SEM).

Microsomal protein quantification was performed (see section 2.3.2) and the expression of similar amounts of protein was confirmed by Western blotting (section 2.3.3) employing antibodies to human POR (Abcam, Cambridge, UK), human CYP17A1 (SantaCruz Inc., Heidelberg, Germany), human CYP19A1 (Abcam) and CYP21A2 (Abcam).

Kinetic parameters were assessed by non-linear regression, using the Michaelis-Menten equation to determine the Michaelis-Menten constant K_m and maximal velocity V_{max} (see section 2.5.2). Catalytic efficiency was defined as the ratio V_{max}/K_m and expressed as percentage of wild type activity. Calculation of enzyme kinetic parameters and subsequent statistical analysis was performed using curve-fitting software (Enzfitter 2.0.9.1; Biosoft, Cambridge, UK).

3.3. RESULTS

3.3.1. Urinary steroid profiling

Gas chromatography/mass spectrometry analysis of urinary steroid metabolite excretion in our patient at the age of 9 years revealed a pattern indicative of PORD, with diagnostic ratios demonstrating combined 21-hydroxylase, 17α-hydroxylase and 17,20-lyase inhibition (**Figure 21 A-D**). 21-hydroxylation as the ratio of the 21-deoxycortisol metabolite pregnanetriolone over cortisol metabolites was significantly compromised as compared to age-specific controls (**Figure 21A**). Similarly, 17α-hydroxylation reflected by the ratio of corticosterone over cortisol metabolites was significantly impaired (**Figure 21B**). 17,20-lyase activity, as assessed by the ratio of 17OHP metabolites over active androgen metabolites was also compromised (**Figure 21C**). Combined inhibition of 17α-hydroxylation and 21-hydroxylation, the hallmark biochemical finding in PORD, was reflected in our patient by a markedly increased ratio of progesterone over cortisol metabolites (**Figure 21D**).

24-h urinary androsterone and etiocholanolone, the main metabolites of androstenedione, testosterone and dihydrotestosterone, were within the age-specific mid normal range (**Figure 21E).** The excretion of the 17-hydroxypregnenolone metabolite 5-PT and also DHEA were increased (**Figure 21E)** indicative of

upregulation of adrenal androgen production. The corticosterone metabolites THB, 5aTHB, and THA were increased and the excretion of free cortisol was decreased, reflecting 17α-hydroxylase and 21-hydroxylase inhibition, respectively.

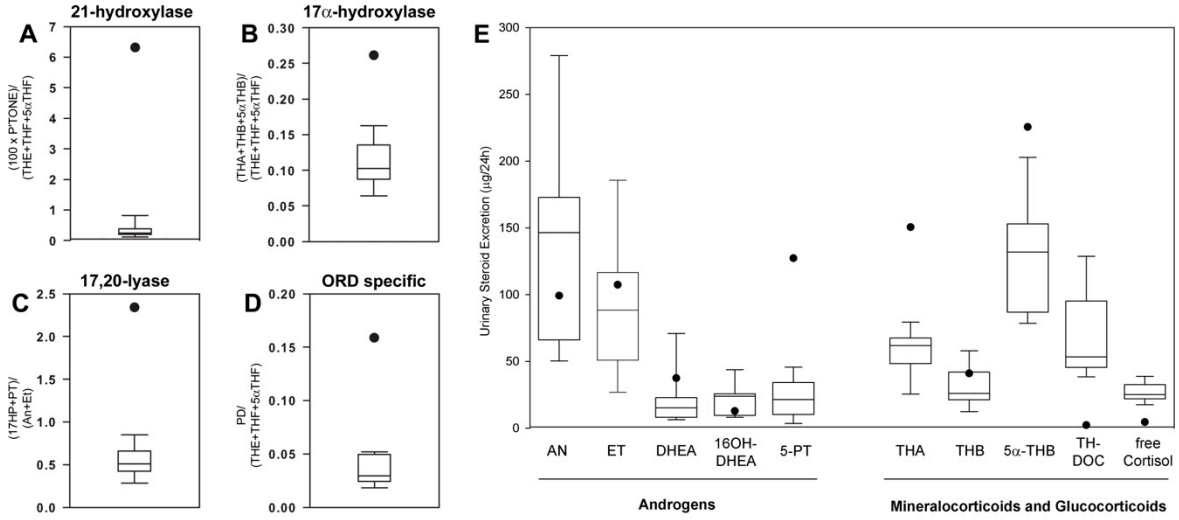

Figure 21: *In vivo* steroidogenic enzyme activity in the patient at the age of 9 years as determined by diagnostic substrate/product ratios (Panels A-D) and total excretion (Panel E) of 24-h urinary steroid metabolites measured by gas chromatography/mass spectrometry and shown in comparison to an age-matched reference cohort (n=10). Box plots represent interquartile ranges (25th to 75th percentile), whiskers the 5th and 95th percentile, respectively, of the normal reference cohort; the patient's results are represented by a closed circle. For steroid metabolite abbreviation and explanation of steroid ratios please see method section.

3.3.2. Genetic analysis

Sequencing of the coding region of the *POR* gene revealed compound heterozygosity for two *POR* mutations (**Figure 22A**). We identified a deletion of guanine in exon 13 (g.32062delG) resulting in a stop codon and subsequent premature truncation of the POR protein 12 amino acids after the frameshift (p.E601*fs*X12). Secondly, we found a missense mutation in exon 14 (g.32171A>G) changing tyrosine at amino-acid position 607 to cysteine (p.Y607C). Segregation analysis demonstrated that the Y607C mutation is located on the maternal allele, while the frameshift mutation is of paternal origin (**Figure 22B**).

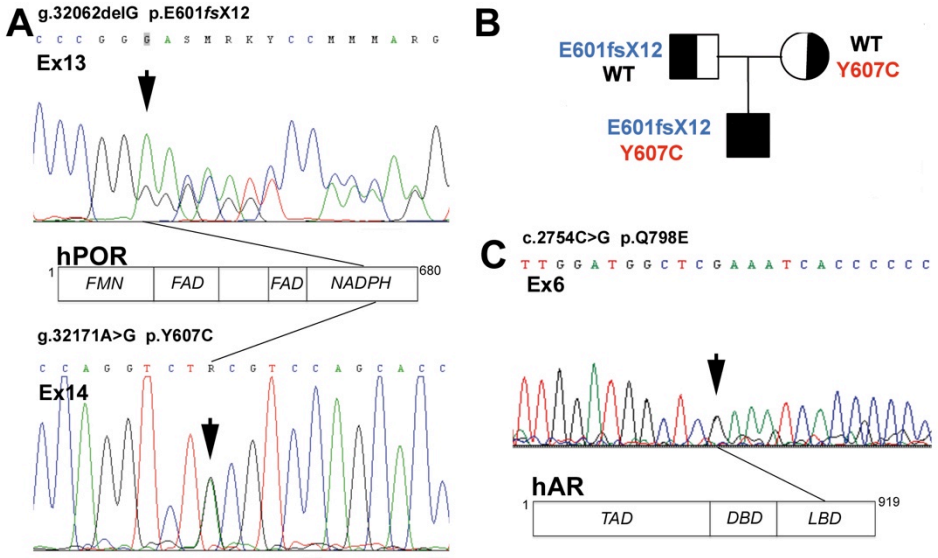

Figure 22: Results of genetic analysis. **Panel A,** electropherogram depicting the compound heterozygous *POR* mutations in our patient. The deletion of the guanine in Exon 13 (g.75,953delG) and the missense mutation in Exon 14 (g.76,062A>G) of the *POR* gene are marked by black arrows. The structure of the POR protein and the approximate location of the mutations are indicated in the schematic representation of the POR protein including its three functional domains, which bind the three partners of the electron transfer chain, FMN (flavin mononucleotide), FAD (flavin adenine dicnucleotide) and NADPH (nicotinamide adenine dinucleotide phosphate). **Panel B**, pedigree of the index family with segregation analysis of the two identified POR mutations. **Panel C**, electropherogram depicting the missense mutation in exon 6 of the *AR* gene (c.2754C>G) marked with a black arrow. The translational effect is indicated in the schematic graph representing the AR protein including its functional domains TAD (transactivation domain), DBD (DNA-binding domain), and LBD (ligand binding domain).

Our collaborators have confirmed the presence of a missense mutation in the *AR* gene by direct sequencing, a glutamine to glutamic acid change (c.2754C>G) resulting in a missense mutation in position 798 within exon 6 of the AR protein (p.Q798E) (**Figure 22C**). This mutation was found in the patient and the mother.

3.3.3. *In vitro* assessment of steroidogenic activity assays

The impact of the maternal Y607C POR mutation on steroidogenic microsomal CYP enzymes was assessed by employing yeast microsomal co-expression of WT or mutant POR with CYP17A1, CYP21A2 or CYP19A1.

Y607C POR decreased catalytic efficiencies of all three enzymes compared to wild type protein (**Figure 23**, **Table 11**). However, a differential pattern of inhibition

was observed. 17α-hydroxylase activity of CYP17A1 showed significant inhibition with a residual catalytic efficiency of 56% as compared to WT (**Figure 23A**, **Table 11**). CYP17A1 17,20 lyase activity was also significantly compromised when looking at the classic pathway, with only 43% residual activity for the conversion of 17-hydroxypregnenolone to DHEA, whereas assessment of 17,20 lyase activity within the proposed alternative pathway demonstrated moderate impairment only, with 66% residual activity for the conversion of 5α-pregnanediolone to androsterone (**Figure 23A**, **Table 11**).

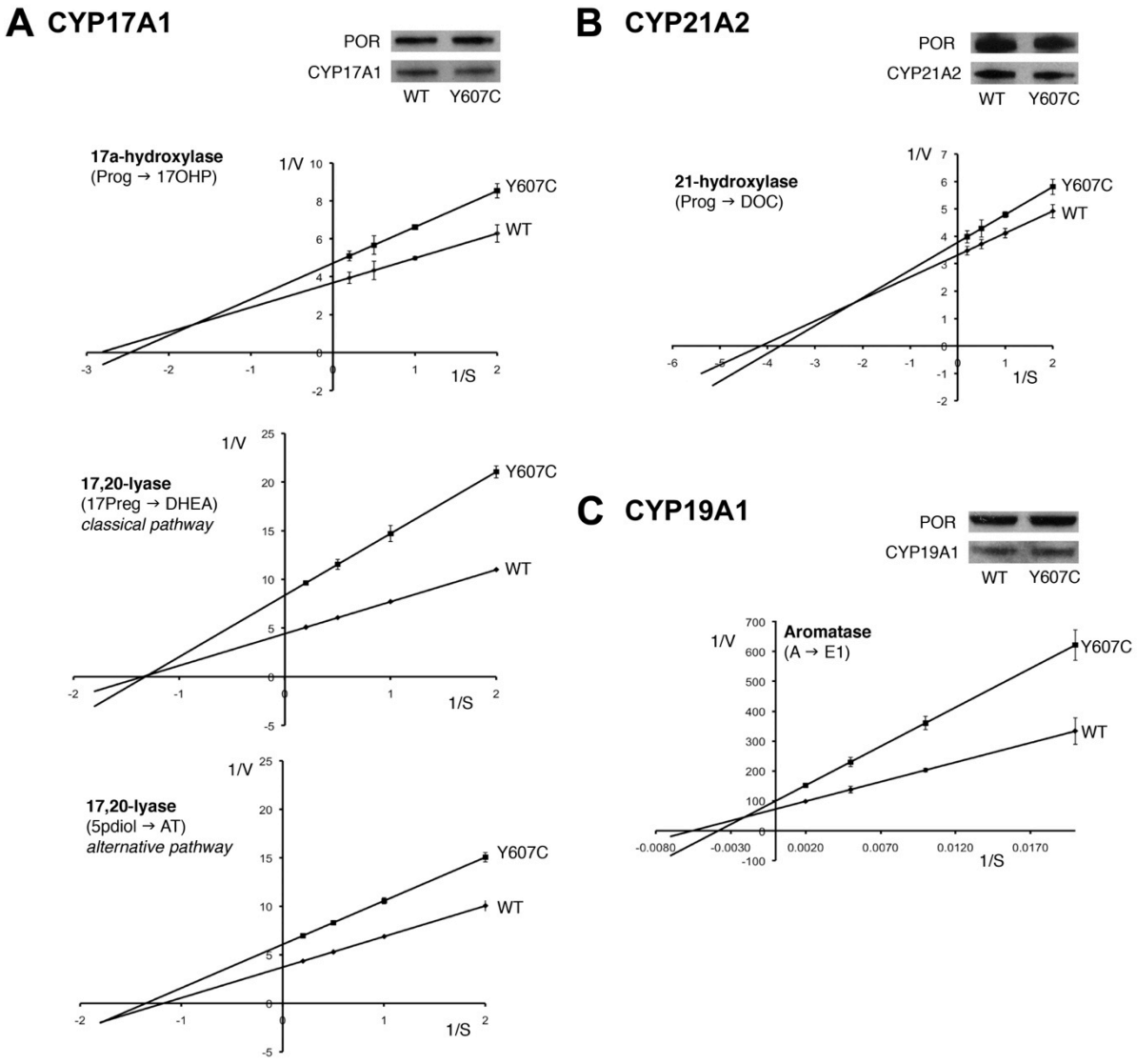

Figure 23: Kinetic analysis of steroidogenic enzyme activities. Lineweaver-Burk plots of steroidogenic activities as assessed by incubation of yeast microsomes co-expressing human wild type (WT) or mutant Y607C POR with human CYP17A1 (A), CYP21A2 (B) or CYP19A1 (C) with either 0.5-5 µM progesterone (for 17α-hydroxylase and 21-hydroxylase activities), 0.5-5 µM 17-hydroxypregnenolone (for 17,20-lyase activity in the classic pathway), 0.5-5 µM 5-pregnanediolone (for 17,20-lyase activity in the alternative pathway) or 50-500 nM androstenedione (for aromatase activity). Representative Western blots demonstrate equal expression of POR and the respective CYP enzyme in the microsomal preparations employed.

In contrast to the pronounced inhibition of 17α-hydroxylase activity, the POR mutant Y607C had only a minor effect on 21-hydroxylation, with 79% residual activity (**Figure 23B**, **Table 11**). CYP19A1 aromatase activity was markedly decreased when co-expressed with Y607C POR with 56% residual activity compared to WT POR

(**Figure 23C**, **Table 11**). Western blotting determined equal amounts of POR and CYP enzyme protein in all employed microsome preparations (**Figure 23A-C**).

Table 11: Kinetic analysis of the POR mutant p.Y607C according to yeast microsomal co-expression assays of either wild type or mutant POR with human CYP17A1, CYP21A2, and CYP19A1. All assays were carried out in three independent triplicate experiments; results are presented as means±SEM. For CYP17A1, both 17α-hydroxylase and 17,20-lyase activities within the classic and alternative androgen pathway were determined.

			CYP17A1		**CYP21A2**	**CYP19A1**
		17α-hydroxylase Prog → 17OHP	17,20-lyase ("classic") 17Preg → DHEA	17,20-lyase ("alternative") 5pdiolone → AT	21-hydroxylase Prog → DOC	Aromatase A'dione → E1
V_{max} (pmol/μg/min)	WT	0.24±0.02	0.22±0.00	0.27±0.01	0.30±0.02	0.014±0.001
	Y607C	0.21±0.02	0.13±0.01	0.16±0.01	0.27±0.02	0.010±0.001
K_m (μM)	WT	0.26±0.10	0.71±0.04	0.85±0.14	0.24± 0.08	180 ± 44
	Y607C	0.41±0.13	0.95 ± 0.11	0.75±0.06	0.27± 0.10	262 ± 54
Catalytic Efficiency V_{max}/K_m (% WT)	Y607C	56±3	44±4	66±3	79±2	56±3

3.4. DISCUSSION

To our knowledge, this is the first report of combined PORD and AIS. At birth, the patient presented with severe 46,XY DSD prompting female gender assignment and bilateral gonadectomy following the diagnosis of AIS. However, at the age of 9 years, i.e. around the time of adrenarche, progressive clitoral enlargement and near normal androgen levels were detected.

The identified AR mutation, Q798E, has been previously associated with the clinical phenotype of PAIS (Quigley et al., 1995; Batch et al., 1992; Bevan et al., 1996; Hiort et al., 1996; Thai et al., 2005). Interestingly, the same mutation was also identified in three patients with azoospermia but no evidence of 46,XY DSD (Wang et al., 1998; Hiort et al., 2000; Ferlin et al., 2006). This phenotypic variability currently remains unexplained. The Q798E mutation is located in the middle of the AR ligand

binding domain, residing in the loop between helix 7-8. Two *in vitro* studies failed to demonstrate impaired AR ligand binding for Q798E (Bevan et al., 1996; Wang et al., 1998). Furthermore, there was no significant impairment of N-terminal /C-terminal interaction, found to be an explanation for the phenotype in some patients with PAIS (Jääskeläinen et al., 2006). This is remarkable as mutations in the AR ligand binding domain usually have significant functional impact. Luciferase reporter assays for Q798E AR function have shown reduced promotor transactivation *in vitro* (Wang et al., 1998; Jääskeläinen et al., 2006; Hiort et al., 1996; Bevan et al., 1996). Of note, its transactivation is restored back to wild type activity with increasing androgen concentrations (Wang et al., 1998; Jääskeläinen et al., 2006), suggesting that increased availability of androgens could enhance mutant Q798E AR action. However, in the previously identified four individuals with Q798E no progressive virilization at time of adrenarche or puberty has been reported.

While patients with AIS due to AR mutations usually have high normal or increased androgen levels, the patient from this study presented neonatally with very low circulating androgens. This suggests an androgen biosynthesis defect. Indeed, this was supported by the results of urinary steroid metabolite analysis at the age of 9 years, which were indicative of PORD. This diagnosis was confirmed by direct sequencing, revealing compound heterozygous mutations. The novel POR frameshift mutation E601*fs*X12 is highly likely to abolish function as previous studies have shown that a premature stop codon result in loss of activity in the R616X POR mutant (Fluck et al., 2007; Agrawal et al., 2008). This indicates that early truncation of *POR* mRNA may result either in nonsense mediated RNA decay or that the integrity of the C-terminus of the POR protein is crucial for electron transfer. The missense mutation Y607C POR has been previously identified when screening a

large cohort of healthy Americans (Huang et al., 2008). However, this is the first time that this mutation has been found in a clinically affected PORD patient and hence has been confirmed as disease causing. Our co-expression assays with Y607C POR demonstrated only a mild impairment of 21-hydroxylase activity but significant inhibition of 17α-hydroxylase. Combined inhibition of both activities is consistent with the biochemical finding of normal baseline cortisol but impaired cortisol response to synacthen. Furthermore, preferential inhibition of 17α-hydroxylase over 21-hydroxylase explains the observation of mineralocorticoid metabolite accumulation in our patient, as previously described for A287P POR (Dhir et al., 2007).

However, one of the most striking features in our patient is the re-emergence of androgen production at the age of 9 years, resulting in progressive clitoral hypertrophy, a phenomenon not reported yet in patients with PORD (Flück and Pandey, 2011; Arlt et al., 2004; Fukami et al., 2009; Krone et al., 2012). This suggests that the disruptive effect of mutant POR on 17,20-lyase activity, resulting in low or non-detectable androgens during the neonatal period, had been partially overcome at time of adrenarche. *In vitro* assays suggested compromised 17,20-lyase activity due to Y607C for both the classic and alternative pathway, though to a lesser degree for the latter. However, clinical biochemical assessment certainly suggested androgen production via the classic pathway, with high normal circulating concentrations of DHEAS and androstenedione, and urinary androgen metabolite specific for the alternative androgen pathway, e.g. 5α-17-hydroxypregnanolone, were not found to be elevated in our patient.

It is obvious that the observed increase in androgen production was of adrenal origin as the patient had undergone bilateral gonadectomy five years earlier. It has been generally agreed that adrenarche and gonadarche are distinct events and

happen independently of each other (see section 1.2.3), and this case study certainly illustrates this. At time of adrenarche there is a physiologic increase in the expression of the co-factor enzyme cytochrome b5 (CYB5A) within the adrenal zona reticularis, the major site of adrenal androgen production (Suzuki et al., 2000). CYB5A expression is low in pre-adrenarchal adrenals but steadily increases after 5 years of age to reach a plateau at the age of 13 years (Nakamura et al., 2009). CYB5A is thought to serve as an allosteric facilitator for the interaction of POR and CYP17A1, stabilizing their interaction by forming a CYP-POR-CYB5 complex. There is currently no information on the exact interaction site of CYB5 with POR. Based on three-dimensional modeling Y607C can be predicted to disrupt the binding of NADPH to the POR NADPH-binding domain (Wang et al., 1997; Huang et al., 2008). However, if one assumes that the hydrophobic surface area near to Y607C could potentially be the interaction area with CYB5, it is conceivable that increasing concentrations of CYB5 at time of adrenarche could partially overcome the effect of the mutant. All microsomal assays in this study were carried in the presence of excess CYB5 concentrations, and consequently it is likely that the disruptive effect of Y607C POR on 17,20-lyase activity would certainly be more significant in a milieu of relative CYB5 deficiency, i.e. prior to adrenarche. To test the effect of varying quantities of CYB5A on Y607C POR would be an interesting experiment for the future. Intriguingly, it was recently demonstrated in the domestic ferret that the majority of gonadectomy-induced androgen-producing adrenal tumours express CYB5, which is physiologically not present in normal ferret adrenals (Wagner et al., 2008). Gonadectomy-induced adrenal tumourigenesis has also been described in certain mouse strains and increased LH stimulation and altered activin/inhibin signalling have been implicated in the pathogenesis (Beuschlein et al., 2003). In humans, increased androgen

production after gonadectomy has not been reported but if such a cross-talk between the gonadal and adrenal axes also exists, it may contribute to the virilization observed in our patient.

Thus, one could speculate that the increase in both androgen production and action at time of puberty is explained by a two-step model. Firstly, the emerging CYB5A expression in the adrenal zona reticularis may ameliorate the disruptive effect of Y607C POR, resulting in an increase in 17,20-lyase activity and adrenal androgen production during adrenarche. Secondly, increasing levels of androgens could then potentially enhance the transactivation capacity of the AR mutant Q798E, as previously observed *in vitro* (Wang et al., 1998; Jääskeläinen et al., 2006). This subsequently results in improved androgen action and the observed clitoral enlargement, which would represent phallic catch-up growth due to increased androgen sensitivity in an individual with a male genetic background, as observed previously in some 46,XY individuals with idiopathic micropenis (Lee and Houk, 2004). Of note, virilization at puberty and the subsequent change of gender identity is not uncommon in 46,XY DSD individuals with HSD17B3 or SRD5A2 deficiencies who where raised as girls (Lee et al., 2007; Cohen-Kettenis, 2005). However, the mechanism in these conditions is different as testicular derived androgens accumulate prior to the enzyme block (androstenedione in HSD17B3 and testosterone in SRD2A2) and are likely to be converted by other isoenzymes (Lee et al., 2007). The observed biological response to a relatively sudden increase in androgen levels in HSD17B3 and SRD5A2 deficiency patients reflects the susceptibility of individuals with a male karyotype to develop phenotypic virilization, similar to our case.

In conclusion, our patient illustrates the close interaction of factors involved in the regulation of androgen synthesis and androgen action, respectively. Furthermore, our case highlights that patients presenting with DSD also require thorough work-up of the adrenal axis and vice versa (Metherell et al., 2009; Ahmed and Rodie, 2010), to ensure that these patients are not exposed to the unrecognized risk of life-threatening adrenal crisis, which fortunately did not occur in our case until the conclusive diagnosis of adrenal insufficiency was established, nine years after the initial presentation with 46,XY DSD.

4. CHAPTER 4: PUBERTAL PRESENTATION IN P450 OXIDOREDUCTASE DEFICIENCY

This chapter has been published as:

Pubertal presentation in seven patients with congenital adrenal hyperplasia due to P450 oxidoreductase deficiency.

Idkowiak J, O'Riordan S, Reisch N, Malunowicz EM, Collins F, Kerstens MN, Köhler B, Graul-Neumann LM, Szarras-Czapnik M, Dattani M, Silink M, Shackleton CH, Maiter D, Krone N, Arlt W.

J Clin Endocrinol Metab. 2011 Mar;96(3):E453-62. doi: 10.1210/jc.2010-1607

4.1. INTRODUCTION

P450 oxidoreductase (POR) deficiency (PORD) is a variant of congenital adrenal hyperplasia caused by mutations in the *POR* gene (Flück et al., 2004; Arlt et al., 2004) (see section 1.3.1.2).

In PORD patients, combined deficiencies of the steroidogenic enzymes CYP17A1 and CYP21A2 represent the most striking biochemical findings. Notably, PORD patients of both sexes may present at birth with DSD, a puzzling finding that can be explained by the existence of an alternative pathway to active androgens (1.3.1.2). The skeletal malformations in PORD patients resemble the malformation phenotype of Antley-Bixler-Syndrome (ABS, OMIM 207410) (Antley and Bixler, 1975).

Neonatal presentation in PORD has been well described (Arlt et al., 2004; Huang et al., 2005; Fukami et al., 2009; Krone et al., 2012). However, there is a paucity of detailed data on the pubertal phenotype that is likely to be affected by impaired sex steroid synthesis.

In this chapter, we have clinically, genetically and biochemically characterized seven patients (five females, two males) with PORD during puberty.

4.2. METHODS

4.2.1. Patients

The cohort consisted of five female and two male patients from six different countries. In all patients appropriate written consent and assent, respectively, had been obtained in accordance with local IRB guidelines. Patient characteristics including genetic and biochemical findings are summarized in **Table 12** for the affected girls and in **Table 13** for the two male patients.

Table 12: Summary of clinical, genetic, and hormonal findings in five female pubertal PORD patients. n.m., not measured; SDS, standard deviation score.

	Case 1	**Case 2**	**Case 3**	**Case 4**	**Case 5**
Ethnicity	White Caucasian	White Caucasian	White Caucasian	White Caucasian	White Caucasian
Karyotype	46,XX	46,XX	46,XX	46,XX	46,XX
POR mutations (p.)	A287P/R457H	A287P/A287P	A287P/A287P	T142A/Y376L*fs*X74	A287P/R223X
46,XX Disordered Sex Development	Yes	Yes	Yes	No	Yes
Skeletal Malformations	Mild	Mild	Mild	Overt at birth	Overt at birth
Age at investigation (years)	16	12	23	19	16
Tanner stages	PH4, B4, M0	PH2, B1, M0	PH3, B3, M0	PH3, B5, M1	PH3, B3, M0
Height (cm)	168 (0.9 SDS)	148 (-1.4 SDS)	166 (0.4 SDS)	182.5 (2.0 SDS)	158.7 (-0.7 SDS)
Target height (cm)	175/168	165/160	172/150	198/166	180/172
Weight (kg)	51.3 (-0.7 SDS)	32.0 (-2.2 SDS)	61.4 (-0.3 SDS)	88.0 (3.1 SDS)	40.2 (-2.4 SDS)
BMI (kg/m^2)	18.2 (-0.9 SDS)	14.61 (-2.1 SDS)	22.3 (0.5 SDS)	26.3 (1.5 SDS)	16.1 (-2.3 SDS)
ACTH (pmol/L)	3.1 (2.2–11)	34.8 (2.2-11)	22 (2.2-11)	19 (2.2-11)	5.3 (2.2-11)
Cortisol (nmol/L)					
baseline	289 (150 – 780)	607 (150 – 780)	149 (150 – 780)	375 (150 – 780)	190 (120-780)
60 min after 250 µg $ACTH_{1\text{-}24}$ i.v.	436 (>550)	717 (>550)	158 (>550)	425 (>550)	314 (>550)
Adrenal insufficiency	Yes	No	Yes	Yes	Yes
Progesterone (nmol/L)					
baseline	8.8 (0.9 – 2.3)	256 (0.3 – 14.1)	45.8 (< 3)	58 (0.9 – 2.3)	28.8 (0.1-5.1)
60 min after 250 µg $ACTH_{1\text{-}24}$ i.v.	53.4	307	181.5	83	>191
17OHP (nmol/L)					
baseline	25.7 (0.45 - 2.9)	72.7 (0.45-2.9)	67.5 (< 5)	25 (0.45 – 2.9)	15 (0.1-8.1)
60 min after 250 µg $ACTH_{1\text{-}24}$ i.v.	53.4	86.8	82.3	36	n.m.
Androstenedione (nmol/L)	2.6 (1.8 – 12.9)	3.45 (2.8 – 6.6)	n.m.	0.6 (3.0 – 9.6)	1.7 (0.1-5.5)
DHEAS (µmol/L)	5.7 (1.1 - 6.2)	2.41 (0.8 – 9.3)	2 (2.5 – 5.25)	1.2 (3.0 – 13.0)	4.2 (0.4-7.9)
Testosterone (nmol/L)	n.m.	n.m.	0.48 (< 2.4)	1.1 (1.0 – 3.5)	0.48 (0.1-1.7)
Estradiol (pmol/L)	53.5 (78-312)	undetectable	n.m.	90 (70 - 530)	84 (66-246)
LH (U/L)	35.0 (1.1-3.7)	19.0 (0.3-1.2)	53.0 (0.7-4.7)	6.1 (1.1-3.7)	19.2 (0.7-4.7)
FSH (U/L)	12.6 (3.1-8.1)	17.0 (1.6-7.3)	29.0 (3.9-7.0)	10.0 (3.1-8.1)	13.1 (3.9-7.0)

Case 1: The neonatal presentation of this case, virilized genitalia (46,XX DSD) and low circulating androgens, has been described previously (Arlt et al., 2004). At the age of 14 years she presented with acute abdominal pain; investigations revealed rupture of a large (4.5cm) left ovarian cyst requiring surgical intervention, with removal of a largely degenerative polycystic ovary. Physical examination also revealed mild dysmorphic features (depressed nasal bridge, arachnodactyly, camptodactyly, restricted elbow extension bilaterally, syndactyly of toes 2/3). Tanner stages were PH4, B4, M0. However, serum E2 was pre-pubertal and gonadotrophins were high (**Table 12**). 17OHP and progesterone were elevated and cortisol showed a subnormal response to $ACTH_{1-24}$ (**Table 12**) and hydrocortisone cover during stress was recommended. After six months of treatment with synthetic progestin, E2 levels slightly increased but gonadotrophins were still high (E2 106 pmol/L; LH 15.3 U/L; FSH 8 U/L). Treatment was changed to an oestradiol/progestin combination. Follow-up one year later showed low E2 levels and elevated gonadotrophins (E2 63 pmol/L; LH 40 U/L, FSH 16 U/L), possibly reflecting compliance problems. At the age of 15.8 years, spontaneous rupture of a right ovarian cyst occurred that required emergency surgical intervention resulting in the removal of the residual right ovary. The patient now receives continuous oestrogen/progestin replacement therapy.

Case 2: The patient (46,XX) was born after 42 weeks of gestation as the third child of non-consanguineous parents of Polish origin. Her genitalia was virilized at birth (clitoromegaly and urogenital sinus). At the age of 11.5 years bilateral ovarian masses were diagnosed by ultrasound and CT and subsequently surgically removed. Histopathology confirmed ovarian follicular cysts. Endocrine assessment revealed undetectable E2 and elevated LH and FSH (**Table 12**). After 10 months, ovarian cysts on both sides recurred and the patient was referred for further endocrine

investigations. Tanner stages were B1, PH2, M0. Several dysmorphic features were noted, including midface hypoplasia, brachycephaly, dysplastic ears, arachno- and camptodactyly and bilaterally restricted elbow extension. Hormonal assessment showed elevated 17OHP, progesterone, and ACTH concentrations; however, cortisol was high normal at baseline and after i.v. cosyntropin (**Table 12**). Medical treatment of the ovarian cysts with a combination of 17β-oestradiol (1mg/d), GnRH superagonists (Dipherelin; 3.75 mg/month) and dexamethasone (0.25 mg/d; reduction to 0.125 mg/48h after 2 months) was initiated. On this regimen, the ovarian cysts partially regressed in size after 12 months of treatment. At 13.5 years her pubertal staging was B4, PH3; she was then started on a combination of triamcinolone 2 mg/d, 17β-oestradiol and synthetic progestin, resulting in regular withdrawal bleeds. The ovarian cysts further decreased in size and until the present age of 18 years there have been no recurrences.

Case 3: The patient was born with ambiguous genitalia after an uneventful pregnancy to consanguineous parents of Italian origin. The baby was raised as a boy until the age of 5 when her gender assignment was reconsidered after the birth of a sister with obvious 46,XX DSD. A diagnostic laparotomy showed the presence of normal internal female genital organs. Multiple genital surgeries including vaginoplasty and partial clitoral reduction were performed between 5 and 12 years of age. Normal psychomotor development, bone age and growth velocity (50^{th} to 75^{th} percentile) were documented. Her younger sister later died aged 8 years after developing signs and symptoms of shock shortly after undergoing an appendectomy.

Pubertal development was induced at the age of 17 years by treatment with equine oestrogens and progesterone. At the age of 23 years she was assessed as having normal female appearance but with only moderate breast development (**Table**

12). Several mild dysmorphic features were noted (narrow hard palate, low set ears, clinodactyly, camptodactyly and brachydactyly of the 4th toe bilaterally). Genetic analysis confirmed a 46,XX karyotype. Hormonal evaluation showed elevated serum progesterone and 17OHP levels whereas serum androgens were low; serum cortisol was low at baseline and did not increase appropriately after i.v. synacthen (**Table 12**). After three months of oestrogen withdrawal, the patient's gonadotrophins were increased (LH 53 U/L, FSH 29 U/L). Concurrently large ovarian cysts up to 7 cm in diameter developed, which regressed partially following reintroduction of oestrogen/progestin treatment, but only resolved after the addition of glucocorticoid treatment (dexamethasone 0.375 mg/d).

Case 4: The patient was the first child born to non-consanguineous parents of Dutch origin. There was no genital ambiguity but she underwent early postnatal assessment for dysmorphic features including frontal bossing, midface hypoplasia, pear shaped nose, low-set ears with flat helices, impaired supination of the forearms, arachnodactyly, synostosis of several distal and interphalangeal joints. However, no precise diagnosis was established and she was subsequently lost to follow-up.

At the age of 19 years she presented with irregular menses. Pubertal development was partially delayed (**Table 12**). Hormonal assessment revealed low E2 with normal gonadotrophins; 17OHP and progesterone were elevated; baseline cortisol was normal but did not increase sufficiently after i.v. $ACTH_{1-24}$ and adrenal androgens were low (**Table 12**). An MRI scan of the pelvic region revealed cystic enlargement of the right ovary (3 x 4 cm) with normal appearance of the left ovary and normal female anatomy of the reproductive system. Combined treatment with E2 (2 mg daily) and dydrogesterone (10 mg daily) was initiated. At present, the patient

has been on hormone replacement therapy for 6 months and repeat imaging has not yet been performed.

Case 5: The girl was born at 36 weeks of gestation after an uneventful pregnancy to non-consanguineous parents of German origin. Postnatally, the girl needed ventilation due to severe respiratory distress associated with bilateral choanal stenosis. At birth there were obvious dysmorphic features including brachycephaly, midface hypoplasia, exophthalmus, retrognathia, depressed nasal bridge, low set ears and bilateral radiohumeral synostosis. The external genitalia were ambiguous with clitoral hypertrophy and an urogenital sinus (Prader stage III). Clitoral reduction and vulvo- and vaginoplasty were performed at 2 years of age. During childhood the girl had multiple reconstructive surgeries for correction of the craniofacial abnormalities.

At 16 years of age, she presented to the endocrine clinic because of primary amenorrhoea. Tanner staging revealed PH3, B3, M0. Bone age was delayed by two years. Pelvic ultrasound revealed an infantile uterus and bilateral polycystic ovaries with the largest cyst measuring 1 cm in diameter and with increased total ovarian volumes of 8.6 and 10 ml, respectively. Hormonal analysis showed a low E2 with upregulated gonadotrophins; baseline cortisol was low and did not increase sufficiently after i.v. cosyntropin and adrenal androgens were normal (**Table 12**). She was started on oestradiol valerate for hormone replacement.

Case 6: The boy was born at 39 weeks of gestation as the first child of a Chinese mother and a Costa Rican father. Both testes were undescended but palpable in the inguinal canal; the scrotum was hypoplastic. Bilateral orchidopexies were performed at the age of 12 months. In addition, at birth, choanal stenosis, facial dysmorphism (brachycephaly, frontal bossing, mid-face hypoplasia, pre-auricular skin

tags) and multiple skeletal abnormalities, including arachnodactyly, shoulder and knee contractures, radio-ulnar synostosis, bilateral coronal synostosis, partial fusions of thoracic vertebrae T3/T4, were noted. No conclusive diagnosis was made and the patient was lost to follow-up.

The patient was referred for endocrine assessment at the age of 10.5 years because of poor genital development (**Table 13**). His genitalia were undermasculinized for age (phallus of 15 mm length with little erectile tissue). Serum gonadotrophins and androgen levels were pre-pubertal (**Table 13**). Cortisol was normal at baseline but insufficiently stimulated after 250 µg $ACTH_{1-24}$ revealing partial adrenal insufficiency (**Table 13**). Hydrocortisone replacement therapy (10 mg/m^2 daily) and early pubertal induction with oral testosterone (40 mg daily) was commenced but the family then dropped out of care and ceased medications.

At age 16 years he presented again after several years of no medication. However, pubertal development had spontaneously progressed and the phallus was 8.5 cm with adequate erectile tissue, appropriate testicular volumes, and advanced pubertal staging (**Table 13**). Hormonal investigations revealed normal androgens but upregulated gonadotrophins (**Table 13**).

Table 13: Summary of clinical, genetic, and hormonal findings in two male pubertal PORD patients. n.m., not measured; SDS, standard deviation score

	Case 6		**Case 7**	
Ethnicity	Hispanic/Asian		White Caucasian	
Karyotype	46,XY		46,XY	
POR mutations (p.)	R457H/Y576X		A287P/IVS7+2dupT	
46,XY Disordered Sex Development	No, but both testicles undescended (inguinal canal)		No, but right testicle undescended (inguinal canal)	
Skeletal malformations	Overt at birth		Overt at birth	
Age at investigation (years)	12	16	12	13.5
Tanner stages	PH1, G1	PH5, G5	PH1, G1	PH3, G2
Testicular volume (right/left) (ml)	1/2	20/25	4/12	25/10
Height (cm)	143 (-0.6 SDS)	166.1 (- 0.9 SDS)	138.2 (-1.6 SDS)	150.9 (-0.8 SDS)
Parental heights father/mother (cm)	172/172		178/157	
Weight (kg)	28.7 (-1.8 SDS)	39.9 (-2.95 SDS)	42.5 (0.2 SDS)	56.6 (0.9 SDS)
BMI (kg/m^2)	14.1 (-2.3 SDS)	15.0 (-3.3 SDS)	22.3 (1.3 SDS)	25.1 (1.60 SDS)
ACTH (pmol/L)	39.6 (2.2-11)	16 (2.2-11)	12.4 (2.2-11)	99.1 (2.2-11)
Cortisol (nmol/L)				
baseline	198 (150 – 780)	217 (150-780)	353 (150 – 780)	n.m.
60 min after 250 µg ACTH$_{1\text{-}24}$ i.v.	229 (>550)	n.m.	411 (>550)	n.m.
Adrenal insufficiency	Yes		Yes	
17OHP (nmol/L)				
baseline	112 (<6)	91.5	14 (0.45 – 2.9)	n.m.
60 min after 250 µg ACTH$_{1\text{-}24}$ i.v.	124	n.m.	54	n.m.
Androstenedione (nmol/L)	5.4 (1.8 – 12.9)	6.0 (2.7-10)	1.1 (1.8 – 12.9)	n.m.
DHEAS (µmol/L)	0.9 (1.1 – 6.2)	1.9 (1.8-10)	0.8 (0.5 – 4.1)	1.3 (1.1-6.2)
Testosterone (nmol/L)	0.8 (0.2-1.5)	26.6 (9-27)	0.7 (0.07-0.8)	10.7 (9-27)
LH (U/L)	0.4 (<1.7)	37 (0.2-6.1)	0.6 (<1.7)	2.4 (0.4-4.6)
FSH (U/L)	1.7 (<2.5)	12.5 (0.5-6.3)	1.9 (<2.5)	4.8 (2.7-4.4)

Case 7: This boy was born after an uneventful pregnancy to non-consanguineous parents of British origin. At birth, several dysmorphic features were noted including choanal stenosis, brachycephaly and joint contractures due to radio-ulnar synostosis. There was no genital ambiguity; however, his right testicle was undescended but palpable in the inguinal canal. Right-sided orchidopexy was undertaken at the age of 12 months and the boy underwent a series of osteotomies for coronal craniosynostosis.

He presented at 12 years of age to the endocrine clinic with lack of pubertal development and testicular volumes of 4 and 12 ml, respectively. Adrenal androgen concentrations were low; testosterone was high-normal in comparison to age-specific reference (**Table 13**). Baseline cortisol was normal but response to i.v. cosyntropin was insufficient (**Table 13**). Hydrocortisone treatment was initiated (10mg/m^2/d) und further pubertal development monitored at 6-monthly intervals. Puberty progressed spontaneously and when assessed at the age of 13.5 years testicular volumes had increased to 10 and 25 ml, respectively (**Table 13**). DHEAS, testosterone and baseline gonadotrophins were within age- specific reference ranges (**Table 13**).

4.2.2. Urinary steroid profiling

Analysis of urinary steroid metabolite excretion was performed as described in section 2.7.1. Steroids quantified included corticosterone metabolites (THB, 5αTHB, THA), the progesterone metabolite PD, 17-hydroxyprogesterone metabolites PT, 17HP, the 17-hydroxypregnenolone metabolite 5-PT, the 21-desoxycortisol metabolite P'TONE, cortisol metabolites THF, 5αTHF and THE; and androgen metabolites An and Et, DHEA and 16-OH-DHEA (see **Table 9** for steroid metabolite abbreviations)

Following quantification of steroid metabolites by GC/MS the following substrate/product ratios to determine the approximate *in vivo* net activity of specific steroidogenic enzymes were calculated: corticosterone over cortisol metabolites (17α-hydroxylase; (THA+THB+5αTHB)/(THF+5αTHF+THE)), 17-hydroxyprogesterone over androgen metabolites (17,20-lyase; (17HP+PT)/(An+Et)), 17-hydroxyprogesterone over cortisol metabolites (21-hydroxylase; (100xPTONE/(THF+5αTHF+THE)), and the ratio of progesterone over cortisol metabolites (combined 21-hydroxylase and 17-hydroxylase activities, i.e. specific for PORD; PD/(THF+5αTHF+THE)). The diagnostic ratios and overall secretion patterns were compared with urinary steroid profiles obtained from a normal reference cohort of boys and girls between 12 and 16 years of age (n=12).

4.2.3. Genetic analysis

The coding sequence of the *POR* gene including exon-intron boundaries was amplified as described in section 2.2.11.

4.3. RESULTS

4.3.1. Clinical and hormonal characteristics

All seven patients presented with absent or incomplete pubertal development leading to the diagnosis of PORD. Three female patients had presented neonatally with 46,XX DSD and five of the seven patients had overt skeletal malformations noted immediately after birth. However, in all cases this had not prompted the establishment of a conclusive diagnosis prior to puberty.

Generally, female patients presented with significant pubertal impairment and ovarian cysts. In case 1, spontaneous cyst rupture required two surgical emergency interventions, resulting in loss of both ovaries despite ongoing oestrogen/progestin

therapy. Ovarian cysts in cases 2 and 3 only resolved following the addition of glucocorticoids and GnRH agonists to ongoing oestrogen/progestin therapy. Four of the five female patients presented with primary amenorrhea and biochemical evidence of primary hypogonadism (**Table 12**). By contrast, both boys showed spontaneous, albeit slightly delayed, pubertal progression, with testicular volumes appropriate for age, and biochemical signs of compensated hypogonadism, with normal testosterone but upregulated gonadotrophins (**Table 13**).

In all patients, adrenal androgens were either normal or low. All cases had elevated 17OHP and progesterone concentrations, accompanied by increased ACTH levels in 5 patients. Baseline cortisol secretion was normal in five and borderline low in two patients. In all but one patient cortisol secretion was not sufficiently stimulated by i.v. cosyntropin, indicative of partial adrenal insufficiency.

Auxological investigations in all seven cases showed a normal height at investigation within the familial target height range.

4.3.2. Urinary steroid profiling

Steroid profiling by GC/MS revealed a typical pattern for PORD in all patients studied (**Figure 24**). 24-h excretion analysis revealed a characteristically increased excretion of metabolites of 17-hydroxypregnenolone (5-PT), progesterone (PD), and 17OHP (17HP, PT, P'TONE) and a mild increase in mineralocorticoid precursor metabolites (e.g. THB, THDOC) (**Figure 24A**), which reflects the concurrent impairment of 17α-hydroxylase and 21-hydroxylase activities. In keeping with impaired 17,20-lyase activity, androgen and androgen precursor metabolite excretion was decreased or low normal (**Figure 24A**). Cortisol metabolites were low or in the lower normal reference range, indicative of impaired 21-hydroxylase activity (**Figure**

24A). Substrate/product ratios clearly demonstrated attenuation of 17α-hydroxylase, 17,20-lyase and 21-hydroxylase activities in all cases examined (**Figure 24B**).

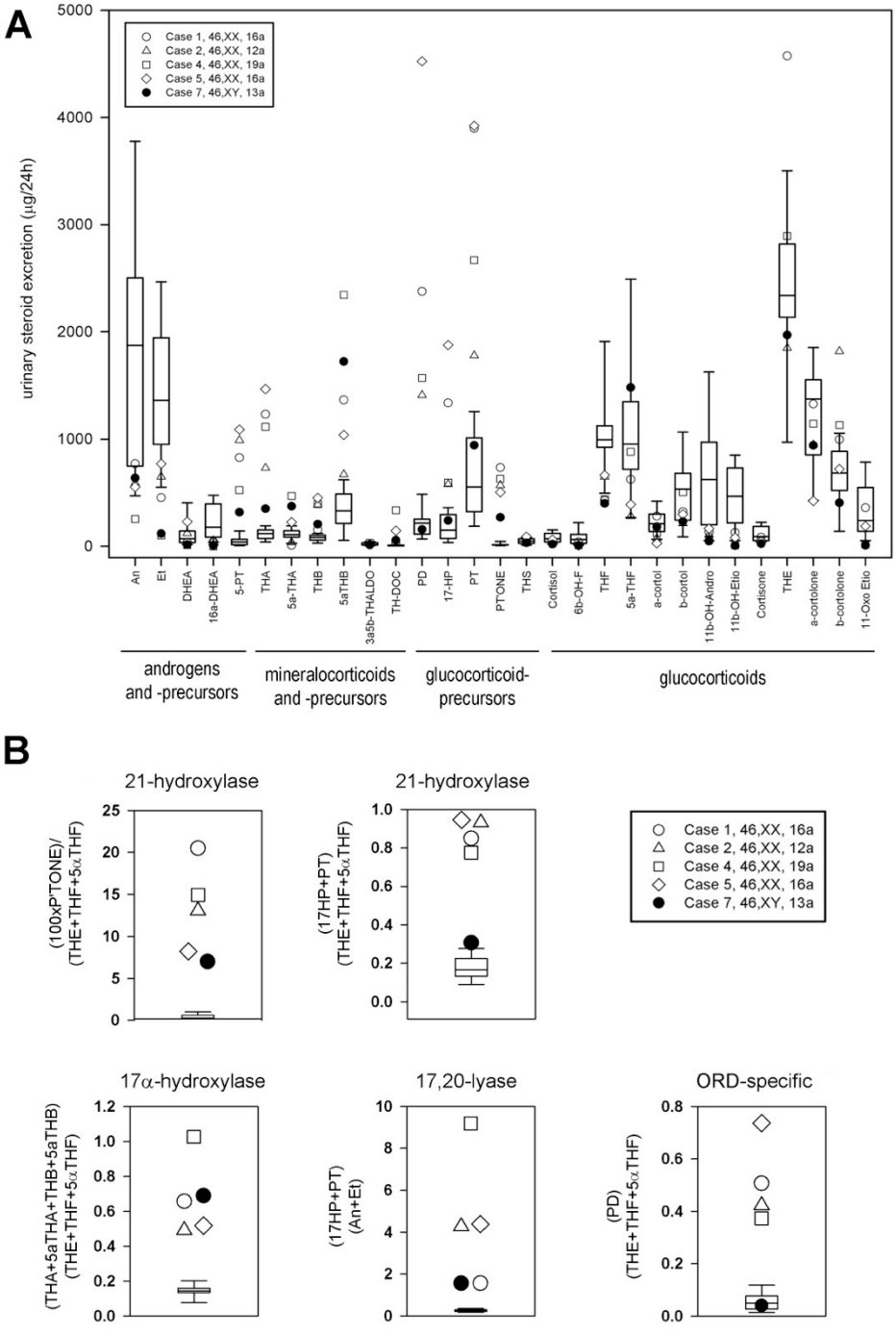

Figure 24: *In vivo* steroidogenic enzyme activities in pubertal PORD patients as determined by total 24-h urinary steroid metabolite excretion (Panel A) and diagnostic steroid substrate/product ratios (Panel B) measured by gas chromatography/mass spectrometry and shown in comparison to an age-matched reference cohort (n=12). Box plots represent the interquartile ranges (25th to 75th percentile), whiskers the 5th and 95th percentile, respectively, of the reference cohort; each pubertal PORD case is represented by specific symbols as indicated in the legend.

4.3.3. Genetic analysis

Sequencing analysis of the *POR* gene revealed compound heterozygous missense mutations p.A287P/p.R457H in case 1. Cases 2 and 3 were homozygous for p.A287P, and case 4 showed compound heterozygous mutations comprising a missense mutation (p.T142A) and a novel frameshift mutation resulting in a premature stop codon (p.Y376L*fs*X74). Case 5 was compound heterozygous, with a p.A287P mutation on one allele, and a novel p.R223X nonsense mutation on the other allele.

Case 6 was compound heterozygous for p.R457H and p.Y567X whereas case 7 was compound heterozygous for p.A287P, and a novel duplication disrupting the splice donor site of intron 7, IVS7+2dupT. The duplication does not yield an alternative splice site according to splice site prediction tool http://www.cbs.dtu.dk/services/NetGene2/, thus resulting in translation of intron 7 until a premature stop codon 64 aa downstream of the last exon 7 codon (p.P277P*fs*X65).

4.4. DISCUSSION

Here, we describe the clinical phenotype as well as biochemical and genetic findings in seven adolescents with PORD all presenting with disturbed pubertal development, manifesting with insufficient pubertal development and primary amenorrhea in four of the five girls and delayed, albeit spontaneously progressive puberty in the two boys.

All five females presented with ovarian cysts. This is a common finding in females affected by steroidogenic disorders and has been reported in 21-hydroxylase deficiency (21OHD) (New, 1993; Hague et al., 1990), 17α-hydroxylase deficiency (17OHD) (Rosa et al., 2007; Kate-Booij et al., 2004; Mallin, 1969), congenital lipoid

adrenal hyperplasia (CLAH) due to mutant steroidogenic acute regulatory protein (StAR) (Fujieda et al., 1997; Shima et al., 2000; Tanae et al., 2000), P450 aromatase deficiency (Belgorosky et al., 2003; Mullis et al., 1997), and also in PORD (Fukami et al., 2005; 2009). Of note, two infants with PORD have been described who even developed large ovarian cysts at two and four months of age, respectively (Fukami et al., 2006; Sahakitrungruang et al., 2009). Excessive LH-mediated ovarian stimulation as a consequence of primary hypogonadism is an obvious underlying mechanism. Interestingly, girls with CLAH often spontaneously undergo puberty and have normal circulating E2 levels (Fujieda et al., 1997) but still present with large ovarian cysts. It has been suggested that this may be the consequence of chronic anovulation rather than LH overstimulation (Shima et al., 2000), a concept that is supported by a study in a patient with amenorrhea, ovarian cysts and inactivating mutations of the LH receptor gene (Latronico et al., 1996). Similarly, multiple ovarian cysts can be found in women with steroidogenic disorders resulting in androgen excess such as 21OHD (Hague et al., 1990; Falhammar et al., 2008), which again could be a consequence of chronic anovulation or potentially direct androgen effects.

A unique mechanism driving ovarian cyst development in females affected by PORD in addition to high gonadotrophins resulting from oestrogen deficiency might be the disruptive impact of mutant POR on sterol synthesis and metabolism (**Figure 25**). 14α-lanosterol demethylase (CYP51A1) requires electron transfer from POR for catalytic activity and catalyses the conversion of lanosterol to meiosis-activating sterols (MAS). FF-MAS (follicular fluid MAS) have been shown to be crucial for the resumption of oocyte meiosis at puberty and also supports oocyte maturation (Byskov et al., 1995; Grondahl et al., 2000; 1998).

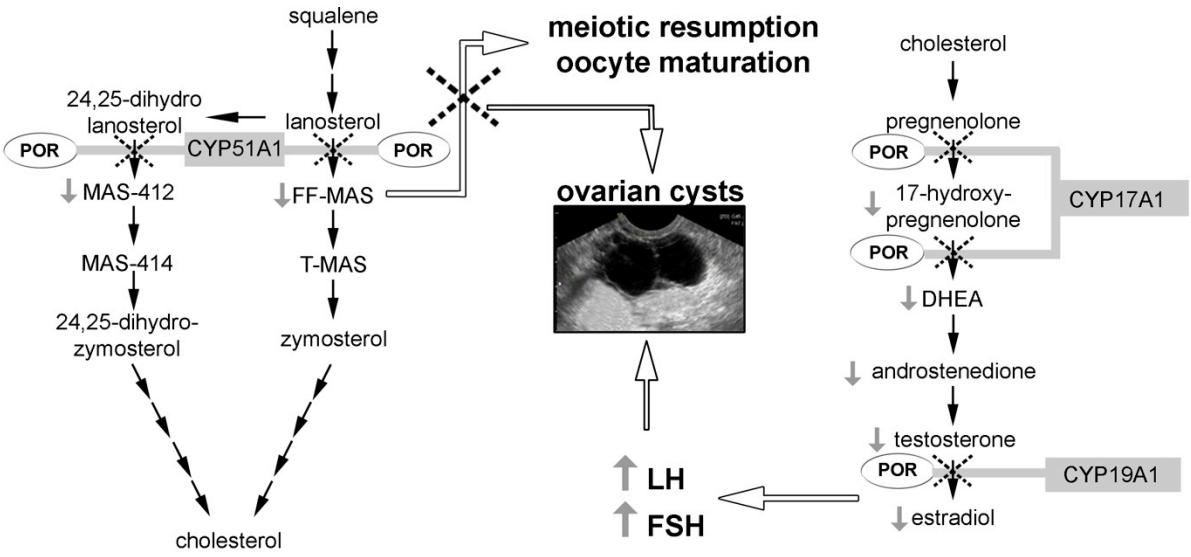

Figure 25: Schematic representation of the possible mechanisms leading to ovarian cysts in female patients with PORD. Impaired sex steroid synthesis results in low estradiol levels (right panel) causing hypergonadotropic hypogonadism with subsequent stimulation of the ovaries by the upregulated gonadotrophins. In addition, mutant POR affects the cholesterol synthesis pathway due to impairment of CYP51A1 activity (left panel) leading to decreased generation of meiosis activating sterols (MAS) that are important for meiotic resumption and oocyte maturation. LH, luteinizing hormone; FSH, follicle stimulating hormone; FF-MAS; follicle fluid MAS; T-MAS, testicular MAS; each black arrow indicates an enzymatic reaction; dotted crosses indicate impairment of pathway reactions; grey arrows indicate increased (or decreased) serum levels.

The detailed mechanism underlying the effects of FF-MAS on oocyte maturation is not clear yet but may involve the PKC pathway (Jin et al., 2006) or hedgehog signalling pathways (Nguyen et al., 2009; Mann and Beachy, 2004). FF-MAS is further converted to T-MAS (testicular MAS), which has been found to be highly expressed in mammalian testis, especially in spermatozoa, suggesting a role in male fertility (Mann and Beachy, 2004); however, its precise role in male human reproduction remains to be elucidated. Importantly, CYP51A1 is highly expressed in murine and human gonads (Rozman et al., 2002) and its inhibition *in vitro* results in oocyte arrest (Wang et al., 2009). Interestingly, it has recently been shown that gonadotrophins induce upregulation of CYP51A1 in mice and rabbits (Wang et al., 2009; 2010), suggesting that POR-dependent CYP51A1 may be a crucial contributor to oocyte maturation at puberty. Thus it is conceivable that female PORD patients

have to take a “double hit” driving ovarian cyst development, disrupted MAS synthesis and high gonadotrophins due to low oestrogen production (**Figure 25**). This may possibly explain why the cysts appeared to be more difficult to control in PORD than in patients with other steroidogenic disorders, with two patients from this case series requiring long-acting glucocorticoids in addition to sex steroid replacement to control the effects of excess LH secretion.

In contrast to the findings in the five female cases, pubertal development in our two male PORD cases was more mildly affected. Case 6 presented with poor development at the age of 10 years but subsequently he and the other male patient spontaneously progressed through puberty with near normal testosterone production. This may indicate that sex steroid production in the testicles during puberty is less dependent on fully functional POR than ovaries or adrenals. Fukami et *al.* (Fukami et al., 2009) previously reported that three out of six male PORD patients had a normal pubertal development while all seven pubertal age girls in their cohort had impaired pubertal development; however, only limited detail on the pubertal findings and no longitudinal data were provided. The only other paper previously reporting on pubertal age PORD patients described two young women aged 17 and 19 years, one of them presenting with normal breast development but primary amenorrhea, the other with complete lack of pubertal development (Sahakitrungruang et al., 2009).

Interestingly, circulating androgens in this case series of pubertal patients were relatively normal, though low androgen levels in infants and younger children with PORD are well documented. The relative increase in androgen production at pubertal age despite POR-dependent inhibition of sex steroid synthesis by CYP17A1 could possibly be explained by increased expression of cytochrome b5 (CYB5) that acts as an allosteric facilitator of POR and CYP17A1 (Auchus et al., 1998) thereby

facilitating CYP17A1 17,20-lyase activity. CYB5 is expressed pre- and postnatally in human adrenal and testicular tissues (Dharia et al., 2004). However, its expression increases in the adrenal zona reticularis around the age of adrenarche (Suzuki et al., 2000) and a similar increase in testicular Leydig cells could enhance 17,20-lyase activity significantly to rectify androgen production during adrenarche and puberty despite partially impaired POR function. The case report of severe 46,XY DSD (chapter 3 of this thesis), who presented with normal adrenal androgens and phallic catch-up growth during adrenarche, supports this hypothesis.

A diagnosis of adrenal insufficiency was established in all but one of our cases at presentation during puberty, generally displaying normal baseline cortisol levels but failure to respond appropriately to ACTH. Of note, despite neonatal presentation with DSD of unknown origin, none of the patients had previously undergone assessment of adrenal function, which had put them at considerable risk of adrenal crisis in case of intercurrent illness, inflammatory stress or surgery. The untimely death of the younger sister of case 3, who also presented with 46,XX DSD and died at the age of 8 years of unexplained shock following a routine appendectomy, illustrates the dramatic consequences that overlooking adrenal insufficiency can have.

Some of the phenotypic variability we observed in our patients may be explained by the differential effects of distinct POR mutations on electron-accepting CYP enzymes (Dhir et al., 2007). Interestingly, the three patients with either homozygous or compound heterozygous missense mutations presented with rather mild skeletal malformations and lack of pubertal progression. By contrast, the four patients carrying a major loss of function mutation in addition to a missense mutation on the other allele presented with severe skeletal malformations but only relatively

mildly impaired pubertal development. Genotype-phenotype analysis in large Caucasian (Krone et al., 2012) and Japanese (Fukami et al., 2009) PORD cohorts confirm that a severe skeletal phenotype is associated with a major loss-of-function mutation on one allele, however the prediction for gential- and biochemical phenotype is poor. The most common POR mutation in Caucasians, p.A287P (Huang et al., 2005), was found on seven alleles in five of our patients. p.R457H, the most common POR mutation in Japan (Adachi et al., 2006), was found in two of the patients, who were of Polish and Chinese origin, respectively. p.A287P decreases 17α-hydroxylase to 20-40% of wild type (WT) activity but retains 70% of 21-hydroxylase WT activity; p.R457H equally disrupts CYP17A1 and CYP21A2 activities (Dhir et al., 2007). p.T142A has been reported to only mildly impair CYP17A1 activity (Huang et al., 2005) and was found in case 4, the only patient with spontaneous menarche and a considerable degree of spontaneous pubertal development.

In summary, pubertal development of children with PORD is impaired and frequently manifests with primary hypogonadism in girls, requiring medical induction of puberty and monitoring for ovarian cyst development. Affected boys may have the capacity for spontaneous pubertal development justifying a primarily observatory approach. Importantly, adequate hydrocortisone replacement and stress dose cover to prevent life-threatening adrenal crisis is crucial in PORD patients. The late diagnosis of adrenal insufficiency in one of the patients and the death of a sibling likely to have suffered from PORD emphasizes the need for concurrent assessment of adrenal and gonadal function not only in PORD but in all DSD patients with an unclear diagnosis. This will facilitate early diagnosis of partial adrenal insufficiency, thus hopefully preventing adrenal crisis-related deaths in PORD, and timely establishment of a conclusive diagnosis in affected patients.

5. CHAPTER 5: BROAD PHENOYTPIC SPECTRUM OF 17ALPHA-HYDROXYLASE (CYP17A1) DEFICIENCY

5.1. INTRODUCTION

17α-hydroxylase deficiency (17OHD, MIM# 202110) is a rare autosomal recessive disorder and a variant of congenital adrenal hyperplasia (CAH) representing about 1% of all CAH cases (section 1.3.1.1). The underlying defect is impaired activity of the cytochrome P450 (CYP) enzyme CYP17A1 (also P450c17), which is located at a major branch point in human steroidogenesis and exhibits two distinct catalytic activities: 17α-hydroxylase, crucial for adrenal GC synthesis, and 17,20 lyase, the key step in the generation of C19 androgen precursors in adrenals and gonads (see section 1.1.8.1. and **Figure 4**).

The *CYP17A1* gene is located on chromosome 10q24.3 and consists of eight exons (Picado-Leonard and Miller, 1987). To date, about 70 mutations in the *CYP17A1* gene have been described (www.hgmd.cf.ac.uk), and the majority is associated with a phenotype of combined 17α-hydroxylase/17,20 lyase deficiency. Lack of CYP17A1 17α-hydroxylase activity results in low cortisol levels. Activation of the HPA axis leads to overproduction of corticosterone and deoxycorticosterone causing hypertension with hypokalaemia. The partial affinity of corticosterone for the glucocorticoid receptor may compensate for low cortisol levels and patients do not present with severe salt-wasting adrenal crisis. The lack of CYP17A1 17,20 lyase activity results in disturbances of sex steroid production leading to disordered sex development (DSD) in genetically male individuals (46,XY DSD) or delayed or absent pubertal development including primary amenorrhoea in 46,XX females. The residual mutant enzyme activity in 17OHD correlates well with the severity of disease expression. A few missense mutations in the *CYP17A1* gene have been described to exhibit only moderate impairment of CYP17A1 17α-hydroxylase activity, while the 17,20 lyase activity was always greatly reduced (see section 1.3.1.1). These patients

with apparently 'isolated' 17,20 lyase deficiency have normal blood pressure and cortisol levels but reduced sex steroid production. This suggests that CYP17A1 17α-hydroxylase activity is the determining component leading to a wider phenotypic spectrum of 17OHD.

5.2. METHODS

5.2.1. Patients

Case 1: The patient (46,XX) was born at term as the third child of non-consanguineous parents of Polish origin. At the age of 15 years she was admitted to an endocrinologist for further investigation of disturbed pubertal development and arterial hypertension. She presented with lack of pubertal development (Tanner stages PH1, B2, M0) and had elevated blood pressure (150/90 mmHg; 3.6/3.0 SDS for height), normal sodium and low-normal potassium (**Table 14**). Further hormonal investigations revealed low plasma renin activity (PRA); ultrasound investigations excluded renal and cardiac hypertension. Baseline cortisol was low and did not increase after $ACTH_{1-24}$ stimulation; 17OHP was normal and ACTH was elevated. Sex steroids including androstenedione and oestradiol (E2) were low with elevated gonadotrophins, indicating hypergonadotrophic hypogonadism (**Table 14**).

Case 2: The boy (46,XY) is the fourth child of consanguineous parents of Afghan origin. He presented at the age of 12 years with learning difficulties, gynaecomastia, microphallus (2.5 cm), glandular hypospadias and cryptorchidism and had a history of orchidopexy for a left undescended testis at the age of 5 years. His Tanner pubertal stages were G1, PH3. His blood pressure was normal, and his serum potassium and sodium levels were within the age and sex specific normal range (**Table 14**). His serum testosterone level was within the lower normal range

and his raised gonadotrophins revealed compensated hypergonadotrophic hypogonadism (**Table 14**). Baseline cortisol was low and did not increase after iv $ACTH_{1-24}$; 17OHP at baseline was mildly elevated (**Table 14**).

Case 3: The older sister (46,XX) of case 2 presented in the endocrine clinic at the age of 15 years because of delayed pubertal development. She had normal breast development (Tanner B4) but did not develop pubic hair nor experienced menarche. Cortisol was low at baseline and did not increase sufficiently after $ACTH_{1-24}$ stimulation (**Table 14**). 17OHP was 2.7 nmol/l at baseline and increased to 3.5 nmol/l after $ACTH_{1-24}$. DHEAS was undetectable by several measurements. E2 was pre-pubertal with gonadotrophins at baseline within the pubertal reference range (**Table 14**). Blood pressure was normal at random baseline measurements and within the age- and height adjusted 50^{th} – 90^{th} centiles in a 24h blood pressure measurement.

Case 4: The 4 week old baby (46,XX) was assessed for prolonged jaundice. A baseline cortisol was 25 nmol/L and did not increase after synacthen stimulation (**Table 14**). ACTH was highly elevated suggesting severe primary adrenal insufficiency. 17OHP was undetectable. Serum potassium and sodium levels were within the normal range. The physical examination showed normal female external genitalia. Urinary steroid profiling with GC/MS showed trace amounts of cortisol metabolites, absence of androgen metabolites with a small amount of corticosterone metabolites indicating incapacity of cortisol and androgen biosynthesis.

***Case 5*:** The patient (46,XY) was born as the only child of non-consanguineous parents of Caucasian origin in Romania. He presented in the endocrine clinic at the age of 23 years due to fertility problems and for consultation for plastic surgery for his small phallus. On examination, there was no phallus detectable with a single perineal

opening. The left testicle was descended and palpable in the scrotum. The blood pressure was normal. Hormonal investigations showed normal cortisol levels at baseline and after $ACTH_{1-24}$ stimulation (**Table 14**). 17OHP and ACTH was within the age-specific reference range. Sodium, potassium, renin and aldosterone were normal. Androgen levels (DHEAS and testosterone) were low but 17-Preg was elevated (57 nmol/L; NR < 13).

Table 14: Summary of clinical, genetic, and hormonal findings from all patients with CYP17A1 deficiency. SDS, standard deviation score

	Case 1	**Case 2**	**Case 3**	**Case 4**	**Case 5**
Karyotype	46,XX	46,XY	46,XX	46,XX	46,XY
CYP17A1 mutation (p.)	P409L/G111V	F53/54del hom.	F53/54del hom.	Y60IfsK88X hom.	A398E/R347H
Age at presentation	2 yrs	birth	15 yrs	3 weeks	birth
Age at investigation	15 yrs	12 yrs	15 yrs	3 weeks	23 yrs
Height cm	168 (0.93 SDS)	159.6 (0.8 SDS)	161.1 (-1.0 SDS)		
Weight kg	49.2 (-0.5 SDS)	36.1 (0.86 SDS)	48.5 (-0.75 SDS)		
BMI kg/m^2	17.4 (-1.1 SDS)	14.2 (-2.1 SDS)	18.7 (-0.29 SDS)		
Blood pressure mmHg	150/90	110/80			120/75
Na; K mmol/L	140; 3.5	140; 4.0		140; 4.5	140; 4.2
PRA ng/ml/h	0.37 (0.5-2.6)				1.5 (0.5-2.6)
Aldosterone nmol/L					0.31 (0.1-0.8)
Cortisol nmol/L					
At baseline	136 (> 150)	105 (> 150)	113 (> 150)	25	375 (> 150)
60 min after ACTH$_{1-24}$	198 (> 550)	151 (> 550)	150 (> 550)	33 (> 550)	621 (> 550)
17OHP nmol/L	2.85 (<5)	17.4 (< 5)	2.7 (< 5)	< 1 (2-10)	7.3 (< 5)
DHEA-sulfate µmol/L	< 0.4 (1.7 - 10.1)	0.4 (1-4)	< 0.4 (1.7-10.1)		0.98 (5.2-12.3)
Testosterone nmol/L		2.4 (0.4-9.5)			0.96 (11-35)
Oestradiol pmol/L	< 70		43		
LH U/L	18.4 (0.4-5.7)	24.4 (0.4-5.7)	2.4 (0.4-5.7)		
FSH U/L	15.3 (2.7-4.4)	14.2 (2.7-4.4)	4.3 (2.7-4.4)		
ACTH pmol/L	110 (2-10)	7.7 (2-10)	9.5 (2-10)	85 (<10)	4.2 (2-10)

5.2.2. Urinary steroid profiling

Analysis of urinary steroid metabolite excretion was performed with GC/MS as described in section 2.7.1. Steroids quantified included corticosterone metabolites THB, 5αTHB, THA, the 17-hydroxyprogesterone metabolite PT and androgen metabolites An, Et, DHEA and 16-OH-DHEA (see **Table 9** for a full list of steroid abbreviations).

Following quantification of steroid metabolites, the following substrate/product ratios were calculated to determine the approximate *in vivo* net activity of specific steroidogenic enzymes: corticosterone over cortisol metabolites (17α-hydroxylase; (THA+THB+5αTHB)/(THF+5αTHF+THE)), 17-hydroxy-progesterone over androgen metabolites (17,20-lyase; (PT)/(An+Et)). These diagnostic ratios were compared to ratios obtained from urine analysis in a healthy, combined male and female reference cohort (n=26; age range 12-30 years).

5.2.3. Genetic analysis

The coding sequence of the *CYP17A1* gene including exon-intron boundaries was amplified as described in section 2.2.11.

5.2.4. Molecular cloning and site-directed mutagenesis

The bicistronic mammalian expression vector pIRES harbouring the human cDNA for WT/mutant CYP17A1 (in MCA) and WT CYB5A (in MCB) was used for *in vitro* functional analysis. Site-directed mutagenesis for p.F53/54del, p.A398E, p.R347H, p.G111V, p.P409L and g.177dupA of CYP17A1 was performed in the pcDNA6 vector as described in section 2.4.3 by using the following primers (the mutated nucleotide is highlighted in bold): C17-R347H-Fwd: 5’-ACTATCAGTGACC**A**TAACCGTCTCCTC-3’; C17-R347H-Rev: 5’-GAGGAGACGG-TTA**T**GGTCACTGATAGT-3’; C17-F53del-Fwd: 5’- GGCCATATGCAATAACAACTT-

CAAGCTGCAGAAAAAATAGGC-3'; C17-F53del-Rev: 5'- GCCATATTTTTTCTGCA-GCTTGAAGTTGTTATGCATATGGCC-3'; C17-A398E-Fwd: 5'- AATCTGTGGG**A**G-CTGCATCAC-3'; C17-A398E-Rev: 5'-GTGATGCAGC**T**CCCACAGATT-3'; C17-G111V-Fwd: 5'-AACCGTAAGG**T**TATCGCCTTC-3'; C17-G111V-Rev: 5'-GAAGGCG-ATA**A**CCTTACGGTT-3'; C17-P409L-Fwd: 5'-TGGCACCAGC**T**GGATCAGTTC-3'; C17-P409L-Rev: 5'-GAACTGATCC**A**GCTGGTGCCA-3'; C17-dupA-Fwd: 5'-GCAG-AAAAAA**A**TATGGCCCCA-3'; C17-dupA-Rev: 5'-TGGGGCCATA**T**TTTTTTCTGC-3'.

Correct insertion of the mutation and integrity of the inserts were checked by direct sequencing. Next, the WT and mutant coding sequences of CYP17A1 (plus V5-tag) were subcloned into the MCA of the pIRES vector harbouring the WT cDNA for CYB5A in its MCB (see section 6.2.5).

5.2.5. *In vitro* functional analysis

HEK293 cells were transfected with 2 µg of pIRES plasmid as described in section 2.1.4. 48h after transfection, cells were incubated at 37°C with 1 ml full MEM supplemented with 200 nM nicotinamide adenine dinucleotide phosphate in the presence of 1000 nmol/litre progesterone for 17α-hydroxylase assays or 500 nmol/litre 17Preg for 17,20 lyase assays. Optimal incubation times for wild type and mutants were assessed in pilot experiments. After incubation, cell supernatant was removed and 10µL of a 1000ng/mL solution of progesterone-d4, 17OHP-d4, 17Preg-d4, DHEA-d4 (all Cambridge Isotope Laboratories Inc., Andover, MA) were added to the medium as an internal standard to normalize extraction efficiency and mass spectrometry variability. Steroids were extracted with 4 ml methyl tert-butyl ether as described in section 2.5.5 and resuspended in 1ml 50/50 (v/v) methanol/water (LC/MS grade). A Waters Xevo mass spectrometer with ACQUITY ultra performance liquid chromatography™ (UPLC) system was used fitted with a HSS T3, 1.8 µM, 1.2

x 50 mm column (Waters Corporation, Milford, MA). Each steroid was quantified by comparison to a calibration series with respect to their internal standard. Quantitation was completed using TargetLynx 4.1 software (MassLynx 4.1, Waters). The assays were linear over a range of 1-500 ng/ml for progesterone and 17OHP and 0.5-500 ng/ml for 17Preg and DHEA (R^2=0.998). Steroid conversion rates were calculated as described in section 2.5.2 and results were visualized in GraphPad Prism Software version 4.0 (GraphPad Inc., San Diego, USA).

Western blot was performed as described in section 2.3.3 using an anti-V5 antibody (Sigma Aldrich, St Louis, MO, USA).

5.3. RESULTS

5.3.1. Urinary steroid profiling

Urinary steroid profiling with GC/MS showed a consistent pattern in all patients (except case 4 whose urinary steroid profile was not available for this study). Mineralocorticoid metabolites (THA, THB, and 5αTHB) as well as progesterone and pregnenolone metabolites (5-PT, PT, and 5-PD) were elevated, but androgen metabolites (An and Et) were low with borderline-low metabolites of active glucocorticoids (THF, 5α-THF, cortolones) (data not shown). This pattern is highly indicative of reduced *in vivo* CYP17A1 enzyme activity, with both catalytic activities significantly impaired. Substrate-product ratios have been applied (**Figure 26**) to compare *in vivo* net activities of CYP17A1 between the four cases analysed. An elevation of this ratio compared to the reference cohort indicates deficiency of the respective enzyme activity. The ratio of mineralocorticoid over glucocorticoid metabolites (THA+THB+5aTHB)/(THE+THF+5aTHF), reflecting the 17α-hydroxylase

activity of CYP17A1, was most severely impaired in case 1 (185.7; NR 0.07-0.18). This ratio was moderately elevated in cases 2 and 3 (6.8 and 12.3, respectively), but only very mildly elevated in case 5 (1.7) (**Figure 26**). The diagnostic ratio reflecting the 17,20 lyase activity of CYP17A1 [(PT)/(An+Et)] was highest in case 5 (10; NR 0.09-0.31) and lower in case 1 (3.6), case 2 (2.2) and case 3 (1.1) (**Figure 26**).

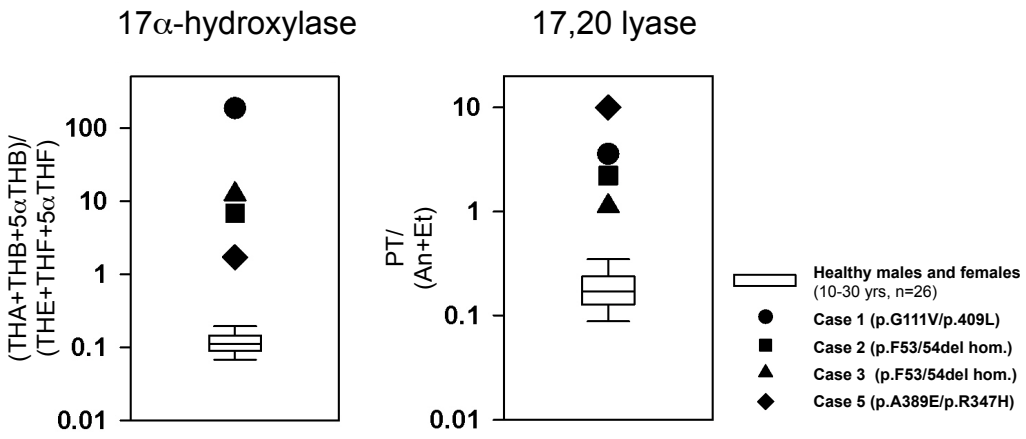

Figure 26: *In vivo* assessment of CYP17A1 17α-hydroxylase and 17,20 lyase activities as indicated by urinary steroid metabolite analysis. Diagnostic steroid metabolite ratios in the four cases analysed with CYP17A1 deficiency are represented by closed symbols (white, case 1; black, case 2; grey, case 3). White box plots represent the interquartile ranges of the reference cohort (healthy males and females, 10-30 years; n=26), whiskers represent the 5th and 95th percentiles, respectively. For steroid abbreviations please see methods.

5.3.2. Genetic analysis

The identification of mutations in the *CYP17A1* gene was carried out by direct sequencing in all 5 cases and is summarized in **Figure 27**.

Case 1 was compound heterozygous for two missense mutations of the *CYP17A1* gene (g.2004 G>T in exon 1 and g.5831 C>T in exon 7) resulting in substitution of glycine by valine at position 111 (p.G111V) and a substitution of proline by leucine at position 409 (p.P409L) of the amino acid sequence. Segregational analysis revealed that the p.P409L mutation derived from the father and the p.G111V mutation was inherited from the mother.

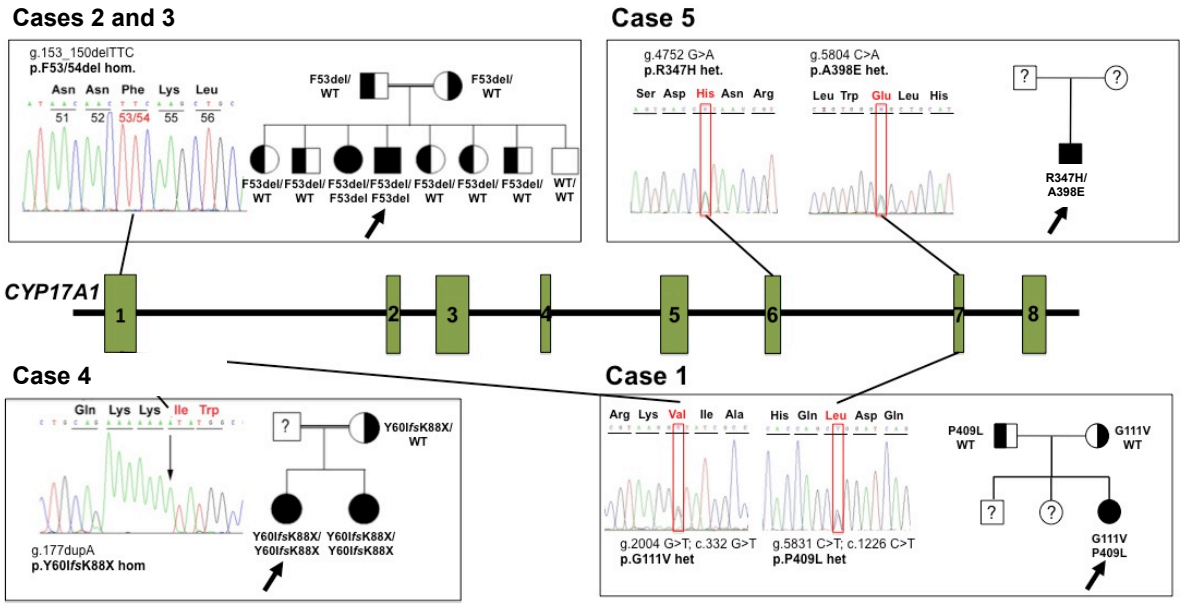

Figure 27: Summary of the genetic findings in the *CYP17A1* gene (exons are indicated by green boxes) including segregational analysis in 5 patients with 17OHD. The following mutations in the *CYP17A1* gene are novel: p.G111V and p.P409L (case 1), p.Y60I*fs*K88X (case 2) and p.A398E (case 5).

Cases 2 and 3 were found to be homozygous of a three nucleotide deletion (g.157_159delTTC) in exon 1 of the *CYP17A1* gene resulting in deletion of a phenylalanine residue of the amino acid sequence (p.F53/54del). Genetic work-up of the family revealed that both consanguineous parents are heterozygous carriers of the p.F53/54del mutation. Moreover, five siblings of the patient have the mutation in the heterozygous state while one sibling carries the wild type sequence on both alleles.

Case 4 carries a novel mutation in exon 1 of the *CYP17A1* gene causing a duplication of adenosine in position 177 of the genomic sequence (g.177dupA). On the protein level, this duplication leads to a frameshift with an introduction of a stop codon at position 88 (p.Y60I*fs*K88X). The older symptomatic sister of the patient carries p.Y60I*fs*K88X mutation on both alleles as well. The mother was the heterozygous carrier of the mutation and the father was not available for genetic analysis.

Case 5 was compound heterozygous for two missense mutations in exon 6 (g.4752 G>A) and in exon 7 (g.5804 C>A) of the *CYP17A1* gene resulting in substitution of an arginine residue by histidine (p.R347H) and substitution of an alanine residue by glutamic acid (p.A398E), respectively. Parental DNA was not available to carry out segregational analysis.

5.3.3. *In vitro* functional assays

All mutants assessed for residual enzymatic activity of both CYP17A1 catalytic reactions show greatly reduced or even absent activity *in vitro* (**Figure 28**). However, three mutants (p.R347H, p.A398E and p.F53/54 del) retain some residual 17α-hydroxylase activity of about 10-15 % of WT activity. Amongst these, the p.347H mutation has the highest residual activity (15.6 %) with p.A398E and p.F53/54del retaining about 10% of WT enzyme activity (**Figure 28A**). The 17,20 lyase activity was greatly reduced to about 1% or less of WT activity for all mutant CYP17A1 protein studied (**Figure 28B**). Amongst all mutant proteins, p.P409L, p.G111V and the frameshift mutation most severely reduce CYP17A1 catalytic function for both 17α-hydroxylase and 17,20 lyase activities, with the two latter mutations completely abolishing protein function.

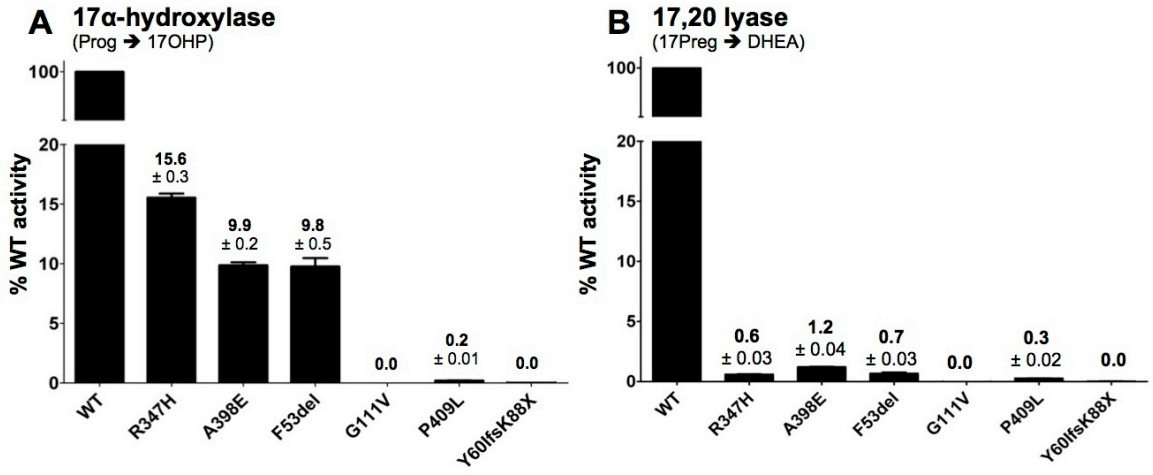

Figure 28: Residual mutant enzyme activity values are depicted for the two catalytic activities of CYP17A1. **Panel A** for the conversion of progesterone (Prog) to 17-hydroxyprogesterone (17OHP), reflecting 17α-hydroxylase activity; **panel B** reflects the 17,20 lyase activity as assessed by the conversion of 17-hydroxypregnenolone (17Preg) to DHEA. Residual enzyme activity is expressed at percentage of wild type (WT) activity, which is defined as 100%. Substrate conversion rate for WT protein was 14.4 ± 0.4 nmol/mg protein/min for Prog and 5.8 ± 1.5 nmol/mg protein/min for 17Preg. All experiments were performed in triplicate in three independent experiments. Error bars represent ± SEM (in percent).

5.4. DISCUSSION

We have described five cases with inactivating mutations in the *CYP17A1* gene causing 17α-hydroxylase deficiency and demonstrated *in vivo* (urinary metabolite analysis) and *in vitro* (functional characterizations) that residual 17α-hydroxylase activity of distinct *CYP17A1* mutations is associated with non-classical manifestations of this disorder.

The complete absence of 17α-hydroxylase activity, as illustrated in case 4, caused by the severe homozygous frameshift mutation, resulted in a severe neonatal presentation with adrenal insufficiency. Neonatal presentation resembling primary adrenal insufficiency is very unusual in 17OHD and has not been reported in the literature so far. The majority of patients present 'classically', i.e. with 46,XY DSD or lack of pubertal development in 46,XX girls, hypokalaemic hyporeninaemic

hypertension and compensated glucocorticoid deficiency due to partial activation of the GC receptor by MC precursors (Goldsmith et al., 1967; Yanase, 1995; Miura et al., 1996; Krone and Arlt, 2009; Miller and Auchus, 2011); this phenotype is illustrated by patient 1 of this case series. Some excretion of MC metabolites in the baby (case 1) - as detected in her urine sample - might have prevented her from severe salt-wasting crisis, but was also directional in establishing the diagnosis as other causes of primary adrenal insufficiency had already been considered (i.e. mutations in *NR5A1*, *DAX1* or *CYP11A1*). Another severe mutation, in a homozygous state, resulting in early truncation of the protein (p.Y27X) was previously reported in an adult woman, who had no signs of pubertal development, and interestingly, did not present with arterial hypertension (Müssig et al., 2005). However, the urinary steroid profile in this patient with high MC metabolites but undetectable 17-oxygenated C21 and C19 steroids represented the typical biochemical fingerprint of severe combined 17α-hydroxylase/17,20 lyase deficiency.

About 10% of patients with 17OHD are normokalaemic and normotensive, despite the fact that they carry severe disease-causing mutations (Kater and Biglieri, 1994; Auchus, 2001). The exact explanation for this phenotypic variability is not known and underlying mechanisms remain to be elucidated.

The p.F53/54del mutation in *CYP17A1* has been frequently reported and is one of the most prevalent mutations in patients of Asian origin, usually associated with partially combined inactivation of 17α-hydroxylase/17,20 lyase activities (Miura et al., 1996; Bao et al., 2011; Yanase et al., 1989). The predominant phenotype of patients with this mutation is 1) a variable degree of hyperaldosteronism with hypokalaemic hypertension not always present and 2) milder sex steroid deficiency with absent or mild DSD in 46,XY individuals and compensated hypergonadotrophic hypogonadism

in both sexes (Yanase, 1995; Miura et al., 1996). These features are consistent with the clinical presentations of the two siblings with homozygous p.F53_54del from this case series (case 2 and 3) and the *in vitro* functional analysis of this mutation retaining about 10% residual activity of 17α-hydroxylase and some residual activity of 17,20 lyase (section 5.3.3) may explain the observed phenotype.

Case 5 presented with the clinical and biochemical features of 'isolated' 17,20 lyase deficiency. Isolated 17,20 lyase deficiency is a rare condition and only around 25 cases have been described in the literature so far (Yanase et al., 1991) (see also sections 1.3.1.1 and 6.4). Importantly, the initial reports on the condition provided only the clinical and hormonal characterizations without identifying a distinct genetic abnormality in six families with 46,XY DSD patients and two families with 46,XX patients that presented with lack of pubertal development [reviewed and discussed in (Yanase et al., 1991)]. So far, 15 cases of isolated 17,20 lyase deficiency with a complete clinical, hormonal, genetic, and functional work-up have been reported Underlying causes were four distinct missense mutations in the *CYP17A1* gene (p.R347H; p.R347C p.R358Q; p.E305G) (Geller et al., 1997; Sherbet et al., 2003; Van Den Akker et al., 2002) and one *POR* missense mutation (p.G539R) (Hershkovitz et al., 2008). Recently, a *CYB5A* nonsense mutation (p.W27X) has been reported resulting in early protein truncation and thus loss of CYB5A function (Kok et al., 2010). Case 5 carried the known missense mutation p.R347H on one allele and a novel missense mutation p.A398E on the other allele. A unifying characteristic of all individuals with 17,20 lyase deficiency is severe sex steroid deficiency, with hormonal measurements confirming a lack of adrenal and gonadal androgen synthesis. However, it is noteworthy that all patients with underlying *CYP17A1* or *POR* mutations concurrently showed significant impairment of

glucocorticoid production, with insufficient cortisol responses to ACTH stimulation; a comprehensive overview of all the published cases with a genetic work-up available is shown in **Table 17**. Of note and to our current knowledge, case 5 is the first patient with isolated 17,20 lyase deficiency due to mutant *CYP17A1* who has normal ACTH-stimulated cortisol levels (**Table 14**), however urinary steroid metabolome analysis demonstrated mild impairment of 17α-hydroxylase activity. A comparison of urinary metabolite ratios reflecting 17α-hydroxylase activities between the patients of this case series shows that this ratio is the lowest in this patient, indicating a higher residual *in vivo* 17α-hydroxylase activity (**Figure 26**). In addition, the degree of 17α-hydroxylase inhibition reflected by this ratio mirrors the *in vitro* functional 17α-hydroxylase activity of the mutant enzymes (**Figure 28**). A comparison of these ratios reflecting between the cases from this thesis and published cases presenting with either classical combined CYP17A1 deficiencies (Neres et al., 2010) or isolated 17,20 lyase deficiencies (Tiosano et al., 2008) is shown in **Figure 29**. This figure also depicts the three siblings with isolated 17,20 lyase deficieny due to mutant CYB5A, as described in Chapter 6, and data from the Birmingham cohort of patients with PORD (Krone et al., 2012). Clearly, case 5 (represented by the open diamond) has only a mild elevation the 17α-hydroxylase ratio; however, biochemically, the enzymatic activity is inhibited, although there is no clinical or hormonal evidence for impaired GC production or MC excess.

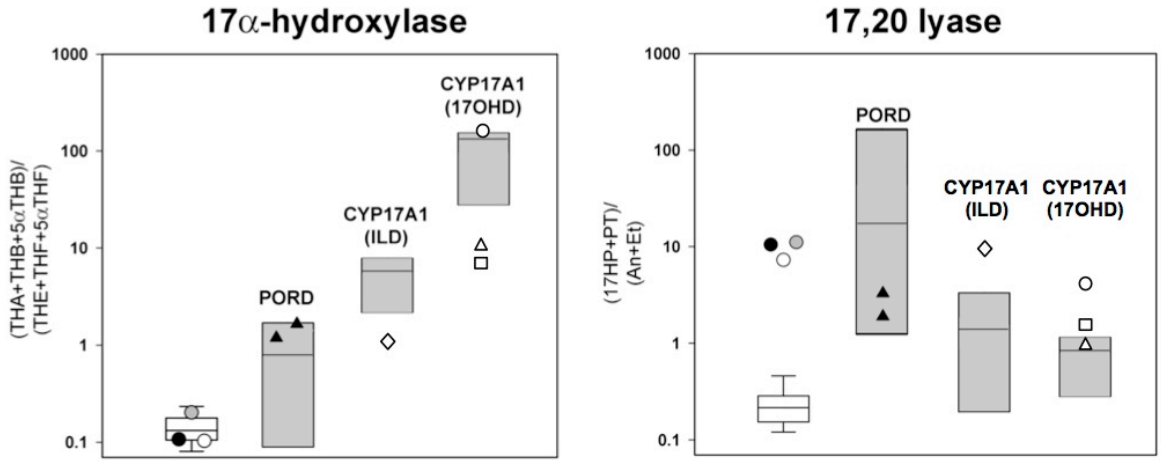

Figure 29: *In vivo* assessment of CYP17A1 17α-hydroxylase and 17,20 lyase activities as indicated by urinary steroid metabolite analysis. Diagnostic steroid metabolite ratios in the three siblings with isolated 17,20 lyase deficiency (ILD) due to homozygous p.H44L CYB5A are represented by closed circles on the left of each panel (white, case 1; black, case 2; grey, case 3). The white diamond symbol represents the ratio obtained from the patient with ILD due to mutant CYP17A1 (case 5 in this chapter; p.A398E/p.R347H) and the three patients with a more classical presentation of 17OHD (circle: case 1, p.G111V/p.P409L; triangle: case 2; square: case 3, both p.F53_54del hom). White box plots represent the interquartile ranges of the reference cohort (healthy males and females, 4-20 years; n=98), whiskers represent the 5th and 95th percentiles, respectively. Grey box plots indicate the ranges and medians for the same steroid ratios measured in 20 patients with classic 17α-hydroxylase deficiency (CYP17A1 17OHD; Neres et al. 2010); six patients with apparently isolated 17,20 lyase deficiency due to CYP17A1 p.E305G (CYP17A1 ILD; Tiosano et al. 2008), and 21 patients with P450 oxidoreductase deficiency (Krone et al. 2012). The triangles represent two patients with the POR mutation p.G539R reported as associated with apparently isolated 17,20 lyase deficiency (Hershkovitz et al., 2008). For steroid abbreviations please see methods.

Thus, urinary steroid profiling represents a powerful diagnostic tool, not only to simplify diagnosis of distinct steroidogenic disorders but also to potentially predict the severity of the mutation, as illustrated in this case series. Importantly, true isolated 17,20 lyase deficiency, i.e. no clinical, hormonal or biochemical evidence of impaired GC or MC biosynthesis and action, is not observed in mutations of the *CYP17A1* and *POR* genes.

6. CHAPTER 6: MUTANT CYTOCHROME B5 (CYB5A) CAUSES TRUE ISOLATED 17,20 LYASE DEFICIENCY OF CYP17A1

This chapter has been published as:

A missense mutation in the human cytochrome b5 gene causes 46,XY disorder of sex development due to true isolated 17,20 lyase deficiency.

Idkowiak J, Randell T, Dhir V, Patel P, Shackleton CH, Taylor NF, Krone N, Arlt W.

J Clin Endocrinol Metab. 2012 Mar;97(3):E465-75. doi: 10.1210/jc.2011-2413. Epub 2011 Dec 14.

6.1. INTRODUCTION

Androgen synthesis in humans crucially relies on the CYP17A1 that is primarily expressed in the adrenals and the gonads (see section 1.1.8.1): CYP17A1 exhibits two distinct catalytic activities. Its 17α-hydroxylase activity facilitates adrenal glucocorticoid synthesis. The 17,20-lyase activity of CYP17A1 converts 17-Preg to the principal androgen precursor dehydroepiandrosterone (DHEA) and, with 50-fold lesser efficiency (Auchus et al., 1998), 17OHP to androstenedione. Both the 17α-hydroxylase and the 17,20 lyase activities of CYP17A1 require electron transfer from NADPH via the electron donor POR. CYP17A1 17,20 lyase activity requires additional interaction of CYP17A1 and POR with the haeme-containing protein cytochrome b5 (CYB5A) (Onoda and Hall, 1982). Previous studies suggest that CYB5A is not directly involved in electron transfer but rather facilitates allosteric interaction of the POR and CYP17A1 proteins, thereby enhancing electron flux (Auchus et al., 1998).

Isolated 17,20 lyase deficiency results in sex steroid deficiency and clinically presents with male undermasculinization, i.e. 46,XY disorder of sex development (46,XY DSD), and with absent or disturbed pubertal development in both 46,XY and 46,XX individuals. In accordance with lack of impairment of 17α-hydroxylase activity, affected patients have been reported to not present with cortisol deficiency or mineralocorticoid excess, which are typically observed in classic, complete CYP17A1 deficiency (Yanase, 1995; Miller and Auchus, 2011). To date, four different missense mutations in *CYP17A1* have been reported to cause apparently isolated 17,20 lyase deficiency (Geller et al., 1997; Van Den Akker et al., 2002; Sherbet et al., 2003). A recent case report described a patient presenting with isolated 17,20 lyase deficiency and normal *CYP17A1* sequence, in whom an inactivating mutation in the *POR* gene

was identified as the cause of disease (Hershkovitz et al., 2008). Recently, a nonsense mutation resulting in early truncation of the CYB5A protein has been described in a 46,XY DSD patient diagnosed with isolated 17,20 lyase deficiency (Kok et al., 2010).

6.2. METHODS

6.2.1. Patients

I have investigated three siblings with 46,XY DSD and a biochemical presentation suggestive of isolated 17,20 lyase deficiency from a consanguineous family of Pakistani origin; the parents were first cousins.

The index patient (Case 1) was born at 41 weeks gestation after an uneventful pregnancy and delivery; routine ultrasound examinations during pregnancy had predicted a female baby. However, at birth, ambiguous, predominantly female genitalia were observed, with enlarged, mildly scrotalized labia majora that contained palpable gonads. The phallus appeared similar to a female clitoris (7mm stretched length). Due to a skinfold between the labia, the urethral orifice and vaginal opening were not clearly detectable but the baby was able to pass urine. The karyotype was 46, XY. Hormonal measurements three days after birth revealed elevated 17OHP (120 nmol/L; NR < 5.0), a normal testosterone (7.2 nmol/L; NR 5-15) normal androstenedione (1.8 nmol/L; NR < 7.7), and low gonadotrophins (LH < 0.5 U/L, FSH < 0.5 U/L). Serum electrolytes were normal when measured three weeks after birth (Na 140 nmol/L, NR 135-145; K 5.2 nmol/L, NR 3.5-5.5). An hCG stimulation test was performed at the age of 6 weeks and again at 5 months, both times revealing a low baseline testosterone that did not increase sufficiently three days after hCG administration (**Table 15**). The decision was taken to raise the baby as a boy.

The older sister (case 2) did not develop any signs of puberty by the age of 13 yrs. On examination her genitalia looked predominantly female but with a single perineal opening, separate labio-scrotal folds with no palpable gonads and a mildly enlarged clitoris (15 mm). Clinically, she had an entirely pre-pubertal appearance including absence of pubic or axillary hair, indicating lack of adrenarche (Tanner stages B1, PH1). Her karyotype was 46,XY. Biochemical investigations revealed low androgens, a pre-pubertal oestradiol and early pubertal gonadotrophins (**Table 15**). There was a normal cortisol response in the short synacthen test but adrenal androgen precursors remained undetectable; 17OHP was mildly elevated (**Table 15**).

Table 15: Summary of hormonal investigations in three siblings with cytochrome B5 deficiency. Hb: haemoglobin; MetHb: methaemoglobin. *: hCG test performed at 5 months of age; **: measured at 13 years before the removal of bilateral intra-abdominal gonads.

	Sibling 1 (Index case)	**Sibling 2**	**Sibling 3**
Age at presentation	neonatal	12.75 yrs	neonatal
Karyotype	46,XY	46,XY	46,XY
Age at time of investigation	5 yrs	15 yrs	8 months
Cortisol (nmol/L)			
at baseline	194	107	386
60 min after ACTH1-24	807 (> 550)	726 (> 550)	901 (> 550)
17OHP (nmol/L)	1.1 (2.0 -9.0)	9.5 (2.0-9.0)	30.0 (0-12.0)
DHEAS (μmol/L)			
at baseline	< 0.4 (0.4-3.7)	< 0.4 (8.3-49)	< 0.4 (0.5-20)
60 min after ACTH1-24	< 0.4	< 0.4	< 0.4
Androstenedione (nmol/L)			
at baseline	< 1.1 (1.5-2.7)	< 1.1 (1.8-4.8)	< 1.1 (1.5-2.7)
60 min after ACTH1-24	< 1.1	< 1.1	< 1.1
Testosterone (nmol/L)			
at baseline	0.2* (0.5-2.0)	1.1 (fem. NR: 0-2.8.0)	0.6 (0.5-2.0)
3 days after 1,500 U hCG	0.2*	n.m.	
Oestradiol (pmol/L)		60**	
LH (U/L)	0.8	2.1** (0.3-2.5)	
FSH (U/L)	2.8	3.2** (1.3-6.6)	
MetHb (mmol/mmol Hb)	0.063 (< 0.015)	0.061 (< 0.015)	0.085 (< 0.015)

The youngest child of the family (case 3; 46,XY) was born with ambiguous genitalia, including bifid scrotum, a very small penis with hardly any corporal tissue present and perineal hypospadias. His testes were not descended into the scrotum

but palpable in the inguinal region. He had an elevated 17OHP and a normal cortisol response to ACTH (**Table 15**). Corrective surgery for hypospadias and bifid scrotum are scheduled for after the child's first birthday.

All 3 affected siblings had elevated clinically inapparent methaemoglobin levels (**Table 15**).

6.2.2. Urinary steroid profiling

Analysis of urinary steroid metabolite excretion was performed as described in section 2.7.1. Steroids quantified included corticosterone metabolites THB, 5αTHB and THA, the progesterone metabolite PD, 17-hydroxyprogesterone metabolites PD and 17HP, the 17-hydroxypregnenolone metabolite 5-PT, the 21-desoxycortisol metabolite P'TONE, cortisol metabolites THF, 5αTHF and THE, and androgen metabolites An, Et, DHEA and 16-OH-DHEA (see **Table 9** for steroid abbreviations).

Following quantification of steroid metabolites by GC/MS I have calculated substrate metabolite/product metabolite ratios to reflect the net *in vivo* activity of 17α-hydroxylase, i.e. corticosterone over cortisol metabolites (THA+ 5αTHA+THB+5αTHB)/(THF+5αTHF+THE), and 17,20-lyase, i.e. 17OHP over androgen metabolites (17HP+PT)/(An+Et).

6.2.3. Genetic analysis

DNA analysis was performed after obtaining informed assent and consent from patients and parents, respectively, with approval from institutional research ethics committees. Genomic DNA was extracted from peripheral blood leukocytes for cases 1-3 and the parents, using a DNA blood and cell culture kit (Qiagen, GmbH, Hilden, Germany). From all other siblings and parents, DNA was extracted from

saliva using a commercially available kit (Oragene DNA OG250 and OG300, DNA Genotek, Ontario, Canada).

The coding sequences of the *CYB5A, POR* and *CYP17A1* genes including exon-intron boundaries were amplified as described in section 2.2.11 for the index patient. For all other family members, only exon 2 of the *CYB5A* gene was amplified and sequenced.

6.2.4. *In silico* analysis

The x-ray structure of human oxidized microsomal cytochrome b5 was used as a template for *in silico* analysis (PDB ID: 2I96; M. Nunez-Quintana, G. Truan, C. van Heijenhoort. Solution structure of human cytochrome b5). The structural representations were generated using the program Molsoft ICM Browser Pro (Molsoft L.L.C., La Jolla, CA).

6.2.5. Molecular cloning and site-directed mutagenesis

Human CYP17A1 cDNA was tagged with the V5 epitope by sub-cloning into the pcDNA6 vector (section 2.4.1.2). The CYP17A1 template cDNA was derived from human CYP17A1 cDNA in the yeast expression vector V10 (see section 2.4.1.1). The following hybrid primers were designed for PCR-based cloning with the In-Fusion® cloning system (section 2.4.2.3), containing HindIII (5') and BamHI(3') restriction sites (gene-specific sequence is highlighted in bold): Fwd_HindIII: 5'-GTTTAAACTTAAGCTT**ATGTGGGAGCTCGTGGCTCTCTTG-3'**; Rev_BamHI: 5'-CTGGACTAGTGGATCC**GGTGCTACCCTCAGCCTGGGCT**-3'. For the PCR, high fidelity Pfu-polymerase (Roche, Basel, Switzerland) was employed. The integrity of the inserts was checked by direct sequencing.

Human CYB5A cDNA in the yeast expression vector V10 was kindly donated by Dr Richard Auchus (Ann-Arbor, Michigan, USA). Site-directed mutagenesis for

p.H44L CYB5A was performed as described in section 2.4.3 by using the following primer (the mutated nucleotide is highlighted in bold): Fwd: 5'-CA-AATTTCTGGAAGAGC**T**TCCTGGTGGGGAAGAAG-3'; Rev: 5'- CTTCTTCCCCACC-AGGA**A**GCTCTTCCAGAAATTTG-3'.

Then the V5-tagged CYP17A1 cDNA and human WT and mutant (p.H44L) CYB5A cDNA were cloned into the bi-cistronic expression vector pIRES (section 2.4.1.3) by using the PCR-based Infusion® cloning approach. Primers were generated to clone CYP17A1-V5-6xHis from pcDNA6 into the MCA of pIRES, employing restriction sites NheI (5') and MluI (3') (gene-specific sequence highlighted in bold): Fwd: 5'-CTCACTATAGGCTAGC**ATGTGGGAGCTCGTGGC**-3'; Rev: 5'-TGCATGCTCGACGCGT**TCAATGGTGATGGTGATGATG**-3'. WT and mutant CYB5A were cloned in the MCB of pIRES, employing restriction site SalI (5') and NotI (3'): Fwd: 5'-ATCCTCTAGAGTCGAC**ATGGCAGAGCAGTCGGAC-3';** Rev: 5'-TAAAGGGAAGCGGCCGC**CAGTCCTCTGCCATGTATAGGC**-3'. Correct insertion of the mutation and integrity of the inserts were checked by direct sequencing.

6.2.6. *In vitro* functional analysis

For *in vitro* functional analysis, the human embryonic kidney cell line HEK293 (section 2.1.1) was used for transient transfection with the generated pIRES constructs and analysis of both catalytic activities of CYP17A1 was performed as follows: cells were transfected with three types of pIRES plasmids as decribed in section 2.1.4: (1) WT CYP17A1 with WT CYB5A; (2) WT CYP17A1 with p.H44L CYB5A and (3) WT CYP17A1 alone (empty MCSB in pIRES). Kinetic constants were determined 48 h following transfection. For 17α-hydroxylase activity assays, cells were incubated in 500 µl MEM full growth medium with 0.5, 1, 2, and 5 µmol/L progesterone in the presence of 0.2 µCu ^{3}H-labelled progesterone (101.3 Ci/mol;

Perkin Elmer, Waltham, MA). For 17,20 lyase activity assays, cells were incubated with 0.25, 0.5, 1.25 and 2.5 µmol/L 17-Preg containing 0.2 µCu ^{3}H-labelled 17-Preg (53.7 Ci/mol; Perkin Elmer, Waltham, MA). To enhance the efficiency of the enzymatic reaction, NADPH was added to the medium in a final concentration of 200 nmol/L. Steroids were extracted and then separated by thin layer chromatography and quantified (section 2.5.6). Kinetic parameters were calculated as described in section 2.5.2.

Protein amounts were measured using the Bradford method (section 2.3.2) after lysing the cells in PBS containing protease inhibitors and 0.1% Triton X-100. To ensure similar expression levels, Western blotting was performed as described in section 2.3.3 with some minor modifications. In brief, cell lysates (8-15 µg) were separated by SDS-PAGE electrophoresis, transferred onto nitrocellulose membranes (Amersham Biosciences) at 30 V for 90 min and blocked with 5% skimmed milk powder (w/v) in PBST (PBS, 0.1% (v/v) Tween 20) for 1-2 hours. Primary antibodies were incubated overnight employing the following dilutions: rabbit polyclonal to cytochrome b5 (Abcam) 1:250; mouse monoclonal to V5 (Invitrogen) 1:1,000; mouse monoclonal to β-actin (Abcam) 1:25,000. Secondary horseradish-peroxidase conjugated antibodies and detection by enhanced chemiluminescence (Immobilon, Millipore, Watford, UK) was performed according to the manufacturer's protocol.

6.3. RESULTS

6.3.1. Urinary steroid profiling

GC/MS analysis of urinary steroid metabolites revealed low androgen metabolite excretion with increased excretion of the 17-Preg metabolite pregnenetriol

(5PT), suggestive of 17,20 lyase deficiency; concurrently, mineralocorticoid and glucocorticoid metabolite excretion appeared normal, suggesting preserved 17α-hydroxylase activity (**Figure 30**). In keeping with these findings, 17α-hydroxylation as assessed by the ratio of corticosterone over cortisol metabolites was not compromised in either sibling whereas 17,20 lyase activity as determined by the ratio of 17OHP over androgen metabolites was significantly elevated, suggestive of isolated 17,20 lyase deficiency (**Figure 31**).

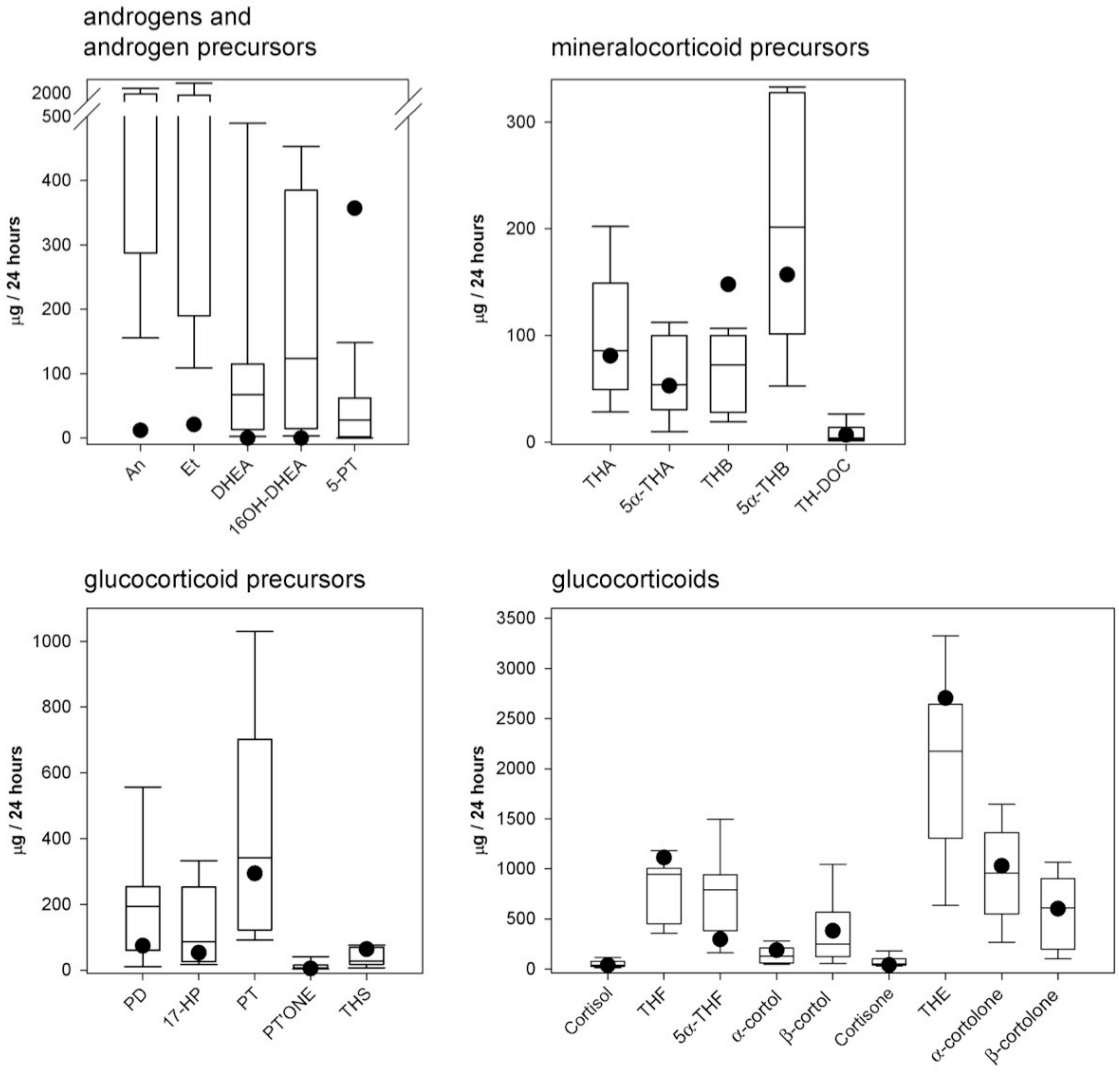

Figure 30: Urinary steroid profile as determined by total 24-h steroid metabolite excretion analysis by GC/MS in one of the affected patients at the age of 13.5 years (case 2; represented as closed circles) in comparison to an age- and sex-matched reference cohort (box plots). For steroid metabolite abbreviations please refer to the methods section.

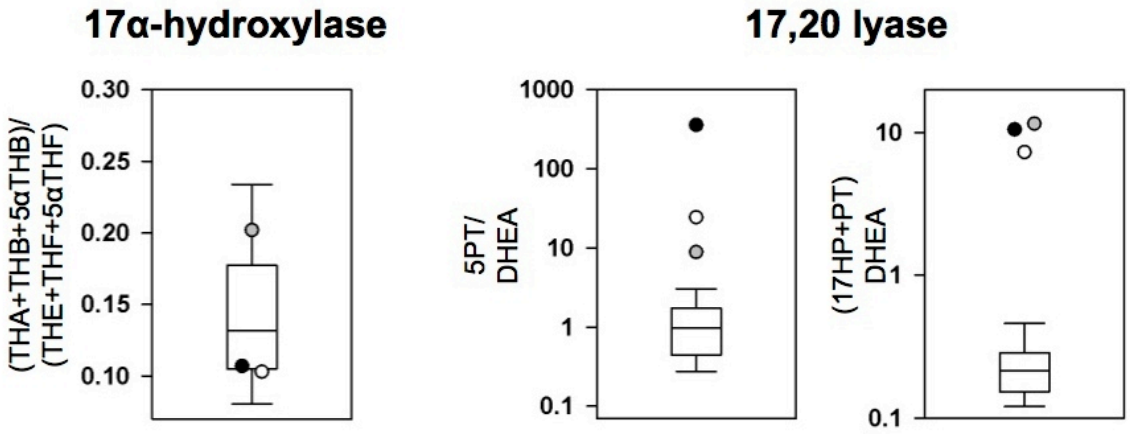

Figure 31: *In vivo* assessment of CYP17A1 17α-hydroxylase and 17,20 lyase activities as indicated by urinary steroid metabolite analysis. Diagnostic steroid metabolite ratios in the three siblings with isolated 17,20 lyase deficiency due to homozygous p.H44L CYB5A are represented by closed circles (white, case 1; black, case 2; grey, case 3). White box plots represent the interquartile ranges of the reference cohort (healthy males and females, 4-20 years; n=98), whiskers represent the 5th and 95th percentiles, respectively. For steroid abbreviations please see methods.

6.3.2. Genetic analysis

Sequencing of the coding regions of the *CYP17A1* and *POR* genes did not reveal mutations in any of the three affected siblings. However, we identified a homozygous missense mutation at the beginning of exon 2 of the *CYB5A* gene (g.28,400 A>T) changing a histidine at position 44 to leucine (p.H44L) (**Figure 32A**). Segregation analysis demonstrated heterozygosity for the p.H44L variant in both father and mother. Further sequencing analysis of the other clinically unaffected siblings revealed heterozygous p.H44L CYB5A in four and WT CYB5A in the remaining four of the siblings (**Figure 32B**).

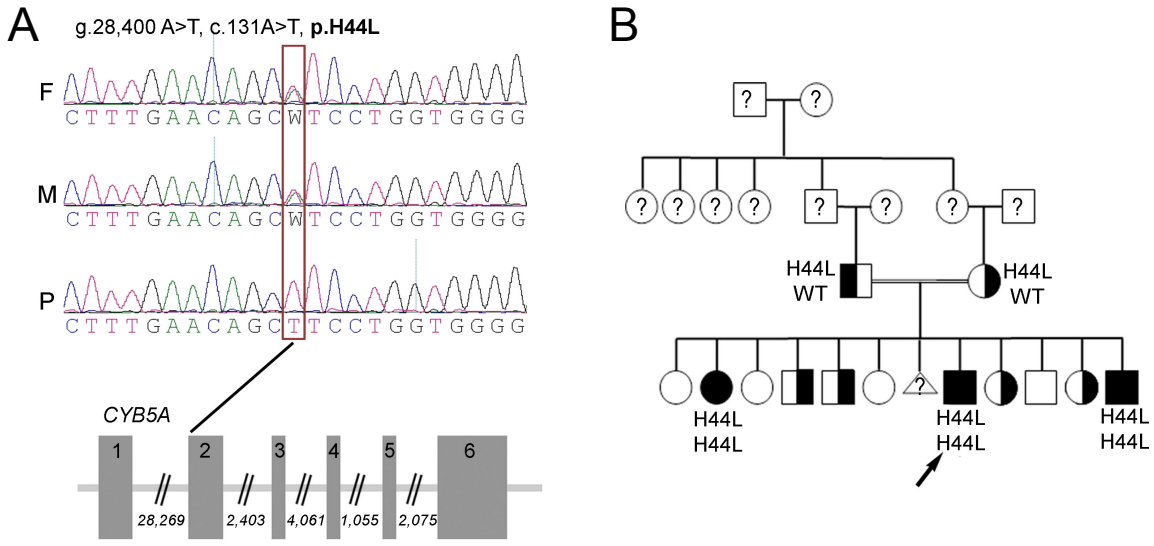

Figure 32: **Panel A,** electropherogram depicting the homozygous missense mutation in the *CYB5A* gene identified in the index patient (P), with heterozygosity in mother (M) and father (F). The mutation g.28,400 A>T is located at the beginning of exon 2 as indicated in the schematic representation of the *CYB5A* gene. Exons are shown as grey rectangles and introns as thin lines; numbers indicate the sizes of the intronic regions. **Panel B,** pedigree of the index family with segregation analysis of the identified *CYB5A* mutation. The arrow depicts the index patient.

6.3.3. *In vitro* functional assays

The observed catalytic constants for the 17α-hydroxylase reaction did not differ following co-expression of CYP17A1 with and without wild type or mutant CYB5A (**Figure 33**, **Table 16**). In contrast, CYP17A1 17,20 lyase activity (Bhattacharya et al., 1999; Schröder et al., 2012; Hershkovitz et al., 2008) was greatly reduced in the presence of p.H44L CYB5A as compared to incubations with WT CYB5A, almost down to the level observed after the expression of CYP17A1 without CYB5A (**Figure 33B**). This decrease in catalytic efficiency was mainly a consequence of a marked reduction of the maximal reaction velocity V_{max} while K_m (indicative of substrate affinity) appeared not to be affected by p.H44L (**Table 16**). The residual activity of the p.H44L mutant on the 17,20 lyase reaction was about 5% of WT (**Figure 33C**).

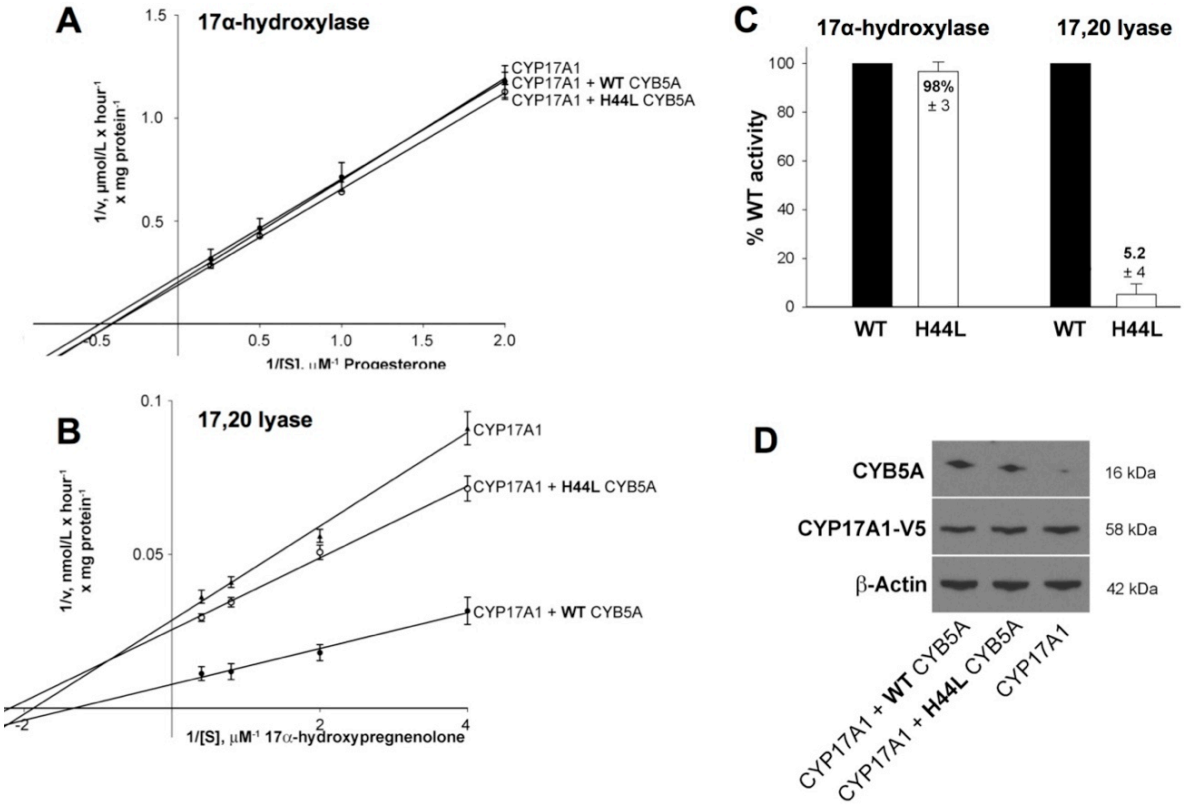

Figure 33: **Panels A+B**, results of kinetic analysis of CYP17A1 activities. The panels show Lineweaver-Burk plots of 17α-hydroxylase (**A**) and 17,20 lyase (**B**) activities as assessed in HEK293 cells transiently transfected with CYP17A1 with or without wild type (WT) or mutant p.H44L CYB5A. **Panel C**, residual enzyme activity expressed as percentage of wild type (WT) activity, defined as 100%, based on measurements carried out at substrate concentrations around Km, i.e. 1µM and 0.5 µM for 17α-hydroxylase and 17,20 lyase activitiy, respectively. For defining the impact of p.H44L on 17,20 lyase activity, the conversion rate observed following expression of CYP17A1 alone was subtracted from those observed after co-expression of CYP17A1 with WT and mutant CYB5A, respectively, prior to calculation of residual activities. **Panels A-C**: Error bars represent the mean ± SEM (%) of at least three independent triplicate experiments. **Panel D**, a representative Western blot demonstrating equal expression levels of WT and mutant CYB5A and CYP17A1 with β-actin as a control for equal loading

Table 16: Kinetic constants (± SEM) of human CYP17A1 catalytic activities after equal co-expression of human wild type CYP17A1 with either human wild type (WT) or mutant (p.H44L) cytochrome b5 (CYB5A) as compared to the expression of CYP17A1 without CYB5A in HEK293 cells.

	17α-hydroxylase	**17,20 lyase**
Vmax	*(μmol/mg x hour)*	*(nmol/mg x hour)*
CYP17A1 + CYB5A **WT**	4.71 ± 0.24	118 ± 5
CYP17A1 + CYB5A **H44L**	5.24 ± 0.16	41 ± 2
CYP17A1	4.99 ± 0.19	35 ± 2
Km	*(μM)*	*(μM)*
CYP17A1 + CYB5A **WT**	2.3 ± 0.25	0.55 ± 0.07
CYP17A1 + CYB5A **H44L**	2.4 ± 0.15	0.48 ± 0.06
CYP17A1	2.4 ± 0.20	0.48 ± 0.07
Catalytic efficiency	*(Km/Vmax)*	*(Km/Vmax)*
CYP17A1 + CYB5A **WT**	2.05	214
CYP17A1 + CYB5A **H44L**	2.18	85
CYP17A1	2.08	73

6.3.4. *In silico* analysis

The histidine residue at position 44 is localized in the haeme-binding pocket within the core domain of the CYB5A protein (**Figure 34A**). The imidazole side chain of H44 appears to coordinate the haeme iron and keep the redox active haeme molecule attached to the CYB5A protein (**Figure 34B**) (Mathews, 1985). Substitution with non-polar lysine in the same position appears to disrupt the interaction between the CYB5A core domain and the haeme molecule (**Figure 34C**).

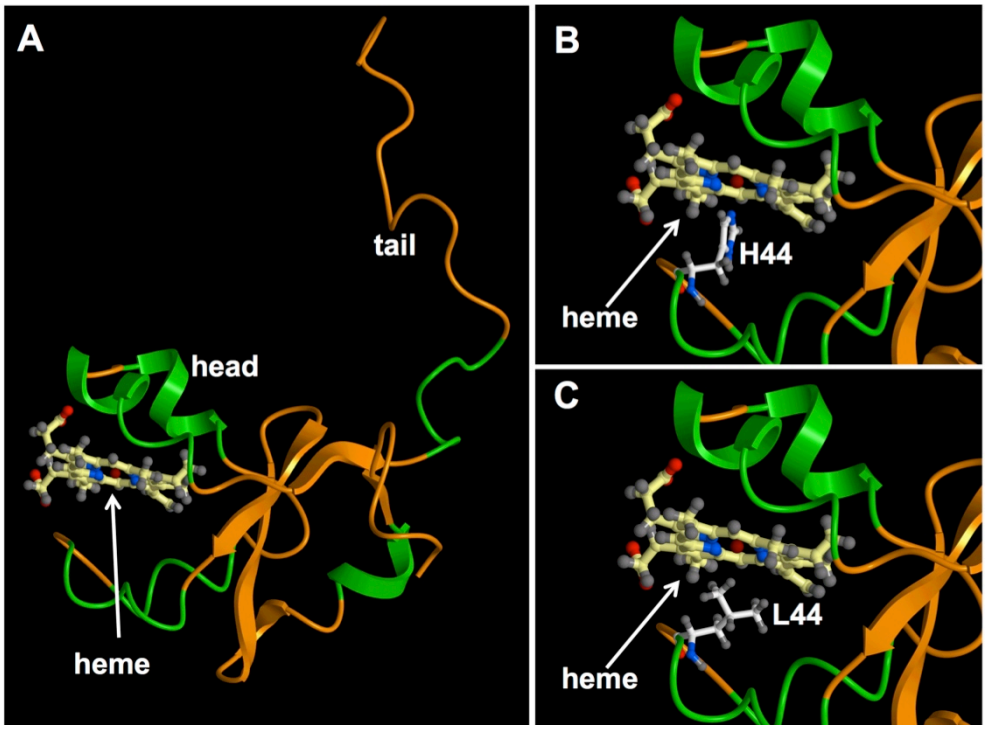

Figure 34: Panel A, three-dimensional model of CYB5A. The protein is composed of a core domain containing the haeme molecule and a hydrophobic tail domain. **Panel B**, magnification of the core domain highlights residue H44 in close proximity to the central iron atom of the haeme molecule. **Panel C,** L44 disrupts the interaction with the haeme molecule.

6.4. DISCUSSION

Here we have described the first human *CYB5A* missense mutation identified in three children from a large consanguineous family presenting with 17,20 lyase deficiency, 46,XY DSD and mild methaemoglobinaemia.

Isolated 17,20 lyase deficiency is a rare condition and only around 25 cases have been described in the literature so far (Yanase, 1995; Geller et al., 1997; Hershkovitz et al., 2008; Simsek et al., 2005; Van Den Akker et al., 2002; Sherbet et al., 2003; Tiosano et al., 2008; Kok et al., 2010). The commonly agreed hormonal phenotype of isolated 17,20 lyase deficiency comprises a selective decrease in DHEA and androstenedione biosynthesis and normal glucocorticoid and mineralocorticoid production (Gupta et al., 2001). Importantly, the initial reports on

the condition provided only the clinical and hormonal characterizations without identifying a distinct genetic abnormality in six families with 46,XY DSD patients (Goebelsmann et al., 1976; Campo et al., 1979; Forest et al., 1980; Zachmann et al., 1982; Kaufman et al., 1983) and two families with 46,XX patients that presented with a lack of pubertal development (Larrea et al., 1983; de Peretti et al., 1984). These reports have been summarized and discussed in the review of Yanase et al. (Yanase et al., 1991).

So far, 15 cases of isolated 17,20 lyase deficiency with a complete clinical, hormonal, genetic, and functional work-up have been reported (**Table 17**). Underlying causes were three distinct missense mutations in the *CYP17A1* gene (p.R347H; p.R358Q; p.E305G) (Geller et al., 1997; Van Den Akker et al., 2002; Sherbet et al., 2003) and one *POR* missense mutation (p.G539R) (Hershkovitz et al., 2008). It appears likely that another patient suggesting 17,20 lyase deficiency, presenting with 46,XX DSD and low circulating androgens (de Peretti et al., 1984), may also have suffered from POR deficiency, but at the time no genetic work-up was performed. Recently, a *CYB5A* nonsense mutation (p.W27X) has been reported resulting in early protein truncation and thus loss of CYB5A function (Kok et al., 2010) (**Table 17**). A unifying characteristic of all these individuals is severe sex steroid deficiency. However, it is noteworthy that all patients with underlying *CYP17A1* or *POR* mutations concurrently showed significant impairment of glucocorticoid production, with insufficient cortisol responses to ACTH stimulation (**Table 17**). This is further reflected by *in vitro* results that show a reduction of 17α-hydroxylase activities to 13-65% and 46% of wild type activity for the *CYP17A1* and *POR* mutations, respectively (**Table 17**). The only exception is the CYP17A1 mutant E305G for which normal or enhanced 17α-hydroxylase activity has been found *in vitro* (Sherbet et al., 2003).

Table 17: Overview of patients with 17,20 lyase deficiency that have been reported with complete information on clinical, biochemical and genetic work-up, including the functional work-up of the causative mutations. All mutations were found in the homozygous state.

				Hormonal investigations			***In vitro* functional analysis**		
Gene	**Mutation**	**Reference**	**Clinical presentation**	Baseline 17OHP nmol/L (<2)	Baseline cortisol nmol/L	Max cortisol after ACTH nmol/L (> 550)	17α-hydroxylase (%WT activity)	17,20 lyase (% WT activity)	*In vitro* expression system
CYP17A1	p.R347H	Geller et al. 1997	46,XY DSD (bifid scrotum, perineal hypospadias), both testes descended, female gender assignment.	1.2	223	n/a	65%	< 5%	Transient transfection in COS1 cells, scintillation counting
		van den Akker et al. 2002	Two siblings with 46,XY DSD.	1.3	190-270	385-427			
CYP17A1	p.R358Q	Geller et al., 1997	46, XY DSD, male gender assignment, gynecomastia at 14yrs (Tanner B5, PH4), 4.5 cm phallus, bifid scrotum, left testes descended, right in inguinal canal	36.4	469	469	65%	< 5%	Transient transfection in COS1 cells, scintillation counting
CYP17A1	p.E305G	Sherbet et al. 2003 Tiosano et al. 2008	A large kindred with four cases of 46,XY DSD, and two 46,XX individuals (one is pre-pubertal, the other had delayed puberty and ovarian cysts).	2.2-21.0	67-192	200-383	not impaired	decreased for D5 pathway, increased for D4 pathway	Yeast microsomes, kinetic analysis, thin-layer chromatography
POR	p.G539R	Hershkowitz et al. 2008	Four patients with 46,XY DSD from a large consanguineous Israeli family, various degrees of undermasculinisation (micropenis to bifid scrotum/scrotal hypospadias)	16.3-41.8	193-224	209-292	46 %	8 %	Yeast microsomes, kinetic analysis, thin-layer chromatography
CYB5A	p.W28X	Kok et al. 2010	46, XY DSD (bifid scrotum, scrotal hypospadias), testes descended	20.3	714	888			Not done
CYB5A	p.H44L	This chapter	Three siblings with 46,XY DSD, various degrees of undermasculinisation from clitoral enlargement and intra-abdominal testes (46,XY female) to ambiguous genitalia (hypospadias, bifid scrotum) with inguinal testes	1.1-30.0	107-386	726-901	96 %	5.5 %	Transient transfection in HEK293 cells, kinetic analysis, thin-layer chromatography

However, patients homozygous for this mutation failed to show an appropriate cortisol response to ACTH and urinary steroid metabolite analysis demonstrated significantly impaired 17α-hydroxylase activity (Tiosano et al., 2008). Hence, although the impairment of 17,20 lyase activity dominates, none of the previously reported mutations in *CYP17A1* or *POR* cause truly isolated 17,20 lyase deficiency. This is of clinical importance, as those patients will require not only sex steroid but also hydrocortisone replacement to avoid adrenal crisis during intercurrent illness or surgery. Future studies in patients with isolated 17,20 lyase deficiency including a complete genetic and hormonal characterization will show whether preservation of CYP17A1 17α-hydroxylase activity can only be observed in CYB5A deficiency.

In our family, clinical investigations, hormonal measurements and *in vitro* functional assays clearly document true isolated 17,20 lyase deficiency in the presence of completely preserved 17α-hydroxylase activity. Similarly, the recently reported patient carrying a homozygous *CYB5A* nonsense mutation showed an entirely normal cortisol response in the short synacthen test (Kok et al., 2010).

The low excretion of urinary androgen metabolites was consistent with the documented low or non-detectable circulating androgens, with the exception of an apparently normal early neonatal testosterone level in case 1, an observation most likely due to cross-reactivity of the assay with foetal steroids that are still circulating in high concentrations during the early days of life. The urinary steroid profile analysis carried out in our patients also had a pivotal role in establishing the correct diagnosis in our family, but also impressively illustrated that CYB5A deficiency is the only condition that shows normal 17α-hydroxylase activity in the presence of 17,20 lyase deficiency. By contrast, 17α-hydroxylase activity, as reflected by the corticosterone over cortisol metabolite ratio, was clearly compromised in previously reported patients with apparently isolated 17,20 lyase deficiency due to mutant CYP17A1 or

POR, although to a lesser degree than in patients considered to have classical, complete 17OHD (Neres et al., 2010; Tiosano et al., 2008).

At the molecular level, it has been reported that CYB5A is not directly involved in electron transfer when facilitating the interaction between CYP17A1 and POR (Auchus et al., 1998), even though it carries a haeme molecule and is therefore potentially able to reduce interaction partners. This is based on *in vitro* observations that CYP17A1 17,20 lyase activity was not altered if co-incubated with apo-b5, i.e. cytochrome b5 devoid of the haeme, or with the haeme-containing holo-protein. This has also been demonstrated for the interaction of cytochrome b5 with the drug-metabolising enzyme CYP3A4 (Auchus et al., 1998; Yamazaki et al., 1996a). Distinct amino acid residues within CYB5A, specifically p.E48 and p.E49, have been shown to retain normal electron transfer properties when mutated, whilst resulting in severely reduced capacity to support 17,20 lyase activity, lending support to the assumption that CYB5A acts as an allosteric facilitator rather than as an electron donor in supporting 17,20 lyase activity (Naffin-Olivos and Auchus, 2006). *In silico* analysis of the CYB5A mutation detected in our patient reveals close proximity of wild type histidine 44 to the haeme molecule, with polar bonds between the positively charged imidazole ring of histidine and the core haeme iron atom (**Figure 34B**). Replacement with leucine at this position, i.e. creating p.H44L, appears to disrupt this interaction (**Figure 34C**), which is highly likely to result in loss of the haeme moiety. This assumption is further supported by previous studies with rat CYB5A that have shown that the haeme-holding ability of cytochrome b5 depends mostly on the strong axial ligation provided by histidine residues 39 and 63 (Falzone et al., 1996; Wang et al., 2003) which are equivalent to histidines 44 and 68 in the human CYB5A protein (**Figure 34C**). Loss of the haeme, i.e. the transition from the CYB5A holo-protein to the apo-protein, has been shown to result in a striking conformational change

(Mukhopadhyay and Lecomte, 2004), which is likely to occur in p.H44L. From this we conclude that the haeme group of CYB5A may be of more significance in supporting CYP17A1 17,20 lyase activity than previously assumed, which challenges the previous concept that the haeme is not required.

Of note, in addition to supporting 17,20 lyase activity, cytochrome b5 is also involved in a number of other processes requiring interaction with this distinct haeme-containing protein, including drug metabolism (Yamazaki et al., 1996a), fatty acid desaturation (Guillou et al., 2004) and, importantly, hemoglobin reduction. Thus, CYB5A deficiency represents another multi-system disorder due to co-factor mutations. This is similar to POR deficiency, which results not only in disordered steroidogenesis but also in impaired drug metabolism (Tomalik-Scharte et al., 2010), and PAPS synthase 2 (PAPSS2) deficiency (Noordam et al., 2009) that disrupts DHEA sulfation, to cause androgen excess, and also other sulfation processes including hepatic drug metabolism.

In our three affected siblings we found mild, clinically inapparent methemogobinemia, in keeping with the findings in the recently reported patient with a *CYB5A* nonsense mutation (Kok et al., 2010) resulting in a non-functional protein. Of note, one further *CYB5A* mutation has been reported previously, resulting in a 16 bp deletion due to a splice site mutation (Giordano et al., 1994). This patient presented with severe cyanosis seven days after birth and significant methaemoglobinaemia of 12-19% (Hegesh et al., 1986), which is more similar to the range of methaemoglobin increases commonly found in cytochrome b5 reductase (CYB5R3) deficiency, i.e. recessive congenital methaemoglobinaemia (Percy and Lappin, 2008). A clinical work-up later revealed 46,XY DSD with an entirely female genital phenotype (Giordano et al., 1994); however, the patient did not undergo endocrine assessment. Importantly, as methaemoglobinaemia is not expected in

17,20 lyase deficiency due to mutant CYP17A1 or POR, assessing methaemoglobin levels in patients with isolated 17,20 lyase deficiency is very likely to represent a useful and presumably highly predictive screening tool for the detection of CYB5A deficiency.

In conclusion, we have described the first human *CYB5A* missense mutation, which results in true isolated 17,20 lyase deficiency as documented by *in vivo* and *in vitro* assessment. The mutation is highly likely to result in loss of CYB5A haeme binding, suggesting that presence of the haeme is crucial for support of 17,20 lyase deficiency. Lack of impairment of 17α-hydroxylase activity can be considered as highly suggestive of *CYB5A* mutations in patients presenting with biochemical evidence of 17,20 lyase deficiency, whereas, impaired 17α-hydroxylation points towards mutant CYP17A1 or POR as the cause of disease. Future studies will need to clarify the impact of *CYB5A* mutations on other organs and systems, with methaemoglobinaemia commonly present.

7. CHAPTER 7: MOLECULAR REGULATION OF DHEA SULFATION BY THE TWO HUMAN PAPS SYNTHASE ISOFORMS

7.1. INTRODUCTION

DHEA sulfation has been previously identified as a novel mechanism of pre-receptor metabolism, regulating the availability of active androgens (Noordam et al., 2009): a molecular defect of the PAPS synthase isoform 2 (PAPSS2) results in decreased DHEA inactivation to DHEAS with subsequent downstream conversion of DHEA to testosterone (see sections 1.1.9.1 and 1.3.1.4). This discovery reveals DHEA sulfation as a gatekeeper of androgen activation. However, based on this seminal case, it is unclear and intriguing why the other PAPSS1 isoform, which is ubiquitously expressed, cannot compensate for defect PAPSS2.

Here, we investigate the molecular interplay of proteins involved in DHEA sulfation, namely SULT2A1 and its co-factors PAPSS1 and PAPSS2.

7.2. METHODS

7.2.1. Plasmids and transient overexpression in HEK293 cells

For all overexpression experiments in this chapter, the cDNA of the PAPSS2b sequence variants was employed (in the progress of this chapter simply referred to as ‘PAPSS2’). For overexpression experiments, the bicistronic vector pIRES™ was employed in order to equally express SULT2A1 with a PAPSS isoform (see section 2.4.1.3). The constructs harbouring SULT2A1 in MCS B and with PAPSS1, PAPSS2 or without a coding sequence in MCS A as well as pIRES constructs harbouring PAPSS isoforms tagged with the cDNA of the fluorescent dye, enhanced green fluorescent protein (eGFP), were generated and kindly donated by Dr Vivek Dhir (University of Birmingham, UK). For the functional studies on subcellular localization of PAPSS variants, cDNAs of PAPSS isoforms cloned into the mammalian

expression vector pEGFP-N1 were kindly donated by Dr Jonathan Mueller (then: University of Duisburg-Essen, Germany) (**Table 18**).

Table 18: Overview of PAPSS sequence variants with their sub-cellular expression pattern [observed by Schroeder et al. (2012)].

PAPSS isoform	Variant (p.)	subcellular localization
PAPSS1	WT	Nuclear > cytoplasmic
	RR111,112AA	Nuclear
	KK9,10AA	Cytoplasmic
PAPSS2	WT	Cytoplasmic > nuclear
	RR101,102AA	Nuclear
	KK6,8AA	Cytoplasmic

These constructs were transiently co-transfected with a pcDNA6 plasmid containing SULT2A1 cDNA generated by restriction digest of SULT2A1 from pIRES with subsequent ligation into linearized pcDNA6, employing the HindIII and XbaI restriction sites. Transfections of 2 µg PAPSS/SULT2A1-pIRES and 1 µg PAPSS-pEGFP-N1 with 1 µg SULT2A1-pcDNA6 plasmids in HEK293 cells were carried out in 6-well plates as described in section 2.1.4.

7.2.2. siRNA knock-down

Small interfering RNAs (siRNAs) were designed with the Block-iT™ RNAi designer tool (http://rnaidesigner.invitrogen.com/rnaiexpress). This tool identifies suitable siRNA oligos within the mRNA sequence of the gene of interest based on guidelines for highly-efficient siRNA knock-down (Ui-Tei, 2004).

Three siRNA oligos were selected for each target (*PAPSS1*, *PAPSS2* and *SULT2A1*). A custom-made control siRNA oligo, which is not directed to any mRNA, served as a negative control for all knock-down experiments. The green fluorescent positive control BLOCK-iT™ (Invitrogen/Life Technologies, Grand Island, NY, USA) was added to each experiment to estimate transfection efficiency.

Table 19: Sequences (sense strand only) of siRNA oligonucleotides used for transfection in the knock-down experiments for PAPSS1, PAPSS2 and SUL2A1.

Target (mRNA position)	**RNA sequence (Sense strand)** (5'→3')
PAPSS1 (309)	CCUGGUUUGUCAUGGUAUU
PAPSS1 (419)	GCAUCGCAGAAGUUGCUAA
PAPSS1 (1380)	GCAGGAUACCCAUAAGCAA
PAPSS2 (612)	CCAGCUUUAUUUCUCCAUU
PAPSS2 (899)	GCAGAACAUUGUACCCUAU
PAPSS2 (1180)	CCGUCUCUGCAGAGGAUAA
SULT2A1 (169)	GCAUAGCUUUCCCUACUAU
SULT2A1 (622)	GGUCAUGGUUUGACCACAU
SULT2A1 (763)	CCGAAGAACUGAACUUAAU
control	GCCACGUAAGAUGAGUCAA

NCI-H295R cells (section 2.1.3) were seeded, 4 x 10^4 cells per well in 24-well plates, to grow to 30-40% confluence. After 24 hours, cells were transfected with siRNA oligos using the Jet-SI ENDO transfection reagent (Peqlab, Erlangen, Germany): for each well, 49 µl of serum-free medium and 1 µl of transfection reagent were mixed in a 1.5 ml reaction tube and incubated for 10 minutes at room temperature. In a separate tube, 48.75 µl of serum-free medium was mixed with 1.25 µl of pooled siRNA from a 2 mM stock (i.e. 50 nM final concentration). Then, the 50 µl transfection reagent solution was added to the 50 µl of siRNA oligo solution. After swift and gentle mixing by vortexing for 10 seconds at medium velocity, the mixture was incubated for 15 minutes at room temperature. Finally, all 100 µl were pipetted drop wise into the well followed by gently swirling the plate. To avoid toxicity, the medium was removed after 6 hours and replaced by 500 µl of full growth medium. Previous experiments from our group showed that the efficiency of the knock-down was greater if the transfection was performed twice. Therefore, the procedure was repeated after 72 hours of incubation and the cells were processed for expression analysis and *in vitro* functional analysis 24 hours after the second transfection.

7.2.3. DHEA sulfation assays

48 hours after transfection of the vector DNA, HEK293 cells were incubated with 0.5 ml full growth medium in the presence of 250 nM DHEA and 0.2 µCi ^{3}H-labelled DHEA (101.3 Ci/mol, Perkin Elmer, Waltham, USA) at 37°C in a cell culture incubator. For siRNA knock-down studies, NCI-H295R cells were incubated 24 hours after the second siRNA knock-down in the presence of 1 µM trilostane, a HSD3B inhibitor, in 0.5 ml serum-free medium at 37°C. After one hour, the medium was replaced with 0.5 ml serum free medium containing 1µM trilostane, 100 nM DHEA and 0.2 µCi ^{3}H-labelled DHEA and cells were incubated for one hour at 37°C in a cell culture incubator. Steroids were extracted from medium with 5 ml of dichloromethane as described in section 2.5.5 with the following modifications: to increase the extraction efficiency of (intracellular) DHEAS, cell membranes were ruptured by adding 1 ml 100% methanol to the cells followed by 10 min incubation at room temperature on an orbital shaker. The methanol and dichloromethane were combined in one glass tube, evaporated on a heat block at 55°C and then separated by TLC followed by quantification of DHEA and DHEAS peaks on a bioscanner as described in section 2.5.6.

7.2.4. mRNA expression analysis by real-time quantitative PCR

Total RNA has been isolated from whole cells after *in vitro* functional analysis as described in section 2.2.1. cDNA was generated by reverse transcription of mRNA (section 2.2.3) and real-time PCR performed as described in section 2.2.10. The following customised, exon-spanning gene expression assays have been employed (all: TaqMan® Assays, Life Technologies™, Grand Island, NY, USA): SULT2A1: Hs00234219_m1; PAPSS1: Hs00968937_m1; PAPSS2: Hs00989921_m1. An assay to detect eukaryotic 18S ribosomal RNA (HS99999901_s1) was employed as a

control to correct for equal loading and to calculate dCt values. All probes were labelled with 6-carboxyfluorescein (FAM), the 18S probe with the VIC® fluorophore.

mRNA expression was quantified as delta Ct values for each target gene (see section 2.2.10). To calculate the 'fold change' following si-RNA knock-down experiments, dCTs of the respective gene after targeted si-RNA knockdown were subtracted from the dCt values of the same gene and within the same experiment following transfection with control siRNA (i.e. delta delta Ct, ddCt), then by applying the following equation:

$$Fold\ change = 2^{(-ddCT)}$$

7.2.5. Immunofluorescence studies

For indirect immunofluorescence, NCI-H295R1 cells were seeded on sterilized cover slips placed in 6-well plates at 20,000 cells per well and grown in full growth medium to attach overnight. Cell were fixed with 100% ice-cold methanol and incubated at -20°C for 20 mins. Cells were washed three times in PBS. To avoid unspecific binding, cells were incubated with 5% (m/v) bovine serum albumin (BSA) in PBS supplemented with 0.1% (v/v) Triton X100 (all Sigma, Pool, UK). Cells were incubated at 4°C overnight with monoclonal mouse antibodies against PAPSS1 and PAPSS2 at a concentration of 1:50 diluted in PBS/0.1% Triton X100/1% BSA (PAPSS1: ab56398; PAPSS2: ab56393; Abcam, Cambridge, USA). After washing three times with PBS/0.1% Triton X100, the samples were incubated with a fluorescein-labelled (FITC) anti-mouse IgG antibody (1:200 in PBS/0.1% Triton X100/1% BSA) at room temperature for 1 hour. After washing the cells three times, coverslips were mounted on microscope slides with Vectashield® mounting medium containing DAPI for nuclear staining (Vector Laboratories, Burlingame, USA).

Cells transiently transfected with pIRES vectors containing eGFP-tagged *PAPSS* cDNA seeded on coverslips were fixed 48 hours after transfection with 1 ml of Glyo-Fixx solution (Thermo Scientific, Cramlington, UK) for 2 hours at room temperature on an orbital shaker. After washing the cover slips three times with PBS, cells were incubated with 85% ethanol for 1 hour and washed again with PBS/0.1% Triton X100. Nuclei were stained with a propidium iodide solution (1:100 in PBS/0.1% Triton X100, containing 100µg/ml RNAse A; all Invitrogen, Carlsbad, USA) at 37°C for 20 mins. Images were obtained from a cell culture microscope (Leica, Wetzlar, Germany) for live-cell imaging and on a confocal microscope (Zeiss, Jena, Germany).

7.2.6. Western blot

To assess expression levels of PAPSS isoforms and SULT2A1 on the protein level after overexpression and knock-down experiments, cells were harvested in cold PBS (with Complete® proteinase inhibitor; Roche, Basel, Switzerland) 48 or 24 hours after transfection, respectively. For protein expression, an extra well of transfected cells has been prepared, which was not used for steroid extraction as the necessary methanol treatment (7.2.3) denatures the protein, making it unsuitable for Western blot analysis. SDS-PAGE and Western blot has been performed as described in section 2.3.3.

Table 20: Primary and secondary antibodies used for Western blot and immunofluorescence studies.

Target	Species, type	Product no	Supplier	Concentration WB (IF)
Primary antibodies:				
PAPSS1	Mouse, monoclonal	ab56398	Abcam	1:1,000 (1:50)
PAPSS2	Mouse, monoclonal	ab56393	Abcam	1:1,000 (1:50)
SULT2A1	Rabbit, polyclonal	ab38416	Abcam	1:200
β-Actin	Mouse, monoclonal	Ab20272	Abcam	1:25,000
α-tubulin	Mouse, monoclonal	Sc-5286	Santa Cruz	
Lamin	Mouse, monoclonal	ab8980	Abcam	1:1000
Secondary antibodies:				
Anti-mouse IgG, HRP-conjugated	Goat, polyclonal	A5278	Sigma	1:1,000
Anti-rabbit IgG, HRP-conjugated	Goat, polyclonal	A6667	Sigma	1:1,000
Anti-mouse, Alexa Fluor® 488	Goat, polyclonal	P36930	Life technologies	(1:100)

7.2.7. Extraction of cytosolic and nuclear fractions from whole cell lysates

A nuclear extraction kit (Chemicon/Millipore®, Billerica, USA) was used to isolate nuclear and cytoplasmic fractions of four different mammalian cell lines: NCI-H295R1, NCI-H295R3, HEK293 and the hepatocellular carcinoma cell line Hep G2.

Cells were grown to 70-90% confluence and pelleted after short (2-5 minutes) trypsinisation (section 2.1) from 6 x T75 flasks (Greiner Bio-One, Stonehouse, UK). Cells were washed twice in 40 ml ice-cold PBS and all subsequent steps were performed on ice/4°C. The volume of the pellet was estimated and five cell pellet volumes of chilled Cytoplasmic Lysis Buffer was added; to homogenise the cells, the tube was then gently inverted. The cell suspension was incubated for 15 minutes and subsequently centrifuged at 250 x g for 5 minutes. The supernatant was discarded and the pellet was re-suspended in two volumes of Cytoplasmic Lysis Buffer. Then, cytoplasmic cell lysis was facilitated by drawing the cell homogenate into a syringe with a 27-gauge needle and ejecting the content back in to the tube. The procedure was repeated five times. The disrupted cell suspension was centrifuged at 8,000 x g

for 20 minutes and the supernatant containing the cytosolic fraction of the cells was snap-frozen and stored at -80°C until further processing.

To extract the nuclear fraction, the cell pellet was re-suspended in 2/3 of its original volume in Nuclear Extraction Buffer. Nuclei were disrupted by drawing and ejecting the pellet five times into a fresh syringe with a 27-gauge needle. Then, the suspension was agitated on an orbital shaker for 45 minutes and centrifuged at 16,000g for 5 minutes. The supernatant, containing the nuclear extract, was stored at -80°C until further processing. Protein content was measured by using the BioRad method (section 2.3.2) and 20 µg of each fraction as well as whole cell lysate were loaded per lane.

7.3. RESULTS

7.3.1. Effects of PAPS synthases on DHEA sulfation *in vitro*

7.3.1.1. Overexpression studies

HEK293 cells were transiently transfected with three different pIRES constructs/combinations: (1) SULT2A1 alone or in the presence of (2) PAPSS isoforms 1 or (3) PAPSS2. An empty vector served as a negative control. After transfection, expression analysis was carried out on the mRNA (**Figure 35**) and protein level (**Figure 36**).

Transfection of pIRES constructs resulted in strong expression of the respective ORFs for all for all targets investigated, indicating successful transcription (**Figure 35**). Baseline target mRNA expression was observed at dCt values of about 21-22 cycles at baseline (transfection with empty vector) and increased to dCt values of 4-5 after transient transfection of the respective constructs. There were no statistical differences of mRNA levels between the different experimental set-ups. The dCt

values for SULT2A1 were of similar range between the three different settings with equally high expression of PAPSS mRNA in constructs that also contained the PAPSS 1 and 2 ORFs (**Figure 35**).

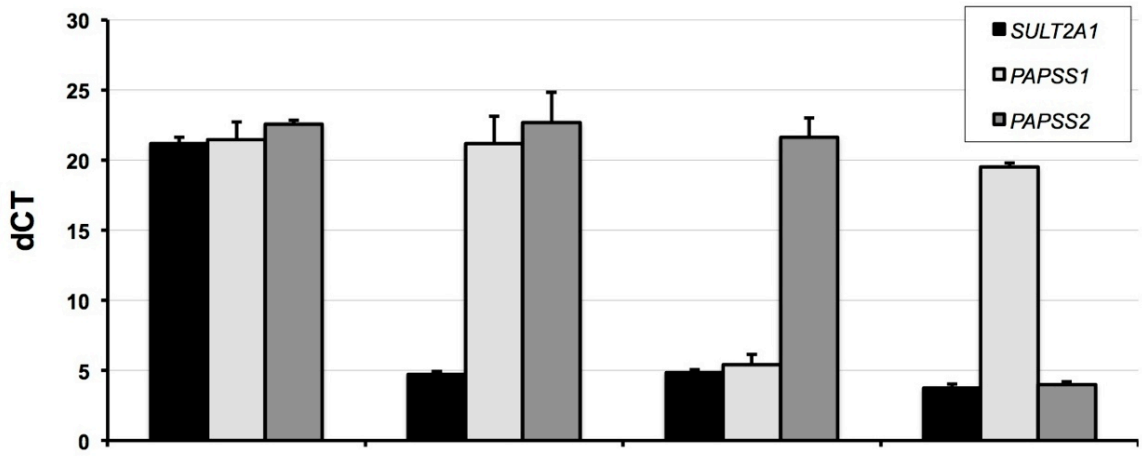

dCT	empty/empty	empty/SULT2A1	PAPSS1/SULT2A1	PAPSS2/SULT2A1
SULT2A1	21.15 ± 0.48	4.73 ± 0.2	4.85 ± 0.22	3.74 ± 0.28
PAPSS1	21.46 ± 1.26	21.19 ± 1.92	5.43 ± 0.71	19.5 ± 0.31
PAPSS2	22.55 ± 0.29	22.66 ± 2.16	21.62 ± 1.36	4.0 ± 0.21

Figure 35: mRNA expression represented as delta Ct (dCt) values of SULT2A1, PAPSS1 and PAPSS2 following transient transfection of pIRES constructs harbouring cDNAs of either SULT2A1 alone or in the presence of PAPSS1 or PAPSS2 in HEK293 cells. An empty pIRES vector served as a negative control. The data were obtained from three independent experiments and variation of mRNA expression is represented as ± standard deviation (SD), illustrated as error bars.

On the protein level, Western blot analysis detected strong staining for SULT2A1 and PAPSS 1/2 in the cell lysates of transfected HEK293 cells, indicating successful transcription of mRNA into protein (**Figure 36**). However, the intensity of the SULT2A1 band is decreased when co-expressed with PAPSS1. This finding was confirmed in five repeats of the Western blot of independent experiments.

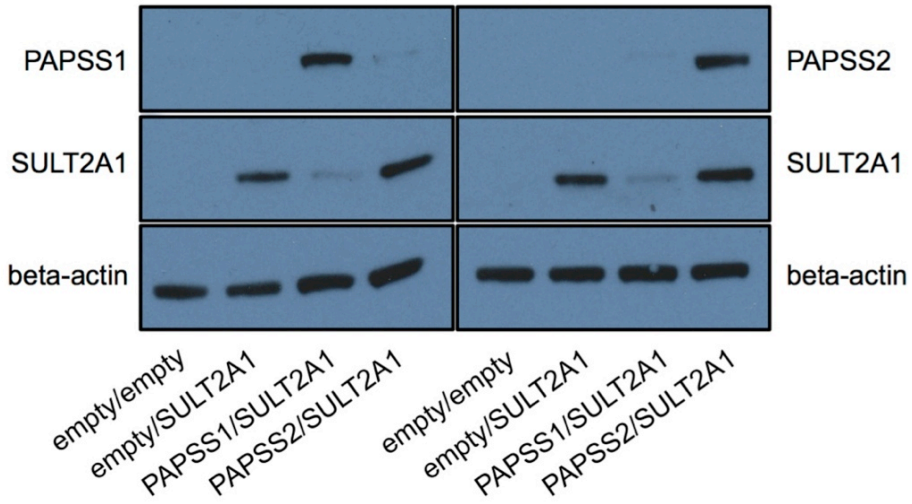

Figure 36: A representative Western Blot of transiently transfected HEK293 cells with pIRES constructs harbouring cDNAs of SULT2A1 alone or in the presence of PAPSS isoforms 1 and 2. Cells transfected with an empty pIRES vector served as a negative control. As PAPSS1 and PASS2 have nearly the same molecular weight, two membranes were incubated with the respective PAPSS antibody. 10 µg of total protein were loaded for each lane. Beta-actin staining served as a control for equal loading.

To assess the impact of the two PAPSS isoforms on SULT2A1 activity on a functional level, DHEA sulfation assays were performed in transfected HEK293 cells (**Figure 37**). Co-expression of PAPSS1 with SULT2A1 resulted in a significant decrease of DHEA sulfation to about 60% of the activity observed when SUL2A1 is present alone. In contrast, co-expressing PAPSS2 strongly increased DHEA to DHEAS conversion and was about 5-6 fold higher as observed when SUL2A1 is expressed on its own. This also reached statistical significance.

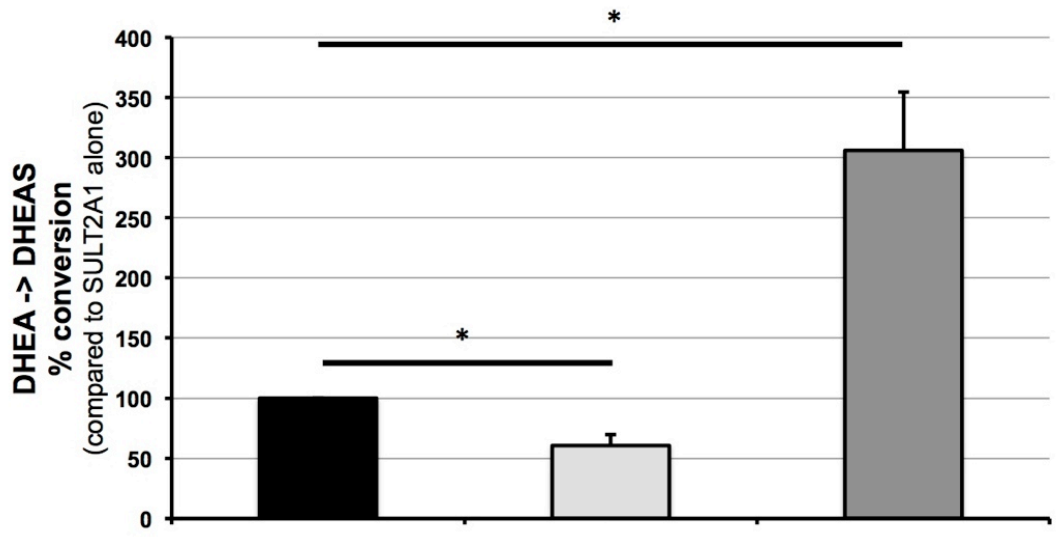

% conversion *(compared to SULT2A1 alone)*	**100**	**61 ± 9.22**	**306 ± 48.6**
p-value		0.0178	0.0181

Figure 37: DHEA sulfation (% DHEA to DHEAS conversion) carried out in HEK293 cells transiently transfected with pIRES constructs harbouring cDNAs of SULT2A1 alone or in the presence of PAPSS isoforms. To assess the impact of either PAPSS isoforms on SULT2A1 activity, the conversion rates were compared to SULT2A1 alone, which is 100%. The data were obtained from three independent experiments and variation of DHEA sulfation is represented as ± standard deviation (SD), also illustrated as error bars. An unpaired Student's T-Test was performed to calculate the p-value for significance levels.

7.3.1.2. siRNA knock-down studies

As a mirror image approach, transient siRNA knock-down of SULT2A1, PAPSS1 and PAPSS2 was performed in the adrenal NCI-H295R1 cell line. SiRNA knockdown was successful for all three targets and knock-down efficiency varied between 60% to 80% (**Figure 38**). To further investigate potential co-regulatory mechanism on the transcriptional level, mRNA expression of *SULT2A1* and *PAPSS* isoforms was measured by real-time PCR for each knock-down scenario (**Figure 38**): siRNA knock-down of *SULT2A1* resulted in a significant increase of *PAPSS2* expression ($p = 0.044$; **Figure 38**, left panel). Knock-down of PAPSS1 did not affect the expression levels of *SULT2A1*, but *PAPSS2* mRNA expression was significantly up regulated ($p = 0.013$; **Figure 38** middle panel). Finally, both mRNAs of *SULT2A1*

and *PAPSS1* were higher expressed in cells were *PAPSS2* was knocked down, however only the *SULT2A1* up-regulation reached statistical significance (SULT2A1: p = 0.039; PAPSS1: p = 0.109; **Figure 38** right panel).

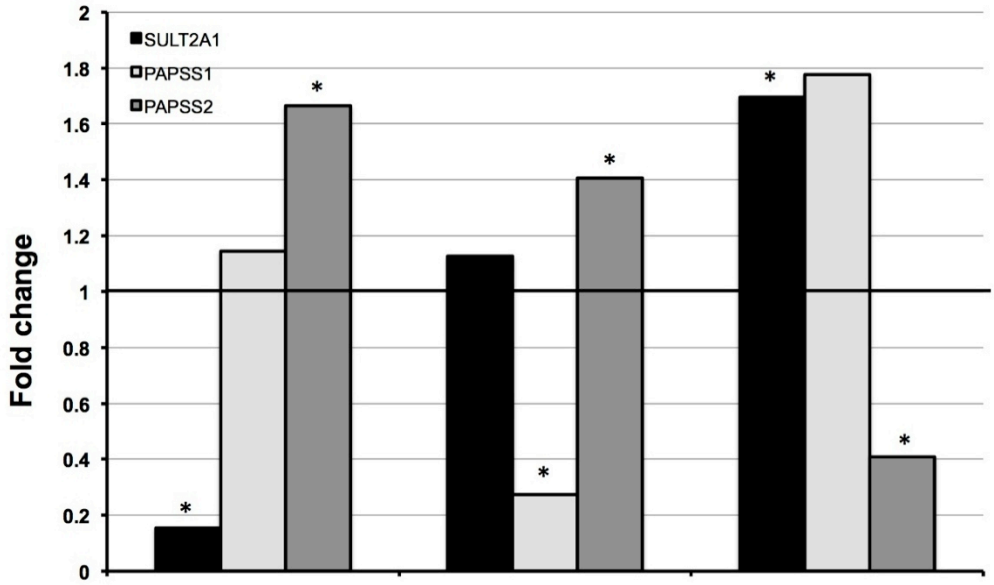

dCT	siSULT2A1 (control)	siPAPSS1 (control)	siPAPSS2 (control)
SULT2A1	**15.84 ± 0.87** (13.79 ± 0.72)	**16.72 ± 0.19** (16.58 ± 0.22)	**15.1 ± 0.54** (15.82 ± 0.41)
PAPSS1	**12.76 ± 1.51** (12.9 ± 1.6)	**17.27 ± 1.63** (15.25 ± 1.48)	**15.97 ± 0.61** (15.43 ± 0.44)
PAPSS2	**13.08 ± 0.48** (13.81 ± 0.46)	**15.25 ± 0.74** (16.07 ± 0.68)	**17.56 ± 0.43** (15.9 ± 1.15)

Figure 38: mRNA expression after transient siRNA knock-down of SULT2A1, PAPSS1 and PAPSS2 in adrenal NCI-H295R cells. Data are presented as fold change based on delta dCt (ddCt) values for comparison to a control knock-down using random, non-targeted siRNA-oligos (control = 1). The dCt values are listed in the table below the bar graph. All experiments were performed in at least three independent experiments. * = $p < 0.05$.

To investigate the effects of these siRNA knock-down experiments on the protein level, Western blot experiments were carried out from whole cell lysates of NCI-H295R1 cells. Knock-down of SULT2A1 resulted in stronger expression of PAPSS2 but also PAPSS1 protein (**Figure 39**, left). Knock-down of PAPSS1 resulted in a mild increase of SULT2A1 and PAPSS2 expression (**Figure 39**, middle). In cells were PAPSS2 expression was decreased, SULT2A1 expression was stronger compared to control (**Figure 39**, right).

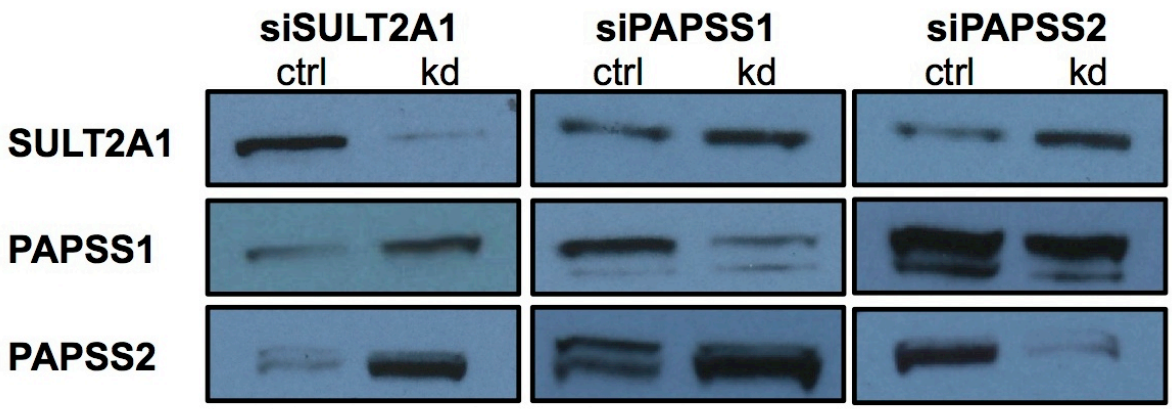

Figure 39: A representative Western blot from adrenal NCI-H295R whole cell lysates after siRNA knock-down (kd) of SULT2A1, PAPSS1 and PAPSS2 (ctrl: cells transfected with a non-targeted control oligo). 20µg of protein were loaded per lane.

To further assess the functional impact of siRNA knock-down of either SULT2A1, PAPSS1 and PAPSS2, *in vitro* DHEA sulfation assays were performed following each knock-down scenario (**Figure 40**).

Knock-down of *SULT2A1* mRNA dramatically reduced DHEAS generation in these cells. Knock-down of the PAPSS1 isoform in the presence of SULT2A1 no effect on DHEA sulfation; intruigingly, knock-down of the PAPSS2 isoform reduced DHEA sulfotransferase activity to about 30 % compared to control (**Figure 40**).

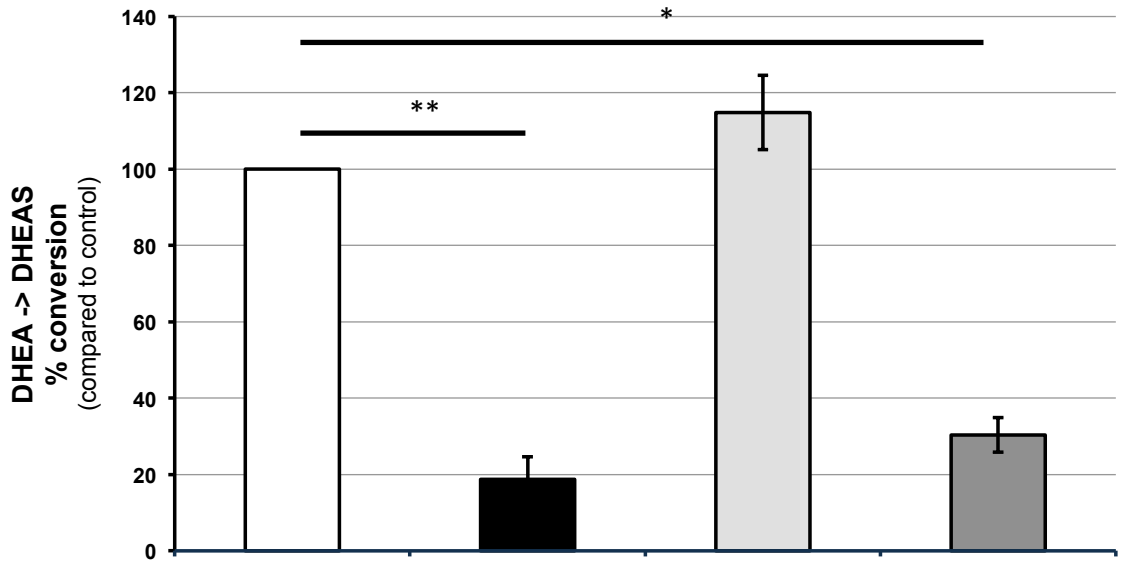

	Control	siSULT2A1	siPAPSS1	siPAPSS2
% conversion *(compared to control)*	**100**	**18.7 ± 5.9**	**114.8 ± 9.7**	**30.3 ± 4.6**
Substrate conversion rate *(nmol DHEA/hour)*	**1.22 ± 0.07**	**0.23 ± 0.03**	**1.38 ± 0.06**	**0.37 ± 0.04**
p-value *(compared to control)*		0.009	0.39	0.015

Figure 40: DHEA sulfation (% DHEA to DHEAS conversion) in adrenal NCI-H295R cells following transient siRNA knock-down of SULT2A1, PAPSS1 and PAPSS2. The conversion rates for each knock-down experiment were compared to a control knock-down with an untargeted siRNA oligo, which is 100%. The data were obtained from three independent experiments and variation of DHEA sulfation is represented as ± standard deviation (SD), also illustrated as error bars. An unpaired Student's T-Test was performed to calculate the p-value for statistical significance.

7.3.2. Subcellular localization studies

To further investigate underlying mechanisms why PAPSS1 can not compensate for defect PAPSS2, expression studies focusing on the subcellular localisation of molecules involved in DHEA sulfation were performed.

7.3.2.1. Fractionation studies

Nuclear and cytoplasmic fractions of NCI-H295R cells (substrains 1 and 3) as well as the liver carcinoma cell line Hep G2 were isolated and Western blot for the two PAPSS isoforms was performed (**Figure 41**). I have verified the integrity and quality of the two fractions by co-staining with the nuclear marker lamin and the

cytosolic marker α-tubulin, and have observed very little contamination of each fraction (data not shown).

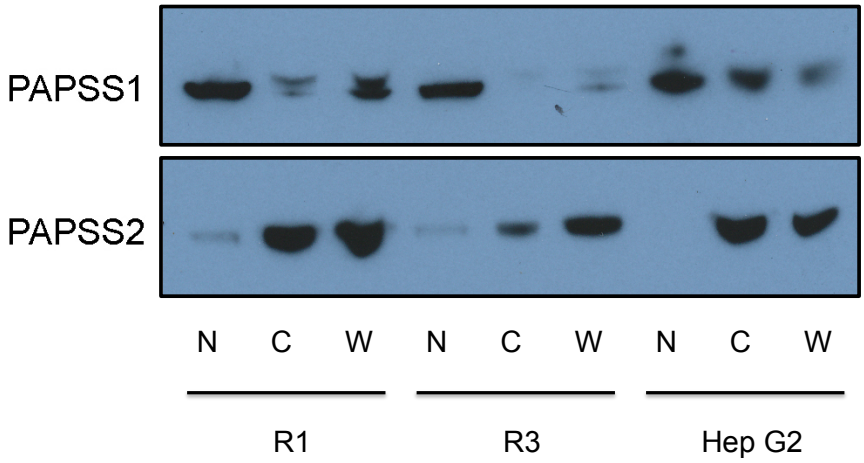

Figure 41: Western blot showing protein staining for PAPSS isoforms in nuclear (N), cytosolic (C) extracts and whole cell lysates (W) from two NCI-H295R substrains (R1 and R3) and the liver carcinoma cell line Hep G2.

PAPSS1 protein was predominantly detected in the nuclear fraction of all three cell types and comparably reduced in the cytosolic fractions. In contrast, an increased expression of PAPSS2 was found in the cytoplasmic compared to the nuclear fraction, with minimal PAPSS2 detection in the nuclear compartments of the adrenal cell substrains and no detection in the nuclear fraction of the Hep G2 cell line.

7.3.2.2. Immunofluorescence studies

To extend the sub-cellular localization studies of the PAPSS isoforms further, immunofluorescence studies were carried out in the adrenal NCI-H295R cell line. Firstly, indirect immunofluorescence with commercially available primary antibodies was performed in methanol-fixed cells (**Figure 42**): both PAPSS isoforms were expressed predominantly in the nuclear compartment, however, a less intense cytoplasmic stain has been observed for both PAPSS isoforms, which was slightly stronger for PAPSS2 compared to PAPSS1.

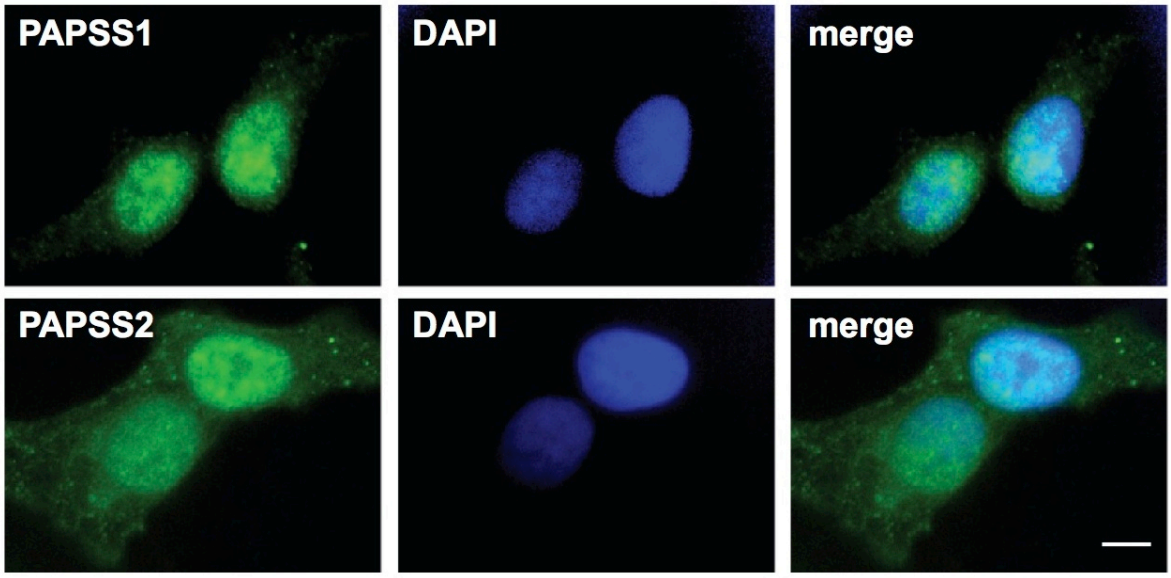

Figure 42: Indirect immunofluorescence of PAPSS isoforms in adrenal NCI-H295R cells. Bar: 50 µm.

As cross-reactivity of the primary antibodies could potentially lead to inaccurate staining of the PAPSS isoforms by indirect immunofluorescence, I have transiently transfected NCI-H295R1 cells with pIRES constructs harbouring the cDNAs of PAPSS 1 and 2 tagged with eGFP. Here, a similar pattern is found as observed in the indirect immunofluorescence studies: PAPSS1-eGFP appears to be predominantly expressed in the nuclear compartment, both in living cells (**Figure 43A**) and after fixation and co-staining with the nuclear marker propidium iodide (**Figure 43 B**). For PAPSS2, I have observed a stronger staining intensity in the nuclear compartment, but also some cytosolic staining both in living cells as well as after fixation. Confocal imaging suggests that the staining distribution varies and the staining intensity can also be found equally strong in both the cytosol as well as in the nucleus in some cells (**Figure 43 B**).

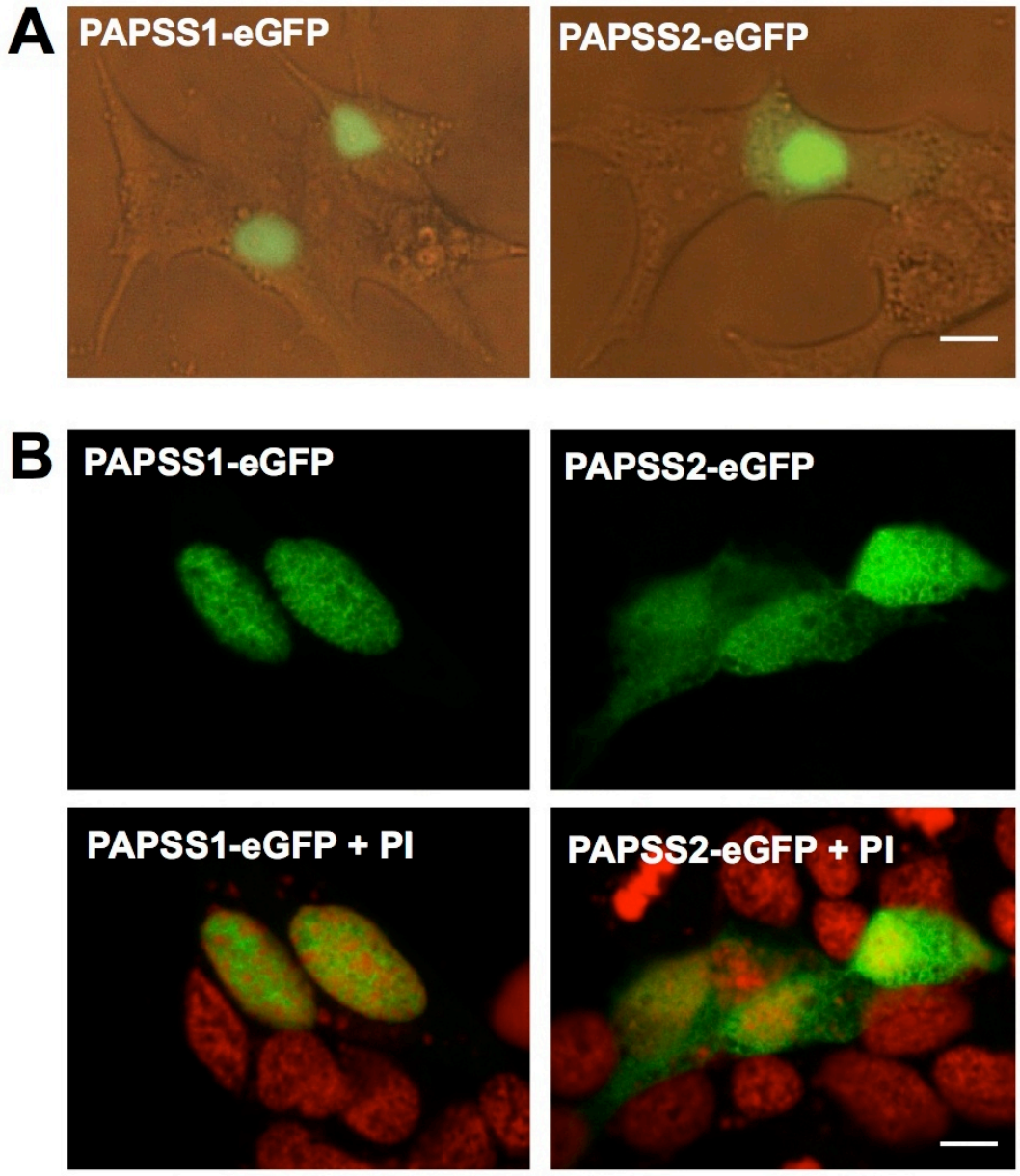

Figure 43: Imaging of living cells (**panel A**) and confocal microscopy (**panel B**) of NCI-H295R cells transiently transfected with the pIRES vector harbouring eGFP-tagged PAPSS1 (left) and PAPSS2 (right) cDNAs. Nuclei were visualized in panel B with propidium iodide (PI, red signal). Bar in panel A: 100 µm, panel B: 75 µm.

7.3.2.3. Functional consequences of subcellular localization of PAPS synthases

To assess the functional consequences of a cytosolic versus nuclear localization of PAPSS1 and PAPSS2, I have performed *in vitro* DHEA sulfation

assays in HEK293 cells of PAPSS variants that are exclusively expressed in the cytoplasm or the nucleus co-transfected with SULT2A1. These sequence variants of PAPSS isoforms were generated by site-directed mutagenesis and identified based on a mutagenesis screen to show a nearly exclusive cytosolic or nuclear expression pattern (Schröder et al., 2012).

A

PAPSS variant (co-transfected with WT SULT2A1)	**Subcellular localization**	**Substrate conv. rate** (nmol DHEA/ hour)	**p-value** (comp. to WT)
EV		2.03 ± 0.13	
P1 WT	nuc > cyt	13.87 ± 1.33	
P1 KK9,10AA	cyt	8.51 ± 0.83	0.035
P1 RR111,112AA	nuc	10.04 ± 0.67	0.02
P2 WT	cyt < nuc	29.1 ± 1.95	
P2 KK6,8AA	cyt	26.9 ± 1.29	0.35
P2 RR101,102AA	nuc	22.56 ± 1.22	0.009

B

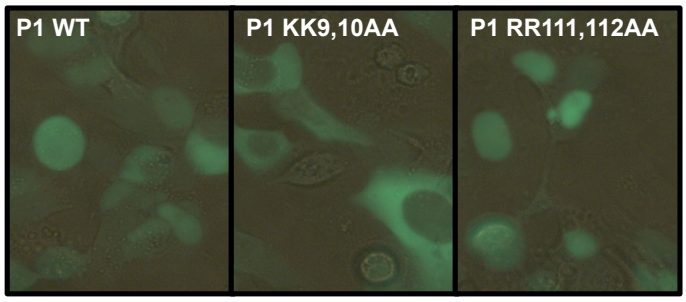

C

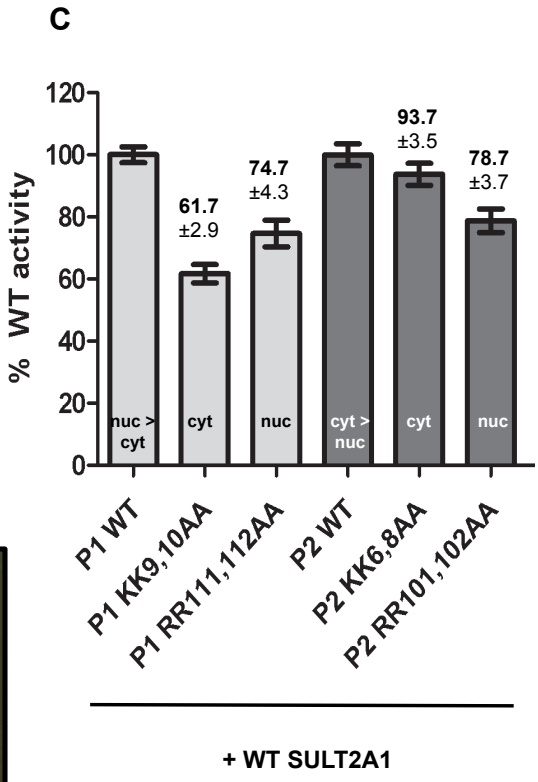

Figure 44: Functional analysis of PAPSS sequence variants co-transfected in HEK293 cells with SULT2A1. **Panel A**: DHEA substrate conversion rates of the four localization variants and empty vector (EV) control compared to wild type PAPSS; the subcellular localization of the respective variants are indicated as nuclear (nuc) and cytoplasmic (cyt). **Panel B**: Live-cell imaging of transfected HEK293 cells with eGFP-tagged PAPSS1 variants to illustrate the subcellular localization pattern. **Panel C**: Substrate conversion rates expressed as %WT activity. All values are expressed as the mean (± SEM) of triplicate assays from three independent experiments. An unpaired student's t-test was performed to calculate the p-values.

For all four sequence variants examined, I have observed a decrease in SULT2A1 activity compared to the respective WT PAPSS isoform, which reached statistical significance for both the cytoplasmic and nuclear PAPSS1 variant (p.KK9,10AA and p.RR111,112AA), but only for the nuclear-expressed PAPSS2 variant (p.RR101,102AA) (**Figure 44**). The DHEA conversion rates were generally

lower for all PAPSS1 variants and SULT2A1 activity was decreased to about 50% when co-transfected with WT PAPSS1 compared to WT PAPSS2 (**Figure 44A**). The most marked decrease was observed for the cytoplasmic PAPSS1 variant, which was 61% of WT PAPSS1 activity (**Figure 44B**).

mRNA and protein expression levels indicate successful overexpression of SULT2A1 and PAPS synthases (**Figure 45** and **Figure 46**). However, the dCt levels of SULT2A1 were about one dCt value higher when co-expressed with PAPSS1 variants, suggesting decreased mRNA expression. At the same time, the PAPSS1 mRNA levels were higher compared to PAPSS2 variants with a difference of two to three dCt values.

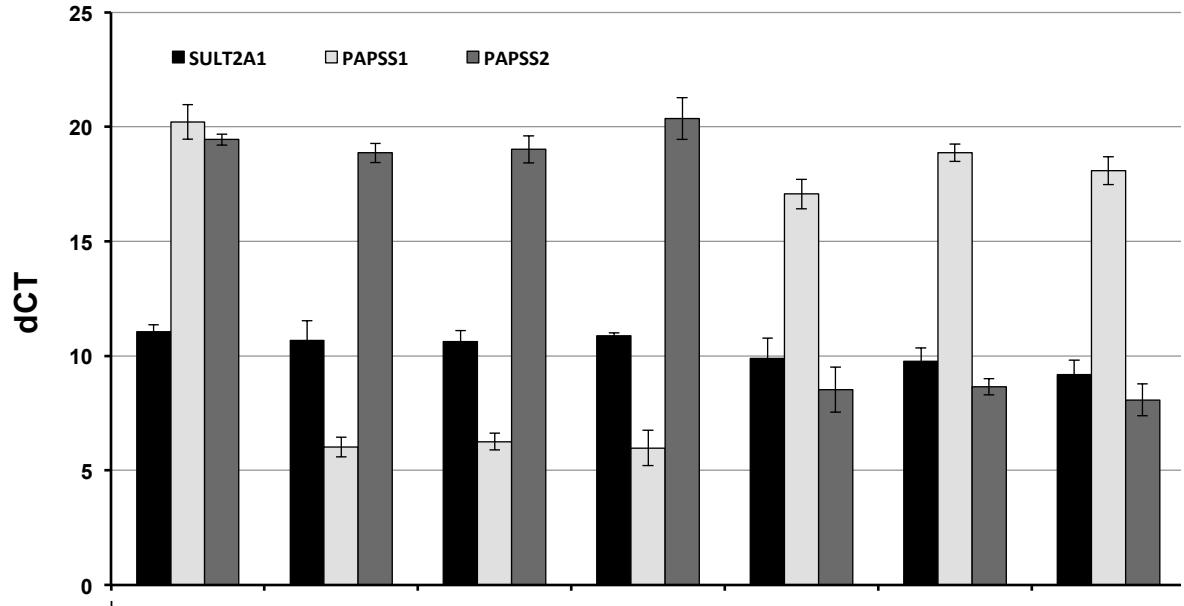

dCT	EV	PAPSS1 WT	PAPSS1 KK9,10AA	PAPSS1 RR111,112AA	PAPSS2 WT	PAPSS2 KK6,8AA	PAPSS2 RR101,102AA
	+ SULT2A1						
SULT2A1	11.04 ± 0.32	10.67 ± 0.86	10.63 ± 0.48	10.86 ± 0.12	9.89 ± 0.89	9.75 ± 0.58	9.18 ± 0.63
PAPSS1	20.21 ± 0.75	6.01 ± 0.43	6.25 ± 0.36	5.97 ± 0.77	17.07 ± 0.64	18.86 ± 0.38	18.08 ± 0.61
PAPSS2	19.44 ± 0.23	18.86 ± 0.42	19.01 ± 0.59	20.36 ± 0.91	8.53 ± 0.98	8.64 ± 0.35	8.08 ± 0.70

Figure 45: mRNA expression represented as delta Ct (dCt) values of SULT2A1, PAPSS1 and PAPSS2 following transient co-transfection in HEK293 cells of p-eGFP-N1 constructs harbouring cDNAs for PAPSS1 and 2 sequence variants with SULT2A1 in pcDNA6. The empty vector (EV) refers to empty p-eGFP-N1 co-trasnfected with SULT2A1. The data were obtained from three independent

experiments and variation of mRNA expression is represented as ± standard deviation (SD), illustrated as error bars.

The variation of SULT2A1 expression as indicated by the real-time mRNA expression data is also reflected on the protein level by Western blot analysis (**Figure 46**): The SULT2A1 bands appear less intense in the lysates derived from cells co-transfected with PAPSS1 variants. Also, the SULT2A1 protein expression is lower in the cells co-transfected with empty pEGFP-N1 vector (EV). In addition, a strong and slightly 'higher' PAPSS2 band has been observed when PAPSS1 was co-transfected; this suggests strong cross-reactivity of the PAPSS2 antibody with PAPSS1 (**Figure 46**).

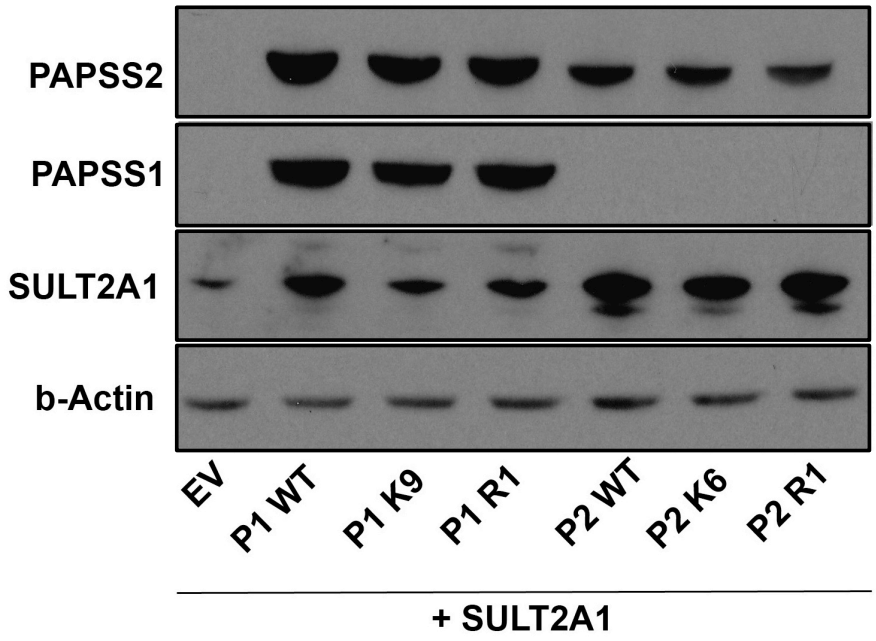

Figure 46: A representative Western blot from HEK293 whole cell lysate after co-transfection of PAPSS1 and 2 variants with SULT2A1. 15µg of protein were loaded per lane and beta-actin was used as a control for equal loading.

7.4. DISCUSSION

Both in the overexpression studies and in the siRNA knock-down experiments, I could recapitulate *in vitro* that PAPSS2 but not PAPSS1 supports SULT2A1 and DHEA sulfation, an observation that was made from a previously published case study (Noordam et al., 2009).

Transient co-expression of SULT2A1 with PAPSS2 resulted in a 300% increase of DHEA sulfation compared to when SULT2A1 only relies on the endogenously expressed PAPS synthases of HEK293 cells. Notably, not only the PAPSS1 overexpression reduces SULT2A1 activity, it also reduces the protein expression of SULT2A1, which I have observed in several replicates of the experiment. To rule out technical artefacts related to the IRES cassette not consistently expressing both cDNAS as described recently (Mansha et al., 2012), I have performed co-transfections with two pcDNA6 plasmids harbouring the cDNAs of PAPSS and SULT2A1, respectively, which gained essentially the same results (data not shown). To exclude a cell-type specific effect, I have also repeated the experiments in the monkey kidney cell line COS7 and obtained similar results (data not shown). As *SULT2A1* mRNA expression was equal in each co-expression scenario, reduced SUL2A1 protein expression could indicate an interaction between PAPSS1 and SULT2A1 on the post-translational level. High levels of PAPSS1, which is endogenously lowly expressed in HEK293 cells, could destabilize SULT2A1 protein or increase its metabolism within the cell, either by exerting direct effects or mediated by other factors. To elucidate underlying mechanism and to identify possible interaction partners would be an important question to address for future studies.

Whilst there may be still unresolved uncertainties concerning the overexpression system, the data generated from the siRNA knock-down studies

clearly show the dependence of SULT2A1 on PAPSS2 as its knock-down reduces the enzyme's activity dramatically; in contrast, PAPSS1 knock-down did not change its activity. Additionally, I have also observed interaction of PAPSS isoforms with SULT2A1 on the transcriptional level and found significant up-regulation of SULT2A1 mRNA expression in cells where PAPSS2 was down regulated. The Western blot data suggest that this is also reflected on the protein level. Interestingly, PAPSS1 knockdown did not change SULT2A1 expression not mirroring the findings from the overexpression studies. The different molecular environment of the adrenal NCI-H295 cells compared to the non-steroidogenic kidney cell could explain this different behaviour; moreover, a dose-dependency could be an explanation as the PAPSS1 expression levels are extremely high after transfection (dCt: 5-6) compared to its much lower endogenous expression levels of NCI-H295R cells (dCt: 15-16). However, the expression data from both experiments strongly indicate interaction of PAPSS isoforms with each other as well as SULT2A1, on the transcriptional and post-transcriptional level.

In the search for potential mechanism underlying the findings that PAPSS1 can not compensate for PAPSS2, different routes of investigations have been proposed and have partly been addressed in previous studies: Different catalytic activities for PAPSS isoforms have been reported with a 10-15fold higher global activity for PAPSS2 compared to PAPSS1 in one study (Fuda et al., 2002). However, these findings were not confirmed by Grum et al. investigating the catalytic activity of the APS kinase domain of the two PAPSS isoforms in isolation and upon hetero-dimer formation (Grum et al., 2010). The same group has investigated PAPS synthases for protein stability and strikingly found that the PAPSS2 unfolded protein has a very short half-life time of several minutes compared to PAPSS1, which essentially remains structurally intact under physiological conditions (van den Boom et al.,

2012). Interestingly, the PAPSS2 isoform is stabilized by low concentrations of nucleotide adenosine-5'phosphosulfate (APS), which is also the product of its ATP sulfurylase activity (van den Boom et al., 2012); APS therefore may represent an intracellular modulator of PAPS formation and sulfation processes as a whole (Mueller and Shafqat, 2013). Therefore, future studies aiming to identify other molecules or proteins that interact with, stabilize or modify PAPS synthases are required in order to understand sulfation processes in their particular cell-type specific environment.

Another line of observations potentially leading to a better understanding of their differential roles derives form the distinct subcellular localization patterns of PAPS synthases. Besset reported that the human PAPSS1 isoform is located in the nucleus of mammalian cells and is functionally active in sulfation-depleted yeast cells; in contrast, human PAPSS2 is expressed in the cytosol of mammalian cells, but re-locates into the nucleus when co-expressed with PAPSS1 (Besset et al., 2000). I have confirmed these findings in steroidogenic and non-steroidogenic cells, with PAPSS1 being mostly localized in the nucleus; in contrast to these findings, I have also found that the PAPSS2 isoform is expressed more heterogeneously being also localized to a lesser extend in the cytoplasm. In addition, I have observed that some cells express PAPSS2 equally in the cytoplasm and the nucleus. These findings were confirmed in recent study employing a quantitative approach in mammalian non-steroidogenic cell lines and the authors report a predominant nuclear expression of PAPSS1 but a predominant cytoplasmic distribution for PAPSS2 (Schröder et al., 2012). Through mutagenesis-screen based on *in silico* analysis of the PAPSS proteins, distinct motifs crucial for cytoplasmic-nuclear shuttling have been identified; here, a distinct nuclear localization signal (NLS) at the N-terminus of the protein is present in both PAPSS isoforms and appears to be stronger for PAPSS1 than

PAPSS2; this motif consists of a highly conserved lysine pattern (KK-x-K) and replacement of these residues with non-polar alanine results in a striking re-location of PAPSS1 and PAPSS2 to the cytoplasm *in vitro* (Schröder et al., 2012). In addition, for nuclear export a highly conserved Arg-Arg motif within an α-loop of the APS kinase domain has been identified, which is crucial for cytosolic re-location (Schröder et al., 2012). Through collaboration with this group I have investigated the functional impact of these PAPSS localization variants in order to determine whether an exclusively nuclear or cytosolic localization of the PAPSS isoforms supports or inhibits SULT2A1 activity. I have observed a decrease of DHEA sulfation for all PAPSS variants, apart from the cytoplasmic PAPSS2 variant, which does not change SULT2A1 activity compared to WT PAPSS2. Interestingly, also the nuclear PAPSS1 variant reduces SULT2A1 activity, although the nucleus has been reported as the natural environment for the PAPSS1 isoform (Besset et al., 2000; Schröder et al., 2012). This suggests that at least some cytoplasmic PAPSS1 expression is required for PAPS generation of this isoform to support DHEA sulfation.

The fact that the DHEA conversion rate does not dramatically differ for each 'dislocalized' PAPSS variant (i.e. the nuclear PAPSS2 and the cytoplasmic PAPSS1) compared to the WT activity is a surprise, but could be explained by the high expression of PAPSS and SULT2A1, providing un-physiological high levels of PAPS. As PAPS is a small molecule, it can pass the nuclear membrane freely and its ample production, independent of its site of generation, would deliver abundant activated sulfate to support SULT2A1.

In summary, my data indicate that the expression of the molecular compounds of the DHEA sulfation cascade, SULT2A1, PAPSS1 and PAPSS2, are co-regulated suggesting compensatory mechanism. Strikingly, PAPSS2 only supports DHEA sulfation *in vitro*, confirming the previously reported *in vivo* findings (Noordam et al.,

2009). Subcellular localisation of PAPSS isoforms might explain their differential roles and I have observed different patterns of sub-cellular distribution, confirming data from a recent study (Schröder et al., 2012). The *in vitro* system I have employed for functional studies on PAPSS variants did not deliver any clear results, which enhance our understanding that subcellular localisation of PAPSS plays a role in the DHEA sulfation process. Future studies would need to focus on the identification of interaction partners of PAPS synthases and SULT2A1 in order to explain mechanistically the co-regulative expression of the proteins as well as the differential roles of PAPSS1 and PAPSS2.

8. CHAPTER 8: THE STEROID METABOLOME OF PATIENTS WITH STEROID SULFATASE (STS) DEFICIENCY REVEALS A PHYSIOLOGICAL ROLE OF STS IN ANDROGEN ACTIVATION BEFORE PUBERTY

8.1. INTRODUCTION

8.1.1. Steroid sulfatase (STS) and sex steroid metabolism

STS hydrolyses the sulfate moiety of sulfated 3β-hydroxysteroids and has high substrate affinity to DHEAS, the most abundant hormone in the human circulation. This generates DHEA, the principal sex steroid precursor (**Figure 47**; section 1.1.9). DHEA is synthesized from cholesterol in the adrenal ZR, which also expresses the enzyme DHEA sulfotransferase (SULT2A1) in high levels. SULT2A1 catalyses the sulfation of DHEA to generate the hydrophilic sulfate ester DHEAS, the main product of the ZR.

DHEAS has virtually no affinity to the androgen receptor; it is essentially inactive. Mainly due to its chemical properties being highly amphiphilic and bound to plasma albumin, it cannot freely pass the cell membrane and be converted to active androgens by intracellular steroidogenic enzymes (**Figure 9**). The DHEAS plasma concentration, however, is much higher than any other steroid, and its half-life in blood is much longer than the half-life of DHEA (20 hours for DHEAS vs. 6 hours for DHEA).

Indeed, DHEAS is the most abundant steroid hormone in the human circulation. As it does not exhibit any androgenic or oestrogenic properties itself, it has been thought to serve as a constant storage pool for the regeneration of DHEA, which can be downstream-converted to active androgen or oestrogens like dihydrotestosterone or oestradiol (**Figure 47**).

In this context, STS is the key enzyme responsible to regenerate DHEA from inactive DHEAS and thereby counteracting adrenal SULT2A1 activity (**Figure 47**). Hence, circulating androgen levels are therefore considered to be partly regulated by

the production of DHEA in the adrenal cortex as well as the metabolism of DHEA regulated by SULT2A1 and STS enzymatic activities.

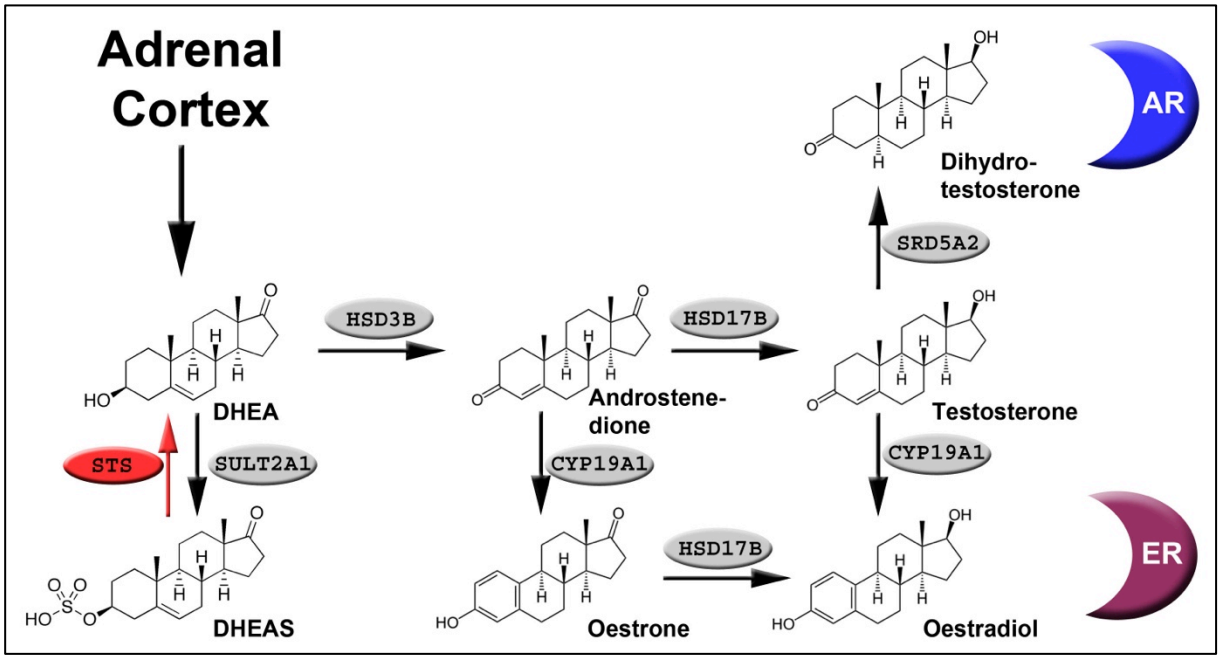

Figure 47: STS and adrenal sex steroid generation and metabolism. STS regenerates DHEA from inactive DHEAS in peripheral target tissues and counteracts the enzyme SULT2A1 expressed in the adrenal ZR. Subsequently, DHEA can be downstream converted to active sex steroids activating sex steroid receptors.

A defect of DHEA sulfation due to a mutations in the *PAPSS2* gene, a crucial co-factor of SULT2A1, has been previously reported to *increase* circulating androgen levels in humans (Noordam et al., 2009). On the contrary, it seems plausible that a defect of the opposite enzymatic reaction, DHEA de-sulfation catalysed by STS, results in reduced sex steroid levels. However, the role of STS *in vivo* has not been entirely elucidated yet.

STS has an important role during pregnancy and is highly expressed in the placenta. In fact, the placenta serves as an endocrine organ on its own and converts the vast amounts of DHEAS produced by the foetal adrenals into oestrogens by placental STS and P450 aromatase (CYP19A1). Hence, placental STS creates the 'oestrogenic environment' of pregnancy.

A previous study in healthy adult men shows that STS has no impact on androgen re-activation from DHEAS: After intravenous infusion of DHEAS, volunteers did not show any increase of DHEA; in contrast both DHEA and DHEAS, including downstream androgens, increased after an oral dose of DHEA (Hammer, 2005).

Only a few studies in adult men with STSD/XLI explored sex steroid metabolism, but without providing detailed clinical information on pubertal development or clinical features in these patients (Lykkesfeldt et al., 1985a; Milone et al., 1991; Delfino et al., 1998). However, severe androgen deficiency has not been reported yet in patients with STSD/XLI; and in fact, infertility is not part of the clinical spectrum of STSD/XLI (Fernandes et al., 2010).

Therefore, this study aimed to explore androgen metabolism in a genetically characterized cohort of patients with XLI/STSD employing steroid metabolomics in serum und urine.

8.1.2. STS deficiency (X-linked ichthyosis)

Mutations or deletions of the *STS* gene result in a skin condition called x-linked recessive ichthyosis (XLI), which is in 80-90% of cases due to complete deletions of the *STS* gene (Fernandes et al., 2010; Bonifas et al., 1987; Ballabio et al., 1989). It is one of the common inherited metabolic disorders with a frequency of 1:2000 – 1:6000 life births (Delfino et al., 1991; Shapiro et al., 1978).

Generally, ichthyosis refers to genetically and acquired disorders of the skin characterized by abnormal keratinisation; the skin of often resembles ‘fish scales’, explaining the origin of the term ichthyosis from greek ‘ichthys’ = ‘fish’. XLI has first been recognized as a distinct form of ichthyosis in the 1960s (Wells and Kerr, 1965; 1966). The pathophysiology of the deficient STS enzyme resulting in the typical dark-

coloured scaling in patients is not fully understood. However, as STS is expressed within the epidermis, it is thought to play a role in cutaneous regulation of lipid metabolism (Fernandes et al., 2010). An increased amount of cholesterol-sulfate has been found in the stratum corneum of patients with XLI/STSD (Williams and Elias, 1981). Hence, a pathological increase of hydrophilic cholesterol-sulfate in the epidermis might be responsible for disturbed desquamation and excess scaling. Clinically, XLI is characterized by large, dark-brown scales primarily located symmetrically on the trunk, neck and the extensor surfaces (**Figure 48**). The scalp is nearly always affected, however plantar and palmar surfaces are spared. Clinical symptoms start a few months after birth, and generally tend to improve during the summer months.

Figure 48: Typical dermatological finding in a patient with XLI: large, dark-brown, tightly-adherent scales on the extensor surfaces. Reprinted with kind permission from Fernandes et al. 2010.

Extra-cutaneous manifestations have been reported in patients with STSD, mainly ocular abnormalities and cryptorchidism. Corneal opacities are the most common ocular abnormalities, occurring in 20-50% of XLI patients (Jay et al., 1968;

Costagliola et al., 1991). These are usually asymptomatic and have a fine, flour-like appearance due to deposits in the posterior corneal stroma or Descemet membrane. Interestingly, these can also be found in about 25% of female carriers (Costagliola et al., 1991).

Cryptorchidism has been reported in up to 20% of patients with XLI (Bradshaw and Carr, 1986; Lykkesfeldt et al., 1985b; Traupe and Happle, 1983; Harkness, 1982; Traupe and Ropers, 1982). As the patients from these reported case series were not genetically characterized, it is unclear whether the testicular maldescend is a direct consequence of STS deficiency or secondary to deletions of genes adjacent to the *STS* locus. Indeed, syndromic presentations with XLI due to contiguous gene deletions are reported, including Conradi syndrome (limb shortening, epiphyseal stripplig, craniofacial defects, short stature) and Rud syndrome (cryptorchidism, retinitis pigmentosa, epilepsy and mental retardation) (Bick et al., 1989; Ballabio et al., 1991; Wulfsberg et al., 1992; Bouloux et al., 1993; Paige et al., 1994; Maya-Nunez et al., 1999; Stoll and Eyer, 1999; Langlois et al., 2009). Concomitant deletions of the neighbouring *KAL1* locus result in Kallmann syndrome characterized by hypogonadotropic hypogonadism and anosmia.

An association between STSD and testicular cancer independent of testicular descend has been hypothesised and reported in two patients with XLI (Lykkesfeldt et al., 1983); however, these reports are the only ones published so far.

Recent studies have shown an association of XLI with behavioural disorders, including autism, attention-deficit-hyperactivity disorder (ADHD) and social communication deficits; however, in the affected subjects large gene deletions have been found that included the *NLGN4* gene encoding neuroligin 4, a synaptic peptide that has been previously implicated in x-linked autism and mental retardation (Kent et al., 2008). However, the same group performed genotyping of the *STS* gene in 384

patients with ADHD and identified two single nucleotide polymorphisms of the *STS* gene that are significantly associated with ADHD (Brookes et al., 2008). The authors hypothesised that disturbed neuronal DHEA-DHEAS metabolism might result in altered neurotransmitter function contributing to the observed behavioural abnormalities. Of note, the key phenotype in *sts* deficient mice is a behavioural disorder that resembles human ADHD (Davies et al., 2009; Trent et al., 2012).

The very first clinical presentation of XLI may occur at birth, and women carrying a child affected by XLI frequently experience prolonged labour due to insufficient dilatation of the cervix (cervical dystocia) (Harkness, 1982; Lykkesfeldt and Bock, 1985; Bradshaw and Carr, 1986). This can be a severe and unexpected birth complication and perinatal death has been reported in STSD (Rizk and Johansen, 1993). Prenatal diagnosis of STSD is possible as maternal oestrogen excretion is decreased; GC/MS analysis of maternal urine also distinguishes foetal STSD from other conditions (like aromatase deficiency) as sex steroid precursor metabolites are found at normal levels (Glass et al., 1998; Shackleton, 2011).

8.2. MATERIALS AND METHODS

8.2.1. Patients

Patients were recruited from an existing cohort of STSD patients based in the Department of Paediatric Dermatology at the Birmingham Children's Hospital. In addition, the study was advertised through the website and newsletters of the Ichthyosis Support Group, UK. Healthy volunteers were invited to join the study following advertisement in the Birmingham Children's Hospital in- and outpatient departments, children of staff or children of families who heard of the study via study participants or staff. Inclusion criteria: boys and young men with confirmed diagnosis

of X-linked ichthyosis/ STS deficiency (cases only; either clinically or following biochemical or genetic testing), age-range for all participants was 6-30 years. Exclusion criteria: chronic severe disease potentially affecting DHEA secretion (i.e. rheumatoid arthritis, ulcerative colitis, cancer, etc); chronic glucocorticoid or sex steroid treatment over the past 12 months; impairment of liver or kidney function due to concomitant disease or medication.

8.2.2. Study Protocol

Prior to the study visit, a urine collection bottle (empty, no additives) was posted by mail together with detailed instructions for the a 24h-urine collection. Participants arrived at the Wellcome Trust Research Facility (Birmingham Children's Hospital and Queen Elisabeth Hospital for young men ≥ 17 yrs) between 8:00 and 12:00. At baseline, participants were assessed by taking a clinical history and physical examination, including a detailed assessment of pubertal development (Tanner stages and testicular volume) and a dermatological assessment. Height, weight, BMI was measured by the study nurse. Testicular volumes were measured with a Prader orchidometer. Blood samples were obtained at baseline for all participants, including serum for steroid hormone measurements as well as EDTA blood for DNA extraction and genetic analysis of the *STS* gene. The study protocol was approved by the Coventry and Warwickshire Research Ethics Committee. All patients or parents/ guardians (in patients younger than 16 years who are not deemed Gillick competent) gave written informed consent prior to enrolment.

8.2.3. Genetic analysis

DNA was extracted from peripheral blood leukocytes as described in section 2.2.11. 90% of the genetic abnormalities in patients with X-linked ichthyosis are deletions of the *STS* gene. To detect complete or partial *STS* deletions, multiplex-

ligation-dependent probe amplification (MLPA) was employed. This assay was designed by MRC Holland (Amsterdam, The Netherlands) and comprised 10 probes each specifically targeting the coding exons of the *STS* gene. In addition, the assay also targets the coding exons of the neighbouring *KAL1* locus as well as the *HDHD1* locus. The assay was performed by MRC Holland on a research basis as part of a collaboration (Dr Raymon Vijzelaar). In patients without any abnormalities in the MLPA analysis, PCR amplification of the entire coding region of the *STS* gene (9 fragments) including intron/exon boundaries from genomic DNA was performed (conditions: see section 2.2.11; primer: see **Table 21**). Direct sequencing was carried out using an ABI3730 sequencer (Applied Biosystems Inc., Foster City, CA, USA) and sequencing analysis was carried out using the CLC Main Workbench software (CLC bio, Cambridge, MA, USA).

Table 21: Primer for PCR amplification and sequencing of the STS gene.

Name	Sequence (5'-3')	GC (%)	T_m (°C)	Length (bp)	Fragment length (bp)
STS EXON1 FWD	TCCGCCTCACATTATCTG	50	55	18	347
STS EXON1 REV	TGCAACACAAGCAGGTAG	50	56	18	
STS EXON 2 FWD	TGGGCAACATAACAAGAC	44	53.3	18	422
STS EXON 2 REV	CTATGAATACAGCCATGTG	42	54	19	
STS EXON 3/4 FWD	TGGGTGACAGAGTGAGAT	50	55.7	18	482
STS EXON 3/4 REV	CCCATTCCCATACCTATAGA	45	55.6	20	
STS EXON 5 FWD	GTAATACCTTAGCGTTTGTG	40	53.3	20	665
STS EXON 5 REV	TCCACGAGAAATAACCCAG	47	55	19	
STS EXON 6 FWD	GACACAACAGAGACTTACC	47	54.6	19	375
STS EXON 6 REV	ACAAGGAGGCAAAGACTTA	42	55	19	
STS EXON 7 FWD	TCCACCTTGAGAAATTAGCC	45	56.3	20	334
STS EXON 7 REV	AAGTAGCAGAAGAACTATGG	40	54.3	20	
STS EXON 8 FWD	ACATTGAGCACGAAAGAG	44	55.8	18	393
STS EXON 8 REV	AATTGACCTGCCTCAAAC	44	55	18	
STS EXON 9 FWD	AGAAGGACATTTGAGAACAC	40	55	20	365
STS EXON 9 REV	TGTGACCAGAACGAAAAGAG	45	56	20	
STS EXON 10 FWD	CACATGGCAGCATAATTTC	42	54.1	19	585
STS EXON 10 REV	AATCAGTCCAAATCCAAGGT	40	57	20	

8.2.4. Serum steroid hormone measurements

Steroids were extracted from 200 µl of serum via liquid–liquid extraction using 2 ml tert-butyl-methyl-ether for DHEA and downstream androgens. Sulfated compounds (DHEAS and cholesterol sulfate) were extracted by a protein-crash method employing 20µl $ZnSO_4$ (0.1 mM) and 100 µl acetonitrile. See section 2.7.3 for further details.

8.2.5. Urinary steroid metabolites

Analysis of steroid hormone metabolites excretion was performed by a quantitative gas chromatography/mass spectrometry (GC/MS) selected ion-monitoring method, as described in section 2.6. For steroid abbreviations, please refer to **Table 9**.

Beside the global excretion (expressed in µg/24 hours), a distinct set of ratios was applied to further explore androgen metabolism. Global 5α-reductase activity was assessed by calculating substrate/product ratios employing 5α-reduced metabolites as numerators (5α-THF, 5α-THB, An), and their 5β-reduced counterpart as denominator (THF, THB, Et, respectively). The relation between active androgen metabolites and androgen precursor metabolites was expressed as a ratio of (An + Et)/ (DHEA+16OH-DHEA+5PT+5PD).

8.2.6. Statistical Analysis

For comparison, a non-parametric test (Mann-Whitney-Wilcoxon) was used to compare the two independent parameters from each cohort (control vs. affected). A p-value of 0.05 was assumed to be statistical significant. Data were expressed as median (± interquartile [boxes] and ± 10^{th}/90^{th} centile [whiskers] ranges). The software GraphPad Prism® was used for statistical analysis.

8.3. RESULTS

8.3.1. Patients characteristics

30 patients with STSD and 38 healthy volunteers (controls) were enrolled in this study. There were no significant differences between weight, height, BMI and age (**Table 22**). 13 STSD patients and 15 controls and were clinically pre-pubertal according to testicular volumes. One patient (age 6.7 years) had an undescended testicle on the left side. No patient had delayed puberty (i.e. pubertal onset after the age of 14 years) with physical development (Tanner stages) and testicular volumes being appropriate for chronological age.

Table 22: Subject characteristics. Values are mean ± SD. Values are compared by using the t-test and did not reach statistical significance for all categories.

	STSD (n=30)	Controls (n=38)
Height (cm)	155.85 ± 21.42	158.27 ± 22.13
Height SDS	0.374 ± 1.11	0.04 ± 1.16
Weight (kg)	48.96 ± 20.22	56.0 ± 20.67
Weight SDS	0.309 ± 1.30	0.58 ± 1.0
BMI (kg/m2)	19.31 ± 4.10	21.38 ± 3.48
BMI SDS	0.093 ± 1.42	0.66 ± 1.02
Age (years)	13.94 ± 5.85	16.5 ± 7.38

All patients had clinically typical dermatological findings of X-linked ichthyosis with different degrees of severity. In the majority of the STSD patients, the diagnosis has been established based on clinical findings (n=20); in 7 patients, a lymphocyte assay for STS activity has been performed, which showed decreased activity; 3 patients underwent genetic testing to confirm the diagnosis.

There were four pairs of siblings and another three brothers amongst the STSD patients. There was no consanguinity reported in any of the patient's families and there were no infertility problems reported in any of the patient's family histories.

11 patients had additional conditions, mostly atopic disease like mild asthma (n=6) and/or hayfever (n=4), eczema (n=1) or multiple allergies (n=1); one patient has been diagnosed with attention deficit hyperactivity disorder (ADHD). No patient was on regular steroid medication, including inhalers.

13 patients were pre-pubertal, according to testicular volumes (≤ 3ml) and physical changes (Tanner stages; see **Table 23**). Another 5 patients were peri-

pubertal with testicular volumes between 4 and 10 ml and low Tanner stages; the remaining 12 STSD patients were post-pubertal with testicular volumes > 10ml and physically fully developed secondary characteristics as assessed by Tanner stages (**Table 23**). According to the clinical assessment, baseline gonadotrophins (**Table 23**) and also medical history from the post-pubertal subjects, no STSD participant had delayed puberty according to standard guidelines (no signs of pubertal development until the age of 14 years). One six-year old boy from the STSD cohort had an undescended left-sided testicle, which prompted a referral to the paediatric endocrine service for further investigation.

For further analysis and comparison of two cohorts (STSD and controls), subjects were assembled into two subgroups according to their pubertal development: 1) the pre-/peri-pubertal subgroup (STSD n=18; controls n= 19) and 2) the post-pubertal subgroup (STSD n=12; control n=19).

Table 23: Characteristics of the STSD cohort emphasising pubertal assessment (Tanner stages, testicular volumes and baseline gonadotrophins). Tanner stages: P = pubic hair, G = genitals, A = axillary hair. LH=luteinizing hormone, FSH=follicle stimulating hormone; n.m. = not measured

				Tanner pubertal stages			Testicular volume		Gonadotrophins	
	Study Number	Age (yrs)	BMI (kg/m^2)	P	G	A	Left (ml)	Right (ml)	LH (U/L)	FSH (U/L)
Pre-pubertal	P12	6.15	13.74	1	1	1	2	2	<0.5	0.7
	P15	6.73	23.01	1	1	1	n.d.	2	<0.5	<0.5
	P11	6.86	16.17	1	1	1	2	2	<0.5	0.9
	P10	7.54	14.96	1	1	1	3	3	<0.5	<0.5
	P14	7.60	18.13	1	1	1	3	3	<0.5	0.6
	P06	9.09	15.19	1	1	1	2	2	n.m.	n.m.
	P22	9.18	14.59	1	2	1	3	3	<0.5	<0.5
	P16	9.22	24.08	1	1	1	3	3	<0.5	1
	P09	9.97	16.46	1	1	1	3	3	<0.5	0.7
	P23	10.83	16.11	1	1	1	3	3	<0.5	1.8
	P02	11.01	14.60	1	1	1	3	3	0.9	1.3
	P07	11.14	17.33	1	1	1	2	2	<0.5	1.4
	P17	11.22	23.16	1	1	1	3	3	0.8	2.3
Peri-pubertal	P08	11.67	17.47	1	2	1	4	3	1	4.9
	P01	12.75	18.58	2	2	1	4	4	n.m.	n.m.
	P05	13.28	16.62	1	2	1	3	4	1.8	2
	P19	13.43	14.79	1	2	1	5	4	1.1	1.6
	P21	13.43	16.89	1	2	1	5	5	1.3	1.7
Post-pubertal	P03	14.29	19.32	5	5	2	10	15	5.1	3.4
	P20	15.81	17.75	5	5	2	20	20	4.4	2.1
	P13	15.83	23.52	5	4	2	20	20	2.2	1.8
	P04	15.93	20.71	5	5	2	25	25	3.9	3
	P18	16.27	24.28	5	5	2	15	15	2.4	6.2
	P096	18.03	15.55	5	5	2	20	20	6.6	3.8
	P099	19.57	24.99	6	5	2	25	20	6.5	1.4
	P100	20.80	19.31	5	5	2	20	20	4.2	3.6
	P098	22.86	23.87	6	5	2	20	20	6.2	2.6
	P095	24.75	25.74	6	5	2	25	25	5.9	1.7
	P094	26.45	24.93	5	5	2	20	20	6.3	8.5
	P097	26.56	27.47	6	5	2	20	20	9	1.7

8.3.2. Genetic analysis

Genetic abnormalities of the *STS* gene have been confirmed in all patients. As 90% of the alterations of the *STS* gene are deletions (Ballabio et al., 1989), multiplex ligand-probe amplification (MLPA) was performed in the first place in all patient's DNA samples. Examples of graphical representations of the MLPA analysis are shown in **Figure 49**. 27 patients of this cohort had complete deletions of the *STS* and of the *HDHD1A* genes, but no deletions of further exons at the Xp22.31/32 locus; in particular, there were no deletions of the *KAL1* gene in all patients of this study (**Figure 49** panel B). One patient (patient 5) had a deletion of exon 7 only (**Figure 49** panel C; **Table 22**). In two brothers there were no alterations in the MLPA analysis and Sanger sequencing of the *STS* gene was performed and both patients had the same hemizygous non-synonymous missense mutation in exon 9 (**Table 22**): a cytosine to thymidine change at position g.114,414 results in the replacement of arginine to cysteine on the protein level (p.R454C); this mutation has been previously reported in a patient with XLI (González-Huerta et al., 2003).

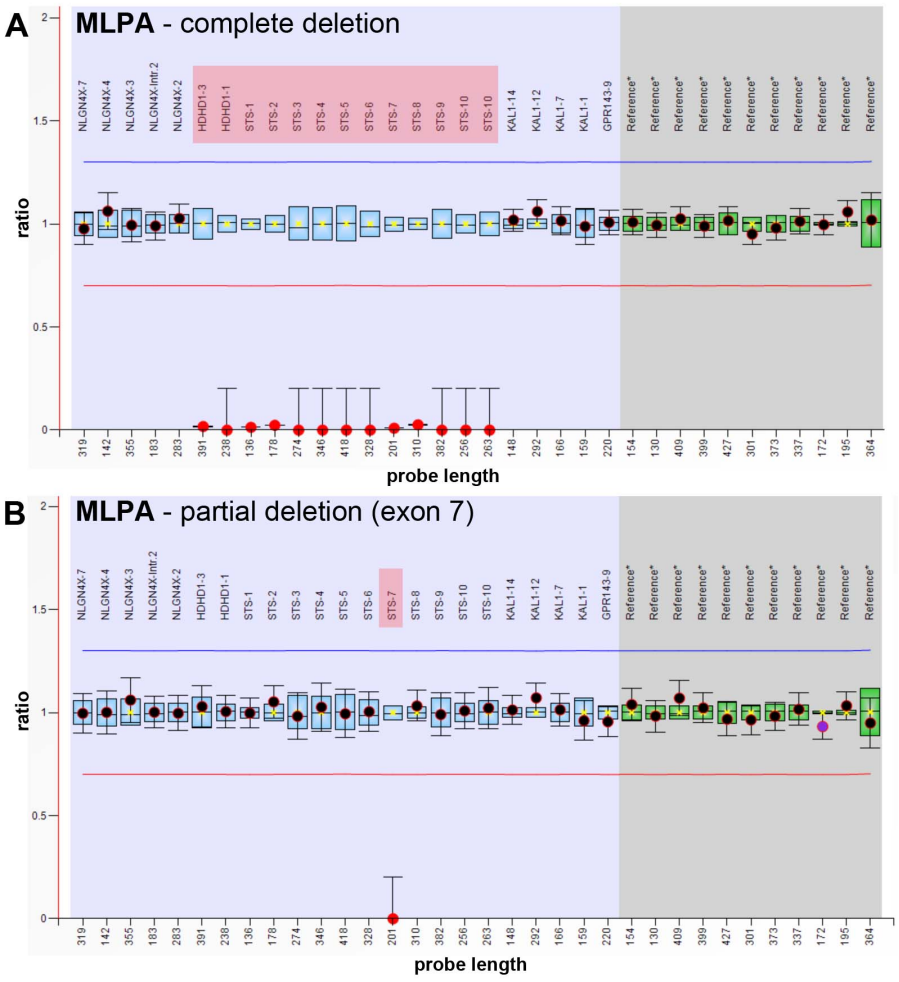

Figure 49: Representation of the results of the genetic analysis. **Panel A and B**: exemplary graphical representations of multiplex ligation-dependent probe amplification (MLPA). **Panel A** shows a complete deletion of the *STS* and the *HDHD1A* genes; **panel B** shows the one patient with a deletion of exon 7. Blue boxes represent the variation of the reference samples. Dots indicate the ratio of the analysed sample with whiskers representing the variation of the probe ratio of the sample compared to the reference runs. The red horizontal line indicates the threshold for deletions (below 0.75), whereas the green horizontal line marks the threshold for duplications (above 1.3). The red box indicates the position of deleted exons of the *STS* gene. Probe lengths in the grey-shaded area at the right side of the panels indicate reference probes that are used to create a normalization constant for data-normalization. Numbers on the x-axis indicate the lengths of the amplification probes. **Panel C**: Sanger sequencing analysis of exon 9 in two patients reveal a non-synonymous substitution at position g.114,414 (cytosine to thymidine) resulting in p.R454C. The NCBI reference sequence is shown at the top with the yellow bar indicating the coding sequence of exon 9; the blue bar indicates the beginning of the downstream intron.

8.3.3. Serum steroid analysis

The serum androgen precursor DHEA, its sulfate ester DHEAS and the active androgen testosterone were measured in all study subjects at baseline from a morning blood sample. In addition, cholesterol-sulfate levels were assessed as a biochemical marker for STSD and found to be highly elevated in the entire STSD cohort (**Table 24**).

DHEA levels were lower in the entire STSD cohort with high statistical significance for both pre-pubertal and peri-/post-pubertal subgroups (**Table 24**, **Figure 52B**). DHEAS levels were significantly higher in the pre-/peri-pubertal subgroup; however in the post-pubertal STSD subgroup DHEAS levels did not differ (**Table 24**, **Figure 52A**).

Table 24: Serum steroid hormone measurements including Cholesterol-sulfate in STSD patients compared to controls. Values are expressed as median (25^{th}, 75^{th} centile). For statistical analysis a Mann-Whitney-U test was applied for non-parametric data.

	subgroup	STSD	Controls	P-value
DHEA nmol/L	All	6.60 (3.1, 9.1)	19.97 (13.1, 31.7)	**< 0.0001**
	Pre-pubertal	5.04 (4.2, 2.4)	20.14 (14.2, 32.8)	**< 0.0001**
	Post-pubertal	10.73 (9.0, 6.8)	18.43 (11.1, 29.9)	**0.0033**
DHEAS µmol/L	All	5.14 (4.1, 7.5)	3.50 (1.37, 9.61)	0.3783
	Pre-pubertal	4.57 (2.0, 5.9)	1.37 (0.71, 3.02)	**0.002**
	Post-pubertal	7.13 (6.2, 9.6)	10.08 (6.58, 13.03)	0.3498
DHEA/DHEAS	All	0.87 (0.10, 1.43)	4.86 (2.29, 16.89)	**< 0.0001**
	Pre-pubertal	0.43 (0.14, 0.95)	15.81 (8.50, 36.89)	**< 0.0001**
	Post-pubertal	1.23 (0.03, 1.5)	2.56 (1.27, 4.48)	**0.0196**
Testosterone nmol/L	All	4.0 (0.35, 11.0)	10.07 (0.35, 17.62)	0.1455
	Pre-pubertal	0.35 (0.35, 0.69)	0.35 (0.35, 1.21)	0.9745
	Post-pubertal	11.81 (10.41, 15.62)	22.56 (15.28, 25.0)	**0.0251**
Cholesterol-sulfate µmol/L	All	51.20 (29.49, 68.22)	0.80 (0.75, 1.16)	**< 0.0001**
	Pre-pubertal	50.72 (39.04, 72.52)	0.77 (0.73, 1.0)	**< 0.0001**
	Post-pubertal	51.20 (25.92, 56.68)	1.12 (0.82, 1.27)	**< 0.0001**

To express the individual *in vivo* capacity for DHEA sulfation, a ratio of DHEA over DHEAS has been calculated, which reflects SULT2A1 activity. A higher DHEA/DHEAS ratio suggests increased STS activity with a shift towards DHEA and active androgens. This ratio was significantly lower in all STSD subjects compared to controls; subgroup analysis shows a higher significance level for the pre-/peri-pubertal subgroup ($p < 0.0001$ vs. p 0.0196). With the DHEA/DHEAS ratio being less than 1 in all STSD subjects throughout all age groups, I have found a marked increase of the DHEA/DHEAS ratio in the younger control subgroup (**Table 24** and **Figure 51**). This ratio decreases from a mean pre-pubertal value of 15.8 to 2.5 in normal/healthy post-pubertal boys (**Table 24**) and is a consequence of equally high DHEA and lower DHEAS levels before puberty (during adrenarche) (**Figure 51**). This suggests increased physiological STS activity prior to puberty.

Testosterone levels were lower in STSD in the post-pubertal subgroup (**Table 24**, **Figure 52**). As expected, testosterone levels were generally low and almost at the limit of detection in the pre-/peri-pubertal subgroups of STSDs and controls (**Figure 52**).

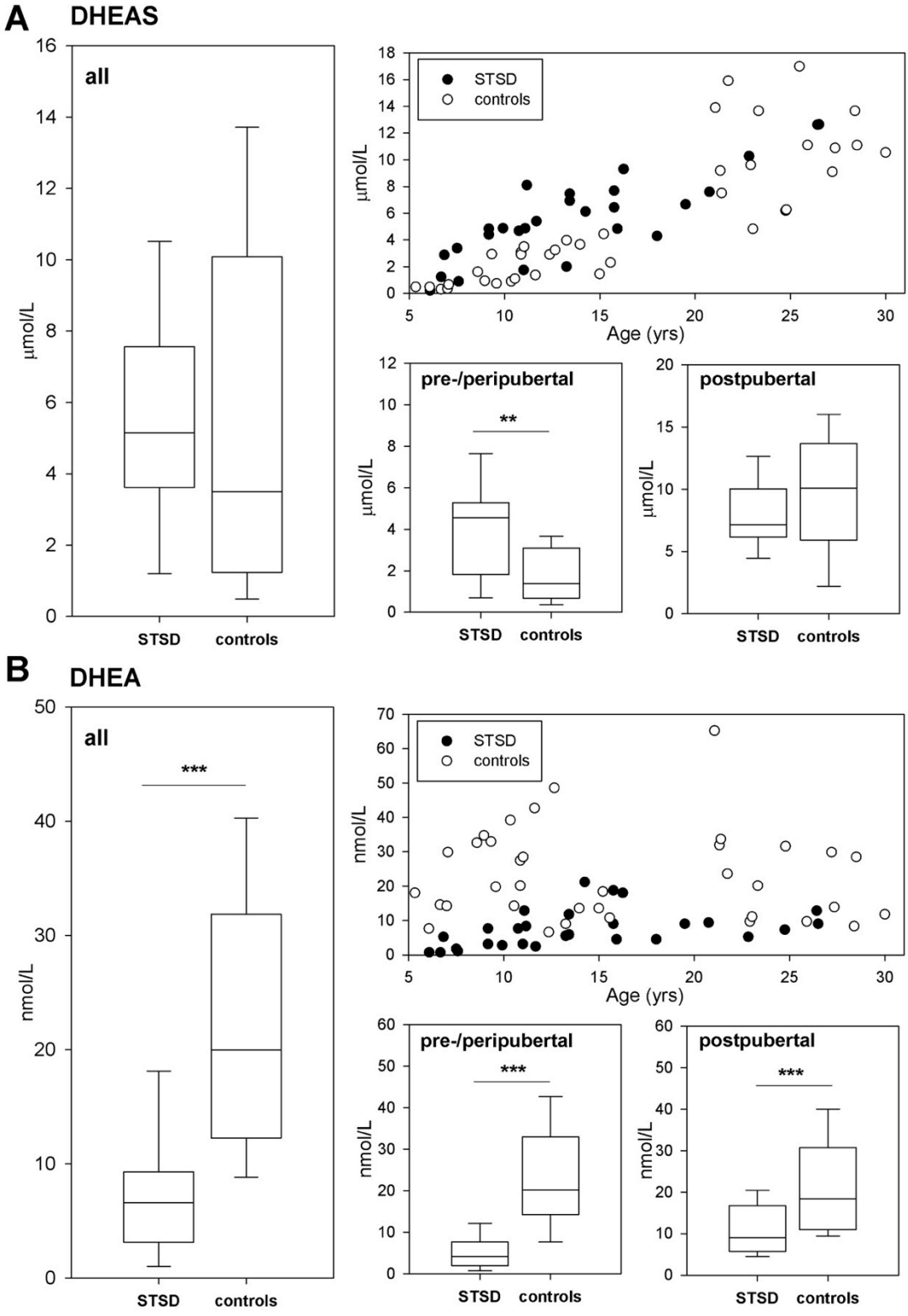

Figure 50: Serum DHEA (panel A) and DHEAS (panel B) levels in STSD patients compared to controls. The graph in the right upper corner of each panel shows each single value plotted against age (open circle: control, closed circle: STSD). The box plots indicate the median and the interquartile ranges, whiskers the 10th and 90th centile, respectively. Values (y-axis) are expressed in µmol/L for DHEAS and nmol/L for DHEA. For statistical analysis a Mann-Whitney-U test was applied for non-parametric data. ** p<0.001; *** p< 0.0001.

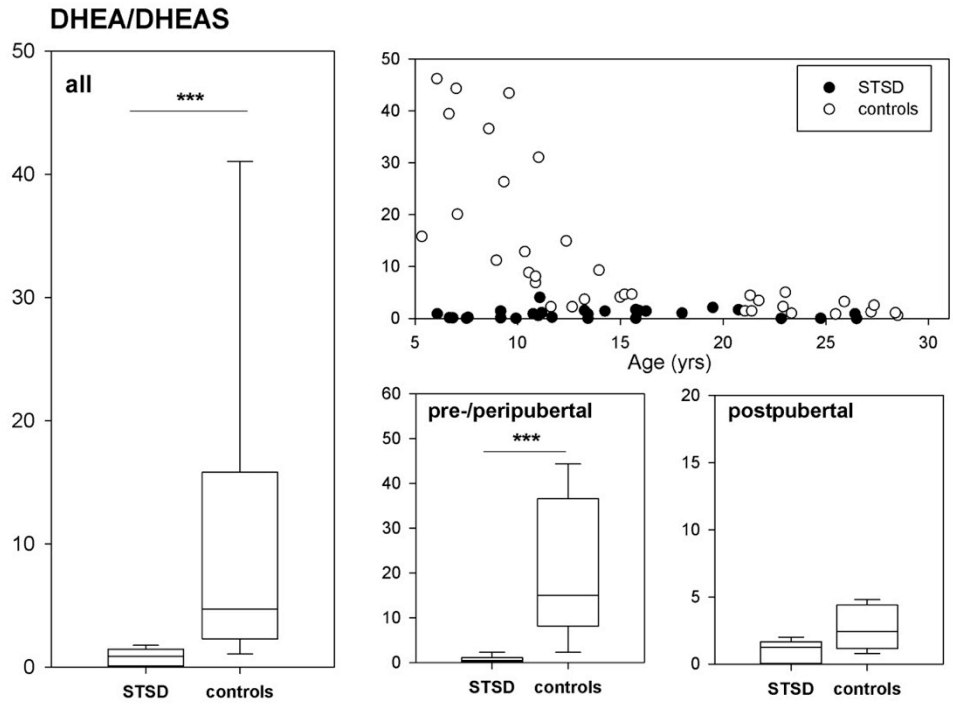

Figure 51: Graphic representations of the serum DHEA over DHEAS ratios in patients with STSD and controls. The box plots indicate the median and the interquartile ranges, whiskers the 10th and 90th centile, respectively. Values (y-axis) are expressed in µmol/L for DHEAS and nmol/L for DHEA. For statistical analysis a Mann-Whitney-U test was applied for non-parametric data. *** p< 0.001.

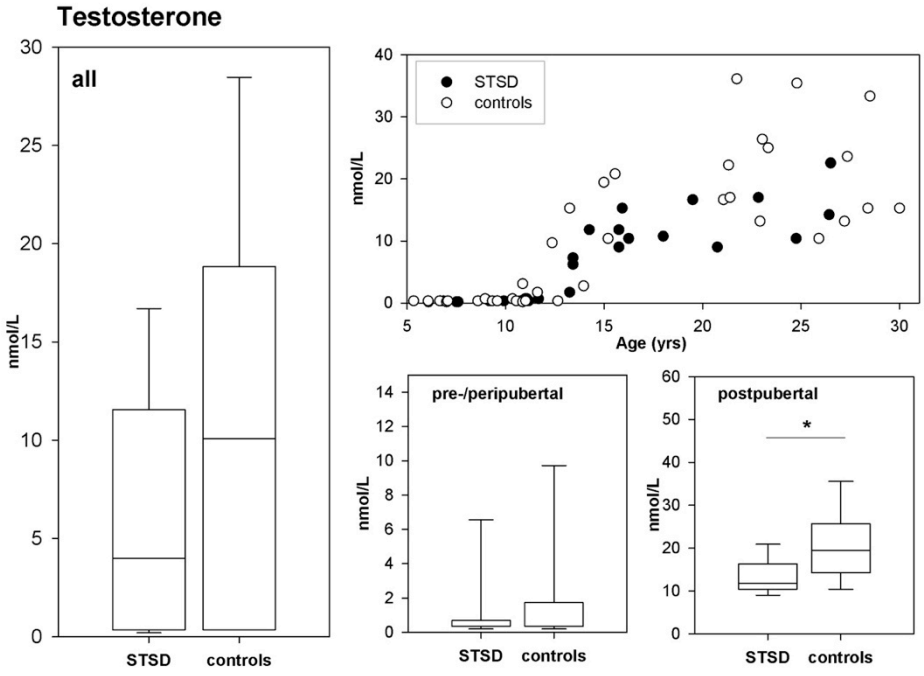

Figure 52: Serum testosterone levels in STSD patients compared to controls. The graph in the right upper corner shows each single value plotted against age (open circle: control, closed circle: STSD). The box plots indicate the median and the interquartile ranges, whiskers the 10th and 90th centile, respectively. Values (y-axis) are expressed in µmol/L for DHEAS and nmol/L for DHEA. For statistical analysis a Mann-Whitney-U test was applied for non-parametric data. * p<0.05.

8.3.4. Urinary androgen metabolite analysis

According to their origin, urinary androgen metabolites were grouped into metabolites derived from active androgens (An and Et) and metabolites from androgen precursors (DHEA, 16-OH DHEA, 5-PT and 5-PD); their excretion rates over 24 hours were compared between STSD subjects and controls (**Table 25**).

There was tendency of lower amounts of secreted active androgen metabolites (An and Et) in post-pubertal STSD subjects, however this did not reach statistical significance (**Table 25**). In contrast, androgen precursor metabolites were significantly higher in STSD subjects compared to controls (**Table 25**). The DHEA detected during the GC/MS analysis reflects excretion of both sulfated and unsulfated DHEA, with DHEAS contributing to the majority (< 95%) of the DHEA (our unpublished findings). Urinary DHEA (=DHEAS) is higher in all STSD subjects and reaches high statistical significance in both STSD subgroups (**Table 25**). Also, the 16α-hydroxylated DHEA compound is elevated in all STSD subjects.

Androgen precursor metabolites upstream of DHEA, like 5-pregnetriol (5-PT) and pregnenediol (5-PD), derived from pregnenolone and 17-pregnenolone, respectively, are also elevated in all STSD subjects, indicating increased androgen generation. The total excretion rates for 5-PD and 5-PT reach statistical significance in both STSD subgroups apart from 5-PT excretion in the post-pubertal subgroup (**Table 25**).

Table 25 (next page): 24-hours excretion rates of urinary androgen metabolites in STSD subjects and controls. Androsterone (An) and Etiocholanolone (Et) are derived from active androgen metabolites; DHEA, 5-pregnenetriol (5-PT), pregnenediol (5-PD) and 16-hydroxy DHEA (16OH DHEA) are derived from androgen precursor metabolites. Excretion rates are expressed as µg/24 hours as means (interquartile ranges). For statistical analysis a Mann-Whitney-U test was applied for non-parametric data.

	Metabolite	subgroup	STSD	Controls	P-value
Active Androgens (µg/24h)	An	All	409 (155, 2192)	403 (117, 2301)	0.8203
		Pre-pubertal	143 (60, 309)	124 (56.3, 206.4)	0.476
		Post-pubertal	2440 (1521, 3670)	2468 (2035, 3365)	0.8663
	Et	All	231 (96, 1018)	329 (98, 1569)	0.3093
		Pre-pubertal	109 (70, 130)	110 (40, 229)	0.7604
		Post-pubertal	1021 (917, 1332)	1663 (1045, 2048)	0.1605
	An + Et	All	604 (231, 3526)	2295 (235, 4067)	0.5887
		Pre-pubertal	237 (177, 415)	311 (96, 414)	0.8588
		Post-pubertal	4055 (2722, 4779)	4563 (3184, 5461)	0.5874
Androgen precursors (µg/24h)	DHEA	All	207 (117, 716)	43 (10, 165)	**0.0009**
		Pre-pubertal	105 (52, 236)	11 (3, 34)	**<0.0001**
		Post-pubertal	626 (291, 1905)	165 (62, 784)	**0.0453**
	5-PT	All	160 (82, 318)	51 (13, 163)	**0.0048**
		Pre-pubertal	77 (53, 169)	14 (4, 42)	**0.0001**
		Post-pubertal	338 (189, 792)	234 (78, 366)	0.0695
	5-PD	All	401 (295, 657)	143 (92, 317)	**0.0008**
		Pre-pubertal	289 (180, 380)	79 (54, 131)	**0.0008**
		Post-pubertal	687 (529, 1062)	317 (215, 364)	**0.0014**
	16OH-DHEA	All	520 (211, 767)	115 (39, 366)	**0.0003**
		Pre-pubertal	217 (137, 535)	39 (13, 76)	**0.0003**
		Post-pubertal	744 (656, 985)	398 (170, 580)	**0.0008**
	DHEA+16OH-DHEA+5-PT+5-PD	All	1355 (889, 2419)	453 (215, 1410)	**0.0225**
		Pre-pubertal	787 (389, 1297)	212 (156, 315)	**0.0007**
		Post-pubertal	2499 (1675, 5311)	1410 (834, 2898)	0.0923
Ratio	(An+Et)/ (DHEA+ 16OH-DHEA+ 5-PT+5-PD)	All	0.490 (0.289, 1.042)	1.985 (0.984, 3.325)	**<0.0001**
		Pre-pubertal	0.327 (0.203, 0.428)	1.119 (0.82, 1.925)	**0.0005**
		Post-pubertal	1.017 (0.685, 1.991)	3.325 (1.809, 4.174)	**0.0233**

In order to express a relation of urinary androgen precursor metabolites to active androgen metabolites, a ratio of (An + Et)/(DHEA + 16OHDHEA + 5-PT + 5-PD) was calculated to assess the relationship between androgen activation towards androgen generation. This ratio was decreased in all STSD subgroups and reached statistical significance (**Table 25**, **Figure 53**).

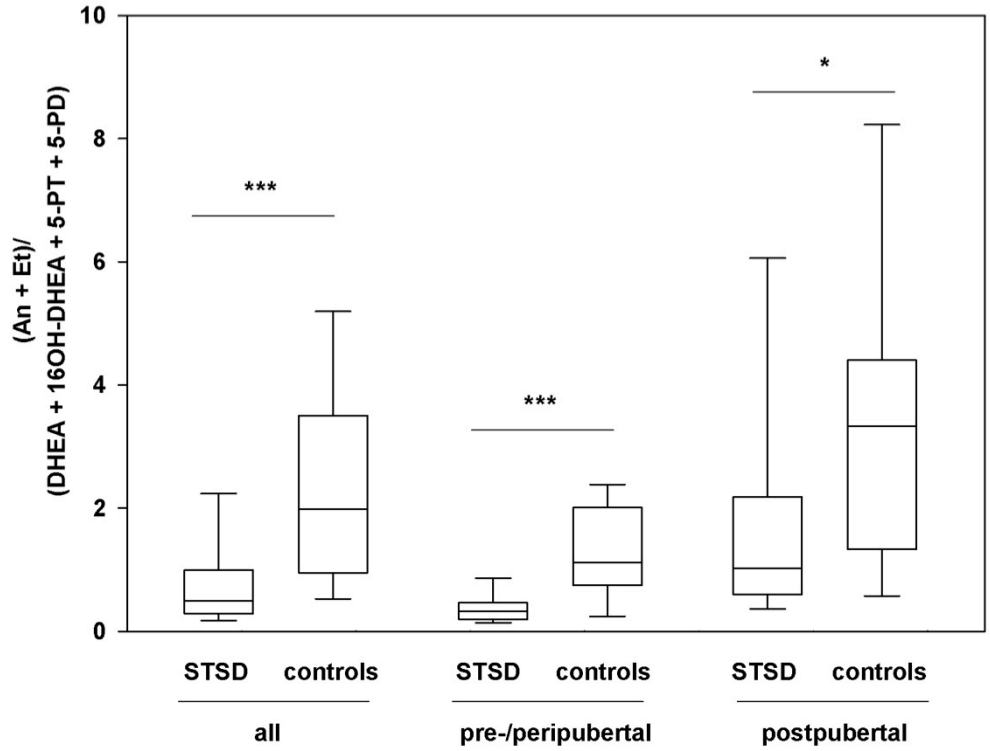

Figure 53: Androgen metabolism in patients with STSD compared to healthy controls as reflected by a ratio of active androgen metabolites (An and Et) over androgen precursor metabolites (DHEA, 16OH-DHEA, 5-PT and 5-PD). The box plots indicate the median and the interquartile ranges, whiskers the 10^{th} and 90^{th} centile, respectively. Values (y-axis) are expressed in µmol/L for DHEAS and nmol/L for DHEA. For statistical analysis a Mann-Whitney-U test was applied for non-parametric data. * $p<0.05$; *** $p< 0.0001$.

Global 5α-reductase activity was assessed by three different diagnostic ratios composed of 5α-reduced compounds (5αTHF, 5αTHB, An) over their respective 5β-reduced counterpart (THF, THB and Et). An increased ratio indicates increased global 5α-reductase activity. These ratios were elevated in all STSD subjects, however statistical significance was only achieved for the 5αTHF/THF ratio (all subgroups) and in the post-pubertal subgroup for 5αTHB/THB (**Table 26**, **Figure 54**).

Table 26: Global 5α-reductase activities as assessed by three different diagnostic ratios composed of 5α-reduced urinary metabolites over their respective 5β-reduced counterpart. Values are expressed as mean (interquartile range). For statistical analysis a Mann-Whitney-U test was applied for non-parametric data.

Ratio	subgroup	STSD	Controls	P-value
5αTHF/THF	All	2.5 (1.8, 3.2)	1.39 (0.95, 1.7)	< 0.0001
	Pre-pubertal	2.37 (1.55, 3.11)	1.23 (0.9, 1.32)	< 0.0001
	Post-pubertal	2.69 (1.94, 3.39)	1.57 (1.07, 2.26)	0.0029
5αTHB/THB	All	5.55 (4.63, 7.35)	4.44 (2.59, 5.2)	0.0067
	Pre-pubertal	5.07 (3.18, 6.5)	4.46 (2.54, 4.99)	0.1305
	Post-pubertal	6.26 (5.52, 7.58)	4.3 (3.07, 5.2)	0.0115
An/Et	All	2.05 (1.39, 2.96)	1.57 (0.96, 2.1)	0.0906
	Pre-pubertal	1.73 (0.88, 2.35)	1.27 (0.92, 1.27)	0.118
	Post-pubertal	2.53 (1.32, 3.15)	1.92 (1.46, 2.4)	0.2537

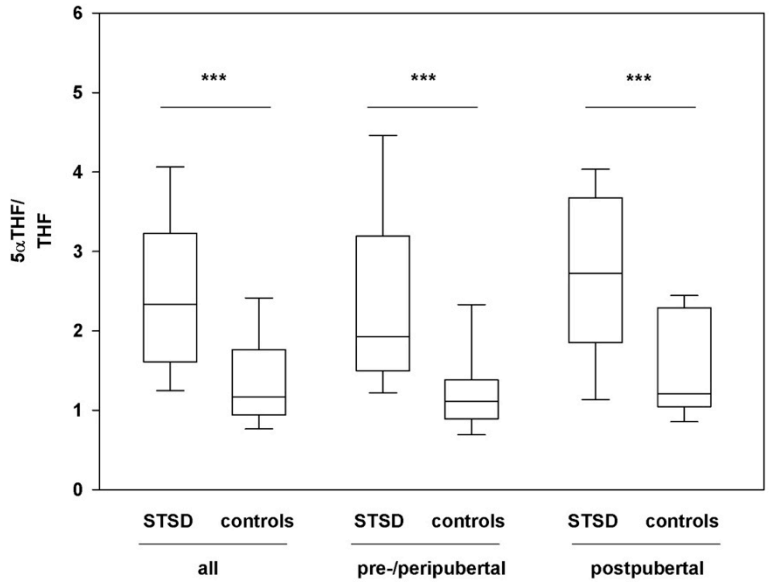

Figure 54: Global 5α-reductase activity as assessed by the ratio of 5α-reduced THF over THF in patients with STSD compared to controls. Box plots indicate the median with interquartile ranges, whiskers represent the 90th and 10th centiles, respectively. For statistical analysis a Mann-Whitney-U test was applied for non-parametric data. * p< 0.05; *** p< 0.0001.

8.4. DISCUSSION

Here, we have explored androgen metabolism and pubertal development in a large, genetically fully characterized paediatric cohort of patients with STSD/XLI. I found no gross abnormalities regarding the pubertal/physical development in children with STSD, but their steroid metabolome is indicative of mild androgen deficiency; in addition, mechanisms of compensation are an increase of androgen activation (global 5α-reductase activity) and possibly also an increase of (adrenal) androgen generation. In addition, we found evidence for an increase of STS activity in healthy boys prior to puberty.

We have genetically characterized the entire cohort and found genetic abnormalities of the *STS* gene in all patients. Complete deletions were detected in 27/30 of STSD patients. Complete deletions of the *STS* gene are the commonest genetic abnormality in XLI and reported in 80-90% of patients (Ballabio et al., 1987b; Bonifas et al., 1987). Importantly, deletions of the neighbouring *KAL1* gene resulting in Kallman syndrome were not present in this cohort, which – if present - would be an exclusion criteria due to its presentation with central hypogonadism. In a similar way, there were not any other forms of contiguous gene syndromes detected, which are frequently described in patients with XLI (Maya-Nunez et al., 1999; Langlois et al., 2009); see 8.1.2). The *HDHD1* gene upstream of the *STS* locus, however, was deleted in all patients of this cohort with complete deletions of the *STS* gene. In fact, the absence of *HDHD1* has been reported in the majority of patients with *STS* deletions (Hernandez-Martin et al., 1999; Preumont et al., 2010). *HDHD1* encodes for a pseudouridine-5'-phosphatase involved in RNA metabolism and its molecular function has only been described in detail recently (Preumont et al., 2010). It dephosphorylates pseudouridine 5'-phosphate, a modified RNA nucleotide present in

tRNAs, rRNAs and small nuclear RNAs; pseudouridine is excreted in urine and serves as a biomarker for certain cancers (Seidel et al., 2006). The importance of HDHD1 in normal physiology is not well understood; an *Hdhd1* knock-out mouse has not been reported yet. One can speculate that HDHD1 contributes to some extra-cutaneous manifestations observed in patients with XLI, however detailed genotype-phenotype studies are lacking and partially due to insufficient genetic characterization of XLI patients of earlier cohorts. Preumont and co-workers speculate that the absence of pseudouridine 5'-phosphatase activity may contribute to the development of testicular cancer and cryptorchidism as this has not been observed in patients with missense mutations or partial deletions of the *STS* gene (Preumont et al., 2010). The one patient with an undescended testis from this cohort also had a *HDHD1* deletion. Most certainly this hypothesis needs to be challenged by re-investigating larger XLI cohorts and providing evidence for functional involvement of HDHD1 in the testicular descent.

One patient in this cohort has a partial deletion of exon 7 of the *STS* gene. Although partial *STS* deletions have been reported in XLI (Nomura et al., 1995; Valdes-Flores et al., 2001), the deletion of exon 7 appears to be a novel finding. In addition, two brothers of this study carried the known p.R454C missense mutation, previously described in a patient with XLI; *in vitro* functional analysis employing radiolabelled ^{3}H-DHEA assays with patient's leukocytes showed reduced STS activity (González-Huerta et al., 2003).

Pubertal and physical development was not abnormal in this cohort of STSD patients: Tanner stages, testicular volumes and height SDS are not different to the control group or what is considered to be normal according to standard guidelines assessing childhood growth and puberty. The onset of pubertal changes observed in this cohort is between 11 and 11.5 years, which is considered to be the normal onset

of puberty in males (Raine et al., 2011; Marshall and Tanner, 1970). However, we have only assessed five boys who were clinically at the beginning of puberty according to their testicular volume and Tanner stages. Of those, three did not develop any pubic hair at the age of 13, which is slightly at the late side. Hence, to make accurate estimations on the beginning of pubertal development in STSD boys, this study is certainly underpowered.

One patient had an undescended testicle on the left side, which was not palpable within the inguinal canal including the groin. The testicle has been discovered intra-abdominal, just above the left inner inguinal ring and orchidopexy was successfully performed.

Serum steroid hormone measurements in this cohort of STSD patients indicate mild androgen deficiency with increased DHEAS levels, which as been reported as well in studies investigating androgen metabolism in adult STSD patients (Delfino et al., 1998; Milone et al., 1991; Bergner and Shapiro, 1988; Lykkesfeldt et al., 1985a; Muskiet et al., 1983; Ruokonen et al., 1980); however there are contradicting findings and DHEAS was not consistently elevated in all studies (**Table 27**).

Table 27: Overview of studies investigating androgen and androgen metabolite levels in serum of STSD patients.

Study	Subjects	Findings	Steroid quantification
Delfino et al., 1998	33 STSD, 33 controls, age 3-70 yrs	DHEAS increases during puberty but not significant. Cholesterol-sulfate always elevated.	GC/MS
Milone et al., 1991	15 STSD, 15 controls; age 22-33 years	DHEAS elevated when measured with GC/MS (not RIA)	GC/MS and RIA
Lykkesfeldt et al., 1985a	20 STSD (age 20-60 yrs), 100 controls (age 20-70 yrs)	Tendency of higher DHEAS in STSD (n.s.), no decline with age; d4dione, E2 were lower in STSD; higher LH in STSD	RIA
Muskiet et al., 1983	7 STSD, 20 controls (adult age range)	DHEAS was normal apart from one STSD patient	GC/MS
Ruokonen et al., 1980	5 STSD, 10 controls	All steroid sulfates not significantly higher in STSD	RIA

The most comprehensive study was done in an adult Danish cohort of 20 XLI patients and 40 age-matched male controls (Lykkesfeldt et al., 1985a). Although, there were no detailed information available on the physical development of the patients, the investigators found biochemical evidence of mild androgen deficiency with increased levels of DHEAS, illustrating for the first time an effect of STS on peripheral sex steroid activation. In addition, LH was higher in STSD, suggesting (compensatory) activation of the HPG axis. My study focused on a paediatric cohort of STSD patients with detailed clinical information and a full genetic characterization. My findings concur with those of (Lykkesfeldt et al., 1985a) and the consequences of STS deficiency on sex steroid metabolism are only marginal.

Serum DHEA levels were not measured in neither of these previous studies, possibly due to previous technical challenges with non-specifity/ cross-reactivity of the antibodies employed for the radio-immuno assays (Lykkesfeldt et al., 1985a). However, with both DHEA and DHEAS measurements the contribution of STS to androgen re-activation from DHEAS can be more accurately estimated. In this context, my data suggest novel insights regarding the activity/role of the STS enzyme during childhood. As it appears that the contribution of STS on DHEA metabolism is low in adult patients (Hammer, 2005) and a dissociation of DHEA and DHEAS is rarely observed (Arlt et al., 2006), this study suggests that the activity of the STS enzyme based on the ratio of DHEA/DHEAS is higher before puberty (during adrenarche) and decreases when puberty starts (**Figure 51**). As this observation comes from the healthy controls, the STSD cohort serves here as a ‘control’ to substantiate that the dissociation of DHEA and DHEAS is due to increased STS activity and not due to an inhibition of SULT2A1.

Little is known about the regulation of STS in normal physiology. Certain cytokines (Il-6, TNFa) and growth factors (FGFs, IGF1) have been reported to

increase STS activity *in vitro*, independently of promotor activation, rather via post-translational modification (Reed and Purohit, 1997). A few rodent and *in vitro* studies employing breast-cancer cell lines examined the effect of steroid hormones modulating STS activity, in particular androgens and progesterone (Moutaouakkil et al., 1984; Lam and Polani, 1985; Schneider et al., 1971). In this context, the raise of gonadal sex steroids during puberty would likely to have an inhibitory effect on STS activity.

We have found from urinary steroid metabolite analysis an increase of 5α-reductase activity based on substrate-product ratios. Increased global 5α-reductase activity would result in increased conversion of testosterone to DHT, i.e. enhanced (peripheral) androgen activation, and could therefore mechanistically compensate for the mild androgen deficiency observed in XLI/STSD. However, I have not found a statistically significant difference between the 5α- and 5β-reduced urinary androgen metabolites androsterone and etiocholoanolone; differences were only apparent between urinary the 5α- and 5β-reduced GC (and to a lesser extend MC) metabolites.

Increased 5α-reductase activity is frequently observed in androgen excess conditions like adult PCOS (Stewart et al., 1990; Vassiliadi et al., 2009; Rodin et al., 1994), but not in children with premature adrenarche (Silfen et al., 2002). Stewart et al. proposed the hypothesis that increased 5α-reduction in PCOS comes first in a pathophysiological chain of events leading to enhanced hepatic cortisol clearance with compensatory HPA axis activation and adrenal androgen secretion (Stewart et al., 1990). The underlying cause for the increase of 5α-reductase activity, either *a priori* or as a secondary event, is still unknown. Obesity affects 5α-reductase activity and can be an explanation for its dyregulation in PCOS, which is strongly associated with metabolic risk. However, in a recent study it is not only confined to the

overweight PCOS subgroup (Vassiliadi et al., 2009). All subgroups from this study are non-obese and BMI-matched, making an obesity-related 5α-reductase dysregulation unlikely. Androgens themselves may play a role in 5α-reductase expression, and the expression of SRD5A2 mRNA in dermal paplillae of hirsute women are positively correlated with circulating androgen levels (Skałba et al., 2006). A regulatory effect of androgens on the SRD5A promotor can be hypothesized in this context, however functional studies are not available.

In summary, we have found based on steroid metabolome analysis minimal impact of STS on androgen metabolism during childhood, suggesting that the sulfotransferase reaction inactivating DHEA to DHEAS is the predominating reaction within the context of DHEA pre-receptor metabolism with potentially more severe clinical implications (Noordam et al., 2009). However, DHEA and DHEAS dissociate before puberty, suggesting that STS is more active during early childhood/adrenarche and shuts down during adolescence and increased gonadal androgen production. Lastly, we have observed increased global 5α-reductase activity, most likely a compensatory mechanism for mild androgen deficiency. The results from this study do not suggest that patients with STSD require a routine endocrine follow-up as they seem to progress through puberty without significant abnormalities.

9. CHAPTER 9: FINAL CONCLUSIONS AND FUTURE DIRECTIONS

9.1. FINAL CONCLUSIONS

Disturbed androgen biosynthesis can result in a broad variety of phenotypes presenting with androgen deficiency or androgen excess. In this work we have investigated the impact of mutations of androgenic and androgen metabolizing enzymes, with particular emphasis on steroidogenic co-factors aiming towards a deeper understanding of the regulation of adrenal androgen biosynthesis.

9.1.1. Androgen deficiency – CYP17A1 and its co-factors POR and CYB5A

We have demonstrated that urinary steroid profiling underpinned by a detailed phenotypic work up of patients affected by androgen deficiency invariably leads to the correct underlying diagnosis. Hence, GC/MS analysis represents a powerful diagnostic tool for unraveling androgen deficiency conditions presenting as 46,XY DSD or absent/lack of pubertal development. Therefore we suggest that urinary steroid profiling should be a first-line investigation in patients with suspected disorders of androgen biosynthesis.

P450 oxidoreductase deficiency (PORD) is a well-described condition since its molecular basis has been discovered about a decade ago (Flück et al., 2004; Arlt et al., 2004). Since then, a large number of studies have further illuminated this frequent cause of CAH with a large variety of mutations being described in patients presenting with DSD, (partial) adrenal insufficiency and skeletal malformations occurring from birth. Here, we have investigated selected cases of children with PORD presenting later in childhood and characterized their phenotypes with regards to their pubertal

development. We have found that testicular function might be preserved in boys and their progression during puberty is only marginally affected by the condition. In contrast, girls tend to develop large ovarian cysts, which are difficult to treat and severe complications may occur, providing important information for clinicians on the management of children with PORD. In addition we have shown that late-onset (or 'non-classical') presentations can occur in PORD with none or mild phenotypes from birth. Importantly, these cases have a typical urinary steroid fingerprint demonstrating concomitant inhibition of 17a-hydroxylase/17,20 lyase and 21-hydroxylase activities, invariably leading to the correct diagnosis.

In addition, the value of urinary GC/MS analysis is in particular exemplified in those patients presenting with 'isolated 17,20 lyase deficiency', a condition previously reported in children harboring mutations in *CYP17A1*, *POR* and *CYB5A* genes (Geller et al., 1997; 1999; Van Den Akker et al., 2002; Sherbet et al., 2003; Hershkovitz et al., 2008; Kok et al., 2010). We could show based on analysis of the steroid metabolome of published case reports and the cases analyzed in this thesis that the urinary metabolome of the three different genetic disorders are distinct and unique for each condition. Of note, true isolated 17,20 lyase deficiency, i.e. without impairment of CYP17A1 17α-hydroxylase activity, can only be found in patients with mutant *CYB5A*. The *in vivo* and *in vitro* investigations from the family harboring the first CYB5A missense mutation (p.H44L) therefore conclusively strengthens previous *in vitro* findings (Auchus et al., 1998) that CYB5A exclusively supports the 17,20 lyase activity of CYP17A1, i.e. the principal androgen producing step in human steroidogenesis.

9.1.2. Androgen excess and DHEA/DHEAS inter-conversion

Previous work from our group has identified genetic abnormalities in the *PAPSS2* gene in a girl with androgen excess, a co-factor supporting DHEA sulfotransferase (SULT2A1) activity and thus revealing DHEA sulfation as a gatekeeper of downstream androgen activation (Noordam et al., 2009). In this work we have further explored DHEA/DHEAS inter-conversion both on the molecular level as well as in a clinical study investigating patients with steroid sulfatase (STS) deficiency.

For the *in vitro* work we further explored the interplay of the two PAPSS isoforms PAPSS1 and PAPSS2 in the context of DHEA sulfation. Firstly, we could show by *in vitro* knock-down and overexpression experiments, that indeed PAPSS2, but not PAPSS1, supports SULT2A1 activity. This confirms previous findings from the prismatic case report (Noordam et al., 2009) underpinning that only the PAPSS2 isoform supports DHEA sulfation. Secondly, based on *in vitro* expression studies, we have shown that PAPSS1, PAPSS2 and SULT2A1 are tightly co-regulated and the expression levels change upon siRNA mediated knock-down; in particular, SULT2A1 expression increases when *PAPSS2* mRNA is low, which suggests compensatory mechanisms. To further elucidate a mechanism for their differential role, we have attempted to investigate the effect of different subcellular localization of PAPSS proteins but found surprisingly that the PAPSS variants decrease SULT2A1 activity apart from the exclusively expressed PAPSS2 variant. Importantly, PAPSS isoforms are dynamically regulated proteins being expressed both in the nucleus and in the cytoplasm, confirming recently published data (Schröder et al., 2012).

To further investigate DHEA/DHEAS inter-conversion we have examined boys and young men with STS deficiency and could confirm the finding from a previous study (Hammer, 2005) suggesting that DHEA sulfation, i.e. DHEA inactivation, is the

predominant direction under physiological conditions. However, in addition our data suggest that STS is active in younger boys prior to puberty, amplifying androgen generation in peripheral target tissues, until gonadal androgen production starts and possibly inhibits STS activity. This finding provides important novel insights into the physiological regulation of STS, which is more active prior to puberty.

9.2. FUTURE DIRECTIONS

Androgen excess in childhood is a common disorder being clearly recognized as a risk factor for metabolic as well as fertility disturbances in later life and of unknown (idiopathic) origin in most of the cases (see 1.3.2). To further explore the regulation of DHEA sulfation on the molecular level has the potential to discover novel players in this network in order to potentially develop drugs that can ameliorate androgen excess conditions.

Previous studies have found low or undetectable DHEAS in 5-10% of children presenting with early-onset androgen excess (Ibáñez et al., 2000; Paterson et al., 2010), suggestive of a potentially significant role of dysregulation of this pathway in the pathogenesis of premature adrenarche.

Some clinical studies have investigated the impact of genetic variants of SULT2A1 and PAPSS2 on patients with androgen excess or circulating DHEAS levels (Louwers et al., 2013; Haring et al., 2013; Goodarzi et al., 2007; Utriainen et al., 2012). However, these studies are either focusing on only a few known or common SNPs or were conducted in small patient cohorts. Certainly, a broader approach employing dense genotyping in large cohorts of patients with premature adrenarche/PCOS is needed for future studies. However, given that only one patient with *PAPSS2* mutations has been identified with an ‘isolated’ androgen excess phenotype (Noordam et al., 2009) and only a few patients are reported, who

presented with SEMD, i.e. a severe bone phenotype (Haque et al., 1998; Miyake et al., 2012; Tüysüz et al., 2013), suggests that PAPSS2 deficiency is a rare cause of (isolated) androgen excess. Certainly, increasing awareness is needed amongst (paediatric) endocrinologists to detect those patients with androgen excess who have low DHEAS levels. We would therefore suggest to include DHEA measurements into the diagnostic work-up of patients, as the DHEA/DHEAS ratio would be a robust screening tool to identify impaired DHEA sulfation. Currently, the measurement of DHEA is challenging (insensitive and expensive) with conventional RIAs, but hopefully this will be overcome in the future with the entry of LC/MSMS technologies in clinical routine (Krone et al., 2010).

With co-factors POR, CYB5A and PAPSS2 being expressed in other tissues, including liver, disturbed electron flux or PAPS provision, respectively, in affected patients will also affect other metabolic pathways apart from androgen production; therefore co-factor deficiencies represent multi-system disorders including hepatic detoxification of endogenous substances (steroid hormones) and drug metabolism (see **Figure 55**). An *in vivo* study from our group in a patient with PORD revealed impaired activity of key drug metabolizing enzymes, including CYP3A4, which is responsible for detoxification of about 80% of drugs, including steroid hormones (Tomalik-Scharte et al., 2010). This finding illustrates the importance of widening the horizon above steroidogenesis when consulting patients with co-factor mutations and stresses the necessity for further research to clearly delineate the impact on other organ systems. To do this, global metabolome analysis employing mass-spectrometry approaches is a promising tool to discover novel metabolic pathways (Suhre, 2014; Prosser et al., 2014). Importantly, these findings are likely to be directly translated into patient's care.

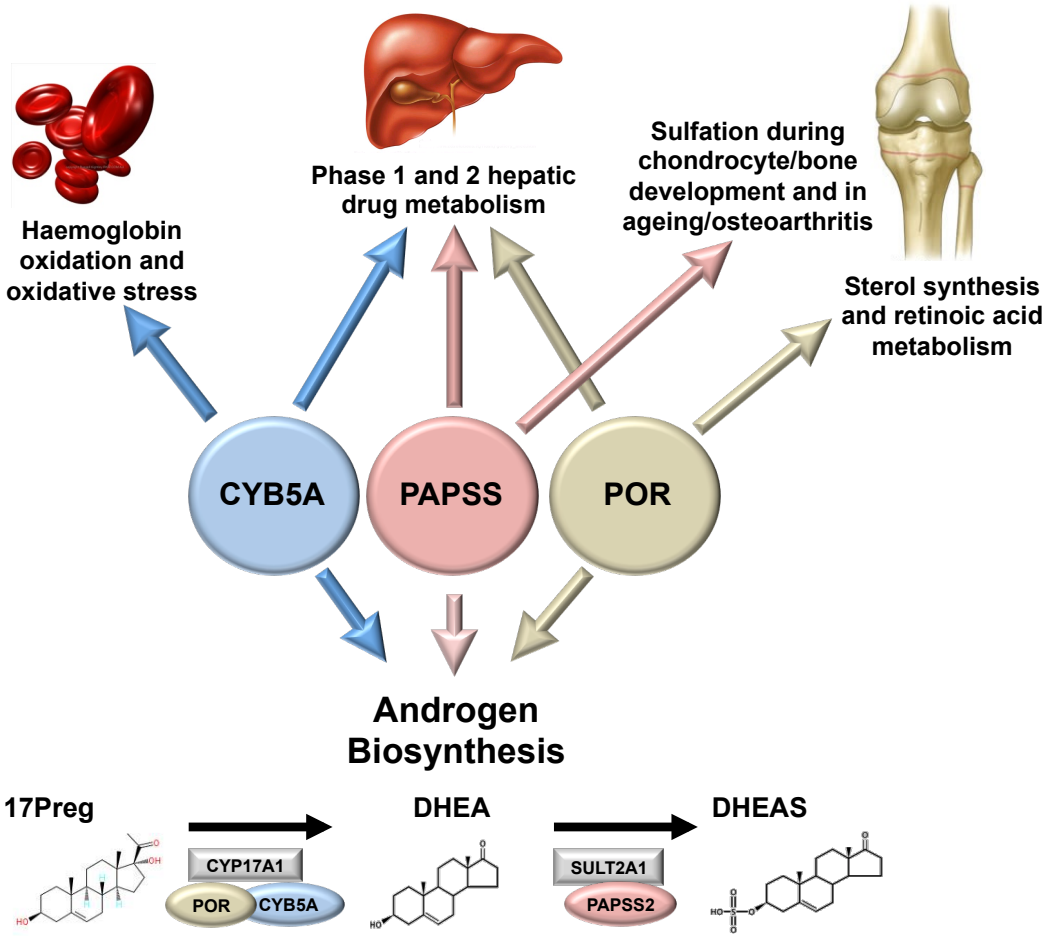

Figure 55: Schematic diagram illustrating the known implications of co-factors CYB5A, PAPSS and POR beyond androgen biosynthesis on haemoglobin, hepatic and chondrocyte metabolism.

10. REFERENCES

Adachi, M., Asakura, Y., Matsuo, M., et al. (2006) POR R457H is a global founder mutation causing Antley-Bixler syndrome with autosomal recessive trait. **American journal of medical genetics Part A**, 140 (6): 633–635

Adachi, M., Tachibana, K., Asakura, Y., et al. (2004) Compound heterozygous mutations of cytochrome P450 oxidoreductase gene (POR) in two patients with Antley-Bixler syndrome. **American journal of medical genetics Part A**, 128A (4): 333–339

Agarwal, A.K. and Auchus, R.J. (2005) Minireview: cellular redox state regulates hydroxysteroid dehydrogenase activity and intracellular hormone potency. **Endocrinology**, 146 (6): 2531–2538

Agarwal, A.K., Monder, C., Eckstein, B., et al. (1989) Cloning and expression of rat cDNA encoding corticosteroid 11 beta-dehydrogenase. **The Journal of biological chemistry**, 264 (32): 18939–18943

Agrawal, V., Huang, N. and Miller, W. (2008) Pharmacogenetics of P450 oxidoreductase: effect of sequence variants on activities of CYP1A2 and CYP2C19. **Pharmacogenetics and genomics**, 18 (7): 569–576

Aguilar, A., Wu, S. and De Luca, F. (2009) P450 oxidoreductase expressed in rat chondrocytes modulates chondrogenesis via cholesterol- and Indian Hedgehog-dependent mechanisms. **Endocrinology**, 150 (6): 2732–2739

Ahmed, S.F. and Rodie, M. (2010) Investigation and initial management of ambiguous genitalia. **Best practice & research Clinical endocrinology & metabolism**, 24 (2): 197–218

Albright, F. (1947) Osteoporosis. **Annals of internal medicine**, 27 (6): 861–882

Andersson, S. and Russell, D.W. (1990) Structural and biochemical properties of cloned and expressed human and rat steroid 5 alpha-reductases. **Proceedings of the National Academy of Sciences of the United States of America**, 87 (10): 3640–3644

Andersson, S., Berman, D.M., Jenkins, E.P., et al. (1991) Deletion of steroid 5 alpha-reductase 2 gene in male pseudohermaphroditism. **Nature**, 354 (6349): 159–161

Antley, R. and Bixler, D. (1975) Trapezoidocephaly, midfacial hypoplasia and cartilage abnormalities with multiple synostoses and skeletal fractures. **Birth Defects Orig Artic Ser**, 11 (2): 397–401

Arlt, W. (2006) Androgen therapy in women. **European journal of endocrinology / European Federation of Endocrine Societies**, 154 (1): 1–11

Arlt, W., Callies, F., van Vlijmen, J., et al. (1999) Dehydroepiandrosterone replacement in women with adrenal insufficiency. **The New England journal of medicine**, 341 (14): 1013–1020

Arlt, W., Hammer, F., Sanning, P., et al. (2006) Dissociation of serum dehydroepiandrosterone and dehydroepiandrosterone sulfate in septic shock. **The Journal of Clinical Endocrinology and Metabolism**, 91 (7): 2548–2554

Arlt, W., Martens, J., Song, M., et al. (2002) Molecular evolution of adrenarche: structural and functional analysis of p450c17 from four primate species. **Endocrinology**, 143 (12): 4665–4672

Arlt, W., Walker, E.A., Draper, N., et al. (2004) Congenital adrenal hyperplasia caused by mutant P450 oxidoreductase and human androgen synthesis: analytical study. **Lancet**, 363 (9427): 2128–2135

Armengaud, J.-B., Charkaluk, M.-L., Trivin, C., et al. (2009) Precocious pubarche: distinguishing late-

onset congenital adrenal hyperplasia from premature adrenarche. **The Journal of Clinical Endocrinology and Metabolism**, 94 (8): 2835–2840

Asuncion, M., Calvo, R.M., San-Millan, J.L., et al. (2000) A prospective study of the prevalence of the polycystic ovary syndrome in unselected Caucasian women from Spain. **Journal of Clinical Endocrinology & Metabolism**, 85 (7): 2434–2438

Auchus, R. (2001) The genetics, pathophysiology, and management of human deficiencies of P450c17. **Endocrinology and metabolism clinics of North America**, 30 (1): 101–19, vii

Auchus, R. (2004) The backdoor pathway to dihydrotestosterone. **Trends in endocrinology and metabolism: TEM**, 15 (9): 432–438

Auchus, R. and Miller, W. (1999) Molecular modeling of human P450c17 (17alpha-hydroxylase/17,20-lyase): insights into reaction mechanisms and effects of mutations. **Molecular endocrinology (Baltimore, Md)**, 13 (7): 1169–1182

Auchus, R. and Rainey, W. (2004) Adrenarche - physiology, biochemistry and human disease. **Clinical endocrinology**, 60 (3): 288–296

Auchus, R., Lee, T. and Miller, W. (1998) Cytochrome b5 augments the 17,20-lyase activity of human P450c17 without direct electron transfer. **The Journal of biological chemistry**, 273 (6): 3158–3165

Augarten, A., Pariente, C., Gazit, E., et al. (1992) Ambiguous genitalia due to partial activity of cytochromes P450c17 and P450c21. **J Steroid Biochem Mol Biol**, 41 (1): 37–41

Balducci, R., Boscherini, B., Mangiantini, A., et al. (1994) Isolated precocious pubarche: an approach. **The Journal of Clinical Endocrinology and Metabolism**, 79 (2): 582–589

Ballabio, A., Carrozzo, R., Parenti, G., et al. (1989) Molecular heterogeneity of steroid sulfatase deficiency: a multicenter study on 57 unrelated patients, at DNA and protein levels. **Genomics**, 4 (1): 36–40

Ballabio, A., Parenti, G., Carrozzo, R., et al. (1987a) Isolation and characterization of a steroid sulfatase cDNA clone: genomic deletions in patients with X-chromosome-linked ichthyosis. **Proceedings of the National Academy of Sciences of the United States of America**, 84 (13): 4519–4523

Ballabio, A., Sebastio, G., Carrozzo, R., et al. (1987b) Deletions of the steroid sulphatase gene in “classical” X-linked ichthyosis and in X-linked ichthyosis associated with Kallmann syndrome. **Human Genetics**, 77 (4): 338–341

Ballabio, A., Zollo, M., Carrozzo, R., et al. (1991) Deletion of the distal short arm of the X chromosome (Xp) in a patient with short stature, chondrodysplasia punctata, and X-linked ichthyosis due to steroid sulfatase deficiency. **American Journal of Medical Genetics**, 41 (2): 184–187

Bao, X., Ding, H., Xu, Y., et al. (2011) Prevalence of common mutations in the CYP17A1 gene in Chinese Han population. **Clinica chimica acta; international journal of clinical chemistry**, 412 (13-14): 1240–1243

Barrett, P.Q., Bollag, W.B., Isales, C.M., et al. (1989) Role of calcium in angiotensin II-mediated aldosterone secretion. **Endocrine reviews**, 10 (4): 496–518

Batch, J.A., Williams, D.M., Davies, H.R., et al. (1992) Androgen receptor gene mutations identified by SSCP in fourteen subjects with androgen insensitivity syndrome. **Human Molecular Genetics**, 1 (7): 497–503

Belgorosky, A., Pepe, C., Marino, R., et al. (2003) Hypothalamic-pituitary-ovarian axis during infancy, early and late prepuberty in an aromatase-deficient girl who is a compound heterocygote for two new point mutations of the CYP19 gene. **The Journal of Clinical Endocrinology and Metabolism**, 88

(11): 5127–5131

Bergner, E.A. and Shapiro, L.J. (1988) Metabolism of 3H-dehydroepiandrosterone sulphate by subjects with steroid sulphatase deficiency. **Journal of inherited metabolic disease**, 11 (4): 403–415

Berta, P., Hawkins, J.R., Sinclair, A.H., et al. (1990) Genetic evidence equating SRY and the testis-determining factor. **Nature**, 348 (6300): 448–450

Besset, S., Vincourt, J.B., Amalric, F., et al. (2000) Nuclear localization of PAPS synthetase 1: a sulfate activation pathway in the nucleus of eukaryotic cells. **The FASEB journal : official publication of the Federation of American Societies for Experimental Biology**, 14 (2): 345–354

Beuschlein, F., Looyenga, B.D., Bleasdale, S.E., et al. (2003) Activin induces x-zone apoptosis that inhibits luteinizing hormone-dependent adrenocortical tumor formation in inhibin-deficient mice. **Molecular and cellular biology**, 23 (11): 3951–3964

Bevan, C.L., Brown, B.B., Davies, H.R., et al. (1996) Functional analysis of six androgen receptor mutations identified in patients with partial androgen insensitivity syndrome. **Human Molecular Genetics**, 5 (2): 265–273

Bhattacharya, S., Falzone, C.J. and Lecomte, J.T. (1999) Backbone dynamics of apocytochrome b5 in its native, partially folded state. **Biochemistry**, 38 (8): 2577–2589

Bick, D., Curry, C.J., McGill, J.R., et al. (1989) Male infant with ichthyosis, Kallmann syndrome, chondrodysplasia punctata, and an Xp chromosome deletion. **American Journal of Medical Genetics**, 33 (1): 100–107

Binder, G., Weber, S., Ehrismann, M., et al. (2009) Effects of dehydroepiandrosterone therapy on pubic hair growth and psychological well-being in adolescent girls and young women with central adrenal insufficiency: a double-blind, randomized, placebo-controlled phase III trial. **The Journal of Clinical Endocrinology and Metabolism**, 94 (4): 1182–1190

Birnboim, H.C. and Doly, J. (1979) **A rapid alkaline extraction procedure for screening recombinant plasmid DNA.**, 7 (6): 1513–1523

Bischof, L.J., Kagawa, N., Moskow, J.J., et al. (1998) Members of the meis1 and pbx homeodomain protein families cooperatively bind a cAMP-responsive sequence (CRS1) from bovine CYP17. **The Journal of biological chemistry**, 273 (14): 7941–7948

Bonifas, J.M., Morley, B.J., Oakey, R.E., et al. (1987) Cloning of a cDNA for steroid sulfatase: frequent occurrence of gene deletions in patients with recessive X chromosome-linked ichthyosis. **Proceedings of the National Academy of Sciences of the United States of America**, 84 (24): 9248–9251

Bouloux, P.M., Kirk, J., Munroe, P., et al. (1993) Deletion analysis maps ocular albinism proximal to the steroid sulphatase locus. **Clinical genetics**, 43 (4): 169–173

Bradshaw, K.D. and Carr, B.R. (1986) Placental sulfatase deficiency: maternal and fetal expression of steroid sulfatase deficiency and X-linked ichthyosis. **Obstetrical & gynecological survey**, 41 (7): 401–413

Brookes, K.J., Hawi, Z., Kirley, A., et al. (2008) Association of the steroid sulfatase (STS) gene with attention deficit hyperactivity disorder. **American journal of medical genetics. Part B, Neuropsychiatric genetics : the official publication of the International Society of Psychiatric Genetics**, 147B (8): 1531–1535

Buckingham, J.C. (2006) Glucocorticoids: exemplars of multi-tasking. **British journal of pharmacology**, 147 Suppl 1 (S1): S258–68

Burger, H.G. (2002) Androgen production in women. **Fertility and sterility**, 77 Suppl 4: S3–5

Byskov, A.G., Andersen, C.Y., Nordholm, L., et al. (1995) Chemical structure of sterols that activate oocyte meiosis. **Nature**, 374 (6522): 559–562

Campbell, B.C. (2011) Adrenarche and middle childhood. **Human nature (Hawthorne, N.Y.)**, 22 (3): 327–349

Campo, S., Stivel, M., Nicolau, G., et al. (1979) Testicular function in post pubertal male pseudohermaphroditism. **Clinical endocrinology**, 11 (5): 481–490

Cannon, W.B. (1915) **Bodely Changes in Pain, Hunger Fear and Rage**

Caprio, M., Fève, B., Claës, A., et al. (2007) Pivotal role of the mineralocorticoid receptor in corticosteroid-induced adipogenesis. **The FASEB journal : official publication of the Federation of American Societies for Experimental Biology**, 21 (9): 2185–2194

Chomczynski, P. and Sacchi, N. (1987) Single-step method of RNA isolation by acid guanidinium thiocyanate-phenol-chloroform extraction. **Analytical biochemistry**, 162 (1): 156–159

Cohen-Kettenis, P.T. (2005) Gender change in 46,XY persons with 5alpha-reductase-2 deficiency and 17beta-hydroxysteroid dehydrogenase-3 deficiency. **Archives of sexual behavior**, 34 (4): 399–410

Conley, A.J., Bernstein, R.M. and Nguyen, A.D. (2012) Adrenarche in nonhuman primates: the evidence for it and the need to redefine it. **Journal of Endocrinology**, 214 (2): 121–131

Cosma, M.P., Pepe, S., Annunziata, I., et al. (2003) The multiple sulfatase deficiency gene encodes an essential and limiting factor for the activity of sulfatases. **Cell**, 113 (4): 445–456

Costagliola, C., Fabbrocini, G., Illiano, G.M., et al. (1991) Ocular findings in X-linked ichthyosis: a survey on 38 cases. **Ophthalmologica. Journal international d'ophtalmologie. International journal of ophthalmology. Zeitschrift für Augenheilkunde**, 202 (3): 152–155

Counts, D.R., Pescovitz, O.H., Barnes, K.M., et al. (1987) Dissociation of adrenarche and gonadarche in precocious puberty and in isolated hypogonadotropic hypogonadism. **The Journal of Clinical Endocrinology and Metabolism**, 64 (6): 1174–1178

Cutler, G.B., Glenn, M., Bush, M., et al. (1978) Adrenarche: a survey of rodents, domestic animals, and primates. **Endocrinology**, 103 (6): 2112–2118

Dacou-Voutetakis, C. and Dracopoulou, M. (1999) High incidence of molecular defects of the CYP21 gene in patients with premature adrenarche. **The Journal of Clinical Endocrinology and Metabolism**, 84 (5): 1570–1574

Davies, W., Humby, T., Kong, W., et al. (2009) Converging pharmacological and genetic evidence indicates a role for steroid sulfatase in attention. **Biological psychiatry**, 66 (4): 360–367

Dawson, P.A. (2011) Sulfate in fetal development. **Seminars in cell & developmental biology**, 22 (6): 653–659

de Peretti, E. and Forest, M.G. (1976) Unconjugated dehydroepiandrosterone plasma levels in normal subjects from birth to adolescence in human: the use of a sensitive radioimmunoassay. **The Journal of Clinical Endocrinology and Metabolism**, 43 (5): 982–991

de Peretti, E. and Forest, M.G. (1978) Pattern of plasma dehydroepiandrosterone sulfate levels in humans from birth to adulthood: evidence for testicular production. **Journal of Clinical Endocrinology & Metabolism**, 47 (3): 572–577

de Peretti, E., Pradon, M. and Forest, M.G. (1984) 17,20-desmolase deficiency in a female newborn, paradoxically virilized in utero. **Journal of steroid biochemistry**, 20 (1): 455–458

del Balzo, P., Borrelli, P., Cambiaso, P., et al. (1992) Adrenal steroidogenic defects in children with

precocious pubarche. **Hormone research**, 37 (4-5): 180–184

Delfino, M., De Ritis, G., Fabbrocini, G., et al. (1991) [Sweat-gland function in patients with X-linked ichthyosis]. **Recenti progressi in medicina**, 82 (12): 677–678

Delfino, M., Procaccini, E.M., Illiano, G.M., et al. (1998) X-linked ichthyosis: relation between cholesterol sulphate, dehydroepiandrosterone sulphate and patient's age. **The British journal of dermatology**, 138 (4): 655–657

Dharia, S., Slane, A., Jian, M., et al. (2004) Colocalization of P450c17 and cytochrome b5 in androgen-synthesizing tissues of the human. **Biology of reproduction**, 71 (1): 83–88

Dhir, V., Ivison, H.E., Krone, N., et al. (2007) Differential inhibition of CYP17A1 and CYP21A2 activities by the P450 oxidoreductase mutant A287P. **Molecular Endocrinology**, 21 (8): 1958–1968

Dhom, G. (1973) The prepuberal and puberal growth of the adrenal (adrenarche). **Beiträge zur Pathologie**, 150 (4): 357–377

Dierks, T., Lecca, M.R., Schmidt, B., et al. (1998) Conversion of cysteine to formylglycine in eukaryotic sulfatases occurs by a common mechanism in the endoplasmic reticulum. **FEBS letters**, 423 (1): 61–65

Dierks, T., Schmidt, B., Borissenko, L.V., et al. (2003) Multiple sulfatase deficiency is caused by mutations in the gene encoding the human C(alpha)-formylglycine generating enzyme. **Cell**, 113 (4): 435–444

Draper, N., Walker, E.A., Bujalska, I.J., et al. (2003) Mutations in the genes encoding 11beta-hydroxysteroid dehydrogenase type 1 and hexose-6-phosphate dehydrogenase interact to cause cortisone reductase deficiency. **Nature Genetics**, 34 (4): 434–439

Eggers, S. and Sinclair, A. (2012) Mammalian sex determination—insights from humans and mice. **Chromosome research : an international journal on the molecular, supramolecular and evolutionary aspects of chromosome biology**, 20 (1): 215–238

Ehrmann, D.A. (2005) Polycystic ovary syndrome. **The New England journal of medicine**, 352 (12): 1223–1236

El-Khairi, R. and Achermann, J.C. (2012) Steroidogenic factor-1 and human disease. **Seminars in reproductive medicine**, 30 (5): 374–381

Ellis, J., Gutierrez, A., Barsukov, I.L., et al. (2009) Domain motion in cytochrome P450 reductase: conformational equilibria revealed by NMR and small-angle x-ray scattering. **Journal of Biological Chemistry**, 284 (52): 36628–36637

Esteban, N.V. and Yergey, A.L. (1990) Cortisol production rates measured by liquid chromatography/mass spectrometry. **Steroids**, 55 (4): 152–158

Falany, C.N. (1997) Enzymology of human cytosolic sulfotransferases. **The FASEB journal : official publication of the Federation of American Societies for Experimental Biology**, 11 (4): 206–216

Falany, C.N., Vazquez, M.E. and Kalb, J.M. (1989) Purification and characterization of human liver dehydroepiandrosterone sulphotransferase. **The Biochemical journal**, 260 (3): 641–646

Falhammar, H., Thorén, M. and Hagenfeldt, K. (2008) A 31-year-old woman with infertility and polycystic ovaries diagnosed with non-classic congenital adrenal hyperplasia due to a novel CYP21 mutation. **Journal of endocrinological investigation**, 31 (2): 176–180

Falzone, C.J., Mayer, M.R., Whiteman, E.L., et al. (1996) Design challenges for hemoproteins: the solution structure of apocytochrome b5. **Biochemistry**, 35 (21): 6519–6526

Ferlin, A., Vinanzi, C., Garolla, A., et al. (2006) Male infertility and androgen receptor gene mutations: clinical features and identification of seven novel mutations. **Clinical endocrinology**, 65 (5): 606–610

Fernandes, N.F., Janniger, C.K. and Schwartz, R.A. (2010) X-linked ichthyosis: an oculocutaneous genodermatosis. **Journal of the American Academy of Dermatology**, 62 (3): 480–485

Fluck, C., Nicolo, C. and Pandey, A. (2007) Clinical, structural and functional implications of mutations and polymorphisms in human NADPH P450 oxidoreductase. **Fundam Clin Pharmacol**, 21 (4): 399–410

Fluck, C., Pandey, A., Huang, N., et al. (2008) P450 oxidoreductase deficiency - a new form of congenital adrenal hyperplasia. **Endocrine development**, 13: 67–81

Flück, C.E. and Pandey, A.V. (2011) Clinical and biochemical consequences of p450 oxidoreductase deficiency. **Endocrine development**, 20: 63–79

Flück, C.E., Tajima, T., Pandey, A.V., et al. (2004) Mutant P450 oxidoreductase causes disordered steroidogenesis with and without Antley-Bixler syndrome. **Nature Genetics**, 36 (3): 228–230

Forest, M.G., Lecornu, M. and de Peretti, E. (1980) Familial male pseudohermaphroditism due to 17-20-desmolase deficiency. I. In vivo endocrine studies. **Journal of Clinical Endocrinology & Metabolism**, 50 (5): 826–833

Fuda, H., Shimizu, C., Lee, Y.C., et al. (2002) Characterization and expression of human bifunctional 3“-phosphoadenosine 5-”phosphosulphate synthase isoforms. **The Biochemical journal**, 365 (Pt 2): 497–504

Fujieda, K., Tajima, T., Nakae, J., et al. (1997) Spontaneous puberty in 46,XX subjects with congenital lipoid adrenal hyperplasia. Ovarian steroidogenesis is spared to some extent despite inactivating mutations in the steroidogenic acute regulatory protein (StAR) gene. **The Journal of clinical investigation**, 99 (6): 1265–1271

Fukami, M., Hasegawa, T., Horikawa, R., et al. (2006) Cytochrome P450 oxidoreductase deficiency in three patients initially regarded as having 21-hydroxylase deficiency and/or aromatase deficiency: diagnostic value of urine steroid hormone analysis. **Pediatric research**, 59 (2): 276–280

Fukami, M., Horikawa, R., Nagai, T., et al. (2005) Cytochrome P450 oxidoreductase gene mutations and Antley-Bixler syndrome with abnormal genitalia and/or impaired steroidogenesis: molecular and clinical studies in 10 patients. **The Journal of Clinical Endocrinology and Metabolism**, 90 (1): 414–426

Fukami, M., Nishimura, G., Homma, K., et al. (2009) Cytochrome P450 Oxidoreductase Deficiency: Identification and Characterization of Biallelic Mutations and Genotype-Phenotype Correlations in 35 Japanese Patients. **The Journal of Clinical Endocrinology and Metabolism**, 94 (5): –1731

Ganguly, A. (1992) Atrial natriuretic peptide-induced inhibition of aldosterone secretion: a quest for mediator(s). **The American journal of physiology**, 263 (2 Pt 1): E181–94

Gazdar, A.F., Oie, H.K., Shackleton, C.H., et al. (1990) Establishment and characterization of a human adrenocortical carcinoma cell line that expresses multiple pathways of steroid biosynthesis. **Cancer research**, 50 (17): 5488–5496

Geller, D., Auchus, R. and Miller, W. (1999) P450c17 mutations R347H and R358Q selectively disrupt 17,20-lyase activity by disrupting interactions with P450 oxidoreductase and cytochrome b5. **Molecular endocrinology (Baltimore, Md)**, 13 (1): 167–175

Geller, D., Auchus, R., Mendonca, B., et al. (1997) The genetic and functional basis of isolated 17,20-lyase deficiency. **Nature Genetics**, 17 (2): 201–205

Ghali, S.A., Gottlieb, B., Lumbroso, R., et al. (2003) The use of androgen receptor amino/carboxyl-

terminal interaction assays to investigate androgen receptor gene mutations in subjects with varying degrees of androgen insensitivity. **The Journal of Clinical Endocrinology and Metabolism**, 88 (5): 2185–2193

Ghosh, D. (2007) Human sulfatases: a structural perspective to catalysis. **Cellular and molecular life sciences : CMLS**, 64 (15): 2013–2022

Giordano, S.J., Kaftory, A. and Steggles, A.W. (1994) A splicing mutation in the cytochrome b5 gene from a patient with congenital methemoglobinemia and pseudohermaphrodism. **Human Genetics**, 93 (5): 568–570

Glass, I.A., Lam, R.C., Chang, T., et al. (1998) Steroid sulphatase deficiency is the major cause of extremely low oestriol production at mid-pregnancy: a urinary steroid assay for the discrimination of steroid sulphatase deficiency from other causes. **Prenatal Diagnosis**, 18 (8): 789–800

Goebelsmann, U., Zachmann, M., Davajan, V., et al. (1976) Male pseudohermaphroditism consistent with 17,20-desmolase deficiency. **Gynecologic investigation**, 7 (3): 138–156

Goldsmith, O., Solomon, D.H. and Horton, R. (1967) Hypogonadism and mineralocorticoid excess. The 17-hydroxylase deficiency syndrome. **The New England journal of medicine**, 277 (13): 673–677

González-Huerta, L.M., Riviera-Vega, M.R., Kofman-Alfeuro, S.H., et al. (2003) Novel missense mutation (Arg432Cys) in a patient with steroid sulphatase-deficiency. **Clinical endocrinology**, 59 (2): 263–264

Goodarzi, M.O., Antoine, H.J. and Azziz, R. (2007) Genes for enzymes regulating dehydroepiandrosterone sulfonation are associated with levels of dehydroepiandrosterone sulfate in polycystic ovary syndrome. **The Journal of Clinical Endocrinology and Metabolism**, 92 (7): 2659–2664

Goosen, P., Storbeck, K.-H., Swart, A.C., et al. (2011) Cytochrome b5 augments 3β-hydroxysteroid dehydrogenase/Δ5-Δ4 isomerase activity. **The Journal of steroid biochemistry and molecular biology**, 127 (3-5): 238–247

Goosen, P., Swart, A.C., Storbeck, K.-H., et al. (2013) Allosteric interaction between 3β-hydroxysteroid dehydrogenase/Δ^{5}-Δ^{4} isomerase and cytochrome b5 influences cofactor binding. **The FASEB journal : official publication of the Federation of American Societies for Experimental Biology**, 27 (1): 322–332

Goto, M., Piper Hanley, K., Marcos, J., et al. (2006) In humans, early cortisol biosynthesis provides a mechanism to safeguard female sexual development. **The Journal of clinical investigation**, 116 (4): 953–960

Graham, F.L., Smiley, J., Russell, W.C., et al. (1977) Characteristics of a human cell line transformed by DNA from human adenovirus type 5. **The Journal of general virology**, 36 (1): 59–74

Grondahl, C., Lessl, M., Faerge, I., et al. (2000) Meiosis-activating sterol-mediated resumption of meiosis in mouse oocytes in vitro is influenced by protein synthesis inhibition and cholera toxin. **Biology of reproduction**, 62 (3): 775–780

Grondahl, C., Ottesen, J.L., Lessl, M., et al. (1998) Meiosis-activating sterol promotes resumption of meiosis in mouse oocytes cultured in vitro in contrast to related oxysterols. **Biology of reproduction**, 58 (5): 1297–1302

Grum, D., van den Boom, J., Neumann, D., et al. (2010) A heterodimer of human 3“-phospho-adenosine-5-”phosphosulphate (PAPS) synthases is a new sulphate activating complex. **Biochemical and biophysical research communications**, 395 (3): 420–425

Guillou, H., D'Andrea, S., Rioux, V., et al. (2004) Distinct roles of endoplasmic reticulum cytochrome b5 and fused cytochrome b5-like domain for rat Delta6-desaturase activity. **Journal of lipid research**,

45 (1): 32–40

Gupta, M., Geller, D. and Auchus, R. (2001) Pitfalls in characterizing P450c17 mutations associated with isolated 17,20-lyase deficiency. **The Journal of Clinical Endocrinology and Metabolism**, 86 (9): 4416–4423

Gupta, M., Guryev, O. and Auchus, R. (2003) 5alpha-reduced C21 steroids are substrates for human cytochrome P450c17. **Archives of biochemistry and biophysics**, 418 (2): 151–160

Gwynne, J.T. and Strauss, J.F. (1982) The role of lipoproteins in steroidogenesis and cholesterol metabolism in steroidogenic glands. **Endocrine reviews**, 3 (3): 299–329

Hadfield, C., Cashmore, A.M. and Meacock, P.A. (1987) Sequence and expression characteristics of a shuttle chloramphenicol-resistance marker for Saccharomyces cerevisiae and Escherichia coli. **Gene**, 52 (1): 59–70

Hague, W.M., Adams, J., Rodda, C., et al. (1990) The prevalence of polycystic ovaries in patients with congenital adrenal hyperplasia and their close relatives. **Clinical endocrinology**, 33 (4): 501–510

Hammer, F. (2005) No Evidence for Hepatic Conversion of Dehydroepiandrosterone (DHEA) Sulfate to DHEA: In Vivo and in Vitro Studies. **Journal of Clinical Endocrinology & Metabolism**, 90 (6): 3600–3605

Hammes, S.R. and Levin, E.R. (2007) Extranuclear steroid receptors: nature and actions. **Endocrine reviews**, 28 (7): 726–741

Haque, M.F.U., King, L.M., Krakow, D., et al. (1998) Mutations in orthologous genes in human spondyloepimetaphyseal dysplasia

and the brachymorphic mouse. **Nature Genetics**, 20 (2): 157–162

Haring, R., Wallaschofski, H., Teumer, A., et al. (2013) A SULT2A1 genetic variant identified by GWAS as associated with low serum DHEAS does not impact on the actual DHEA/DHEAS ratio. **Journal of molecular endocrinology**, 50 (1): 73–77

Harkness, R.A. (1982) Current clinical problems in placental steroid or aryl sulphatase C deficiency and the related “cervical dystocia” and X-linked ichthyosis. **Journal of inherited metabolic disease**, 5 (3): 142–144

Hazeldine, J., Arlt, W. and Lord, J.M. (2010) Dehydroepiandrosterone as a regulator of immune cell function. **The Journal of steroid biochemistry and molecular biology**, 120 (2-3): 127–136

Hegesh, E., Hegesh, J. and Kaftory, A. (1986) Congenital methemoglobinemia with a deficiency of cytochrome b5. **The New England journal of medicine**, 314 (12): 757–761

Herman-Giddens, M.E., Slora, E.J., Wasserman, R.C., et al. (1997) Secondary sexual characteristics and menses in young girls seen in office practice: a study from the Pediatric Research in Office Settings network. **PEDIATRICS**, 99 (4): 505–512

Hernandez-Martin, A., Gonzalez-Sarmiento, R. and De Unamuno, P. (1999) X-linked ichthyosis: an update. **The British journal of dermatology**, 141 (4): 617–627

Hershkovitz, E., Parvari, R., Wudy, S.A., et al. (2008) Homozygous mutation G539R in the gene for P450 oxidoreductase in a family previously diagnosed as having 17,20-lyase deficiency. **The Journal of Clinical Endocrinology and Metabolism**, 93 (9): 3584–3588

Hiort, O., Holterhus, P.M., Horter, T., et al. (2000) Significance of mutations in the androgen receptor gene in males with idiopathic infertility. **Journal of Clinical Endocrinology & Metabolism**, 85 (8): 2810–2815

Hiort, O., Sinnecker, G.H., Holterhus, P.M., et al. (1996) The clinical and molecular spectrum of androgen insensitivity syndromes. **American Journal of Medical Genetics**, 63 (1): 218–222

Hochberg, Z. (2010) Evo-Devo of child growth III: premature juvenility as an evolutionary trade-off. **Hormone research in pædiatrics**, 73 (6): 430–437

Homma, K., Hasegawa, T., Nagai, T., et al. (2006) Urine steroid hormone profile analysis in cytochrome P450 oxidoreductase deficiency: implication for the backdoor pathway to dihydrotestosterone. **The Journal of Clinical Endocrinology and Metabolism**, 91 (7): 2643–2649

Honda, M. (1976) Effects of ACTH on plasma levels of adrenal steroids in essential hypertension. **Endocrinologia japonica**, 23 (3): 195–202

Horton, J.D., Goldstein, J.L. and Brown, M.S. (2002) SREBPs: activators of the complete program of cholesterol and fatty acid synthesis in the liver. **The Journal of clinical investigation**, 109 (9): 1125–1131

Huang, N., Agrawal, V., Giacomini, K., et al. (2008) Genetics of P450 oxidoreductase: sequence variation in 842 individuals of four ethnicities and activities of 15 missense mutations. **Proc Natl Acad Sci U S A**, 105 (5): 1733–1738

Huang, N., Pandey, A., Agrawal, V., et al. (2005) Diversity and function of mutations in p450 oxidoreductase in patients with Antley-Bixler syndrome and disordered steroidogenesis. **American journal of human genetics**, 76 (5): 729–749

Hughes, I.A. and Deeb, A. (2006) Androgen resistance. **Best practice & research Clinical endocrinology & metabolism**, 20 (4): 577–598

Hughes, I.A. and Evans, B.A. (1987) Androgen insensitivity in forty-nine patients: classification based on clinical and androgen receptor phenotypes. **Hormone research**, 28 (1): 25–29

Ibanez, L., Potau, N., Virdis, R., et al. (1993) Postpubertal outcome in girls diagnosed of premature pubarche during childhood: increased frequency of functional ovarian hyperandrogenism. **Journal of Clinical Endocrinology & Metabolism**, 76 (6): 1599–1603

Ibanez, L., Potau, N., Zampolli, M., et al. (1996) Hyperinsulinemia in postpubertal girls with a history of premature pubarche and functional ovarian hyperandrogenism. **Journal of Clinical Endocrinology & Metabolism**, 81 (3): 1237–1243

Ibanez, L., Virdis, R., Potau, N., et al. (1992) Natural history of premature pubarche: an auxological study. **Journal of Clinical Endocrinology & Metabolism**, 74 (2): 254–257

Ibáñez, L., Aulesa, C., Potau, N., et al. (2002) Plasminogen activator inhibitor-1 in girls with precocious pubarche: a premenarcheal marker for polycystic ovary syndrome? **Pediatric research**, 51 (2): 244–248

Ibáñez, L., de Zegher, F. and Potau, N. (1999) Anovulation after precocious pubarche: early markers and time course in adolescence. **The Journal of Clinical Endocrinology and Metabolism**, 84 (8): 2691–2695

Ibáñez, L., Dimartino-Nardi, J., Potau, N., et al. (2000) Premature adrenarche--normal variant or forerunner of adult disease? **Endocrine reviews**, 21 (6): 671–696

Ibáñez, L., Díaz, R., López-Bermejo, A., et al. (2009) Clinical spectrum of premature pubarche: links to metabolic syndrome and ovarian hyperandrogenism. **Rev Endocr Metab Disord**, 10 (1): 63–76

Ibáñez, L., Potau, N., Chacon, P., et al. (1998) Hyperinsulinaemia, dyslipaemia and cardiovascular risk in girls with a history of premature pubarche. **Diabetologia**, 41 (9): 1057–1063

Ibáñez, L., Potau, N., Zampolli, M., et al. (1997) Girls diagnosed with premature pubarche show an

exaggerated ovarian androgen synthesis from the early stages of puberty: evidence from gonadotropin-releasing hormone agonist testing. **Fertility and sterility**, 67 (5): 849–855

Idkowiak, J., Lavery, G.G., Dhir, V., et al. (2011) Premature adrenarche: novel lessons from early onset androgen excess. **European journal of endocrinology / European Federation of Endocrine Societies**, 165 (2): 189–207

Ilan, Z., Ilan, R. and Cinti, D.L. (1981) Evidence for a new physiological role of hepatic NADPH:ferricytochrome (P-450) oxidoreductase. Direct electron input to the microsomal fatty acid chain elongation system. **The Journal of biological chemistry**, 256 (19): 10066–10072

Iwasaki, Y., Aoki, Y., Katahira, M., et al. (1997) Non-genomic mechanisms of glucocorticoid inhibition of adrenocorticotropin secretion: possible involvement of GTP-binding protein. **Biochemical and biophysical research communications**, 235 (2): 295–299

Javitt, N.B., Lee, Y.C., Shimizu, C., et al. (2001) Cholesterol and hydroxycholesterol sulfotransferases: identification, distinction from dehydroepiandrosterone sulfotransferase, and differential tissue expression. **Endocrinology**, 142 (7): 2978–2984

Jay, B., Blach, R.K. and Wells, R.S. (1968) Ocular manifestations of ichthyosis. **The British journal of ophthalmology**, 52 (3): 217–226

Jääskeläinen, J., Deeb, A., Schwabe, J.W., et al. (2006) Human androgen receptor gene ligand-binding-domain mutations leading to disrupted interaction between the N- and C-terminal domains. **Journal of molecular endocrinology**, 36 (2): 361–368

Jenkins, E.P., Andersson, S., Imperato-McGinley, J., et al. (1992) Genetic and pharmacological evidence for more than one human steroid 5 alpha-reductase. **The Journal of clinical investigation**, 89 (1): 293–300

Jin, S., Zhang, M., Lei, L., et al. (2006) Meiosis activating sterol (MAS) regulate FSH-induced meiotic resumption of cumulus cell-enclosed porcine oocytes via PKC pathway. **Molecular and cellular endocrinology**, 249 (1-2): 64–70

John, M.E., John, M.C., Boggaram, V., et al. (1986) Transcriptional regulation of steroid hydroxylase genes by corticotropin. **Proceedings of the National Academy of Sciences of the United States of America**, 83 (13): 4715–4719

Judd, H.L., Lucas, W.E. and Yen, S.S. (1974) Effect of oophorectomy on circulating testosterone and androstenedione levels in patients with endometrial cancer. **American journal of obstetrics and gynecology**, 118 (6): 793–798

Kampa, M., Kogia, C., Theodoropoulos, P.A., et al. (2006) Activation of membrane androgen receptors potentiates the antiproliferative effects of paclitaxel on human prostate cancer cells. **Molecular cancer therapeutics**, 5 (5): 1342–1351

Kate-Booij, ten, M.J., Cobbaert, C., Koper, J.W., et al. (2004) Deficiency of 17,20-lyase causing giant ovarian cysts in a girl and a female phenotype in her 46,XY sister: case report. **Human reproduction (Oxford, England)**, 19 (2): 456–459

Kater, C.E. and Biglieri, E.G. (1994) Disorders of steroid 17 alpha-hydroxylase deficiency. **Endocrinology and metabolism clinics of North America**, 23 (2): 341–357

Kaufman, F.R., Costin, G., Goebelsmann, U., et al. (1983) Male pseudohermaphroditism due to 17,20-desmolase deficiency. **Journal of Clinical Endocrinology & Metabolism**, 57 (1): 32–36

Kelley, R.I., Kratz, L.E., Glaser, R.L., et al. (2002) Abnormal sterol metabolism in a patient with Antley-Bixler syndrome and ambiguous genitalia. **American Journal of Medical Genetics**, 110 (2): 95–102

Kent, L., Emerton, J., Bhadravathi, V., et al. (2008) X-linked ichthyosis (steroid sulfatase deficiency) is

associated with increased risk of attention deficit hyperactivity disorder, autism and social communication deficits. **Journal of medical genetics**, 45 (8): 519–524

Keohavong, P. and Thilly, W.G. (1989) Fidelity of DNA polymerases in DNA amplification. **Proceedings of the National Academy of Sciences of the United States of America**, 86 (23): 9253–9257

Kerrigan, J.R., Veldhuis, J.D., Leyo, S.A., et al. (1993) Estimation of daily cortisol production and clearance rates in normal pubertal males by deconvolution analysis. **Journal of Clinical Endocrinology & Metabolism**, 76 (6): 1505–1510

Kok, R.C., Timmerman, M.A., Wolffenbuttel, K.P., et al. (2010) Isolated 17,20-Lyase Deficiency due to the Cytochrome b5 Mutation W27X. **The Journal of Clinical Endocrinology and Metabolism**

Kong, A.N., Yang, L., Ma, M., et al. (1992) Molecular cloning of the alcohol/hydroxysteroid form (hSTa) of sulfotransferase from human liver. **Biochemical and biophysical research communications**, 187 (1): 448–454

Kornel, L. (1994) Colocalization of 11 beta-hydroxysteroid dehydrogenase and mineralocorticoid receptors in cultured vascular smooth muscle cells. **American journal of hypertension**, 7 (1): 100–103

Krone, N. and Arlt, W. (2009) Genetics of congenital adrenal hyperplasia. **Best practice & research Clinical endocrinology & metabolism**, 23 (2): 181–192

Krone, N., Dhir, V., Ivison, H., et al. (2007a) Congenital adrenal hyperplasia and P450 oxidoreductase deficiency. **Clinical endocrinology**, 66 (2): 162–172

Krone, N., Hanley, N. and Arlt, W. (2007b) Age-specific changes in sex steroid biosynthesis and sex development. **Best practice & research Clinical endocrinology & metabolism**, 21 (3): 393–401

Krone, N., Hughes, B.A., Lavery, G.G., et al. (2010) Gas chromatography/mass spectrometry (GC/MS) remains a pre-eminent discovery tool in clinical steroid investigations even in the era of fast liquid chromatography tandem mass spectrometry (LC/MS/MS). **The Journal of steroid biochemistry and molecular biology**, 121 (3-5): –504

Krone, N., Reisch, N., Idkowiak, J., et al. (2012) Genotype-phenotype analysis in congenital adrenal hyperplasia due to P450 oxidoreductase deficiency. **The Journal of Clinical Endocrinology and Metabolism**, 97 (2): E257–67

Kushnir, M.M., Blamires, T., Rockwood, A.L., et al. (2010) Liquid chromatography-tandem mass spectrometry assay for androstenedione, dehydroepiandrosterone, and testosterone with pediatric and adult reference intervals. **Clinical chemistry**, 56 (7): 1138–1147

Labrie, C., Bélanger, A. and Labrie, F. (1988) Androgenic activity of dehydroepiandrosterone and androstenedione in the rat ventral prostate. **Endocrinology**, 123 (3): 1412–1417

Labrie, F. (2003) Extragonadal synthesis of sex steroids: intracrinology. **Ann Endocrinol (Paris)**, 64 (2): 95–107

Lam, S.T. and Polani, P.E. (1985) Hormonal induction of steroid sulphatase in the mouse. **Experientia**, 41 (2): 276–278

Langlois, S., Armstrong, L., Gall, K., et al. (2009) Steroid sulfatase deficiency and contiguous gene deletion syndrome amongst pregnant patients with low serum unconjugated estriols. **Prenatal Diagnosis**, 29 (10): 966–974

Larrea, F., Lisker, R., Bañuelos, R., et al. (1983) Hypergonadotrophic hypogonadism in an XX female subject due to 17,20 steroid desmolase deficiency. **Acta endocrinologica**, 103 (3): 400–405

Latronico, A.C., Anasti, J., Arnhold, I.J., et al. (1996) Brief report: testicular and ovarian resistance to luteinizing hormone caused by inactivating mutations of the luteinizing hormone-receptor gene. **The New England journal of medicine**, 334 (8): 507–512

Lavery, G., Walker, E., Tiganescu, A., et al. (2008) Steroid biomarkers and genetic studies reveal inactivating mutations in hexose-6-phosphate dehydrogenase in patients with cortisone reductase deficiency. **The Journal of Clinical Endocrinology and Metabolism**, 93 (10): 3827–3832

Lavery, G.G., Idkowiak, J., Sherlock, M., et al. (2012) Novel H6PDH mutations in two girls with premature adrenarche: 'Apparent' and “true” CRD can be differentiated by urinary steroid profiling. **European journal of endocrinology / European Federation of Endocrine Societies**

Lawson, A.J., Walker, E.A., Lavery, G.G., et al. (2011) Cortisone-reductase deficiency associated with heterozygous mutations in 11beta-hydroxysteroid dehydrogenase type 1. **Proceedings of the National Academy of Sciences of the United States of America**, 108 (10): 4111–4116

Lee, P.A. and Houk, C.P. (2004) Outcome studies among men with micropenis. **Journal of pediatric endocrinology & metabolism : JPEM**, 17 (8): 1043–1053

Lee, Y., Kirk, J., Stanhope, R., et al. (2007) Phenotypic variability in 17beta-hydroxysteroid dehydrogenase-3 deficiency and diagnostic pitfalls. **Clinical endocrinology**, 67 (1): 20–28

Liu, J., Rone, M.B. and Papadopoulos, V. (2006) Protein-protein interactions mediate mitochondrial cholesterol transport and steroid biosynthesis. **The Journal of biological chemistry**, 281 (50): 38879–38893

Lombès, M., Oblin, M.E., Gasc, J.M., et al. (1992) Immunohistochemical and biochemical evidence for a cardiovascular mineralocorticoid receptor. **Circulation research**, 71 (3): 503–510

Lonard, D.M. and O'Malley, B.W. (2006) The expanding cosmos of nuclear receptor coactivators. **Cell**, 125 (3): 411–414

Louwers, Y.V., de Jong, F.H., van Herwaarden, N.A.A., et al. (2013) Variants in SULT2A1 affect the DHEA sulphate to DHEA ratio in patients with polycystic ovary syndrome but not the hyperandrogenic phenotype. **The Journal of Clinical Endocrinology and Metabolism**, 98 (9): 3848–3855

Lowry, O.H., Rosebrough, N.J., Farr, A.L., et al. (1951) Protein measurement with the Folin phenol reagent. **The Journal of biological chemistry**, 193 (1): 265–275

Lu, N.Z., Wardell, S.E., Burnstein, K.L., et al. (2006) International Union of Pharmacology. LXV. The pharmacology and classification of the nuclear receptor superfamily: glucocorticoid, mineralocorticoid, progesterone, and androgen receptors. **Pharmacological reviews**, 58 (4): 782–797

Lund, J., Ahlgren, R., Wu, D.H., et al. (1990) Transcriptional regulation of the bovine CYP17 (P-450(17)alpha) gene. Identification of two cAMP regulatory regions lacking the consensus cAMP-responsive element (CRE). **The Journal of biological chemistry**, 265 (6): 3304–3312

Luo, X., Ikeda, Y. and Parker, K.L. (1994) A cell-specific nuclear receptor is essential for adrenal and gonadal development and sexual differentiation. **Cell**, 77 (4): 481–490

Luu-The, V., Sugimoto, Y., Puy, L., et al. (1994) Characterization, expression, and immunohistochemical localization of 5 alpha-reductase in human skin. **The Journal of investigative dermatology**, 102 (2): 221–226

Lykkesfeldt, G. and Bock, J.E. (1985) Lactation in placental steroid sulphatase deficiency. **British journal of obstetrics and gynaecology**, 92 (2): 179–180

Lykkesfeldt, G., Bennett, P., Lykkesfeldt, A.E., et al. (1985a) Abnormal androgen and oestrogen metabolism in men with steroid sulphatase deficiency and recessive X-linked ichthyosis. **Clinical endocrinology**, 23 (4): 385–393

Lykkesfeldt, G., Høyer, H., Ibsen, H.H., et al. (1985b) Steroid sulphatase deficiency disease. **Clinical genetics**, 28 (3): 231–237

Lykkesfeldt, G., Høyer, H., Lykkesfeldt, A.E., et al. (1983) Steroid sulphatase deficiency associated with testis cancer. **Lancet**, 2 (8365-66): 1456

Mallin, S.R. (1969) Congenital adrenal hyperplasia secondary to 17-hydroxylase deficiency. Two sisters with amenorrhea, hypokalemia, hypertension, and cystic ovaries. **Annals of internal medicine**, 70 (1): 69–75

Mancini, M.A., Song, C.S., Rao, T.R., et al. (1992) Spatio-temporal expression of estrogen sulfotransferase within the hepatic lobule of male rats: implication of in situ estrogen inactivation in androgen action. **Endocrinology**, 131 (3): 1541–1546

Mann, R.K. and Beachy, P.A. (2004) Novel lipid modifications of secreted protein signals. **Annual review of biochemistry**, 73: 891–923

Mansha, M., Wasim, M., Ploner, C., et al. (2012) Problems encountered in bicistronic IRES-GFP expression vectors employed in functional analyses of GC-induced genes. **Molecular biology reports**, 39 (12): 10227–10234

Marshall, W.A. and Tanner, J.M. (1969) Variations in pattern of pubertal changes in girls. **Archives of disease in childhood**, 44 (235): 291–303

Marshall, W.A. and Tanner, J.M. (1970) Variations in the pattern of pubertal changes in boys. **Archives of disease in childhood**, 45 (239): 13–23

Martin, D.D. (2004) The Early Dehydroepiandrosterone Sulfate Rise of Adrenarche and the Delay of Pubarche Indicate Primary Ovarian Failure in Turner Syndrome. **Journal of Clinical Endocrinology & Metabolism**, 89 (3): 1164–1168

Mathews, F.S. (1985) The structure, function and evolution of cytochromes. **Progress in biophysics and molecular biology**, 45 (1): 1–56

Maya-Nunez, G., Torres, L., Ulloa-Aguirre, A., et al. (1999) An atypical contiguous gene syndrome: molecular studies in a family with X-linked Kallmann's syndrome and X-linked ichthyosis. **Clinical endocrinology**, 50 (2): 157–162

Małunowicz, E., Romer, T.E., Szarras-Czapnik, M., et al. (1987) Combined deficiency of 17 alpha-hydroxylase and 21-hydroxylase in an 8 years old girl. **Endokrynologia Polska**, 38 (1): 117–124

Márquez, D.C. and Pietras, R.J. (2001) Membrane-associated binding sites for estrogen contribute to growth regulation of human breast cancer cells. **Oncogene**, 20 (39): 5420–5430

Meijer, O.C. (2002) Coregulator proteins and corticosteroid action in the brain. **Journal of neuroendocrinology**, 14 (6): 499–505

Mendonca, B.B., Domenice, S., Arnhold, I.J.P., et al. (2009) 46,XY disorders of sex development (DSD). **Clinical endocrinology**, 70 (2): 173–187

Mesiano, S. and Jaffe, R.B. (1997) Developmental and functional biology of the primate fetal adrenal cortex. **Endocrine reviews**, 18 (3): 378–403

Metherell, L.A., Naville, D., Halaby, G., et al. (2009) Nonclassic lipoid congenital adrenal hyperplasia masquerading as familial glucocorticoid deficiency. **The Journal of Clinical Endocrinology and Metabolism**, 94 (10): 3865–3871

Meunier, B., de Visser, S.P. and Shaik, S. (2004) Mechanism of oxidation reactions catalyzed by cytochrome p450 enzymes. **Chemical reviews**, 104 (9): 3947–3980

Miki, Y., Nakata, T., Suzuki, T., et al. (2002) Systemic distribution of steroid sulfatase and estrogen sulfotransferase in human adult and fetal tissues. **The Journal of Clinical Endocrinology and Metabolism**, 87 (12): 5760–5768

Miller, W.L. and Auchus, R.J. (2011) The molecular biology, biochemistry, and physiology of human steroidogenesis and its disorders. **Endocrine reviews**, 32 (1): 81–151

Milone, A., Delfino, M., Piccirillo, A., et al. (1991) Increased levels of DHEAS in serum of patients with X-linked ichthyosis. **Journal of inherited metabolic disease**, 14 (1): 96–104

Miura, K., Yasuda, K., Yanase, T., et al. (1996) Mutation of cytochrome P-45017 alpha gene (CYP17) in a Japanese patient previously reported as having glucocorticoid-responsive hyperaldosteronism: with a review of Japanese patients with mutations of CYP17. **Journal of Clinical Endocrinology & Metabolism**, 81 (10): 3797–3801

Miyake, N., Elcioglu, N.H., Iida, A., et al. (2012) PAPSS2 mutations cause autosomal recessive brachyolmia. **Journal of medical genetics**, 49 (8): 533–538

Moore, K.L. (1988) **Essentials of human embryology**. Mosby Inc

Moras, D. and Gronemeyer, H. (1998) The nuclear receptor ligand-binding domain: structure and function. **Current opinion in cell biology**, 10 (3): 384–391

Moutaouakkil, M., Prost, O., Dahan, N., et al. (1984) Estrone and dehydroepiandrosterone sulfatase activities in guinea-pig uterus and liver: estrogenic effect of estrone sulfate. **Journal of steroid biochemistry**, 21 (3): 321–328

Mueller, J.W. and Shafqat, N. (2013) Adenosine-5'-phosphosulfate - a multifaceted modulator of bifunctional 3“-phospho-adenosine-5-”phosphosulfate synthases and related enzymes. **The FEBS journal**

Mukhopadhyay, K. and Lecomte, J.T.J. (2004) A relationship between heme binding and protein stability in cytochrome b5. **Biochemistry**, 43 (38): 12227–12236

Mulder, G.J. (2003) **Conjugation Reactions In Drug Metabolism**. CRC Press

Mullis, P.E., Yoshimura, N., Kuhlmann, B., et al. (1997) Aromatase deficiency in a female who is compound heterozygote for two new point mutations in the P450arom gene: impact of estrogens on hypergonadotropic hypogonadism, multicystic ovaries, and bone densitometry in childhood. **The Journal of Clinical Endocrinology and Metabolism**, 82 (6): 1739–1745

Muskiet, F.A., Jansen, G., Wolthers, B.G., et al. (1983) Gas-chromatographic determination of cholesterol sulfate in plasma and erythrocytes, for the diagnosis of recessive X-linked ichthyosis. **Clinical chemistry**, 29 (7): 1404–1407

Müssig, K., Kaltenbach, S., Machicao, F., et al. (2005) 17alpha-hydroxylase/17,20-lyase deficiency caused by a novel homozygous mutation (Y27Stop) in the cytochrome CYP17 gene. **The Journal of Clinical Endocrinology and Metabolism**, 90 (7): 4362–4365

Naffin-Olivos, J. and Auchus, R. (2006) Human cytochrome b5 requires residues E48 and E49 to stimulate the 17,20-lyase activity of cytochrome P450c17. **Biochemistry**, 45 (3): 755–762

Nakamura, Y., Gang, H.X., Suzuki, T., et al. (2009) Adrenal changes associated with adrenarche. **Rev Endocr Metab Disord**, 10 (1): 19–26

Nebert, D.W. and Russell, D.W. (2002) Clinical importance of the cytochromes P450. **Lancet**, 360 (9340): 1155–1162

Nelson, D.R., Koymans, L., Kamataki, T., et al. (1996) P450 superfamily: update on new sequences, gene mapping, accession numbers and nomenclature. **Pharmacogenetics**, 6 (1): 1–42

Neres, M.S., Auchus, R.J., Shackleton, C.H.L., et al. (2010) Distinctive profile of the 17-hydroxylase and 17,20-lyase activities revealed by urinary steroid metabolomes of patients with CYP17 deficiency. **Arquivos brasileiros de endocrinologia e metabologia**, 54 (9): 826–832

New, M.I. (1993) Nonclassical congenital adrenal hyperplasia and the polycystic ovarian syndrome. **Annals of the New York Academy of Sciences**, 687: 193–205

Nguyen, N.T., Lin, D.P.-C., Yen, S.-Y., et al. (2009) Sonic hedgehog promotes porcine oocyte maturation and early embryo development. **Reproduction, fertility, and development**, 21 (6): 805–815

Nomura, K., Nakano, H., Umeki, K., et al. (1995) A study of the steroid sulfatase gene in families with X-linked ichthyosis using polymerase chain reaction. **Acta dermato-venereologica**, 75 (5): 340–342

Noordam, C., Dhir, V., McNelis, J.C., et al. (2009) Inactivating PAPSS2Mutations in a Patient with Premature Pubarche. **The New England journal of medicine**, 360 (22): 2310–2318

Ono, T. and Bloch, K. (1975) Solubilization and partial characterization of rat liver squalene epoxidase. **The Journal of biological chemistry**, 250 (4): 1571–1579

Onoda, M. and Hall, P.F. (1982) Cytochrome b5 stimulates purified testicular microsomal cytochrome P-450 (C21 side-chain cleavage). **Biochemical and biophysical research communications**, 108 (2): 454–460

Oppenheimer, E., Linder, B. and Dimartino-Nardi, J. (1995) Decreased insulin sensitivity in prepubertal girls with premature adrenarche and acanthosis nigricans. **The Journal of Clinical Endocrinology and Metabolism**, 80 (2): 614–618

Pacak, K., Eisenhofer, G. and Lenders, J. (2008) **Pheochromocytoma**. Wiley-Blackwell

Paige, D.G., Emilion, G.G., Bouloux, P.M., et al. (1994) A clinical and genetic study of X-linked recessive ichthyosis and contiguous gene defects. **The British journal of dermatology**, 131 (5): 622–629

Pandey, A., Kempna, P., Hofer, G., et al. (2007) Modulation of human CYP19A1 activity by mutant NADPH P450 oxidoreductase. **Molecular endocrinology (Baltimore, Md)**, 21 (10): 2579–2595

Parker, K.L. and Schimmer, B.P. (1997) Steroidogenic factor 1: a key determinant of endocrine development and function. **Endocrine reviews**, 18 (3): 361–377

Paterson, W.F., Ahmed, S.F., Bath, L., et al. (2010) Exaggerated adrenarche in a cohort of Scottish children: clinical features and biochemistry. **Clinical Endocrinology**, 72 (4): 496–501

Percy, M.J. and Lappin, T.R. (2008) Recessive congenital methaemoglobinaemia: cytochrome b(5) reductase deficiency. **British journal of haematology**, 141 (3): 298–308

Pescovitz, O.H., Comite, F., Cassorla, F., et al. (1984) True precocious puberty complicating congenital adrenal hyperplasia: treatment with a luteinizing hormone-releasing hormone analog. **Journal of Clinical Endocrinology & Metabolism**, 58 (5): 857–861

Peterson, R.E., Imperato-McGinley, J., Gautier, T., et al. (1985) Male Pseudohermaphroditism Due to Multiple Defects in Steroid-Biosynthetic Microsomal Mixed-Function Oxidases. **The New England journal of medicine**, 313 (19): 1182–1191

Picado-Leonard, J. and Miller, W.L. (1987) Cloning and sequence of the human gene for P450c17 (steroid 17 alpha-hydroxylase/17,20 lyase): similarity with the gene for P450c21. **DNA (Mary Ann Liebert, Inc.)**, 6 (5): 439–448

Pohorecky, L.A. and Wurtman, R.J. (1971) Adrenocortical control of epinephrine synthesis. **Pharmacological reviews**, 23 (1): 1–35

Pompon, D., Louerat, B., Bronine, A., et al. (1996) “[6] Yeast expression of animal and plant P450s in optimized redox environments.” In **Methods in Enzymology**. Methods in Enzymology. vol. Elsevier. pp. 51–64

Potau, N., Williams, R., Ong, K., et al. (2003) Fasting insulin sensitivity and post-oral glucose hyperinsulinaemia related to cardiovascular risk factors in adolescents with precocious pubarche. **Clinical endocrinology**, 59 (6): 756–762

Preumont, A., Rzem, R., Vertommen, D., et al. (2010) HDHD1, which is often deleted in X-linked ichthyosis, encodes a pseudouridine-5'-phosphatase. **The Biochemical journal**, 431 (2): 237–244

Pritchard, L.E., Turnbull, A.V. and White, A. (2002) Pro-opiomelanocortin processing in the hypothalamus: impact on melanocortin signalling and obesity. **The Journal of endocrinology**, 172 (3): 411–421

Prosser, G.A., Larrouy-Maumus, G. and de Carvalho, L.P.S. (2014) Metabolomic strategies for the identification of new enzyme functions and metabolic pathways. **EMBO Reports**, 15 (6): 657–669

Quigley, C.A., De Bellis, A., Marschke, K.B., et al. (1995) Androgen receptor defects: historical, clinical, and molecular perspectives. **Endocrine reviews**, 16 (3): 271–321

Radford, D.J., Wang, K., McNelis, J.C., et al. (2010) Dehdyroepiandrosterone sulfate directly activates protein kinase C-beta to increase human neutrophil superoxide generation. **Molecular endocrinology (Baltimore, Md)**, 24 (4): 813–821

Radominska, A., Comer, K.A., Zimniak, P., et al. (1990) Human liver steroid sulphotransferase sulphates bile acids. **The Biochemical journal**, 272 (3): 597–604

Raine, J.E., Donaldson, M.D.C., Gregory, J.W., et al. (2011) **Practical Endocrinology and Diabetes in Children**. John Wiley & Sons

Rainey, W.E., Saner, K. and Schimmer, B.P. (2004) Adrenocortical cell lines. **Molecular and cellular endocrinology**, 228 (1-2): 23–38

Ray, A. and Prefontaine, K.E. (1994) Physical association and functional antagonism between the p65 subunit of transcription factor NF-kappa B and the glucocorticoid receptor. **Proceedings of the National Academy of Sciences of the United States of America**, 91 (2): 752–756

Recksiek, M., Selmer, T., Dierks, T., et al. (1998) Sulfatases, trapping of the sulfated enzyme intermediate by substituting the active site formylglycine. **The Journal of biological chemistry**, 273 (11): 6096–6103

Reed, M.J. and Purohit, A. (1997) Breast cancer and the role of cytokines in regulating estrogen synthesis: an emerging hypothesis. **Endocrine reviews**, 18 (5): 701–715

Reed, M.J., Purohit, A., Woo, L.W.L., et al. (2005) Steroid sulfatase: molecular biology, regulation, and inhibition. **Endocrine reviews**, 26 (2): 171–202

Rege, J. and Rainey, W.E. (2012) The Steroid Metabolome of Adrenarche. **Journal of Endocrinology**

Remer, T., Boye, K.R., Hartmann, M.F., et al. (2004) Adrenal steroid hormones and metaphyseal bone in children. **Hormone research**, 62 (5): 221–226

Remer, T., Boye, K.R., Hartmann, M.F., et al. (2005) Urinary markers of adrenarche: reference values in healthy subjects, aged 3-18 years. **The Journal of Clinical Endocrinology and Metabolism**, 90 (4): 2015–2021

Rizk, D.E. and Johansen, K.A. (1993) Placental sulfatase deficiency and congenital ichthyosis with intrauterine fetal death: case report. **American journal of obstetrics and gynecology**, 168 (2): 570–

571

Rodin, A., Thakkar, H., Taylor, N., et al. (1994) Hyperandrogenism in polycystic ovary syndrome. Evidence of dysregulation of 11 beta-hydroxysteroid dehydrogenase. **The New England journal of medicine**, 330 (7): 460–465

Rodriguez, H., Hum, D.W., Staels, B., et al. (1997) Transcription of the human genes for cytochrome P450scc and P450c17 is regulated differently in human adrenal NCI-H295 cells than in mouse adrenal Y1 cells. **Journal of Clinical Endocrinology & Metabolism**, 82 (2): 365–371

Rone, M.B., Fan, J. and Papadopoulos, V. (2009) Cholesterol transport in steroid biosynthesis: role of protein-protein interactions and implications in disease states. **Biochimica et biophysica acta**, 1791 (7): 646–658

Rosa, S., Duff, C., Meyer, M., et al. (2007) P450c17 deficiency: clinical and molecular characterization of six patients. **The Journal of Clinical Endocrinology and Metabolism**, 92 (3): 1000–1007

Rosenfield, R.L. (1994) Normal and almost normal precocious variations in pubertal development premature pubarche and premature thelarche revisited. **Hormone research**, 41 Suppl 2: 7–13

Rosenfield, R.L. (2007) Clinical review: Identifying children at risk for polycystic ovary syndrome. **The Journal of Clinical Endocrinology and Metabolism**, 92 (3): 787–796

Rosenfield, R.L., Lipton, R.B. and Drum, M.L. (2009) Thelarche, pubarche, and menarche attainment in children with normal and elevated body mass index. **PEDIATRICS**, 123 (1): 84–88

Rozman, D., Cotman, M. and Frangez, R. (2002) Lanosterol 14alpha-demethylase and MAS sterols in mammalian gametogenesis. **Molecular and cellular endocrinology**, 187 (1-2): 179–187

Ruokonen, A., Oikarinen, A., Palatsi, R., et al. (1980) Serum steroid sulphates in ichthyosis. **The British journal of dermatology**, 103 (3): 245–248

Sahakitrungruang, T., Huang, N., Tee, M.K., et al. (2009) Clinical, genetic, and enzymatic characterization of P450 oxidoreductase deficiency in four patients. **The Journal of Clinical Endocrinology and Metabolism**, 94 (12): 4992–5000

Sajjad, Y., Quenby, S., Nickson, P., et al. (2004a) Immunohistochemical localization of androgen receptors in the urogenital tracts of human embryos. **Reproduction (Cambridge, England)**, 128 (3): 331–339

Sajjad, Y., Quenby, S.M., Nickson, P., et al. (2004b) Expression of androgen receptors in upper human fetal reproductive tract. **Human reproduction (Oxford, England)**, 19 (7): 1659–1665

Salem, M., Tainsh, R.E., Bromberg, J., et al. (1994) Perioperative glucocorticoid coverage. A reassessment 42 years after emergence of a problem. **Annals of surgery**, 219 (4): 416–425

Schenkman, J.B. and Jansson, I. (2003) The many roles of cytochrome b5. **Pharmacology & therapeutics**, 97 (2): 139–152

Schmidt, K., Hughes, C., Chudek, J.A., et al. (2009) Cholesterol metabolism: the main pathway acting downstream of cytochrome P450 oxidoreductase in skeletal development of the limb. **Molecular and cellular biology**, 29 (10): 2716–2729

Schneider, G., French, A., Bullock, L.P., et al. (1971) Absence of androgen stimulation of hepatic steroid sulfatase in the female rat. **Endocrinology**, 89 (1): 308–310

Schröder, E., Gebel, L., Eremeev, A.A., et al. (2012) Human PAPS synthase isoforms are dynamically regulated enzymes with access to nucleus and cytoplasm. **PloS one**, 7 (1): e29559

Seidel, A., Brunner, S., Seidel, P., et al. (2006) Modified nucleosides: an accurate tumour marker for

clinical diagnosis of cancer, early detection and therapy control. **British journal of cancer**, 94 (11): 1726–1733

Sewer, M.B. and Waterman, M.R. (2002) Adrenocorticotropin/cyclic adenosine 3“,5-”monophosphate-mediated transcription of the human CYP17 gene in the adrenal cortex is dependent on phosphatase activity. **Endocrinology**, 143 (5): 1769–1777

Sewer, M.B. and Waterman, M.R. (2003) ACTH modulation of transcription factors responsible for steroid hydroxylase gene expression in the adrenal cortex. **Microscopy research and technique**, 61 (3): 300–307

Shackleton, C., Marcos, J., Malunowicz, E.M., et al. (2004) Biochemical diagnosis of Antley-Bixler syndrome by steroid analysis. **American Journal of Medical Genetics**, 128A (3): 223–231

Shackleton, C.H. (2008) “Genetic disorders of Steroid Metabolsim Diagnosed by Mass Spectrometry.” In Blau, N., Duren, M. and Gibson, K.M. (eds.) **Laboratory Guide to the Methods in Biochemical Genetics**

. 1st ed. Heidelberg: Springer. pp. 549–605

Shackleton, C.H.L. (2011) Role of a Disordered Steroid Metabolome in the Elucidation of Sterol and Steroid Biosynthesis. **Lipids**

Shapiro, L.J., Weiss, R., Buxman, M.M., et al. (1978) Enzymatic basis of typical X-linked icthyosis. **Lancet**, 2 (8093): 756–757

Sherbet, D., Tiosano, D., Kwist, K., et al. (2003) CYP17 mutation E305G causes isolated 17,20-lyase deficiency by selectively altering substrate binding. **The Journal of biological chemistry**, 278 (49): 48563–48569

Shima, M., Tanae, A., Miki, K., et al. (2000) Mechanism for the development of ovarian cysts in patients with congenital lipoid adrenal hyperplasia. **European journal of endocrinology / European Federation of Endocrine Societies**, 142 (3): 274–279

Siiteri, P.K. and Wilson, J.D. (1974) Testosterone formation and metabolism during male sexual differentiation in the human embryo. **Journal of Clinical Endocrinology & Metabolism**, 38 (1): 113–125

Silfen, M.E., Shackleton, C.H.L., Manibo, A.M., et al. (2002) 5 alpha-reductase and 11 beta-hydroxysteroid dehydrogenase activity in prepubertal Hispanic girls with premature adrenarche. **The Journal of Clinical Endocrinology and Metabolism**, 87 (10): 4647–4651

Silverman, S.H., Migeon, C., Rosemberg, E., et al. (1952) Precocious growth of sexual hair without other secondary sexual development; premature pubarche, a constitutional variation of adolescence. **PEDIATRICS**, 10 (4): 426–432

Simoncini, T., Hafezi-Moghadam, A., Brazil, D.P., et al. (2000) Interaction of oestrogen receptor with the regulatory subunit of phosphatidylinositol-3-OH kinase. **Nature**, 407 (6803): 538–541

Simpson, E.R., Mahendroo, M.S., Means, G.D., et al. (1994) Aromatase cytochrome P450, the enzyme responsible for estrogen biosynthesis. **Endocrine reviews**, 15 (3): 342–355

Simsek, E., Ozdemir, I., Lin, L., et al. (2005) Isolated 17,20-lyase (desmolase) deficiency in a 46,XX female presenting with delayed puberty. **Fertility and sterility**, 83 (5): 1548–1551

Sinclair, A.H., Berta, P., Palmer, M.S., et al. (1990) A gene from the human sex-determining region encodes a protein with homology to a conserved DNA-binding motif. **Nature**, 346 (6281): 240–244

Skałba, P., Dabkowska-Huć, A., Kazimierczak, W., et al. (2006) Content of 5-alpha-reductase (type 1 and type 2) mRNA in dermal papillae from the lower abdominal region in women with hirsutism.

Clinical and experimental dermatology, 31 (4): 564–570

Sklar, C.A., Kaplan, S.L. and Grumbach, M.M. (1980) Evidence for dissociation between adrenarche and gonadarche: studies in patients with idiopathic precocious puberty, gonadal dysgenesis, isolated gonadotropin deficiency, and constitutionally delayed growth and adolescence. **Journal of Clinical Endocrinology & Metabolism**, 51 (3): 548–556

Sopher, A.B., Jean, A.M., Zwany, S.K., et al. (2011) Bone Age Advancement in Prepubertal Children With Obesity and Premature Adrenarche: Possible Potentiating Factors. **Obesity (Silver Spring, Md)**

Stein, C., Hille, A., Seidel, J., et al. (1989) Cloning and expression of human steroid-sulfatase. Membrane topology, glycosylation, and subcellular distribution in BHK-21 cells. **The Journal of biological chemistry**, 264 (23): 13865–13872

Stelzer, C., Brimmer, A., Hermanns, P., et al. (2007) Expression profile of Papss2 (3“-phosphoadenosine 5-”phosphosulfate synthase 2) during cartilage formation and skeletal development in the mouse embryo. **Developmental dynamics : an official publication of the American Association of Anatomists**, 236 (5): 1313–1318

Stewart, P.M., Shackleton, C.H., Beastall, G.H., et al. (1990) 5 alpha-reductase activity in polycystic ovary syndrome. **Lancet**, 335 (8687): 431–433

Stocco, D.M. and Sodeman, T.C. (1991) The 30-kDa mitochondrial proteins induced by hormone stimulation in MA-10 mouse Leydig tumor cells are processed from larger precursors. **The Journal of biological chemistry**, 266 (29): 19731–19738

Stocco, D.M., Wang, X., Jo, Y., et al. (2005) Multiple signaling pathways regulating steroidogenesis and steroidogenic acute regulatory protein expression: more complicated than we thought. **Molecular Endocrinology**, 19 (11): 2647–2659

Stoll, C. and Eyer, D. (1999) A syndrome of congenital ichthyosis, hypogonadism, small stature, facial dysmorphism, scoliosis and myogenic dystrophy. **Annales de genetique**, 42 (1): 45–50

Storbeck, K.-H., Swart, A.C., Goosen, P., et al. (2013) Cytochrome b5: novel roles in steroidogenesis. **Molecular and cellular endocrinology**, 371 (1-2): 87–99

Strott, C.A. (2002) Sulfonation and molecular action. **Endocrine reviews**, 23 (5): 703–732

Suhre, K. (2014) Metabolic profiling in diabetes. **Journal of Endocrinology**, 221 (3): R75–85

Suzuki, T., Sasano, H., Takeyama, J., et al. (2000) Developmental changes in steroidogenic enzymes in human postnatal adrenal cortex: immunohistochemical studies. **Clinical endocrinology**, 53 (6): 739–747

Talbot, N.B., Butler, A.M., Burman, R.A., et al. (1943) Excretion of 17-keto steroids by normal and abnormal children. **American Journal of Diseases of Children**, 65: 364–375

Tanae, A., Katsumata, N., Sato, N., et al. (2000) Genetic and endocrinological evaluations of three 46,XX patients with congenital lipoid adrenal hyperplasia previously reported as having presented spontaneous puberty. **Endocrine journal**, 47 (5): 629–634

Tee, M.K. and Miller, W.L. (2013) Phosphorylation of Human P450c17 by p38α Selectively Increases 17,20 Lyase Activity and Androgen Biosynthesis. **Journal of Biological Chemistry**

Temeck, J.W., Pang, S.Y., Nelson, C., et al. (1987) Genetic defects of steroidogenesis in premature pubarche. **The Journal of Clinical Endocrinology and Metabolism**, 64 (3): 609–617

Thai, H.T.T., Kalbasi, M., Lagerstedt, K., et al. (2005) The valine allele of the V89L polymorphism in the 5-alpha-reductase gene confers a reduced risk for hypospadias. **The Journal of Clinical Endocrinology and Metabolism**, 90 (12): 6695–6698

Tiosano, D., Knopf, C., Koren, I., et al. (2008) Metabolic evidence for impaired 17alpha-hydroxylase activity in a kindred bearing the E305G mutation for isolate 17,20-lyase activity. **European journal of endocrinology / European Federation of Endocrine Societies**, 158 (3): 385–392

Tomalik-Scharte, D., Maiter, D., Kirchheiner, J., et al. (2010) Impaired hepatic drug and steroid metabolism in congenital adrenal hyperplasia due to P450 oxidoreductase deficiency. **European journal of endocrinology / European Federation of Endocrine Societies**, 163 (6): 919–924

Tomlinson, J.W., Walker, E.A., Bujalska, I.J., et al. (2004) 11beta-hydroxysteroid dehydrogenase type 1: a tissue-specific regulator of glucocorticoid response. **Endocrine reviews**, 25 (5): 831–866

Traupe, H. and Happle, R. (1983) Clinical spectrum of steroid sulfatase deficiency: X-linked recessive ichthyosis, birth complications and cryptorchidism. **European journal of pediatrics**, 140 (1): 19–21

Traupe, H. and Ropers, H.H. (1982) Cryptorchidism and hypogenitalism in X-linked recessive ichthyosis vulgaris. **Human Genetics**, 60 (2): 206

Trent, S., Dennehy, A., Richardson, H., et al. (2012) Steroid sulfatase-deficient mice exhibit endophenotypes relevant to attention deficit hyperactivity disorder. **Psychoneuroendocrinology**, 37 (2): 221–229

Tüysüz, B., Yılmaz, S., Gül, E., et al. (2013) Spondyloepimetaphyseal dysplasia Pakistani type: expansion of the phenotype. **American journal of medical genetics Part A**, 161 (6): 1300–1308

Ui-Tei, K. (2004) **Guidelines for the selection of highly effective siRNA sequences for mammalian and chick RNA interference**. 32 (3): 936–948

Utriainen, P., Jääskeläinen, J., Romppanen, J., et al. (2007) Childhood metabolic syndrome and its components in premature adrenarche. **The Journal of Clinical Endocrinology and Metabolism**, 92 (11): 4282–4285

Utriainen, P., Laakso, S., Jääskeläinen, J., et al. (2012) Polymorphisms of POR, SULT2A1 and HSD11B1 in children with premature adrenarche. **Metabolism: clinical and experimental**, 61 (9): 1215–1219

Utriainen, P., Voutilainen, R. and Jääskeläinen, J. (2009) Continuum of phenotypes and sympathoadrenal function in premature adrenarche. **European journal of endocrinology / European Federation of Endocrine Societies**, 160 (4): 657–665

Val, P. and Swain, A. (2010) Gene dosage effects and transcriptional regulation of early mammalian adrenal cortex development. **Molecular and cellular endocrinology**, 323 (1): 105–114

Val, P., Jeays-Ward, K. and Swain, A. (2006) Identification of a novel population of adrenal-like cells in the mammalian testis. **Developmental biology**, 299 (1): 250–256

Val, P., Martinez-Barbera, J.-P. and Swain, A. (2007) Adrenal development is initiated by Cited2 and Wt1 through modulation of Sf-1 dosage. **Development (Cambridge, England)**, 134 (12): 2349–2358

Valdes-Flores, M., Kofman-Alfaro, S.H., Vaca, A.L., et al. (2001) Deletion of exons 1-5 of the STS gene causing X-linked ichthyosis. **The Journal of investigative dermatology**, 116 (3): 456–458

van de Wijngaart, D.J., Dubbink, H.J., van Royen, M.E., et al. (2012) Androgen receptor coregulators: recruitment via the coactivator binding groove. **Molecular and cellular endocrinology**, 352 (1-2): 57–69

Van Den Akker, E.L.T., Koper, J.W., Boehmer, A.L.M., et al. (2002) Differential inhibition of 17alpha-hydroxylase and 17,20-lyase activities by three novel missense CYP17 mutations identified in patients with P450c17 deficiency. **The Journal of Clinical Endocrinology and Metabolism**, 87 (12): 5714–5721

van den Boom, J., Heider, D., Martin, S.R., et al. (2012) 3“-Phosphoadenosine 5-”phosphosulfate (PAPS) synthases, naturally fragile enzymes specifically stabilized by nucleotide binding. **Journal of Biological Chemistry**, 287 (21): 17645–17655

Vassiliadi, D.A., Barber, T.M., Hughes, B.A., et al. (2009) Increased 5 alpha-reductase activity and adrenocortical drive in women with polycystic ovary syndrome. **Journal of Clinical Endocrinology & Metabolism**, 94 (9): 3558–3566

Venkatachalam, K.V. (2003) Human 3“-phosphoadenosine 5-”phosphosulfate (PAPS) synthase: biochemistry, molecular biology and genetic deficiency. **IUBMB life**, 55 (1): 1–11

Vickery, L.E. (1997) Molecular recognition and electron transfer in mitochondrial steroid hydroxylase systems. **Steroids**, 62 (1): 124–127

Voutilainen, R., Perheentupa, J. and Apter, D. (1983) Benign premature adrenarche: clinical features and serum steroid levels. **Acta paediatrica Scandinavica**, 72 (5): 707–711

Vuguin, P., Linder, B., Rosenfeld, R.G., et al. (1999) The roles of insulin sensitivity, insulin-like growth factor I (IGF-I), and IGF-binding protein-1 and -3 in the hyperandrogenism of African-American and Caribbean Hispanic girls with premature adrenarche. **The Journal of Clinical Endocrinology and Metabolism**, 84 (6): 2037–2042

Wagner, S., Kiupel, M., Peterson, R.A., et al. (2008) Cytochrome b5 expression in gonadectomy-induced adrenocortical neoplasms of the domestic ferret (Mustela putorius furo). **Veterinary pathology**, 45 (4): 439–442

Wang, C., Xu, B., Zhou, B., et al. (2009) Reducing CYP51 inhibits follicle-stimulating hormone induced resumption of mouse oocyte meiosis in vitro. **Journal of lipid research**, 50 (11): 2164–2172

Wang, F., Yang, J., Wang, H., et al. (2010) Gonadotropin-regulated expressions of lanosterol 14alpha-demethylase, sterol Delta14-reductase and C-4 sterol methyl oxidase contribute to the accumulation of meiosis-activating sterol in rabbit gonads. **Prostaglandins & other lipid mediators**

Wang, M., Roberts, D.L., Paschke, R., et al. (1997) Three-dimensional structure of NADPH-cytochrome P450 reductase: prototype for FMN- and FAD-containing enzymes. **Proceedings of the National Academy of Sciences of the United States of America**, 94 (16): 8411–8416

Wang, Q., Ghadessy, F.J., Trounson, A., et al. (1998) Azoospermia associated with a mutation in the ligand-binding domain of an androgen receptor displaying normal ligand binding, but defective trans-activation. **The Journal of Clinical Endocrinology and Metabolism**, 83 (12): 4303–4309

Wang, W.-H., Lu, J.-X., Yao, P., et al. (2003) The distinct heme coordination environments and heme-binding stabilities of His39Ser and His39Cys mutants of cytochrome b5. **Protein engineering**, 16 (12): 1047–1054

Wells, R.S. and Kerr, C.B. (1965) Genetic classification of ichthyosis. **Archives of dermatology**, 92 (1): 1–6

Wells, R.S. and Kerr, C.B. (1966) Clinical features of autosomal dominant and sex-linked ichthyosis in an English population. **British medical journal**, 1 (5493): 947–950

Werner, R., Grötsch, H. and Hiort, O. (2010) 46,XY disorders of sex development--the undermasculinised male with disorders of androgen action. **Best practice & research Clinical endocrinology & metabolism**, 24 (2): 263–277

Whitnall, M.H., Driscoll, W.J., Lee, Y.C., et al. (1993) Estrogen and hydroxysteroid sulfotransferases in guinea pig adrenal cortex: cellular and subcellular distributions. **Endocrinology**, 133 (5): 2284–2291

Wierman, M.E., Beardsworth, D.E., Crawford, J.D., et al. (1986) Adrenarche and skeletal maturation during luteinizing hormone releasing hormone analogue suppression of gonadarche. **The Journal of**

clinical investigation, 77 (1): 121–126

Wilks, A., Black, S.M., Miller, W.L., et al. (1995) Expression and characterization of truncated human heme oxygenase (hHO-1) and a fusion protein of hHO-1 with human cytochrome P450 reductase. **Biochemistry**, 34 (13): 4421–4427

Willemsen, R., Kroos, M., Hoogeveen, A.T., et al. (1988) Ultrastructural localization of steroid sulphatase in cultured human fibroblasts by immunocytochemistry: a comparative study with lysosomal enzymes and the mannose 6-phosphate receptor. **The Histochemical journal**, 20 (1): 41–51

Williams, M.L. and Elias, P.M. (1981) Stratum corneum lipids in disorders of cornification: increased cholesterol sulfate content of stratum corneum in recessive x-linked ichthyosis. **The Journal of clinical investigation**, 68 (6): 1404–1410

Wilson, J.D. (2003) 5alpha-Androstane-3alpha,17beta-Diol Is Formed in Tammar Wallaby Pouch Young Testes by a Pathway Involving 5alpha-Pregnane-3alpha,17alpha-Diol-20-One as a Key Intermediate. **Endocrinology**, 144 (2): 575–580

Wulfsberg, E.A., Curtis, J. and Jayne, C.H. (1992) Chondrodysplasia punctata: a boy with X-linked recessive chondrodysplasia punctata due to an inherited X-Y translocation with a current classification of these disorders. **American Journal of Medical Genetics**, 43 (5): 823–828

Wurtman, R.J. and Pohorecky, L.A. (1971) Adrenocortical control of epinephrine synthesis in health and disease. **Advances in metabolic disorders**, 5: 53–76

Xia, C., Panda, S.P., Marohnic, C.C., et al. (2011) Structural basis for human NADPH-cytochrome P450 oxidoreductase deficiency. **Proceedings of the National Academy of Sciences of the United States of America**

Xu, Z.H., Otterness, D.M., Freimuth, R.R., et al. (2000) Human 3“-phosphoadenosine 5-”phosphosulfate synthetase 1 (PAPSS1) and PAPSS2: gene cloning, characterization and chromosomal localization. **Biochemical and biophysical research communications**, 268 (2): 437–444

Yamazaki, H., Johnson, W.W., Ueng, Y.F., et al. (1996a) Lack of electron transfer from cytochrome b5 in stimulation of catalytic activities of cytochrome P450 3A4. Characterization of a reconstituted cytochrome P450 3A4/NADPH-cytochrome P450 reductase system and studies with apo-cytochrome b5. **The Journal of biological chemistry**, 271 (44): 27438–27444

Yamazaki, H., Nakano, M., Gillam, E.M., et al. (1996b) Requirements for cytochrome b5 in the oxidation of 7-ethoxycoumarin, chlorzoxazone, aniline, and N-nitrosodimethylamine by recombinant cytochrome P450 2E1 and by human liver microsomes. **Biochemical pharmacology**, 52 (2): 301–309

Yanagibashi, K. and Hall, P.F. (1986) Role of electron transport in the regulation of the lyase activity of C21 side-chain cleavage P-450 from porcine adrenal and testicular microsomes. **The Journal of biological chemistry**, 261 (18): 8429–8433

Yanagisawa, K., Sakakibara, Y., Suiko, M., et al. (1998) cDNA cloning, expression, and characterization of the human bifunctional ATP sulfurylase/adenosine 5'-phosphosulfate kinase enzyme. **Bioscience, biotechnology, and biochemistry**, 62 (5): 1037–1040

Yanase, T. (1995) 17 alpha-Hydroxylase/17,20-lyase defects. **J Steroid Biochem Mol Biol**, 53 (1-6): 153–157

Yanase, T., Kagimoto, M., Suzuki, S., et al. (1989) Deletion of a phenylalanine in the N-terminal region of human cytochrome P-450(17 alpha) results in partial combined 17 alpha-hydroxylase/17,20-lyase deficiency. **The Journal of biological chemistry**, 264 (30): 18076–18082

Yanase, T., Simpson, E.R. and Waterman, M.R. (1991) 17 alpha-hydroxylase/17,20-lyase deficiency: from clinical investigation to molecular definition. **Endocrine reviews**, 12 (1): 91–108

Yang, J. and Fuller, P.J. (2012) Interactions of the mineralocorticoid receptor--within and without. **Molecular and cellular endocrinology**, 350 (2): 196–205

Zachmann, M., Werder, E.A. and Prader, A. (1982) Two types of male pseudohermaphroditism due to 17, 20-desmolase deficiency. **Journal of Clinical Endocrinology & Metabolism**, 55 (3): 487–490

Zhang, L.H., Rodriguez, H., Ohno, S., et al. (1995) Serine phosphorylation of human P450c17 increases 17,20-lyase activity: implications for adrenarche and the polycystic ovary syndrome. **Proceedings of the National Academy of Sciences of the United States of America**, 92 (23): 10619–10623

Ziegler, G.A., Vonrhein, C., Hanukoglu, I., et al. (1999) The structure of adrenodoxin reductase of mitochondrial P450 systems: electron transfer for steroid biosynthesis. **Journal of molecular biology**, 289 (4): 981–990

Zukauskaite, S., Lasiene, D., Lasas, L., et al. (2005) Onset of breast and pubic hair development in 1231 preadolescent Lithuanian schoolgirls. **Archives of disease in childhood**, 90 (9): 932–936

11. PUBLICATIONS ARISING FROM THIS THESIS

1. Reisch N, **Idkowiak J**, Ivison HE, Hughes BA, Haskins Olney A, Blair EM, Dhir V, Shackleton CHL, Krone N, Arlt W. Prenatal diagnosis of congenital adrenal hyperplasia caused by P450 oxidoreductase deficiency. *J Clin Endocrinol Metab*. 2013 Jan 30.

2. Lavery GG, **Idkowiak J**, Sherlock M, Bujalska I, Ride JP, Saqib K, Hartmann MF, Hughes B, Wudy SA, De Schepper J, Arlt W, Krone N, Shackleton CH, Walker EA, Stewart PM. Urinary steroid metabolome analysis refines the diagnosis and spectrum of cortisone reductase deficiencies in patients presenting with premature adrenarche. *Eur J Endocrinol*. 2013 Feb 1;168(2):K19-26

3. **Idkowiak J,** Randell T, Dhir V, Patel P, Shackleton CH, Taylor NF, Krone N, Arlt W. A missense mutation the human *cytochrome b5* gene causes 46,XY disorder of sex development due to true isolated 17,20 lyase deficiency. *J Clin Endocrinol Metab*. 2012 Mar;97(3):E465-75.

4. Krone N, Reisch N, **Idkowiak J**, Dhir V, Ivison HE, Hughes BA, Rose IT, O'Neil DM, Vijzelaar R, Smith MJ, MacDonald F, Cole TR, Adolphs N, Barton JS, Blair EM, Braddock SR, Collins F, Cragun DL, Dattani MT, Day R, Dougan S, Feist M, Gottschalk ME, Gregory JW, Haim M, Harrison R, Olney AH, Hauffa BP, Hindmarsh PC, Hopkin RJ, Jira PE, Kempers M, Kerstens MN, Khalifa MM, Köhler B, Maiter D, Nielsen S, O'Riordan SM, Roth CL, Shane KP, Silink M, Stikkelbroeck NM, Sweeney E, Szarras-Czapnik M, Waterson JR, Williamson L, Hartmann MF, Taylor NF, Wudy SA, Malunowicz EM, Shackleton CH, Arlt W. Genotype-phenotype analysis in congenital adrenal hyperplasia due to P450 oxidoreductase deficiency. *J Clin Endocrinol Metab*. 2012 Feb;97(2):E257-67.

5. **Idkowiak J**, Lavery GG, Dhir V, Barrett TG, Stewart PM, Krone N, Arlt W. Premature adrenarche – novel lessons from early onset androgen excess. *Eur J Endocrinol 2011 Aug; 165(2): 189-207.*

6. **Idkowiak J**, O'Riordan S, Reisch N, Dhir V, Maiter D, Malunowicz EM, Willems P, Dattani M, Shackleton CHL, Kerstens M, Krone N, Collins F, Arlt W. Pubertal presentation in congenital adrenal hyperplasia due to P450 oxidoreductase deficiency. *J Clin Endocrinol Metab* 2011 Mar:96(3):E453-62.

7. **Idkowiak J**, Malunowicz EM, Reisch N, Dhir V, Szarras-Czapnik M, Holmes DM, Davies JD, Hughes IA, Krone N, Arlt W. Concomitant P450 oxidoreductase and androgen receptor mutations result in neonatal 46,XY disordered sex development and androgenisation at adrenarche. *J Clin Endocrinol Metab* 2010 Jul;95(7):3418-27.